Geologic Characteristics of Sediment-and Volcanic-Hosted Disseminated Gold Deposits—Search for an Occurrence Model

U.S. GEOLOGICAL SURVEY BULLETIN 1646

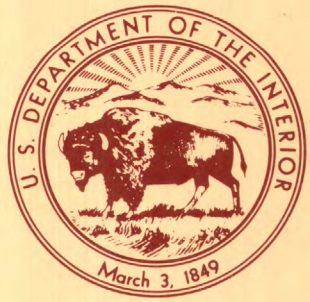

Tooker, ed.— GEOLOGIC CHARACTERISTICS OF SEDIMENT- AND VOLCANIC-HOSTED DISSEMINATED GOLD DEPOSITS— U.S. Geological Survey Bulletin 1646

CORRECTION

The following pages replace pages 97 through 102 in U.S. Geological Survey Bulletin 1646.

valley-fill gravel to the east.

Basin-and-range-associated tectonism during the Miocene (Stewart, 1980) created a steep block-faulted terrain. Three conspicuous basin-and-range fault sets trend east-west, northwest, and northeast within the district. Hawkins (1982) postulated that the east-west-trending fault set may have been active during the Mesozoic, and was followed by the development of northeast- and northwest-trending faults during the basin-and-range event. The Snow Canyon fault, one of the major east-west-trending faults, occurs just north of the Jerritt Canyon window (fig. 57). Similar but smaller scale east-west-trending faults in the Enfield Bell mine are are the Marlboro Canyon, Bell, and Ridge faults (fig. 58), which may have also formed first during the Mesozoic.

Erosion of uplifted blocks along these faults has locally removed the upper-plate rocks and exposed the lower plate as windows in the Roberts Mountains thrust (fig. 58). In most areas, the contact between upper- and lower-plate rocks in the Jerritt Canyon district is thought to be a high-angle fault. Exposure of the Roberts Mountains thrust is limited. Continued erosion has resulted in a steep terrain and the locally thick alluvial and colluvial cover in the district.

REGIONAL STRATIGRAPHY

Most of the rocks in the Jerritt Canyon district are Paleozoic sedimentary and volcanic rocks that have been assigned to the upper and lower plates of the Roberts Mountains thrust (Hawkins, 1973).

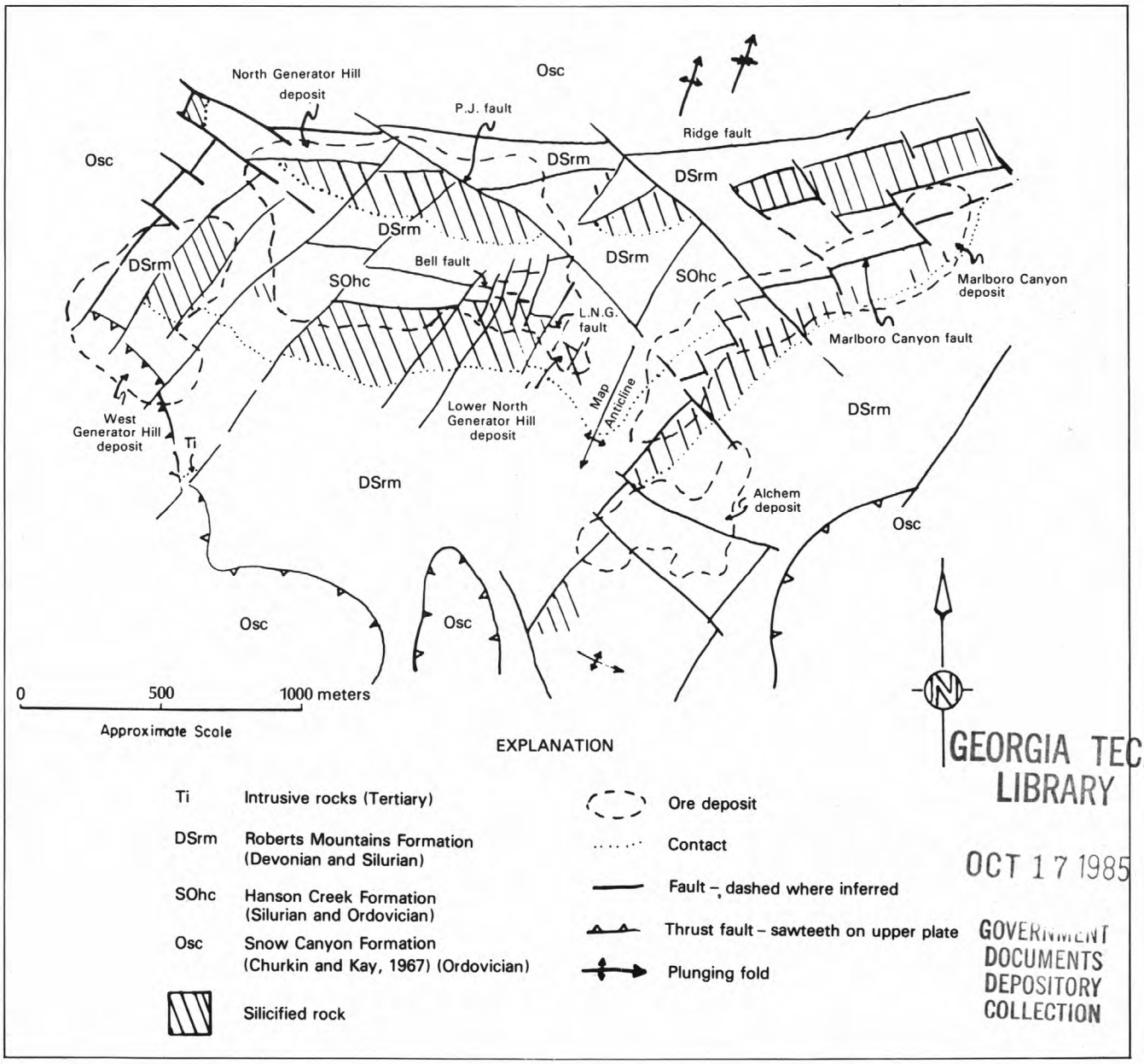

Figure 58. Preliminary geologic map of the Enfield Bell mine, Jerritt Canyon district, Elko County, Nevada.

Lower-plate rocks

Lower-plate stratigraphy within the Independence Mountains was described by Kerr (1962) and Hawkins (1973). Although a continuous, undisturbed stratigraphic section has not yet been recognized, sufficient exposures are present to enable the reconstruction of a complete section from the base of the Eureka Quartzite through the Roberts Mountains Formation (fig. 59).

The Eureka Quartzite of Middle Ordovician age is recognized throughout most of central Nevada as a prominent cliff-forming member of the autochthonous assemblage. Exposures of the formation in the district are limited to the southern parts of the Jerritt Canyon window, where it is composed of thick-bedded orthoquartzite. Fresh rock is generally light grey, with scattered grains of oxidized pyrite; weathered surfaces may be slightly yellow brown. Quartz grains are cemented by silica except near the contact with the overlying Hanson Creek Formation, where carbonate cement may also occur. Although bedding is indistinct, beds are generally massive and more than 3 m thick. Fossils are rare, but local exposures yield graptolite molds. Measured thicknesses of the Eureka Quartzite range from 150 to 190 m. Although the base of the formation has not been well studied, the upper contact is interpreted to be gradational with the Hanson Creek Formation.

The Hanson Creek Formation, considered to be of Late Ordovician and Early Silurian age by Matti and others (1975), is the major host rock at the Bell Enfield mine and is exposed in many parts of the Jerritt Canyon window. On the basis of surface and subsurface data, the Hanson Creek Formation is here subdivided into five lithologic units—unit 1 (youngest) through unit 5 (oldest) (fig. 60). Because the upper parts of the Hanson Creek Formation are much better known and occur more commonly in outcrop than the lower units, the units are numbered consecutively from the top down.

The lower three units of the Hanson Creek Formation, units 3 through 5, are carbonaceous banded limestones. The banding, best developed in unit 3, results from alternating beds of micritic limestone and laminated dolomitic limestone, in which the laminated beds are the most carbonaceous. Pyrite occurs in both types of beds, although it is more abundant in the laminated beds.

The basal unit, unit 5, as measured, consists of 5 to 30 m of dolomitic limestone and thin-bedded micritic limestone, with some laminated calcareous siltstone near the basal contact. Fossils recognized throughout are crinoidal, brachiopod, bryozoan, and radiolarian fragments. Near the top of unit 5, an intraclastic layer has been recognized in which the intraclasts contain fossil debris mixed with carbon stringers and pods and sparry calcite cement. Locally, lenses and pods of black, carbonaceous chert have been recognized.

The overlying unit 4 is a 30- to 40-m-thick sequence of carbonaceous banded limestone containing abundant black chert nodules and lenses, 5 to 25 cm long, oriented parallel to bedding. Micrite beds may be faintly laminated, whereas laminated dolomitic limestone beds are locally absent. Fossil fragments are similar to those found in the basal unit.

The middle unit of the Hanson Creek Formation, unit 3, is a sequence of alternating carbonaceous micritic limestone beds and laminated carbonaceous dolomitic limestone beds. This unit, which is the main host for gold mineralization in the Enfield Bell mine (fig. 60), has been measured at more than 90 m thick in exposures in the southern part of the district. Chert beds, generally less than 0.1 m long and 2 cm thick, occur sporadically in the lower part of the unit. Fossils recognized in this unit are similar to those in the lower two units, with the addition of trilobite fragments. Studies have shown that gold mineralization favors the more permeable laminated beds, which occur locally in tenfold greater abundance than in the micrite beds.

Overlying unit 3 is a varyingly textured, 30-m-thick unit of limestone—unit 2. Four different rock types have been recognized in this unit: (1) thick-bedded limestone, (2) wavy thin-bedded to nodular limestone, (3) oolitic limestone, and (4) wavy-laminated limestone. The rock is weak to noncarbonaceous, weakly pyritic, and locally is entirely composed of dolomite. Fossils are fairly evenly distributed and resemble those recognized in the lower three units; however, trilobite fragments have not been recognized in this unit.

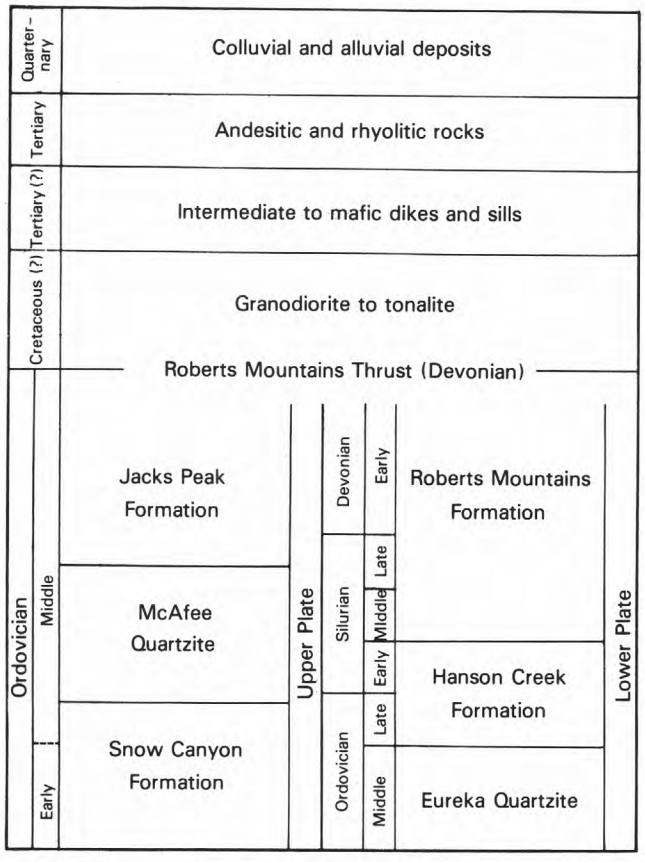

Figure 59. Stratigraphic section of the Jerritt Canyon district. Stratigraphy for upper-plate rocks from Churkin and Kay (1967), and for lower-plate rocks from Mullens and Poole (1972), Matte and others (1975), and Merriam and McKee (1976).

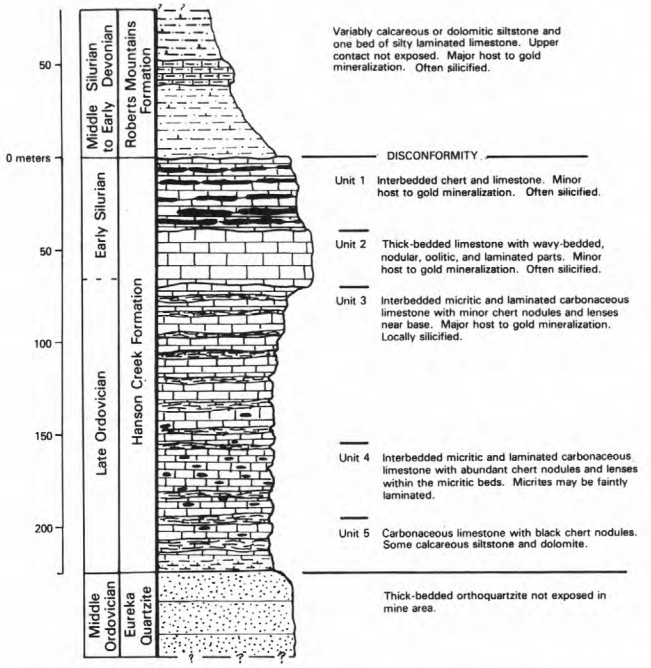

Figure 60. Generalized stratigraphic section of lower-plate rocks in the Enfield Bell mine area.

The uppermost unit of the Hanson Creek Formation, unit 1, is composed of 3 to 40 m of interbedded black chert and carbonaceous limestone. Chert beds are more consistent than in units 3, 4, or 5, and may exceed 1 m in length and 5 cm in thickness. Pinching and swelling of the chert as a result of soft-sediment deformation is common. Sponge spicules, radiolarians, and the absence of diagenetic-replacement textures suggest a sedimentary, nondiagenetic origin for the chert. The limestone beds, which are thicker than the chert beds, compose as much as 75 percent of a measured thickness near the base of the unit. Both laminated and nonlaminated limestone beds have been recognized.

The contact between the Roberts Mountains and Hanson Creek Formations appears to be disconformable, a contention that was also supported by the work of Matti and others (1975). Whereas previously published reports (Mullens and Poole, 1972; Merriam and McKee, 1976) placed the uppermost unit of the Hanson Creek Formation as part of the overlying Roberts Mountains Formation, Freeport Gold Co. geologists cite the sharpness of the contact between this uppermost unit and siltstone of the Roberts Mountains Formation, as well as the similar textures and mineralogy within the five units of the Hanson Creek Formation, as evidence that the uppermost unit, 1, more properly belongs within the Hanson Creek Formation.

The Roberts Mountains Formation of Middle Silurian to Early Devonian age (Matti and McKee, 1977) is exposed throughout the Jerritt Canyon district. The basal 30 m of this formation is host to gold mineralization in the Enfield Bell mine (fig. 60). The estimated thickness of the Roberts Mountains Formation is 300 m; however, the uppermost part has been truncated by the Roberts Mountains thrust, which forms the upper contact of the formation. The major rock type of the Roberts Mountains Formation is a laminated fissile, varyingly calcareous to dolomitic siltstone. The rock is composed of well-rounded, well-sorted quartz silt grains, with carbonate as cement. Accessory minerals include illite-sericite, chlorite, anastamosing carbon filaments, disseminated pyrite, and a distinctive heavy-mineral suite. Black lenses composed of carbon, pyrite euhedra, and fibrous chalcedony, 0.5 cm thick and 2 to 5 cm long, oriented parallel to bedding, are common in the basal part of the formation. Fossils are rare and are limited to graptolite molds on parting surfaces.

A 10- to 15-m-thick bed of laminated to thin-bedded silty limestone occurs near the base of the formation. The more fissile siltstone beds commonly weather into small platy fragments and form gradual slopes, whereas the silty limestone unit is more resistant and can be traced in outcrop for hundreds of meters along strike.

Upper-plate rocks

The upper-plate rocks (western facies) in the Independence Mountains have been correlated with eugeosynclinal rocks of the Ordovician Valmy Group (Churkin and Kay, 1967). Three formations of Ordovician age are recognized locally, in ascending order: The Snow Canyon Formation (Early and Middle Ordovician), the McAfee Quartzite (Middle Ordovician), and the Jacks Peak Formation (Middle Ordovician).

Whereas exposures of the McAfee Quartzite and the Jacks Peak Formation are limited to the northernmost part of the Jerritt Canyon district, the Snow Canyon Formation commonly flanks lower-plate rocks throughout the district. Only the Snow Canyon Formation is described here.

The rocks that compose the Snow Canyon Formation in the Jerritt Canyon district are predominantly siliceous sedimentary rocks, estimated at 350 m thick (Churkin and Kay, 1967). Except for the more resistant members, the Snow Canyon does not crop out well and forms smooth, talus-covered slopes.

Shale, fissile siltstone, and argillite form the bulk of the Snow Canyon section. These rocks are carbonaceous and much less calcareous or dolomitic than those of the Roberts Mountains Formation. Weathered exposures show a characteristic orange-brown staining. Bedding generally is very wavy and contorted, and soft-sediment-compaction features are common. Graptolite molds are locally abundant.

Interspersed with the clastic rocks are multicolored, wavy chert beds that exhibit a knobby texture on their bedding planes, referred to locally as cobblestone texture. Bedding is generally less than 10 cm thick. Bedded grey barite locally occurs with the chert.

Discontinuous layers of grey to brown quartzite, generally less than 3 m thick, occur within the finer grained clastic sequence. A thicker quartzite unit, with scattered shale horizons, apparently caps the Snow Canyon Formation. Both types of quartzite are composed of quartz sand grains and scattered pyrite, cemented with silica or carbonate. Carbon and random quartz veinlets are recognized locally. Crossbedding, though

sparse, has been observed in the thinner quartzite and siltstone beds.

Mafic pillow lavas occur within the Snow Canyon Formation, sandwiched between argillaceous-rock sequences. Chert and limestone can be found sporadically within the lavas. The limestone beds occur between successive pillow structures. Alteration of these lavas has changed the primary minerals to chlorite, sericite, and carbonate. Phenocrysts of plagioclase and pyroxene commonly are totally altered to calcite.

Limestone is the least continuous rock type in the Snow Canyon Formation. Besides occurring within altered mafic lavas, limestone has been recognized interspersed with laminated chert, shale, and siltstone. A section of shaly carbonaceous limestone capped by a cliff-forming intraformational limestone breccia apparently occurs near the base of the formation on the west margin of the Enfield Bell mine area.

GEOLOGY OF THE ENFIELD BELL MINE

The Enfield Bell mine is located in the northern part of the Jerritt Canyon window, in an area approximately 3,300 m long east-west by 1,200 m wide north-south (fig. 58). The mine comprises four known ore deposits, in order of decreasing size: the Marlboro Canyon, North Generator Hill, West Generator Hill, and Alchem deposits. Current reserves are 13.7 million tons (12.5 million t) at an average grade of 0.199 troy oz Au per ton (7.03 g Au/t), occurring in both oxidized and carbonaceous sedimentary rocks. Mineralization is structurally and lithologically controlled within the upper banded limestone of the Hanson Creek Formation, unit 3, and the lower siltstone of the Roberts Mountains Formation (fig. 60). Lesser amounts of ore occur in silicified sections of both formations. Small slices of geochemically barren upper-plate rock have been recognized in the Marlboro Canyon pit. Gold currently is being mined from Marlboro Canyon and a part of North Generator Hill known as Lower North Generator Hill (fig. 58).

Structure

Faulting is common in the Enfield Bell mine area and is the most important structural feature related to mineralization; folding may have been contemporaneous with a premineral set of faults. The four sets of faults in the Enfield Bell mine area range in age from Devonian to Tertiary. The oldest faults are the Roberts Mountains thrust and sympathetic subparallel low-angle normal and reverse faults within the upper- and lower-plate assemblages. The presence of imbricate low-angle faults became evident when detailed mapping revealed reversals and truncations of stratigraphy along brecciated low-angle shears.

East-west-trending faults are the next-younger set of major faults in the mine area. These faults are cut by younger northwest- and northeast-trending faults. The ages of these three fault sets is somewhat equivocal; however, the east-west-trending system is postulated to have formed first during the Mesozoic, with an overprint of Tertiary motion. One such fault is the Snow Canyon fault (Hawkins, 1982), which occurs immediately north of the mine area (fig. 57). Smaller scale east-west-trending faults within the mine area are the Marlboro Canyon fault in the Marlboro Canyon ore body, the Bell and L.N.G. faults in the Lower North Generator Hill ore body, and the Ridge fault, which forms the north boundary of the Jerritt Canyon window (fig. 58).

Figures 61A and 61B show typical cross sections through the Lower North Generator Hill and Marlboro Canyon deposits that illustrate the characteristics of the Bell and Marlboro Canyon faults, which were the main conduits for mineralization in their respective ore bodies. In each deposit, rocks of the Roberts Mountains and Hanson Creek Formations form the footwall block (north) against rocks of the Hanson Creek Formation in the hanging wall (south). Estimated relative vertical displacement on these faults is 100 m. Both faults dip steeply south but change dip and strike directions over short vertical and horizontal distances. The Marlboro Canyon fault changes strike in the western part of the Marlboro Canyon ore body to more northeasterly, whereas the Bell fault changes strike to northeasterly in the east end of the Lower North Generator Hill ore body (fig. 58). Both faults became shallower in dip on progressively deeper mine levels.

The L.N.G. fault is also an east-west-trending fault that may have formed as a result of uplift along the Bell fault; it appears, for the most part, to be a bedding-plane fault. This fault, which dips gently south, is believed to have formed as a result of slippage along the boundary between silicified and unsilicified parts of the Hanson Creek Formation. The amount of displacement on the L.N.G. fault changes to a northwesterly strike on the east side of the Lower North Generator Hill ore body (fig. 58).

After formation of the Marlboro Canyon and Bell faults, the high-angle northwest- and northeast-trending faults were formed during Basin and Range tectonism. Mapping evidence of active mine faces suggests that the northeast-trending faults postdate the northwest-trending faults. However, the fact that the northwest-trending P.J. fault in the North Generator Hill deposit cuts both east-west- and northeast-trending faults indicates that some of the northwest-trending faults postdate the northeast-trending faults. Although the genetic relations of faulting in the mine area is still equivocal, all the faults are interpreted to predate gold mineralization. Ore coincides with faults and blossoms at fault intersections. Figure 62, a geologic map of a typical ore bench in the Lower North Generator Hill pit, shows the relation of these structures.

The Map anticline, a southwest-plunging asymmetric fold that occurs between the North Generator and Marlboro Canyon ore bodies (fig. 58), is believed to have formed as a result of thrusting. The western limb of this fold strikes west-northwest and dips south-southwest, whereas the eastern limb strikes north-northeast and dips east-southeast. Dips on each limb range from 25° to 65°; the eastern limb is the steepest. The fold limbs are delineated by dipping beds of jasperoid, which can be readily seen in aerial photographs.

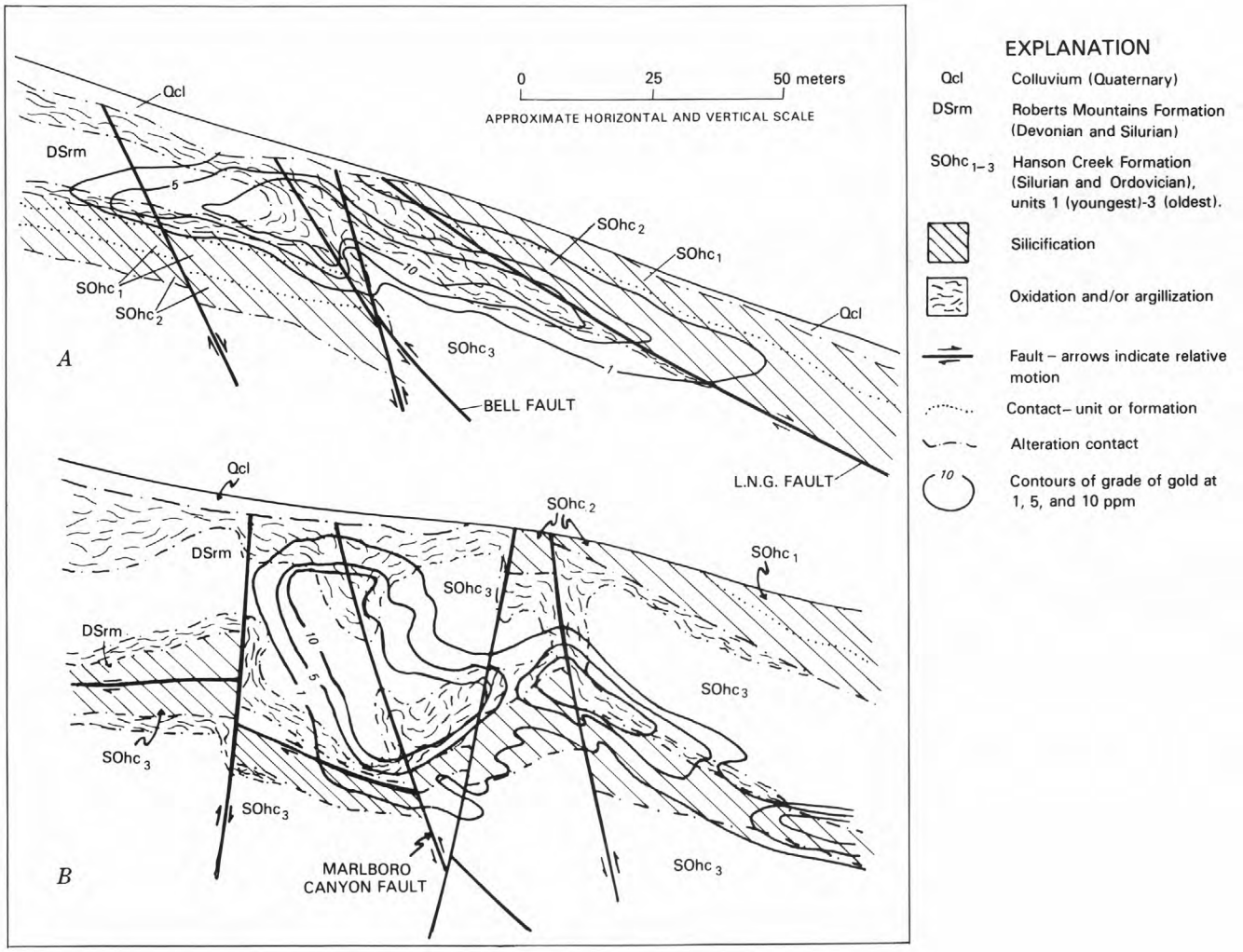

Figure 61. A, North-south cross section through the central part of the Lower North Generator Hill deposit. Contours of gold grade are 1, 5, and 10 ppm. B, North-south cross section, looking eastward, through the central part of the Marlboro Canyon ore body. Gold mineralization is strongly structurally controlled, with greater vertical than horizontal continuity. Contours of gold grade are 1, 5, and 10 ppm.

Ore-body morphology

The ore in the Enfield Bell mine occurs in two distinct modes. The largest ore zone, containing the most continuous and highest grades of gold, are elongate, steeply to moderately dipping tabular zones (Marlboro-type ore zones), which are typical sites for ore deposition in North Generator Hill and in most of Marlboro Canyon. The second type of ore zone (Alchem-type ore zone) is also tabular but is associated with low-angle faults, commonly containing stratiform jasperoid bodies. The bulk of the ore tonnage in the western Marlboro Canyon, Alchem, and West Generator Hill deposits are from Alchem-type ore zones.

Figure 61B shows a cross section of a typical Marlboro-type ore zone. A mushroomlike appearance is created by gold values increasing in large increments from the surface downward, tapering off more gradually below the main ore intervals. Figure 63 shows a typical cross-sectional view of an Alchem-type ore zone. The ore occurs in both unsilicified and silicified parts of the Roberts Mountains Formation and in silicified sections of the underlying Hanson Creek Formation. The contact between these two formations is interpreted to be, at least in part, a low-angle fault. The best ore grades occur in rocks of the Roberts Mountains Formation, and the ore zone may be highly undulatory.

Gold in both types of ore zones is disseminated in the rock—quite typical of ore zones observed in other deposits, such as Carlin. Gold grains observed in thin section may exceed 5 μm in diameter but are generally smaller than 2 μm. Where large enough to be observed petrographically, gold grains commonly are spatially associated with goethite, which may be pseudomorphic after pyrite.

Alteration

Three major hydrothermal events have altered the rocks of the Enfield Bell mine: (1) silicification, (2) oxidation and argillization, and (3) carbonization. Silicification, the predominant event, resulted in alteration of the limestone to hard dense varicolored jasperoid.

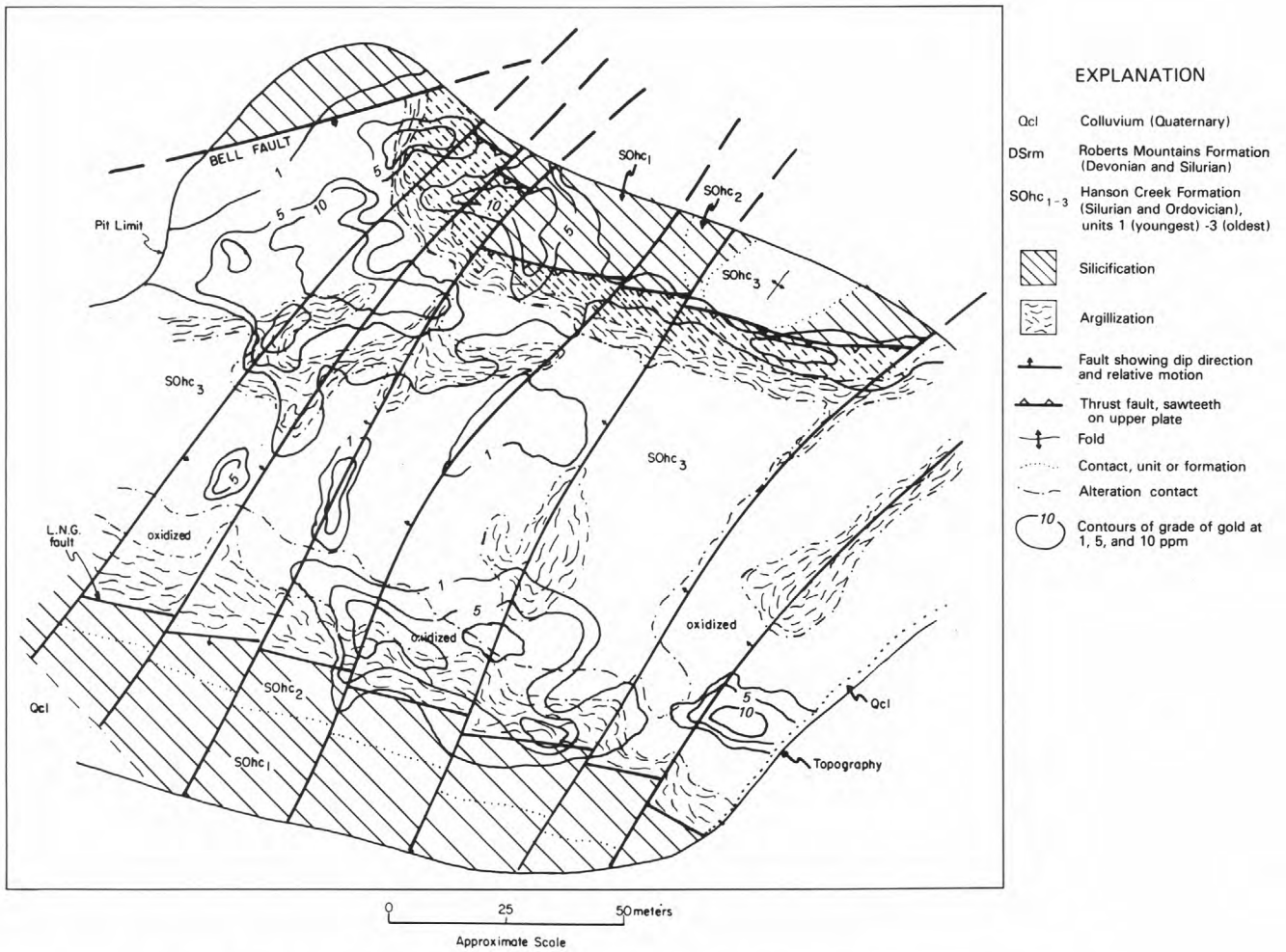

Figure 62. Geologic map of a typical mine level in the Lower Generator Hill ore body.

The jasperoid bodies in the mine area stand out in strong relief from the surrounding terrain and are approximately tabular in shape. Although about 35 to 40 percent of the rocks in the mine area are jasperoid, jasperoid constitutes less than 10 percent of the ore. The degree of silicification recognized in the mine area ranges from scattered quartz veining to complete replacement of the carbonate fraction. Silicification has affected rocks of both the Roberts Mountains and Hanson Creek Formations but is more intense in limestone of the Hanson Creek Formation. Mine mapping suggests that all but, possibly, the latest phase of silicification occurred before Tertiary block faulting. Jasperoid can be seen in razor-sharp contact against unsilicified rocks, horizontally juxtaposed along high-angle faults. The nearly stratiform appearance of the jasperoid bodies is interpreted to be the result of silicification along low-angle faults as well as replacement of chemically favorable rock types. The major stage of silicification that formed the jasperoid bodies is also believed to predate gold mineralization. Gold values occur in silicified and unsilicified rocks on either side of high-angle faults. Gold mineralization does not normally occur in ore-grade concentrations in jasperoid and generally is homogeneously distributed and of lower grade relative to the range of values found in the main ore zones. Locally, the jasperoid bodies may host gold mineralization higher than 30 ppm, but generally it ranges from less than 0.05 to 1.5 ppm.

Oxidation and argillization may be the most economically important alteration events to have taken place in the Enfield Bell mine area; the oxidized and argillized rocks contain the highest gold values and are relatively easy to treat with conventional cyanidation techniques of gold recovery. These two types of alteration coincide spatially and are believed to have similar, but not necessarily contemporaneous, genesis. Oxidation of the Roberts Mountains Formation produced a tan to light-orange-brown semifriable siltstone. Pyrite grains are well oxidized to limonite and goethite, and carbon is generally absent. The rock may also be noncalcareous, owing to associated but limited decalcification. Oxidation within the Hanson Creek Formation is similar to that recognized in the Roberts Mountains Formation, except for (1) local oxidation of black, carbonaceous chert lenses and beds to light-brown chert or black chert with brown rims, and (2) preferential oxidation of the more permeable laminated beds of unit 3 of the Hanson Creek Formation. Again, as in the Roberts Mountains

GPO 591-238/38348

Geologic Characteristics of Sediment-and Volcanic-Hosted Disseminated Gold Deposits—Search for an Occurrence Model

Edwin W. Tooker, Editor

A study of current information
on disseminated gold occurrences
as a basis for developing an
empirical occurrence model

U.S. GEOLOGICAL SURVEY BULLETIN 1646

DEPARTMENT OF THE INTERIOR
DONALD PAUL HODEL, Secretary

U.S. GEOLOGICAL SURVEY
Dallas L. Peck, Director

UNITED STATES GOVERNMENT PRINTING OFFICE : 1985

For sale by the
Superintendent of Documents
U.S. Government Printing Office
Washington, D.C. 20402

Library of Congress Cataloging in Publication Data

Geologic characteristics of sediment- and volcanic-hosted disseminated gold deposits -- search for an occurrence model.

(U.S. Geological Survey Bulletin 1646)
Includes bibliographies.
Supt. of Docs. no.: I 19.3:1646
1. Gold ores--West (U.S.). 2. Disseminated deposits--West (U.S.). I. Tooker, Edwin Wilson, 1923- . II. Series: United States. Geological Survey. Bulletin 1646.
QE75.B9 no. 1646 557.3s 85-600044
[QE390.2.G65] [553.4'1'0978]

CONTENTS

FIGURES

TABLES

Geologic Characteristics of Sediment- and Volcanic-Hosted Disseminated Gold Deposits—Search for an Occurrence Model

Edwin W. Tooker, *Editor*

SUMMARY

Disseminated, "invisible," dispersed, bulk-minable, or Carlin-type gold deposits are all different names for a major new type of ore deposit that is currently being extensively developed in the Western United States. Though discovered originally in Nevada, this type of deposit is now being found elsewhere; thus, a descriptive empirical model that emphasizes the geologic-, geochemical-, and geophysical-occurrence environments and geoeconomic characteristics is needed to assist the mining industry and Government to explore for and assess the resource potential of these deposits in the United States and elsewhere. This report compiles scientific discussions on geologic-occurrence processes and observable factors leading to the definition of such a model, originally presented at a U.S. Geological Survey workshop held in Reno, Nev., in 1982. This workshop comprised conference, field-examination, and discussion sessions; participants included employees of State and Federal geological surveys and industry experts on the subject.

The characteristic genetic processes and observable features of disseminated gold occurrences are considered here in a series of 11 chapters based on reports presented during the workshop sessions. Most of the deposits discussed are in Nevada, where D. E. White observes a genetic tie between the high-temperature active hot-spring systems and fossil (less than 40 m.y. old) epithermal gold-silver deposits. Evolution of volcanic belts seems to be paralleled by closely related sequential formation of volcanic- and fossil-hot-spring-hosted gold deposits. The enigma is that of the sediment-hosted deposits, which generally predate widespread mid-Tertiary volcanism and many, but not all, of which share mineralogic-geochemical characteristics; the genetic tie to volcanism is obscure, but the data base for these early sediment-hosted deposits is still incomplete.

Next, we consider critical aspects of the geochemical and physical characteristics of hydrothermal solutions, derived from evidence of silica-mineral solubility, gold-sulfide-bearing solutions, infusion of meteoric water, and the boiling/rupture cycle of these systems, as well as regional geochemical consequences and the geochronology and duration of the hydrothermal systems. R. O. Fournier's experimental studies demonstrate that specific silica minerals may be used to interpret the geochemical/geothermal conditions of gold deposition. Parameters considered to effect crystallization or recrystallization in various parts of the hydrothermal systems include the silica phases (quartz, chalcedony, β-cristobalite, opal-CT, and glass) present, solution composition and degree of saturation, time, temperature, and confining pressure (or its sudden release).

J. J. Rytuba observes that the mineral assemblages and fluid inclusions of Carlin-type deposits imply that the hydrothermal solution was of low temperature (25°-150°C), low ionic strength in NaCl, and low total sulfide content. Such a solution can transport substantial amounts of gold only as a sulfide complex; iron is present as the $FeCl^+$ complex, and mercury and antimony as the native elements. Changes in arsenic phases reflect a decrease in temperature over time.

A conceptual model for the occurrence of carbonate-hosted disseminated gold deposits, based on geologic, fluid-inclusion, geochemical, and stable-isotope studies of the Carlin and Cortez deposits by R. O. Rye, focuses on the shallow-level meteoric-water hydrothermal system that he believes was mobilized by underlying igneous activity. He proposes that all the ore components, which are mobile in shallow hydrothermal systems, could have been derived from the host Paleozoic sedimentary rocks. Although the identity of the chemical complexes constituting the transporting solution is still uncertain at Carlin, boiling and mixing with low-temperature ground waters do not seem to have been important depositing factors, although they occurred after main-stage gold was deposited.

In addition to such factors as cooling, changes in pH, interaction with wallrocks, oxidation by mixing with meteoric water or by contact with the atmosphere, and physicochemical reactions, boiling or effervescence of the hydrothermal ore fluids can lead to deposition of metals. C. G. Cunningham proposes two theoretical models that show how boiling may cause deposition of gold. Studies of the paragenesis and fluid inclusions at Summitville, Colo., show that boiling at or near the surface releases H_2S from aqueous sulfide solutions and results in the precipitation of gold, barite, and quartz. A second study of the Mahd adh Dahab gold deposit, Saudi Arabia, suggests that effervescence of saline carbonate solutions there increased the pH, lowered the solubility of gold, and resulted in its precipitation.

B. R. Berger describes hot-spring deposits, which are characterized by extensive surficial and near-surface silicification and widespread hydrothermal brecciation. These deposits may progress below the silica caprock into a stockwork-veining zone. Ores are irregularly distributed but generally of higher grade near vents. Trace-element suites commonly include Ag, As, Hg, Sb, Tl, and W; though present in low concentrations, Cu, Pb, and Zn do not seem to have been important components of the hydrothermal solutions at near-surface depths.

M. L. Silberman explores the isotopic (K-Ar) record for the timing and duration of gold deposition in the hydrothermal-alteration and mineralization sequence, with respect to spatially associated igneous rocks. The few existing geochronologic studies suggest that the timespan of hydrothermal activity is in the range 0.6-2.5 m.y.; activity is short lived, transitory, but repetitive.

H. F. Bonham's examination of bulk-minable deposits turns to some broader regional (even plate tectonic) features of these fine-grained replacement deposits. He proposes a system for their classification based on spatial relations with intrusive granitic and extrusive volcanic centers, and indicates special deposit-type attributes to be considered in the discussion of deposit models. He compares a broad array of types of disseminated gold deposits in Nevada and elsewhere.

Field observations made during the workshop included visits to Steamboat Springs and the Borealis and Jerritt Canyon deposits, Nev., descriptions of which follow. D. E. White describes the geologic and geochemical relations at Steamboat Springs, which may be a present-day equivalent of the Tertiary geothermal systems that formed epithermal gold-silver deposits. A descriptive roadlog is included to facilitate personal observation of the geothermal area. Borealis is a moderate-size volcanic-hosted disseminated gold deposit that D. G. Strachan believes contains evidence of fossil geothermal activity. Extensive bleached and altered (silicified and argillized) zones in faulted and brecciated volcanic rocks may define vent centers. The Jerritt Canyon deposit, one of the largest carbonate-hosted types, contains disseminated gold in oxidized and carbonaceous parts of the autochthonous Paleozoic carbonate rocks underlying the Roberts Mountains thrust fault. Low-angle faults provided pathways for solutions upward into favorable zones for deposition. Hydrothermal alteration comprises silicification (including abundant jasperoid), oxidation, argillization, and carbonization; gold is concentrated mostly in altered rock and is accompanied by stibnite, barite, realgar, and orpiment. Reserves amount to as much as 2,562,500 troy oz (79.7 million g).

The initial conclusion of the workshop--that a precise occurrence model(s) is premature--was followed by a decision to test this conclusion by compiling and comparing a "checklist" tabular inventory of the known as well as yet-to-be-determined attributes for each of 13 sediment-, volcanic-, and hot-spring-hosted deposit examples: (1) Carlin, Nev. (including the neighboring Maggie Creek/Gold Quarry deposits), (2) Cortez, Nev., (3) Gold Acres, Nev., (4) Jerritt Canyon, Nev., (5) Alligator Ridge, Nev., (6) Getchell, Nev., (7) Mercur, Utah, (8) Hasbrouck Peak, Nev., (9) McLaughlin, Calif., (10) Sulphur, Nev., (11) Borealis, Nev., (12) Round Mountain, Nev., and (13) DeLamar, Idaho. The results of a comparison of these checklist data (see table 8) clearly indicate that a general model for the occurrence of disseminated gold deposits has emerged. A range of types of depositional environments seems to share many common district and deposit traits. Originally described and developed as economic entities in north-central Nevada, these deposits are beginning to be recognized elsewhere in the western Cordilleran region and beyond. This status report exposes numerous gaps in our knowledge as well as codifying what is presently known.

INTRODUCTION

The current expansion of resource information, particularly on "disseminated" gold, and the improved technologies now available for resource investigations should place us in an enhanced position for developing a better predictive methodology for meeting one of the important responsibilities of the U.S. Geological Survey--to examine and assess the mineral resources of the geologic terranes composing the public (and privately owned) lands of the United States. The first step is systematic organization of these data. Geologic-occurrence models are an effective systematic method by which to organize large amounts of resource information into a logical sequence facilitating its use more effectively in meeting several industry and Survey objectives, which include the exploration for resources and the assessment of resource potential for land-use decisions. Such models also provide a scientific basis for metallogenesis research, which considers the observable features or attributes of ore occurrence and their "fit" into the Earth's resource puzzle. The use of models in making resource assessments/appraisals was addressed by Shawe (1981), who reported the results of a workshop on methods for resource appraisal of Wilderness and Conterminous United States Mineral Appraisal Program (CUSMAP; 1:250,000-scale quadrangles) areas. The Survey's main objective in the 1982 workshop was to evaluate the status of knowledge about disseminated or very fine grained gold deposits and, if possible, to develop an occurrence model(s).

This report on the workshop proceedings has three main objectives: (1) Education through the publication of a summary review and presentation of new thinking and observations about the scientific bases for those geologic processes and environments that foster disseminated gold-ore formation; (2) systematic organization of available geologic, geochemical, and geophysical information for a range of typical disseminated gold deposits (including recognition of gaps in those data); and (3) assessment of current understanding (as presented in objective 2) toward formulating an empirical ore-occurrence model for this type of deposit. As such, this volume represents a preliminary first step at classification and provides a source of pertinent background information.

Readers of this volume will soon discover, however, that full agreement has not yet been achieved in the interpretation of some of the geologic evidence. The resulting variations in tentative occurrence models for these controversial deposits ultimately will be resolved by filling the gaps in information that have already been identified. Thus, this volume does not report a U.S. Geological Survey consensus; the conclusions expressed in each chapter represent the particular interpretations of the various workshop participants.

Characteristics of disseminated gold occurrences

Most disseminated gold deposits were formed from near-surface low-temperature silica-rich hydrothermal solutions that, at least in part, seem to be comparable to those associated with hot-spring systems. The first eight chapters that follow describe the geologic process and environmental attributes that seem to form and characterize these deposits, which locally, at least, apparently occur in certain sedimentary and volcanic host rocks more commonly than was originally believed. At the outset of these discussions, it became evident that an appropriate, yet inclusive, acceptable name was needed for this type of deposit, which has been variously referred to as very fine grained to "invisible," disseminated, Carlin type, dispersed, or bulk minable. Some of these terms also have been used to describe the fine-grained, generally visible "porphyry copper" type of deposit that is formed in a different geologic environment. The dictionary definitions give scant support for rigorous use of the most common terms "disseminated" or "dispersed" for either type. These terms are used interchangeably in the chapters that follow, depending on the authors' choice. A suggestion, after searching the dictionary, is that a case can be made for calling the subvolcanic system, generally considered responsible for formation of the "porphyry copper" deposits, a dispersed system—that is, spread from a fixed center of supply. The invisible-gold deposits, whose source is less distinctly known, can then be called disseminated—that is, spread widely and irregularly in small particles, as in sowing seed; diffuse.

We have adopted in this volume the convention of reporting production data for gold in troy ounces per short ton, with corresponding grams per metric ton in parenthesis. The troy ounce is the international commercial unit for measuring gold; it is the most commonly used value in commodity reports and in the economic-geology literature, and thus will be familiar and useful to most readers. With one exception, all other scalar values are in Système International (S.I.) units. This exception is in the road log to Steamboat Springs, Nev., which gives distances in miles because vehicles most commonly used in traversing the area record distances only in these units; S.I. equivalents are added in parentheses.

Field examination of type disseminated gold deposits and occurrences

Characteristic examples of the varietal types of disseminated gold deposits or presently subeconomic occurrences were visited during the 1982 workshop. Descriptions of the type deposits at Steamboat Springs, Borealis, and Jerritt Canyon, Nev., are included in the last three chapters. Deposit attributes for the Hasbrouck Peak and Round Mountain deposits are included in the checklists at the end of this volume. The field trip, led by Donald E. White, began with observations of the well-known metal-depositing modern hot-spring system at Steamboat Springs, Nev. Possible fossil-hot-spring ore depositing systems were subsequently visited at Borealis, Nev. (leader, Donald G. Strachan) and at Hasbrouck Peak, Nev. (leader, Andy B. Wallace). Although the mine workings in the Round Mountain district could not be visited, the geologic setting and ore-deposit attributes of this volcanic-hosted ore body were described and discussed by Daniel R, Shawe, Joseph V. Tingley, and Byron R. Berger, who have studied the deposit and its regional setting. The final field visit, led by Roger Banghart, was to the large carbonate-hosted deposits in the Jerritt Canyon district, Nev.

Status of the disseminated-gold-occurrence model

The objectives of the concluding workshop session were to focus attention on what is known already and what still needs to be known about the variety of similar yet different types of disseminated gold deposits visited or discussed, and, if possible, to frame an ore-occurrence model for them. First, a checklist of the regional, district, and mine attributes was made for several deposits typical of the sediment-, hot-spring-, and volcanic-hosted deposits: Alligator Ridge, Nev., Borealis, Nev., Carlin, Nev., Cortez, Nev., DeLamar, Idaho, Getchell, Nev., Gold Acres, Nev., Hasbrouck Peak, Nev., Jerritt Canyon, Nev., Maggie Creek/Gold Quarry, Nev., McLaughlin, Calif., Mercur, Utah, Round Mountain, Nev., Round Mountain Mine, Nev., and Sulphur, Nev. A concluding discussion by Edwin W. Tooker enlarges on the regional attributes in terms of their plate-tectonic terrane setting, basement rocks, and Phanerozoic intrusion and volcanism, and compares the district and deposit traits for sediment- and volcanic-hosted deposits.

Vein and Disseminated Gold-Silver Deposits of the Great Basin Through Space and Time

By Donald E. White

CONTENTS

INTRODUCTION

In a recent paper, White and Heropoulos (1983) tabulated all the data currently available on precious-metal deposits of the Great Basin, especially in Nevada and the immediately adjacent parts of surrounding States. Of these deposits (table 1), 48 are in Nevada, 2 each are in nearby parts of California, Idaho, and Utah, and 1 is in Arizona. White and Heropoulos focused on deposits that have been radiometrically dated (45 districts or deposits) or that had at least preliminary data on salinities of ore fluids and (or) temperatures of deposition (from temper-atures of homogenization and freezing-point depressions of fluid inclusions). Many mineralization ages were determined by standard potassium-argon methods on mineral separates of nearly pure adularia (hydrothermal K-feldspar, mainly by Silberman and McKee, 1974, and Silberman and others, 1976, 1979). Although such ages should be relatively reliable, they may not represent the total timespan of ore deposition of a single deposit or a district. Other K-bearing minerals and altered rocks were utilized for dating some deposits without suitable adularia or alunite; these ages are probably less reliable.

Salinity data were available for only nine deposits or districts—far too few to permit reliable conclusions. The fluids of epithermal vein systems are generally dilute, mostly ranging from 0.2 to 2 weight percent NaCl equivalent, but some inclusion fluids from Rochester (Vikre, 1981) and Tenmile (Nash, 1972) range as high as 6 and 7 weight percent NaCl equivalent. For comparison, active geothermal systems do not exceed 0.8 weight percent NaCl equivalent in salinity (Brook and others, 1979; White and Heropoulos, 1984).

Nash (1972) made the most intensive search for suitable fluid inclusions from disseminated deposits. He concluded that Gold Acres is characterized by inclusion fluids of 5.4 to 7.3 weight-percent-NaCl-equivalent salinity, with filling temperatures of about 160°-185°C. These temperatures are considerably lower than those of typical epithermal veins, most of which range from 200° to 300°C and average about 250°C (table 1; Buchanan, 1981).

Of the 55 deposits or districts listed in table 1, 17 have been called disseminated, Carlin type, bulk mining, or invisible gold, as distinguished from those that contain typical precious-metal veins, which generally occur in volcanic rocks. Of these 17 deposits, 7 have mineralization ages of less than 40 m.y. that probably differ little from those of typical volcanic-hosted vein deposits, except for a broader dispersion of the ore metals in sedimentary rather than in volcanic rocks.

At least 10 "disseminated" ore districts and, possibly, many unlisted recent discoveries are in sedimentary rocks older than the widespread mid-Tertiary volcanism of the Great Basin. Do these deposits differ in significant ways other than age and host rocks? Were their ore fluids more saline than the 2 weight percent NaCl equivalent of most volcanic-hosted veins? Were their temperatures, heat sources, hydrodynamics, and tectonic environments also

Table 1. Locations, mineralization ages, ore-fluid salinities, and temperatures of gold-silver deposits of Nevada and adjacent States

[Deposits marked with an asterisk have been variously called disseminated, carbonate hosted, Carlin type, bulk mining, or invisible gold, and differ from classic epithermal-vein deposits; many other similar deposits have recently been discovered, but no age or fluid-inclusion data are available. Age listed is approximate average of range. Adularia was the mineral most commonly dated (see Silberman and others, 1976, and Buchanan, 1981, for summaries of minerals and ages). Salinities were calculated from the freezing-point depression of fluid inclusions. Temperatures are those of homogenization of fluid inclusions, with no pressure correction; they are probably valid for most of these deposits (Buchanan, 1981). References: A, R. P. Ashley (written commun., 1983); B, Bonham (1982); Bu; Buchanan (1981); G, Garside and Schilling (1979); N, Nash (1972); P, Pansze (1975); S, Silberman and others (1976, 1979) and Silberman (1984); V, Vikre (1981); W, A. B. Wallace (written commun., 1983)]

District	Lat N.	Long W.	Age (m.y.)	Salinity (wt pct NaCl equiv)	Temperature (°C)	References
			Nevada			
Adelaide	40°51'	117°30'	14	---	---	S
Aurora	38°17'	118°54'	11	.2-1.7	227-255	Bu, N, S
Blue Star*	40°54'	116°19'	37.5	---	---	B
Borealis*	38°40'	118°45'	5	---	---	B
Buckhorn	40°10'	116°25'	14.6	---	---	Bu, S
Buckskin	38°59'	119°20'	---	---	---	B
Bullfrog	36°55'	116°48'	9	---	---	Bu, S
Bullion*	40°23'	116°43'	35	---	---	S
Camp Douglas	38°21'	118°12'	15	---	---	G, S
Carlin*	40°45'	116°18'	---	---	150-200	N
Cedar Mountain (Bell)*	38°35'	117°47'	---	.2-1.7	250	Bu
Comstock Lode	39°03'	119°37'	13	---	250-300	Bu, S
Cornucopia	41°32'	116°16'	15	---	---	Bu
Cortez*	40°08'	116°37'	35	---	150-200	B, N, S
Cuprite	37°31'	117°13'	---	---	---	A
Divide	37°59'	117°15'	16	---	---	Bu, S
Getchell*	41°12'	117°16'	90	---	---	B, S
Gilbert	38°09'	117°40'	8	---	275	Bu, S
Gold Acres*	40°15'	116°45'	94	5.4-7.3	160-185	B, N
Gold Circle	41°15'	116°47'	15	---	175-200	Bu, S
Gold Strike*	40°59'	116°22'	78.4	---	---	B
Goldfield	37°43'	117°13'	20-23	---	200-300	A, Bu, S
Hasbrouck*	37°59'	117°16'	16	---	---	B
Humboldt	40°36'	118°11'	73	---	---	Bu
Jarbidge	41°52'	115°26'	14	---	---	Bu, S
Manhattan	38°33'	117°02'	16	.4-1.9	220	N, S
National	41°50'	117°35'	15.5	---	---	Bu
Northumberland*	38°57'	116°47'	84.6	---	---	B
Peavine	39°36'	119°55'	---	---	---	A
Pinson*	41°10'	117°17'	90?	---	---	B, S
Pyramid	39°52'	119°37'	21	---	---	A
Ramsey (Lyon)	39°27'	119°19'	10	---	221	Bu, S
Rawhide	39°01'	118°20'	16	---	---	Bu, S
Rochester*	40°17'	118°09'	58-79	6	270-310	N, V
Round Mountain*	38°42'	117°04'	25	.2-1.4	250-260	B, N, S
Searchlight	35°27'	114°55'	---	---	---	Bu
Seven Troughs	40°29'	118°46'	14	---	240-318	S
Silver Dike	38°19'	118°12'	17.3	---	300	G, S
Silver Peak	37°47'	117°43'	5	---	---	Bu, S
Standard*	40°31'	118°12'	73	---	---	B
Steamboat Springs	39°23'	119°45'	3	.2	>90-230	S
Sulphur	40°53'	118°40'	1.8-2.1	---	---	A, W
Talapoosa*	39°27'	119°19'	10	---	---	S
Tenmile	41°02'	117°53'	16	.4-7.3	>135-330	N, S
Tonopah	38°04'	117°14'	19	<1	240-265	Bu, S
Tuscarora	41°17'	116°14'	38	---	---	Bu, S
Widekind	39°35'	119°45'	---	---	---	A
Wonder	39°24'	118°06'	22	---	---	Bu, S

Table 1. Locations, mineralization ages, ore-fluid salinities, and temperatures of gold-silver deposits of Nevada and adjacent States—Continued

District	Lat N.	Long W.	Age (m.y.)	Salinity (wt pct NaCl equiv)	Temperature (°C)	References
			California			
Bodie	38°12'	119°00'	7.2-8.0	---	215-245	S
Monitor	38°42'	119°40'	5	---	---	S
			Arizona			
Oatman	35°02'	114°23'	---	---	220	Bu
			Idaho			
DeLamar	43°02'	116°50'	---	---	---	Bu
Silver City	43°02'	116°44'	15	---	---	Bu, P
			Utah			
Gold Strike*	37°23'	113°53'	78.4	---	---	Bu
Mercur*	40°19'	112°12'	---	---	---	Bu

similar? These and some other unresolved questions are considered below.

Acknowledgments

The concepts proposed in this chapter are the outgrowth of my efforts to resolve some of the questions raised during the 1982 U.S. Geological Survey workshop and a subsequent (1983) conference in Reno, Nev. (White and Heropoulos, 1983), on active and fossil hydrothermal-convection systems of the Great Basin.

Many individuals have provided essential data utilized or reinterpreted by me. Thanks are especially due to M. L. Silberman, H. F. Bonham, Jr., J. H. Stewart, L. J. Buchanan, R. P. Ashley, R. O. Fournier, J. T. Nash, Chris Heropoulos, A. B. Wallace, W. C. Bagby, T. G. Theodore, and Larry Garside. By no means is there general agreement among researchers on those "fossil" systems that are "epithermal gold-silver deposits" hosted by mid-Tertiary and younger volcanic rocks. Many veins in volcanic rocks are underlain by nonvolcanic rocks, generally of Mesozoic or Paleozoic age. The initial selection of deposits for table 1 was primarily based on a comparison of production values from H. F. Bonham's maps of gold production (Bonham, 1976) and silver production (Bonham, 1980). To be included in table 1, a district must have had important production of Au or Ag (4th rank or larger, as categorized on Bonham's maps) but relatively small production of base and other metals; my intent was to eliminate districts mined primarily for Cu or Pb-Zn, but with total production so large that minor Au and Ag indicated first-rank precious-metal production from byproduct Au and Ag. This tentative list was then examined by R. P. Ashley and H. F. Bonham, Jr., or was included in earlier published discussions of epithermal precious-metal deposits by Lindgren (1933), Nolan (1933), or Buchanan (1981). For the deposits of table 1 designated with an asterisk as "disseminated" or "bulk mining," I depended primarily on the map and brief discussions noted by Bonham (1982).

AGES OF ORE DEPOSITS AND THEIR RELATIONS TO VOLCANISM

Cretaceous systems

Nine of the ore systems listed in table 1 have indicated mineralization ages older than 44 m.y. (fig. 1). The Rochester district (Vikre, 1981) may, in part, be as young as 58 m.y., but all the other districts, including part of the Rochester, have ages between 73 and 94 m.y. Only a few of these districts have been dated reliably by adularia closely associated with ore, and so the true mineralization ages are not yet firmly established.

Most of the older deposits are mined primarily for dispersed or "invisible" gold (Bonham, 1982),

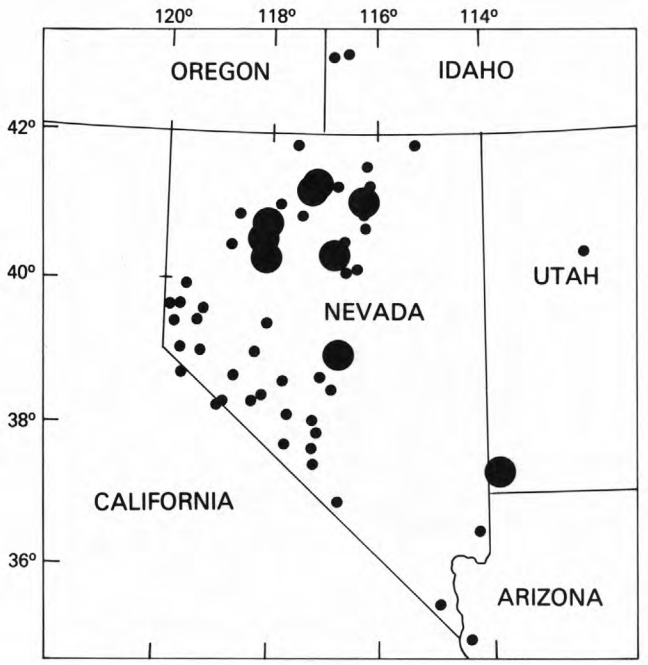

Figure 1. Nevada and parts of adjacent States; large dots denote locations of gold-silver deposits of Cretaceous and early Tertiary age (older than 44 m.y.). Small dots denote all other deposits listed in table 1.

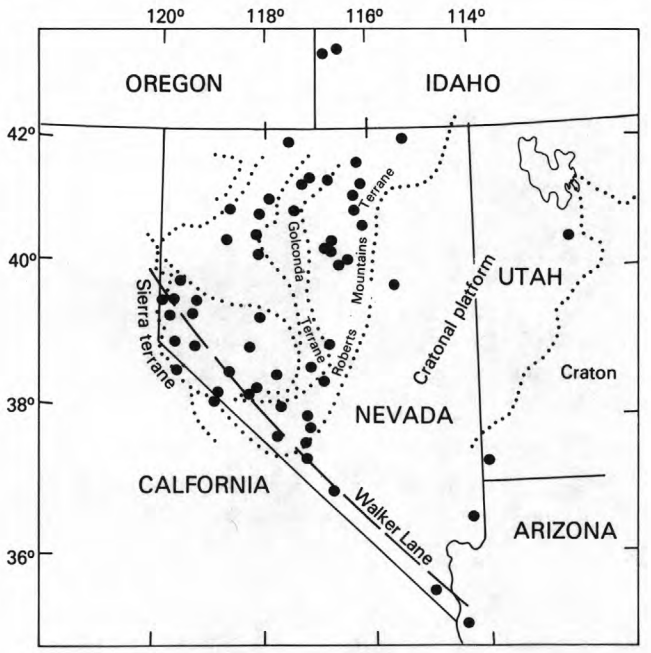

Figure 2. Nevada and parts of adjacent States, showing distribution of miogeosynclinal and accreted terranes (see fig. 64).

although the Rochester district is of interest mainly for its silver. Most districts show little obvious relation to belts of volcanic rocks, although the Rochester, again, is an exception because it occurs in volcanic rocks of the Koipato Group of Mesozoic age.

The distribution of the older deposits shown in figure 1 shows no coherent pattern. A cluster occurs in north-central Nevada which seems to be associated with the accreted Golconda and Roberts Mountains terranes (fig. 2) and are sharply limited by the east boundary of the Roberts Mountains terrane. Exceptions are the Gold Strike district of southwestern Utah, and Alligator Ridge, which have not yet been dated.

A long time lapse may have occurred between Cretaceous and middle Tertiary precious-metal-ore generation, possibly from about 73 to 38 m.y. B.P. Firm conclusions cannot yet be drawn from the limited data; however, many new deposits of the disseminated type have been discovered in the past 5 to 10 years, most of which are not yet reliably dated (or data not yet released). Major thrust faulting and accretion of terranes from elsewhere had already occurred. Crustal extension and thinning, with consequent increased conductive heat flow and early stages of formation of the Great Basin, had not yet started.

Evolving trends of mid-Tertiary and younger volcanic and precious-metal systems

The pattern of mid-Tertiary and younger volcanism and its relations to precious-metal-ore deposits have been interpreted as belts that develop sequentially. Stewart and Carlson (1976) and Stewart and others (1977) emphasized arcuate, generally east-west-trending belts, each successively younger to the south over time. Silberman and others (1976) also emphasized an east-westward trend that migrates southward but rotates into near-coincidence with the northwest-trending Walker Lane (near the common northwest boundary of Nevada and California). North-southward and northeastward trends are not specifically recognized.

Although I depend strongly on the primary data from these authors for most of my interpretations, I prefer to interpret the pattern of evolving volcanism during and after mid-Tertiary time as a sharply flexed arc consisting of an east-northeast-trending southern arm and a north-northeast-trending northern arm, joining in east-central Nevada (fig. 3); over time, this arc broadens and migrates southward and westward. The gold-silver deposits as a whole (bottom, fig. 1; table 1) show a stronger north-northeastward than an east-westward or northwestward trend. In the following sections, I suggest these main trends, with dominance shifting over time. Mineralization trends tend to be short and sharp in space and time, not always coinciding with the crudely contemporaneous volcanic trends.

Trends from 43 to 34 m.y. B.P.

Stewart and others (1977) showed the distribution of volcanic rocks that range in age from 34 to 43 m.y. (fig. 3). Although several interpretations of their generalized distributions have been published, I visualize figure 3 as a sharply flexed arc with west-southwestern and north-northeastern limbs that join at an

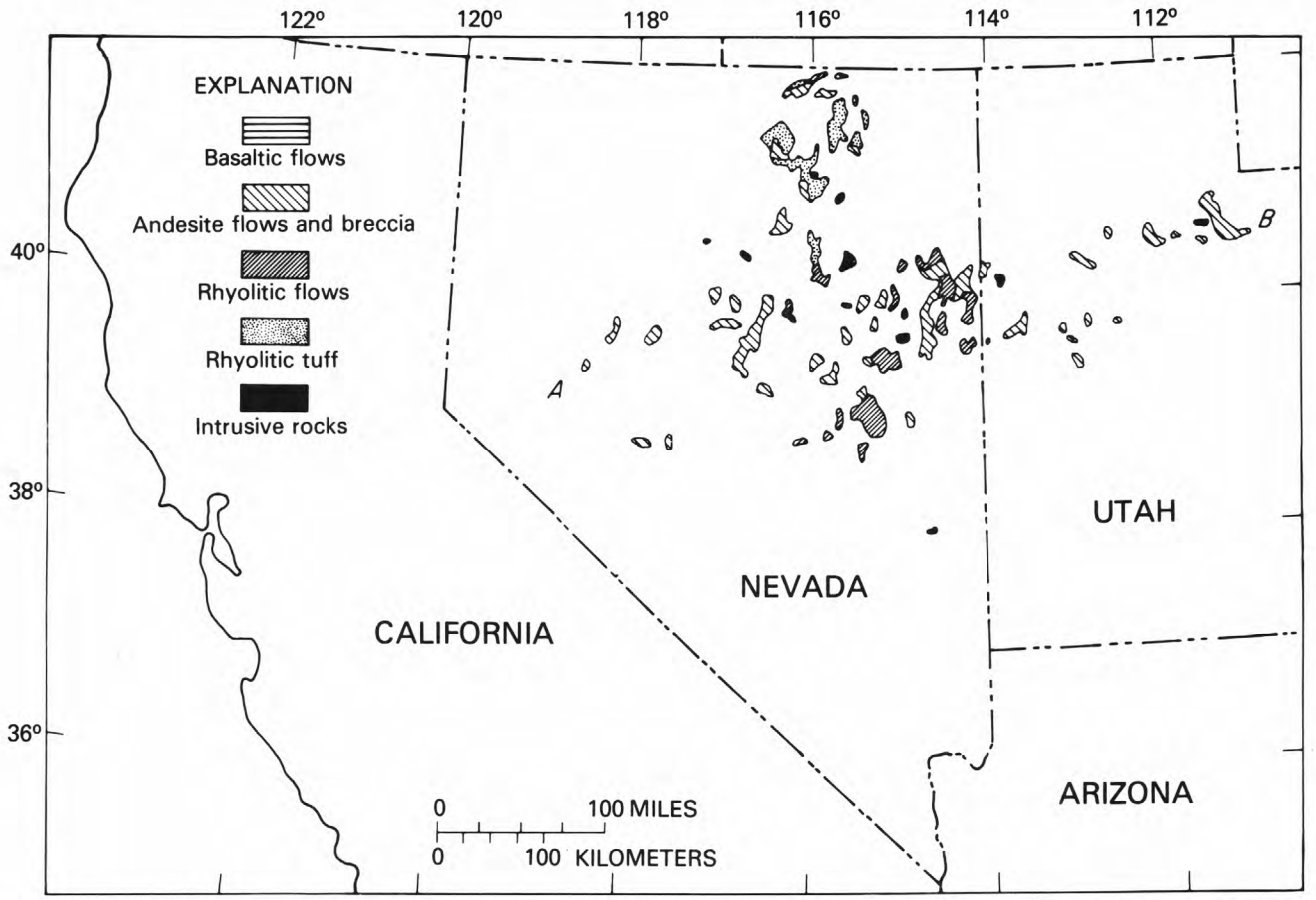

Figure 3. Nevada and parts of adjacent States, showing distribution of volcanic rocks that range in age from 34 to 43 m.y. (from Stewart and others, 1977, fig. 1A).

apex in east-central Nevada. Andesitic flows and breccia are dominant in the southern limb, rhyolitic flows are abundant near the sharp flexure, and rhyolitic tuff is most abundant along the north-northeastern limb. Intrusive rocks are sporadic throughout the arc. Only a single caldera, Mount Lewis, was recognized by Stewart and others (1977) in north-central Nevada south of Battle Mountain, but all mapped rhyolitic ash-flow tuff occurs considerably northeastward of this caldera. The terrane boundaries shown in figure 2 have no apparent influence on the volcanic arc, the types of volcanism, or the positions of calderas.

Four precious-metal districts with indicated ages within the same 34-43-m.y.-age range as the volcanic rocks have been recognized (fig. 4). All four districts are tightly restricted within a timespan of 4 m.y. from 38 to 35 m.y. B.P., are alined along the northeast-trending arm of the volcanic arc of figure 3, and are superposed over the general area of highest concentration of Cretaceous(?) deposits (fig. 1).

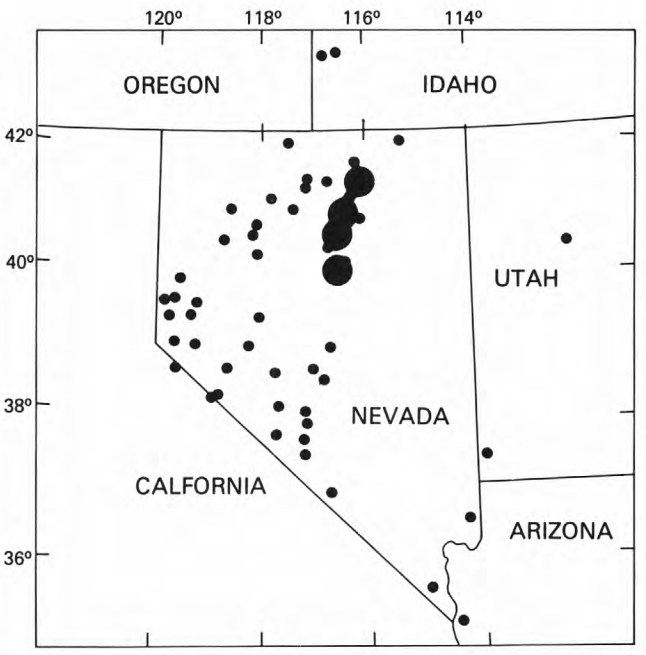

Figure 4. Nevada and parts of adjacent States, showing locations of gold-silver deposits with mineralization ages of 34 to 43 m.y. (large dots).

Trends from 34 to 17 m.y. B.P.

The volcanic evolution of southward-migrating east-west-trending belts that previous authors have emphasized, was most firmly established during

34–17 m.y. B.P. The southern limb of the arc of figure 3 advanced slightly westward, while its east end strengthened and rotated more rapidly southward than its west end. Contemporaneously, the moderately strong northern limb of the arc of figure 3 weakened as it advanced westward (fig. 5). Thus, a strong northwestward trend crudely parallel to the Walker Lane, emphasized by the previously cited authors, became most firmly evident. Rhyolitic ash-flow tuffs were the dominant volcanic rocks in southwestern Nevada and eastern California. Stewart and Carlson (1976, sheet 2) identified 11 definite calderas, 8 probable calderas, and 2 northwest-trending volcanotectonic depressions, the largest approximately 100 km long by 50 km wide. More calderas probably exist, especially in western and northeastern Nevada, where concealed calderas seem likely to account for the distribution of many ash-flow tuffs.

Six epithermal gold-silver districts were generated within this volcanic period, all of which formed within the timespan 25–17 m.y. B.P. (fig. 6), approximately parallel to the Walker Lane. These districts include the important Round Mountain, Tonopah, and Goldfield, Nev., districts, which as a group trend north-south. These ore districts are not restricted to any one volcanic type but occur mainly in areas of andesitic rocks, commonly with later rhyolite tuff. No recognized epithermal mineralization occurred in the volcanic time interval 34–25 m.y. B.P.

Trends from 17 to 6 m.y. B.P.

Most students of Great Basin volcanology consider that all the volcanic rocks erupted from 17 to 6 m.y. B.P. belong to a single broad volcanic period. The volcanic arc of figure 3 had expanded westward and southward during the time interval shown in figure 5, as described above, and then expanded farther to the west (fig. 7). Its southern limb weakened somewhat but remained dominantly rhyolitic. Andesite flows and breccia became dominant in the western part of the expanding arc. In the northern and northeastern limbs of the arc, basalt flows became a major volcanic component, in part in bimodal association with rhyolite flows, especially in northern Nevada and southern Idaho. Only 2 rhyolitic calderas were identified on the northeast limb of the arc, in contrast to 10 mapped and 2 probable calderas shown

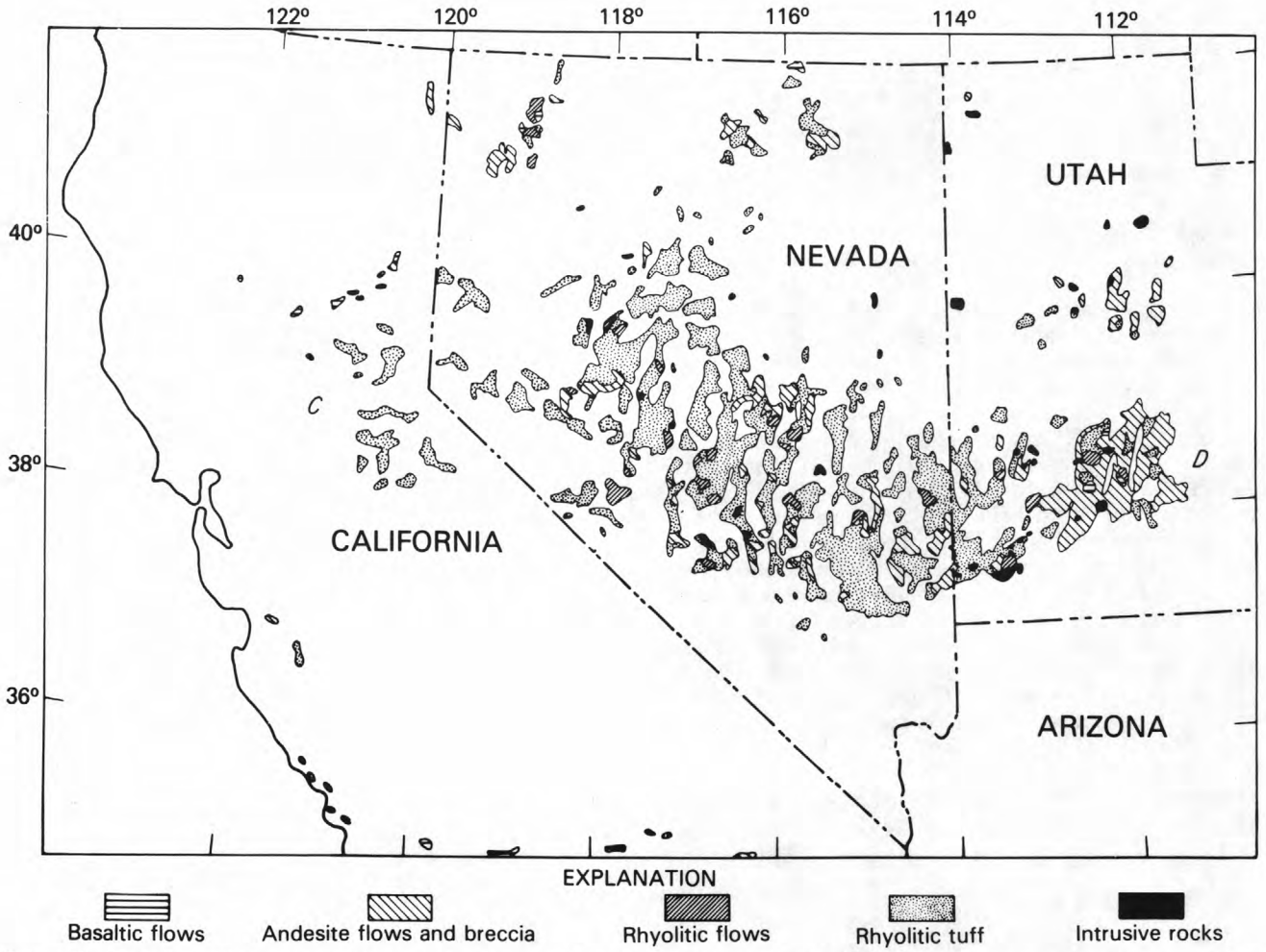

Figure 5. Nevada and parts of adjacent States, showing distribution of volcanic rocks that range in age from 17 to 34 m.y. (from Stewart and others, 1977, fig. 1B; see fig. 3 for key).

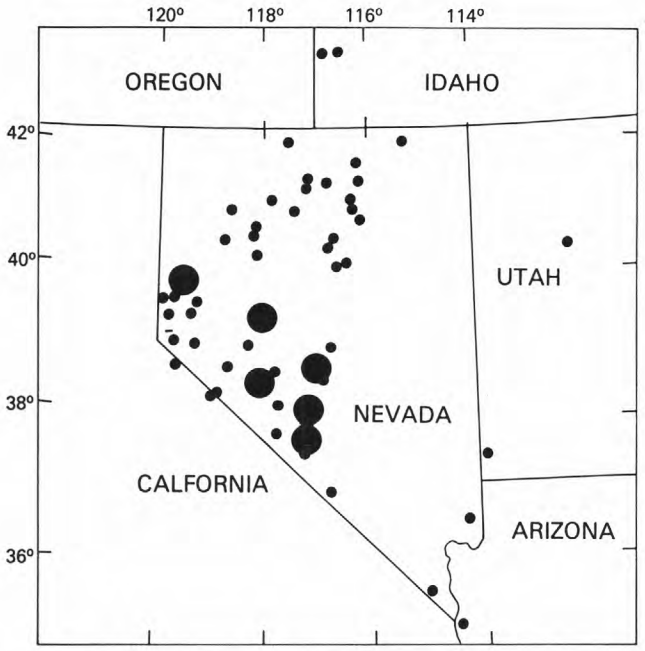

Figure 6. Nevada and parts of adjacent States, showing locations of gold-silver deposits with mineralization ages of 17 to 25 m.y. (large dots).

by Stewart and Carlson (1976, sheet 3) on the southern limb of the volcanic arc.

Although epithermal gold-silver deposits of the volcanic period 17-6 m.y. B.P. are also generally considered as a single group, the pattern of evolution suggests a significant change near 14 m.y. B.P. that justifies subdivision into an older and a younger group. The climax in ore deposition, as viewed by the number of dated ore districts, occurred within the short period 17-14 m.y. B.P. (fig. 8). A total of 15 districts from table 1 are included in this group, none of which are of first rank except, possibly, the Silver City-DeLamar district in southwestern Idaho. The Jarbidge, Manhattan, and National districts are the largest of the age group in Nevada. Seven districts of figure 8 occur within the general Walker Lane of southwestern Nevada, but a relatively distinct cluster of eight districts are in and near north-central Nevada, within the general region of mineralization shown in figures 1 and 3.

The later part of this volcanic period (approx 14-6 m.y. B.P.) was accompanied by a further evolution of the mineralization trends (fig. 9). The Walker Lane trend of ore deposits shifted a little farther southwestward to includes the major Comstock lode, as well as the Aurora and Bullfrog districts of Nevada and Bodie, Calif. Seven Troughs (13.7-14 m.y. old) can be viewed either as a westward extension of the cluster in figure 8 or as a continued but weakening northeastward extension from the apex of ore deposits in figure 9.

Trends from 6 m.y. B.P. to present

During the past 6 m.y., Nevada has been almost devoid of volcanism except for local basalt flows (fig. 10), andesite, and a few rhyolite domes near Steamboat Springs south of Reno. Long Valley caldera in California erupted rhyolite ash-flow tuff and, together with Mono Craters just to the north, extruded small rhyolitic domes (G, fig. 10). Figure 10 shows, however, that westward migration and expansion of volcanism are still continuing, though declining in intensity.

Epithermal ore deposits formed about 5 m.y. B.P. along the Walker Lane trend (Monitor, Calif., and Borealis and Silver Peak, Nev., fig. 11). Steamboat Springs (S, fig. 11), which has been active during the past 3 m.y. (Silberman and others, 1979), and Sulphur, Nev., (1.8-2.1 m.y. old, table 1), are the youngest representatives of the epithermal gold-silver group (White, 1981; White and Heropoulos, 1984). Continuing thermal activity in the resurgent dome of Long Valley caldera, Calif. (G, fig. 10), may also be generating an epithermal ore deposit, as suggested by the presence of Ag and Au in some hot-spring sinters, along with the commonly associated "volatile" elements As, Hg, Sb, and Tl (White and Heropoulos, 1983).

However, the existence of ore-grade Au and Ag in minable amounts (neglecting the problems of mining water-saturated rocks at high temperatures) has not been demonstrated for any active hot-spring system. Sulphur, Nev. (1.8-2.1 m.y. old), continues to exhale sulfur gases and may contain the size and grade of an economic ore deposit (A. B. Wallace, oral commun., 1981).

Although Steamboat Springs, Sulphur, and, possibly, Long Valley are examples of active generation of epithermal gold-silver deposits, this type of mineralization now seems to be declining in frequency and intensity in the Western United States, though possibly not in New Zealand, Kamchatka, and elsewhere.

ENIGMAS OF DISSEMINATED GOLD-SILVER DEPOSITS

In recent years, major attention has been focused on disseminated precious-metal ore deposits, generally minable for their dispersed fine-grained or "invisible" gold. Table 1 and the previous discussion suggest that the existence of at least two types of ore deposits may be causing at least part of the confusion. The younger deposits (less than 40 m.y. old) may be similar in origin, composition of ore fluids, hydrodynamics, tectonic environment, and near-surface generation to the classic "fossil" volcanic-hosted vein deposits, except for differences in physical characteristics of the host rocks. All of these younger deposits may be "volcanic centered" and owe their thermal energy and, probably, part of their mineral content and water to underlying volcanic sources. The distribution of volcanism and ore generation (figs. 3-11) shows convincingly that both of these phenomena are broadly related in space and time, but that ore generation is restricted to short time intervals requiring some special tectonic and other geologic conditions. Much more abundant data on the ages of these ore deposits may provide much new understanding of paleotectonics, for one example. A vein represents a fossil open channel that

was permeable to upward flow of mineralizing fluids. Although this channel was eventually filled with quartz and other "self-sealing" hydrothermal minerals (Keith and others, 1978), the strike of a widening vein was at that time either in the direction, or close to the direction, of minimum horizontal stress. Probably no method other than radiometric dating of K-bearing gangue minerals can provide changes in principal stress directions through a large area over millions of years.

A second type of disseminated deposit seems to differ greatly from the first in its reported ages (generally older than 70 m.y.) and in other characteristics. We have only fragmentary data on the tectonic settings, ages, temperatures of deposition, salinities, and other characteristics of the ore fluids of this group. For many years I assumed that the relative abundances of As, Sb, Hg, and Tl in high-temperature active hot-spring systems and some disseminated deposits (especially Carlin and Getchell) provided strong evidence for closely related origins. However, figure 1 and table 1 demonstrate that many disseminated deposits may be pre-Tertiary, their fluid-inclusion salinities distinctly higher (if Gold Acres and Rochester, Nev., are typical), and their temperatures generally lower than those of many vein deposits and some active hot-spring systems. If their reported age differences are real, the tectonic and volcanic environments of these deposits probably differed also.

Until more reliable data on these older(?) disseminated deposits are available, we should be careful in reaching any firm conclusions on a common origin. My present tendency is to suggest that the older sediment-hosted deposits were saturated by "evolved connate" waters (White, 1981), possibly convectively circulating below a low-permeability barrier that became less permeable over time because of self-sealing. These systems could have been geopressured, with fluids dispersing into surrounding pore water, losing heat by conduction but with little or no venting of fluids directly to the surface, or mixing with meteoric waters.

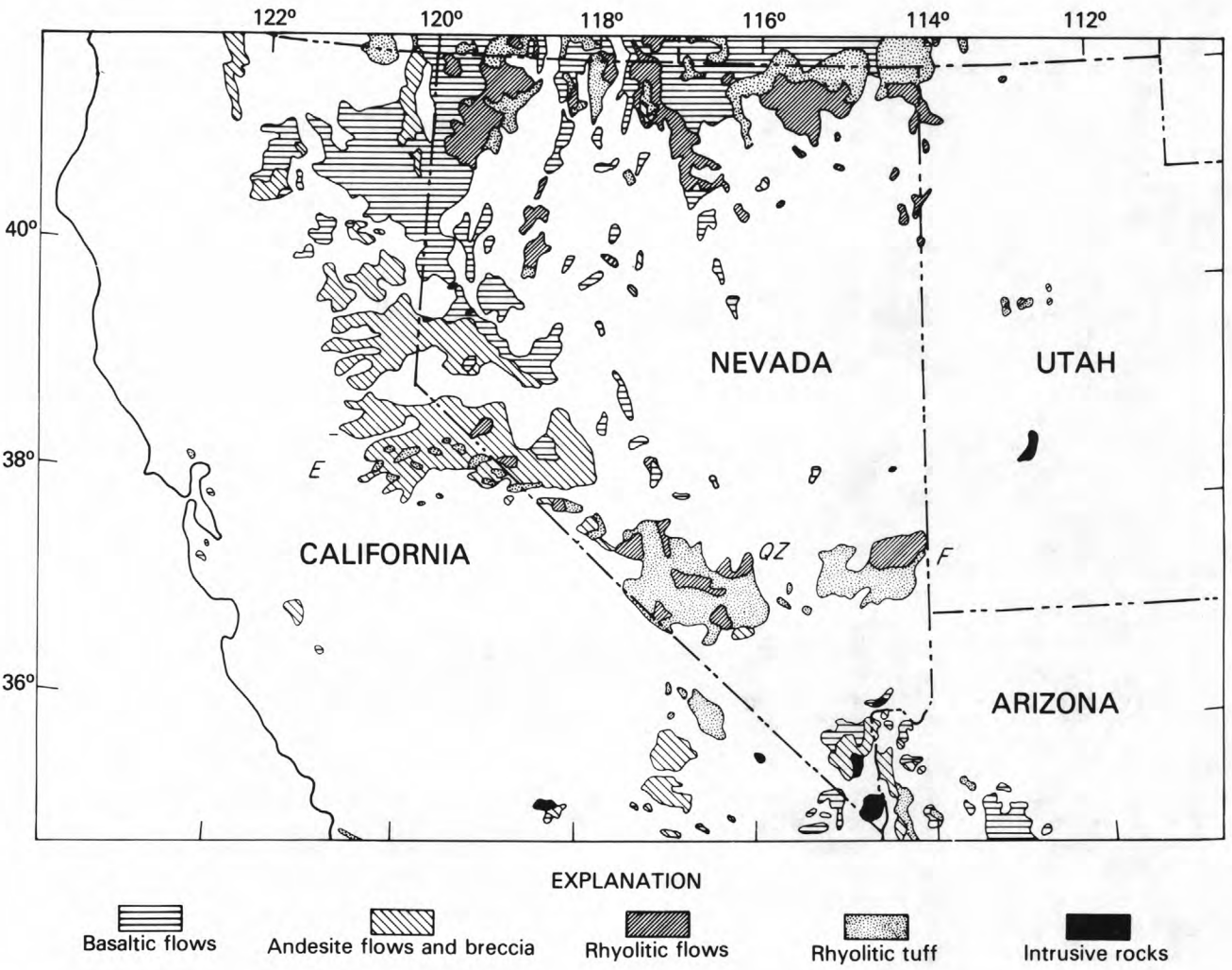

Figure 7. Nevada and parts of adjacent States, showing distribution from volcanic rocks that range in age from 6 to 17 m.y. (from Stewart and others, 1977, fig. 1C).

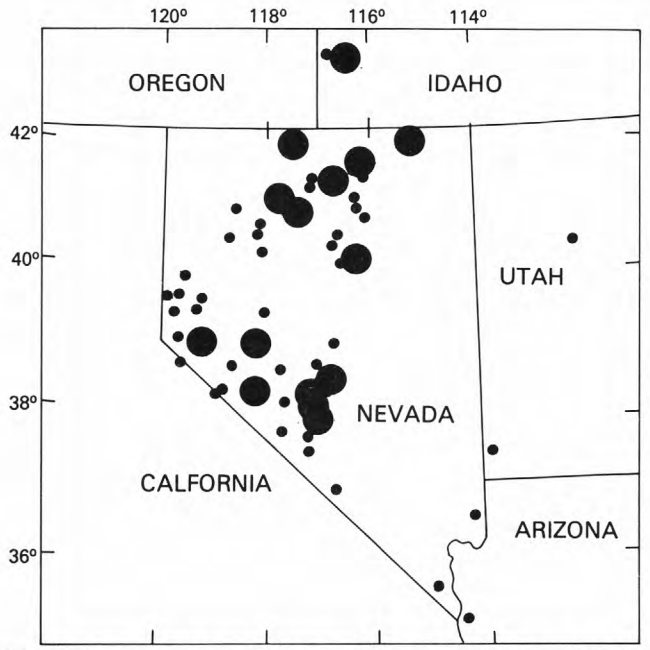

Figure 8. Nevada and parts of adjacent States, showing locations of gold-silver deposits with mineralization ages of 14 to 17 m.y. (large dots).

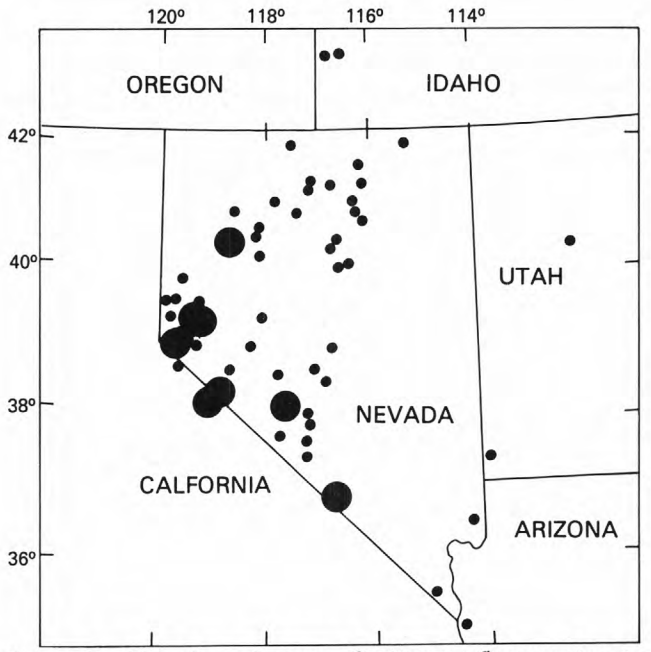

Figure 9. Nevada and parts of adjacent States, showing locations of gold-silver deposits that range in age from 6 to about 14 m.y. (large dots).

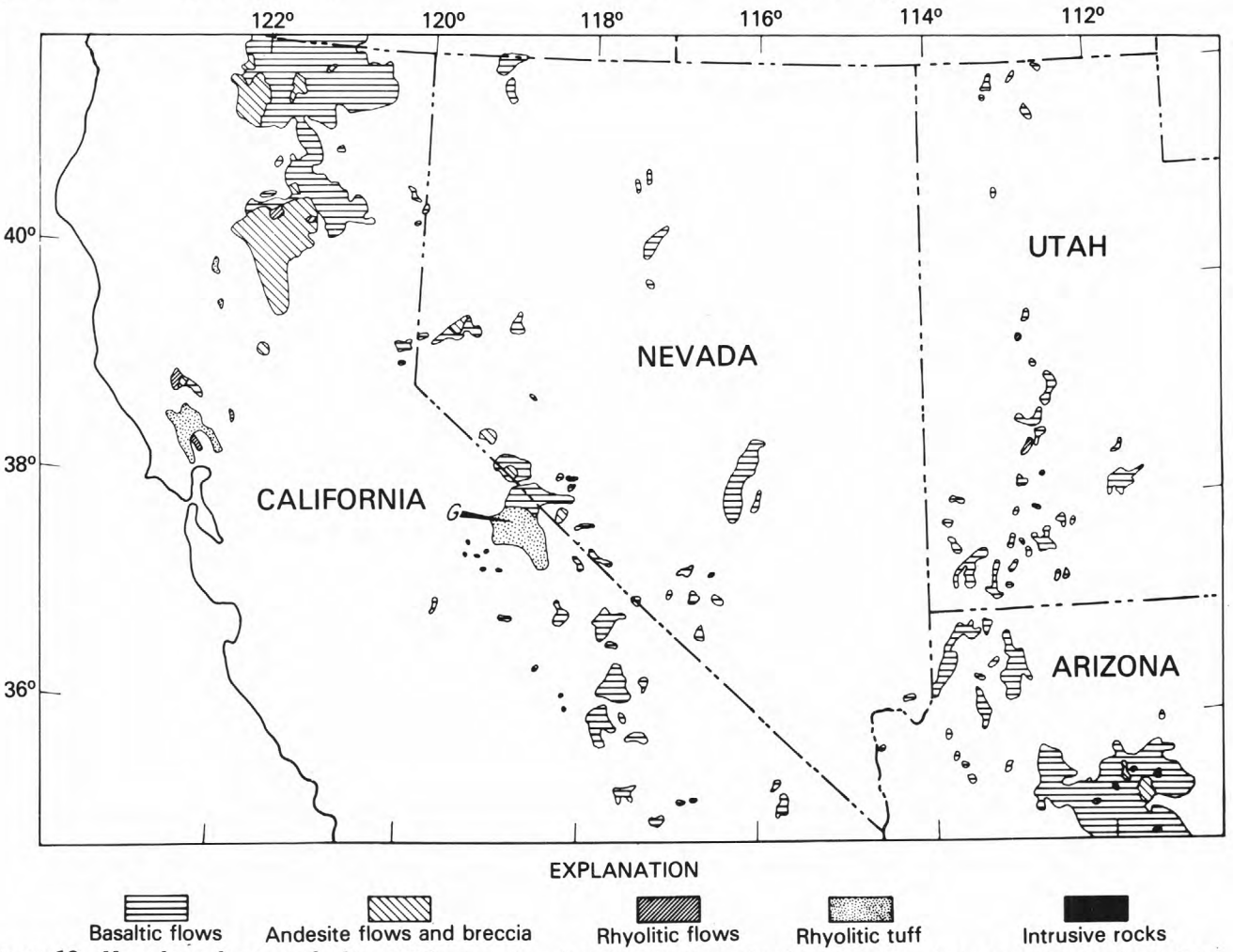

Figure 10. Nevada and parts of adjacent States, showing distribution of volcanic rocks that range in age from 0 to 6 m.y. (from Stewart and others, 1977, fig. 1D).

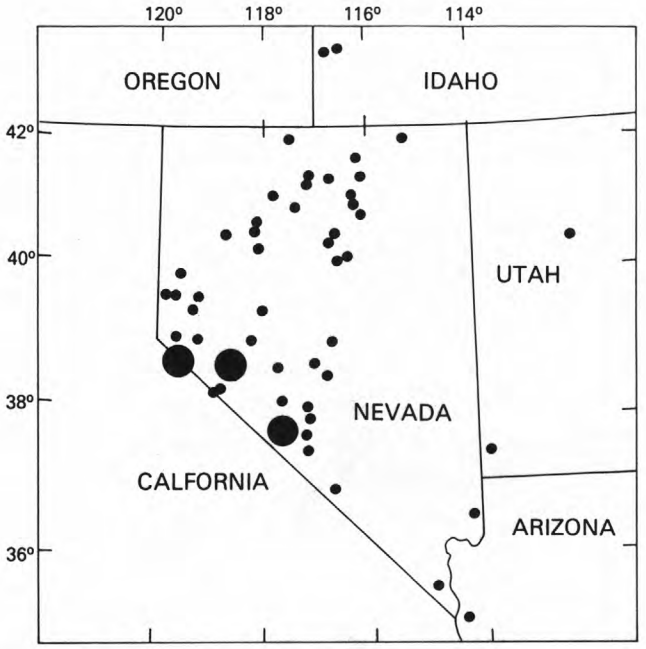

Figure 11. Nevada and parts of adjacent States, showing locations of gold-silver deposits with mineralization ages of 0 to 6 m.y. (large dots). Steamboat Springs (S) is the only active system, but Sulphur (Su) has feeble discharges of warm gases.

REFERENCES CITED

Bonham, H. F., Jr., 1976, Gold producing districts of Nevada (2d ed.): Nevada Bureau of Mines Geologic Map 32, scale 1:1,000,000.

----- 1980, Silver producing districts of Nevada (2d ed.): Nevada Bureau of Mines Geologic Map 33, scale 1:1,000,000.

----- 1982, Reserves, host rocks, and ages of bulk-minable precious metal deposits in Nevada: Nevada Bureau of Mines and Geology Open-File Report 81-1 and Preliminary Report 82-9, 4 p.

Brook, C. A., Mariner, R. H., Mabey, D. R., Swanson, Jr., Guffanti, Marianne, and Muffler, L. J. P., 1979, Hydrothermal convection systems with reservoir temperatures ≥ 90°C, in Muffler, L. J. P., ed., Assessment of geothermal resources of the United States—1978: U.S. Geological Survey Circular 790, p. 18-85.

Buchanan, L. J., 1981, Precious metal deposits associated with volcanic environments in the Southwest, in Dickinson, W. R., and Payne, W. D., eds., Relations of tectonics to ore deposits in the Southern Cordillera: Arizona Geological Society Digest, v. 14, p. 237-262.

Garside, L. J., and Schilling, J. H., 1979, Thermal waters of Nevada: Nevada Bureau of Mines Geology Bulletin 91, 163 p.

Keith, T. E. C., White, D. E., and Beeson, M. H., 1978, Hydrothermal alteration and self-sealing in Y-7 and Y-8 drill holes in northern part of Upper Geyser Basin, Yellowstone Park, Wyoming: U.S. Geological Survey Professional Paper 1054-A, p. A1-A26.

Lindgren, Waldemar, 1933, Mineral deposits (4th ed.): New York, McGraw-Hill, 930 p.

Nash, J. T., 1972, Fluid inclusion studies of some gold deposits in Nevada; in Geological Survey research, 1972: U.S. Geological Survey Professional Paper 800-C, p. C15-C19.

Nolan, T. B., 1933, Epithermal precious-metal deposits, in Ore deposits of the western states (Lindgren volume): New York, American Institute Mining Metallurgical Engineers, p. 623-640.

Pansze, A. J., Jr., 1975, Geology and ore deposits of the Silver City-De Lamar-Flint region, Owyhee County, Idaho: Idaho Bureau of Mines and Geology Pamphlet 161, 79 p.

Silberman, M. L., 1984, Geochronology of hydrothermal alteration and mineralization, in Geothermal Resources Council Conference on Energy and Mineral Resources of the Northern Great Basin, Reno, Nev., 1983. Proceedings [in press].

Silberman, M. L., and McKee, E. H., 1974, Ages of Tertiary volcanic rocks and hydrothermal precious-metal deposits in central and western Nevada, in Guidebook to the geology of four Tertiary volcanic centers in central Nevada: Nevada Bureau of Mines Report 19, p. 67-72.

Silberman, M. L., Stewart, J. H., and McKee, E. H., 1976, Igneous activity, tectonics, and hydrothermal precious-metal mineralization in the Great Basin during Cenozoic time: Society of Mining Engineers Transactions, v. 260, no. 3, p. 253-263.

Silberman, M. L., White, D. E., Keith, T. E. C., and Dockter, R. D., 1979, Duration of hydrothermal activity at Steamboat Springs, Nevada, from ages of spatially associated volcanic rocks: U.S. Geological Survey Professional Paper 458-D, p. D1-D14.

Stewart, J. H., and Carlson, J. E., 1976, Cenozoic rocks of Nevada: Nevada Bureau of Mines and Geology Map 52, scale 1:1,000,000.

Stewart, J. H., Moore, W. J., and Zietz, Isidore, 1977, East-west patterns of Cenozoic rocks, aeromagnetic anomalies, and mineral deposits, Nevada and Utah: Geological Society of America Bulletin, v. 88, no. 1, p. 67-77.

Vikre, P. G., 1981, Silver mineralization of the Rochester district, Pershing County, Nevada: Economic Geology, v. 76, no. 3, p. 580-609.

White, D. E., 1981, Active geothermal systems and hydrothermal ore deposits, in Economic Geology, 75th anniversary volume, p. 392-423.

White, D. E., and Heropoulos, Chris, 1983, Active and fossil hydrothermal convection systems of the Great Basin, in Geothermal Resources Council Conference on Energy and Mineral Resources of the Northern Great Basin, Reno, Nev., 1983, Proceedings.

Silica Minerals as Indicators of Conditions During Gold Deposition

By Robert O. Fournier

CONTENTS

INTRODUCTION

Silica minerals commonly found in association with gold include amorphous silica, poorly crystalline cristobalite, opal-CT, chalcedony, and quartz. Poorly crystalline cristobalite shows broad X-ray-diffraction peaks centered at about 0.41 and 0.25 nm. Opal-CT shows these same X-ray peaks, as well as an additional low-tridymite peak at about 0.43 nm (Jones and Segnit, 1971). Fournier (1973) and, apparently, Schoen and White (1965) used the term "β-cristobalite" both for poorly crystalline cristobalite and for opal-CT.

Figure 12 plots the solubilities of various silica minerals in water at the vapor pressures of the solutions. At temperatures from about 100° to 300°C, the solubilities of these silica minerals are not greatly affected by pressure and most added salts (Fournier, 1983; Fournier and Marshall, 1983). Quartz is the stable form of silica under the pressure-temperature conditions in most hydrothermal systems. For other forms of silica to deposit, the mineralizing solution must become supersaturated with respect to quartz. The various mechanisms by which a silica solution becomes supersaturated may also affect the ability of the solution to transport gold. This chapter attempts to show that the presence of specific silica minerals, in association with gold, may be useful for interpreting the conditions at the time of gold deposition.

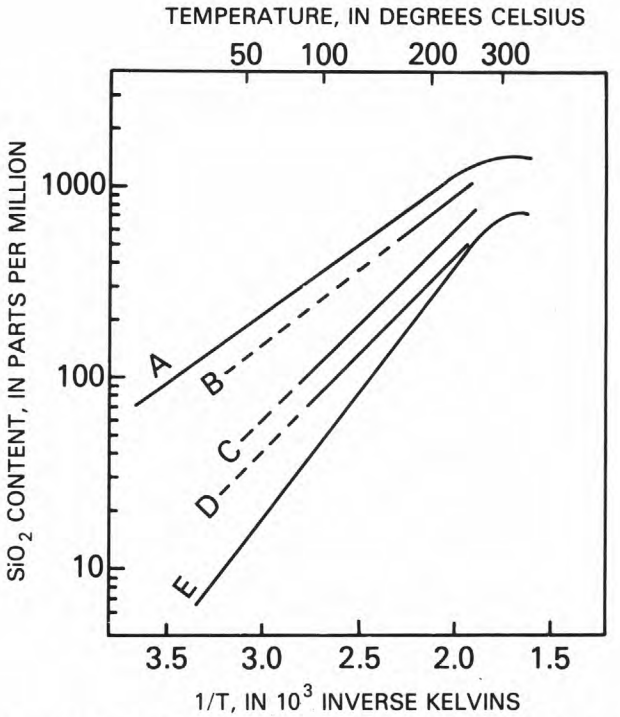

Figure 12. Solubilities of various silica phases in water at the vapor pressure of the solution. A, amorphous silica; B, opal-CT (labeled "β-cristobalite" by Fournier, 1973), C, α-cristobalite; D, chalcedony; E, quartz (from Fournier, 1973, fig. 2).

TRANSPORT AND DEPOSITION OF GOLD IN HYDROTHERMAL SOLUTIONS

I present here a brief discussion of the chemical and physical processes favoring gold transport and deposition in comparison with those that favor transport and deposition of silica minerals. Detailed discussions of the geochemistry of gold relative to disseminated deposits are presented elsewhere in this volume (see Cunningham, this volume; Rye, this volume; Rytuba, this volume).

Because the ore grade required to make a gold mine profitable is very low (presently about 1 mg Au per kilogram of rock), economically exploitable gold deposits are likely to form in more diverse ways than those for metals that require relatively large concentrations for ore grade. Although gold commonly appears to have been coprecipitated with sulfide minerals, the presence of sulfur (as sulfide or other species) is not essential for gold transport or deposition. According to current thought, however, the presence of base metals implies transport in chloride-rich solutions, which are not essential for the transport of gold. The concentrations of gold in the hydrothermal solutions responsible for ore deposition may be very low. Nonetheless, the higher the concentration of dissolved gold, the easier it is to account for the formation of a hydrothermal ore deposit, because only small amounts of transporting fluid are required.

In oxidizing, near-surface environments, the mobility of gold may be affected by complexing with Cl^-, Br^-, $S_2O_3^{2-}$, SCN^-, CN^-, organic materials, and colloids (Goñi and others, 1967; Lakin and others, 1974). Complexes with S_x^{2-} and NH_3 are found in moderately reducing solutions (Skibsted and Bjerrum, 1974). Apparently, chloride and sulfide complexes (Henley, 1973; Seward, 1973) are dominant in most hydrothermal solutions, although, according to Barnes (1979), other complexes with Te, Se, Bi, Sb, and (or) As probably are locally significant. Gold-chloride complexes are important under low-pH oxidizing conditions and high chloride activity (Henley, 1973). Gold-bisulfide complexes are important in near-neutral to slightly alkaline reducing solutions, particularly under conditions where HS^-, S, and SO_4^{2-} coexist (S. B. Romberger, oral commun., 1981). Romberger (1982) summarized the conditions favoring gold deposition as follows: "* * * If gold were transported as chloride complexes, deposition occurs with increased pH, reduction, dilution and/or cooling," and "* * * if gold were transported as bisulfide complexes, oxidation, dilution, pH changes, and/or precipitation of base metal sulfides result in gold deposition." Gold deposition is particularly likely to occur where ascending solutions boil as a result of decreasing hydrostatic pressure, because there is a simultaneous loss of dissolved sulfide, decrease in temperature, and change in pH as volatile constituents, such as H_2S and CO_2, partition into the evolving gas (mostly steam) phase.

I show below that boiling, cooling, dilution, and pH changes may also cause deposition of silica minerals. Oxidation and reduction reactions, however, are unlikely to cause silica to precipitate. Therefore, gold deposition without accompanying silica deposition is likely to occur as a result of oxidation or reduction, with little or no change in the temperature of the solution.

In addition to the chemical factors that favor transport and deposition of gold in hydrothermal solutions, the mechanisms by which hydrothermal solutions might become either acidic and rich in chloride, or near-neutral and rich in sulfide (with or without sulfide), should be studied. Most deeply circulating thermal waters attain moderate to high concentrations of chloride by leaching it from rocks, particularly sedimentary and silicic volcanic rocks (Ellis and Mahon, 1964, 1967, 1977). The attainment and persistence of near-neutrality in hydrothermal solutions are easy to explain on the basis of water-rock reactions. For hydrolysis reactions involving feldspars, pH values are generally between 5 and 7; lower pH values occur in waters with higher salinity (Hemley, 1959; Hemley and others, 1961; Hemley and Jones, 1964). The persistence of high acidity (pH<4) in a hydrothermal solution as it flows underground requires special, but not unreasonable, circumstances. At very high temperatures, the acidic components are mostly associated and unreactive (Helgeson, 1969). As hydrothermal solutions cool, these acidic components dissociate and react vigorously with feldspars and micas. High acidity can be maintained only in nonreactive rocks, such as quartzite and altered rocks that previously have had most of their cations leached, and in fractures that have a protective coating of quartz or other minerals on the walls that prevents ionic diffusion and reaction of the acidic solution with the surrounding rock. Fournier and Truesdell (1970), who studied hot-spring and well waters in Yellowstone National Park, Wyo., reported that when there is no indication of precipitation of silica from a thermal water during ascent from an underground reservoir, there generally is evidence of exchange of cations between the solution and the wallrock during upward flow. The reverse is true where significant amounts of silica precipitate from an ascending thermal water: Little or no cation exchange occurs.

Until very recently, drilling for production of geothermal energy in active hydrothermal systems had encountered extremely acidic conditions at depth at only a few localities in zones of active volcanism, such as Matsao in Taiwan (Chen, 1970, 1975), and Onikobe (Yamada, 1976) and Matsukawa (Nakamura and others, 1970) in Japan. At Matsao and Onikobe, acid-chloride waters with pH less than 2 were found at depths greater than 1,000 m at temperatures exceeding 275°C. The reservoir at Matsao is in quartzite, and at Onikobe a deep reservoir is in andesite altered to pyrophyllite and quartz. It now appears that deep acid-chloride thermal water and (or) deep acidic alteration (pyrophyllite+quartz) is present in many active hydrothermal systems associated with active or relatively young andesitic volcanism. These systems include Biliran (Lawless and Gonzalez, 1982), Nasuji-Sogonon (Seastres, 1982), Palimpinon (Leach and Bogie, 1982), and Baslay-Dauin (Harper and Arevalo, 1982) in the Philippines, and Suretimeat (Heming and others, 1982) in the New Hebrides. In these systems, much of the acidity may come from magmatic gases, including SO_2, H_2S, and HCl.

An acidic hydrothermal solution can be generated in various ways, including interaction of the gases evolved from a crystallizing magma at depth with ground water, hydrolysis of salts or sulfur at high temperature and relatively low pressure, and mixing of alkaline-chloride waters with acid-sulfate waters that form near the Earth's surface and then infiltrate deep underground. Mechanisms of ore deposition involving magmatic emanations have had many advocates over the years and need no further comment here.

HCl may be generated by hydrolysis of NaCl at moderate to high temperatures and low pressures:

$$NaCl+H_2O = NaOH+HCl. \quad (1)$$

Many investigators have found HCl in condensate after circulating dry steam over solid NaCl (Briner and Roth, 1948; Martynova and Samoilov, 1957; Galobardes and others, 1981). In experiments at 600°C, I found that significant amounts of HCl are generated by reaction 1 at pressures below about 35 MPa, and even more at lower pressures. Addition of quartz to the system greatly increases the yield of HCl because NaOH is removed from the solution by reaction with quartz, with precipitated sodium silicates as products. In natural systems, where aluminum is available in micas, clays, plagioclase, and other minerals, albitization is likely to result from the hydrolysis of NaCl. At high temperatures, the HCl that is generated by this process will be highly associated and relatively unreactive. Acidic alteration will occur when water or steam carrying this HCl moves to cooler parts of the hydrothermal system, especially where the steam condenses.

Relatively oxidized, sulfur-rich gases will be evolved where gypsum or anhydrite are involved in hydrolysis reactions. For example, the 1982 eruption of El Chichón Volcano in Mexico contributed far more sulfuric acid to the atmosphere and stratosphere than is common for comparable-size eruptions of other volcanoes, such as Mount St. Helens (O. B. Toon, oral commun., 1982). Gypsum beds occur in the sedimentary section beneath El Chichón but are absent beneath Mount St. Helens. When gypsum (or anhydrite) and halite both are involved in hydrolysis reactions, the resulting relatively oxidized solutions should be ideal for transporting gold as a chloride complex.

Ellis (1977, 1979) attributed the deep acidity found in exploration wells drilled for geothermal energy at Matsao on Taiwan to the reaction of water with deeply buried native-sulfur deposits, producing sulfuric acid and hydrogen sulfide:

$$4S+4H_2O=3H_2S+H_2SO_4. \quad (2)$$

Where the sulfuric acid produced by reaction 2 is neutralized by reaction with the surrounding rock, the resulting solution should be capable of transporting significant gold as a bisulfide complex.

In some places, deep acidity may result from downward movement of water that has become acidic at and near the water table (Ellis and Mahon, 1977; Henley and Ellis, 1983). In the Norris Geyser Basin area of Yellowstone National Park, acidic waters are generated high on a hillside where H_2S is oxidized to sulfate and native sulfur. Some of this water appears to percolate hundreds of meters underground, where it mixes with high-temperature (approx 270°C) neutral water rich in chloride. The resulting "acid-chloride-sulfate" waters, which issue as hot springs and geysers, have been extensively analyzed (Gooch and Whitfield, 1888; Allen and Day, 1935; Rowe and others, 1973). The remarkably constant compositions of some of these springs since they were first analyzed in the late 1880's indicate a large and probably deep reservoir of mixed water.

Solutions that result from mixing of oxidized, acid-sulfate water and alkaline-chloride waters should be capable of transporting gold at high temperatures as a chloride complex. Some of the acid-sulfate surface waters may dissolve considerable native sulfur and carry that constituent underground along with sulfate. By reaction 2 and subsequent water-rock reactions, such a solution might become capable of transporting significant gold as a bisulfide complex, as previously discussed.

BEHAVIOR OF DISSOLVED SILICA IN HYDROTHERMAL SYSTEMS

Iler (1979) presented a comprehensive review of the behavior of silica in water. Much is known about the behavior of dissolved silica in active hydrothermal systems as a result of observations of hot-spring systems and extensive drilling for geothermal resources (White and others, 1956; Mahon, 1966; Fournier, 1973). In long-lived presently active systems, the solubility of quartz has been found to control dissolved-silica concentration in all geothermal-reservoir waters at temperatures greater than about 180°C and in most reservoir waters above about 140°C—in many, above 90°C. Chalcedony has a slightly higher solubility than quartz and commonly controls dissolved-silica concentration at temperatures below 90°-140°C, in some cases as high as 180°C. Under special conditions for short periods, however, cristobalite or volcanic glass may control dissolved-silica concentration, even at very high temperatures. Such special conditions include active faulting, hydrothermal explosions, and "short circuiting" by drilling that allows hot water to come into contact with glass- or cristobalite-rich rock which previously has not been in contact with circulating hot water. When two or more different silica minerals are in contact with a given solution, the most soluble silica phase will generally control dissolved-silica concentration until that phase completely dissolves, is converted to another, more stable phase, or is taken out of contact with the circulating water by formation of intervening alteration products or precipitates.

On the basis of results of experimental studies (Rimstidt and Barnes, 1980) and personal observations of the behavior of silica in hot-spring systems, it appears that slow cooling of a hydrothermal solution generally will result in the deposition of quartz if initial temperatures are above about 200°C. Rapid cooling allows supersaturated silica solutions to form, particularly when the cooling is adiabatic (through boiling in response to lower pressure and without transfer of heat to the wallrock). Supersaturated silica solutions may also evolve where hot water dissolves glass-bearing rocks, where rocks are altered by highly acidic solutions without simultaneous deposition of quartz, and where sudden decreases in fluid pressure occur at high temperature. High alkalinity (high pH) greatly increases the solubility of quartz (Seward, 1974; Fleming and Crerar, 1982), and neutralization of an alkaline solution could lead to the precipitation of amorphous silica. However, this mechanism is generally unimportant in most natural hydrothermal systems with high cation contents because silicate-hydrolysis

reactions, such as those investigated by Hemley (1959), buffer pH values under near-neutral or slightly acidic conditions. High alkalinity might be a factor locally for relatively short periods where boiling allows rapid loss of CO_2, or where a solution comes in contact with silica-deficient rocks (such as peridotite or nepheline syenite) which contain mineral suites that are ineffective in buffering the pH at relatively low values.

Recent experiments in which amorphous silica was precipitated from hydrothermal solutions have been reported by many investigators, including Rothbaum and Rohde (1979), Rothbaum and others (1979), Bohlmann and others (1980), Crerar and others (1981), and Weres and others (1982). Most of these investigations were undertaken to find ways to prevent silica-scale formation during production of geothermal resources. Silica solubilities in water under hydrothermal conditions were determined by Fournier and Rowe (1977) and Chen and Marshall (1982). Large degrees of silica supersaturation with respect to quartz are required for amorphous silica to precipitate (fig. 12). Amorphous silica at 100°C has the same solubility in pure water as does quartz at about 225°C. A dilute solution in equilibrium with quartz at a reservoir temperature of 210°C will yield a solution just saturated with respect to amorphous silica at 100°C, if it rises fast enough for adiabatic cooling to occur and silica does not precipitate during that ascent (fig. 13). Voluminous deposits of siliceous sinter generally

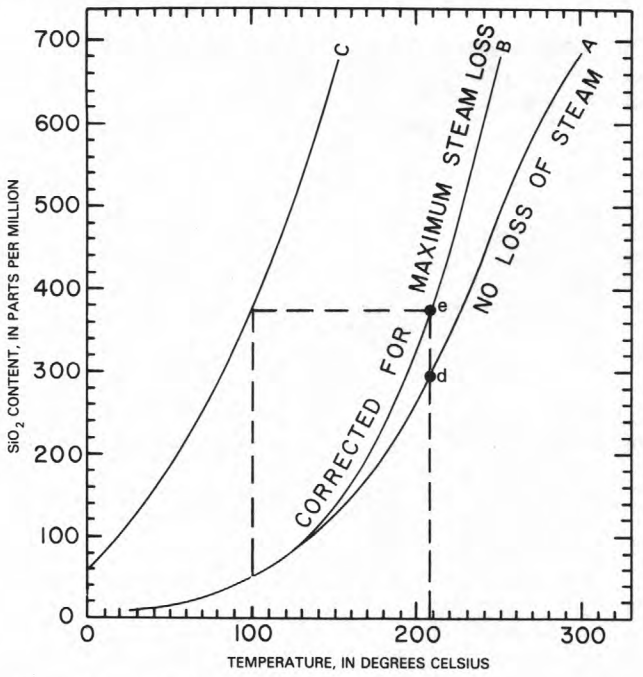

Figure 13. Solubilities of amorphous silica (curve C) and quartz (curve A) at the vapor pressures of the solutions. Curve B illustrates the dissolved-silica concentration after adiabatic cooling (boiling) to 100°C, as a function of the initial temperature of the solution before boiling. d, initial concentration of dissolved silica in equilibrium with quartz at 210°C; e, concentration of dissolved silica after adiabatic cooling of the solution from 210° to 100°C.

indicate deposition from neutral to slightly alkaline (resulting from loss of CO_2 as the waters approach the surface), chloride-rich waters that flowed quickly to the surface from reservoirs with temperatures in the range 200°-270°C. Waters flowing from reservoirs with lower temperatures contain so little silica that amorphous silica can deposit only after the solution cools to well below 100°C (fig. 13); the sinters that form from these waters are generally thin and restricted in area. Sinter deposits do not form where waters flow from reservoirs with temperatures below about 150°C. In contrast, waters flowing from reservoirs with temperatures above about 270°C contain so much dissolved silica that significant amounts precipitate in the channelways leading to the surface, and so hot-spring activity stops before large sinter deposits can develop. Self-sealing of active geothermal systems was discussed by Bodvarsson (1964), Facca and Tonani (1967), White and others (1971), Coplen and others (1973), and Grindley and Browne (1976). Very little silica precipitates from waters with pH below about 4 because high acidity inhibits the precipitation of silica (Kamiya and others, 1974; Rothbaum and others, 1979; Weres and others, 1982).

In some presently active hydrothermal systems, such as Broadlands, New Zealand, quartz appears to precipitate at the interface where relatively saline hot water from deep in the system mixes with overlying less saline colder water (W. A. J. Mahon, oral commun., 1982). Mixing of waters with different initial temperatures generally results in solutions that are supersaturated in silica with respect to the solubility of quartz, as shown by an enthalpy-silica diagram (fig. 14). In enthalpy-concentration diagrams, if heat-of-mixing effects are negligible, the solutions that result from mixing of cold and hot components lie along approximately straight lines joining the end members (Fournier, 1979), such as line A-C in figure 14. Cold ground waters commonly have dissolved-silica concentrations ranging from 10 to 50 ppm. If the solution after mixing has a relatively high enthalpy (high temperature), such as at point D in figure 14, quartz is likely to precipitate. Note that even when two hot waters mix, each in equilibrium with quartz at different temperatures, the resulting solutions may be supersaturated with respect to quartz (segment E-C, fig. 14). However, mixing of some thermal waters, such as at points E and G, may give either supersaturated (segment E-F) or undersaturated (segment F-G) silica solutions, depending on the proportion of the two waters in the mixture. Some amethystine quartz may form as a result of mixing of oxygen-rich relatively cold water coming from shallow regions with hot water from deeper in the system. The color of amethyst is probably due to a relatively high content of ferric iron, indicative of oxidizing conditions (Frondel, 1962).

Slight silica supersaturation with respect to quartz is required for chalcedony to precipitate directly from solution. Chalcedony might precipitate directly from some mixed waters at the appropriate temperatures. If the temperature of the solution after mixing is below 100°C, such as at point B in figure 14, it is likely that little, if any, silica will deposit as a result of the mixing. This conclusion is based on the observation that the silica-mixing model of Truesdell and Fournier (1977)

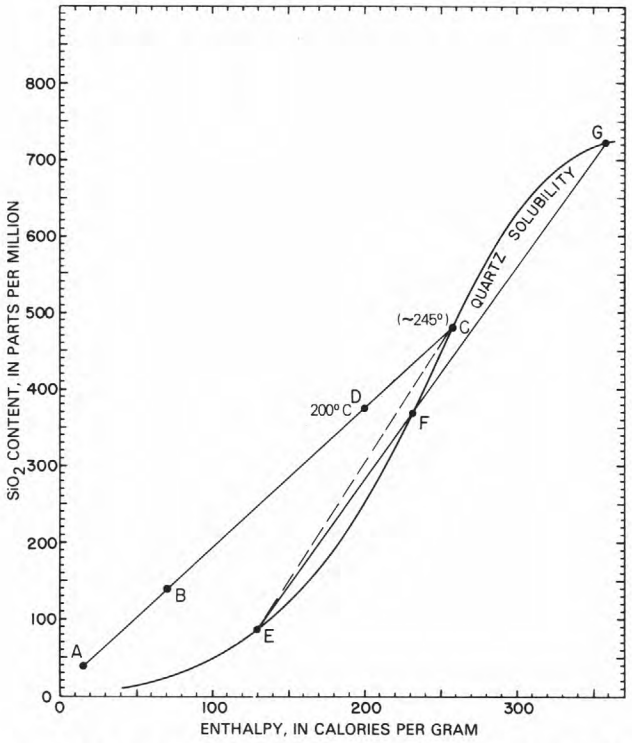

Figure 14. Solubility of quartz as a function of enthalpy at the vapor pressure of the solution. Lines A-C, E-C, and E-G illustrate enthalpy-silica relations in solutions that result from mixing various proportions of hot and cold waters.

works very well when applied to many hot-spring waters with large rates of flow and temperatures below 100°C.

It was noted above that the solubility of glass can control dissolved-silica concentration at high temperatures for short periods where new fractures bring hot water into contact with previously unaltered rock. Laboratory experiments under hydrothermal conditions show that volcanic glass contributes silica to solution to about the same extent as does pure amorphous silica (Dickson and Potter, 1982). In the absence of rapid precipitation of quartz, chalcedony, or cristobalite, any cooling of a solution that has reacted extensively with volcanic glass could result in the precipitation of amorphous silica. The first stage in the precipitation process is likely to be polymerization of the dissolved silica, with formation of colloidal and gelatinous particles that can be swept along in a moving fluid.

Reaction of hot water with previously unaltered glass-rich volcanic rock may explain the exceedingly high dissolved-silica concentrations measured in one vigorously discharging, boiling hot spring in Yellowstone National Park that is presently depositing gold-bearing sinter. That spring first appeared on a hillside in a grove of pine trees near Gibbon Meadows shortly after the M=7.1 Hebgen Lake earthquake in 1959. The size and distribution of these trees indicate that the ground where the spring appeared was not hot before the earthquake. When I first observed and sampled this hot spring, it was discharging more than 300 L/min; the water was fountaining as much as a meter above the vent, and it appeared opalescent owing to dispersed colloidal silica. The deposition of siliceous sinter around the edge of the pool and along the channels where the water overflowed down the hillside was especially rapid where the water came in contact with organic material. One sample of this sinter was analyzed for gold by neutron activation; it contained 0.8 ppm Au. In this water, the gold could have precipitated from an ascending boiling solution at depth while that solution was still at a comparatively high temperature. The precipitated gold could have been incorporated within colloidal-silica particles that also were forming at depth, and then transported to the surface along with that silica.

Amorphous silica is relatively unstable and transforms to poorly crystalline cristobalite or opal-CT, which, in turn, recrystallizes to chalcedony or quartz. These transformations have been studied in the field and experimentally by many investigators (White and others, 1956; Carr and Fyfe, 1958; Fyfe and McKay, 1962; Heydemann, 1964; Ernst and Calvert, 1969; Mizutani, 1970; Murata and Nakata, 1974; Murata and Larson, 1975; Murata and Randall, 1975; Kastner and others, 1977; Hein and Scholl, 1978; Keith and Muffler, 1978; Kano and Taguchi, 1982). Time, high temperature, high pH, high salinity, and the presence of dissolved Mg have all been found to favor the transformation of amorphous silica to poorly crystalline cristobalite or opal-CT and then to quartz (or chalcedony). In a few places in some hot-spring systems, α-cristobalite appears to have precipitated directly from solution (T. E. C. Keith, written commun., 1982), and tridymite crystals have been found apparently growing in some sinter deposits (Sato, 1962).

Recently deposited hot-spring siliceous sinters have been found to be composed predominantly of amorphous material. Sinters a few thousand years old generally appear opaline, especially if buried by younger deposits, and show either a poorly crystalline cristobalite or opal-CT X-ray pattern. According to T. E. C. Keith (written commun., 1982), many X-ray-diffraction patterns of older sinters from Yellowstone National Park indicate poorly crystalline cristobalite, without the low-tridymite peak that is characteristic of opal-CT. In contrast, the silica phase left as a residue in acid-altered and -leached environments in Yellowstone National Park generally exhibits a broad 0.43-nm tridymite X-ray-diffraction peak in addition to broad cristobalite peaks.

Many sinters tens of thousands of years old are chalcedonic, especially if buried and exposed to higher temperatures than those generally prevalent at the Earth's surface. The morphologic features exhibited by some chalcedonic materials, such as dehydration cracks, slump structures, and thicker silica deposits on the bottoms than on the sides and tops of cavities (gravitational settling of amorphous-silica particles), indicate that amorphous silica was present initially. In the absence of such features, the mechanism of formation of a given chalcedony is doubtful. Chalcedonies range in composition from about 90 to 99 weight percent SiO_2; the rest is H_2O and various impurities, particularly Fe_2O_3 and Al_2O_3 (Frondel, 1962). It is not known whether the trace-element contents of primary chalcedonies differ from those

formed by transformation of amorphous silica. Elements that can substitute for silica in tetrahedral coordination with oxygen, such as Ge, Ga, B, Fe, Ti, and Al, are found in opaline sinters (White and others, 1964; Ichikuni, 1968; Ichikuni and Kobayashi, 1969; J. J. Rowe, oral commun., 1978). These elements might be more abundant in chalcedony that formed by transformation of amorphous silica than in directly precipitated chalcedony. It is important to know whether the chalcedony formed as a primary precipitate or by transformation of amorphous silica because of the implications about conditions required to precipitate one or the other.

Where quartz precipitates in open spaces directly from hydrothermal solutions, it exhibits crystal faces. Where these crystal faces are obliterated through interfering growth of adjacent crystals, the early euhedrality of the quartz might be difficult to detect. Evidence for precipitation from solution on crystal faces includes growth bands, defined by solid and fluid inclusions, and c crystallographic directions which are all approximately perpendicular to a surface on which growth occurred initially. Many hydrothermal veins in shallow deposits, however, exhibit bands of randomly oriented anhedral quartz that show no indications of earlier euhedral stages of growth. This texture suggests that the quartz may have formed by growth within a band which was initially amorphous silica or (less likely) chalcedony. If so, fluid inclusions within that quartz either were introduced after crystallization or represent fluid that was trapped at the time of formation of the amorphous or chalcedonic silica and was later remobilized during the transformation to quartz. Therefore, fluid-inclusion-filling temperatures and salinities may give little or no information about the condition of the hydrothermal fluid that initially deposited the siliceous vein material.

Numerous investigators, starting with Kennedy (1950), have shown that increased pressure greatly increases the solubility of quartz at temperatures above about 300°C. A likely mechanism for generating a highly supersaturated silica solution at high temperatures is by a sudden decrease in fluid pressure (fig. 15), possibly from lithostatic to hydrostatic or lower. Grindley and Browne (1976) attributed the formation of strongly silicified (by quartz+adularia, commonly accompanied by pyrite) breccia adjacent to open fissures at Wairakei and Broadlands, New Zealand, to sudden decreases in fluid pressure resulting from hydraulic fractures propagating through self-sealed rock. Keith and Muffler (1978) suggested that at Yellowstone National Park, simultaneous brecciation and deposition of amorphous silica occurred as a result of a sudden decrease in pressure, caused either by fracturing accompanying resurgent doming or by draining of a glacial lake that decreased the local hydrostatic pressure.

Natural hydrothermal waters range from very dilute to concentrated salt solutions. The effects of dissolved salts on the solubility of amorphous silica were investigated by Marshall (1980), Marshall and Warakomski (1980), Chen and Marshall (1982), Marshall and Chen (1982a, b), and Fournier and Marshall (1983). Below about 300°C, most dissolved salts except Na_2SO_4 cause a slight decrease in the solubility of amorphous

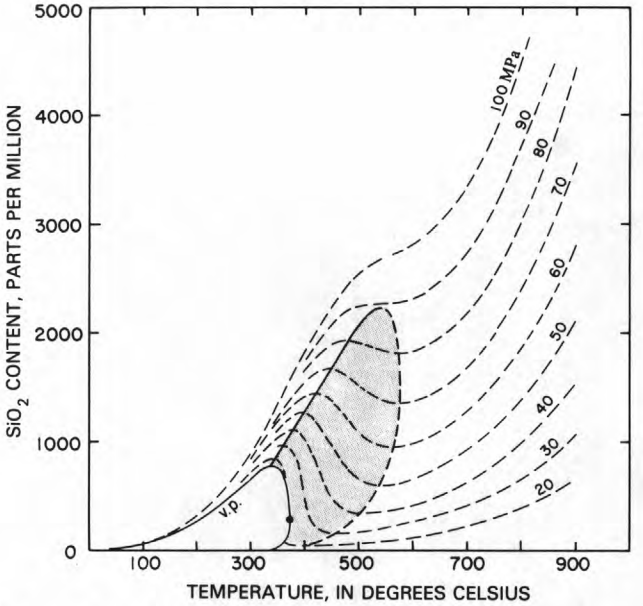

Figure 15. Calculated solubilities of quartz in water as a function of temperature at various pressures (using the equation of Fournier and Potter, 1982). Shaded area emphasizes a region of retrograde solubility.

silica. Solubilities of quartz and other silica minerals should be similarly affected by dissolved salts.

Addition of Na_2SO_4 greatly increases the solubility of amorphous silica at all measured temperatures (Chen and Marshall, 1982; Marshall and Chen, 1982a; Fournier and Marshall, 1983), apparently by the formation of a silica-sulfate complex (Marshall and Chen, 1982b; Fournier and Marshall, 1983). It is not known whether sodium is involved in that complex, or if other dissolved sulfates also form complexes with silica. The formation of a silica-sulfate complex also should increase the solubility of quartz in Na_2SO_4-rich solutions. These silica-sulfate complexes may occur to a large extent in some hydrothermal systems; at Cesano, Italy, a hot Na-K-SO_4-rich brine, containing more than 356,000 ppm total dissolved solids at 200° to 300°C, was penetrated in a 1,435-m-deep geothermal well (Calamai and others, 1976). However, the concentration of dissolved silica in the brine at Cesano is not well known.

Above about 300°C and at low to moderate pressures, added NaCl greatly increases the solubility of quartz (Fournier and others, 1982; Fournier, 1983), as shown in figure 16. In figure 16, note the solubility maximums even at very high concentrations of dissolved NaCl. Point A marks the intersection of the 18-weight-percent-NaCl solution with the vapor-pressure curve (that is, the solution boils). When a solution is heated at constant pressure, eventually either it will boil, or a field of retrograde quartz solubility will be entered. In either event, precipitation of quartz should decrease the permeability in the highest temperature part of a convecting hydrothermal system. This precipitation of quartz (and other minerals) is likely to occur at about 350° to 550°C, depending on the depth of circulation and the salinity of

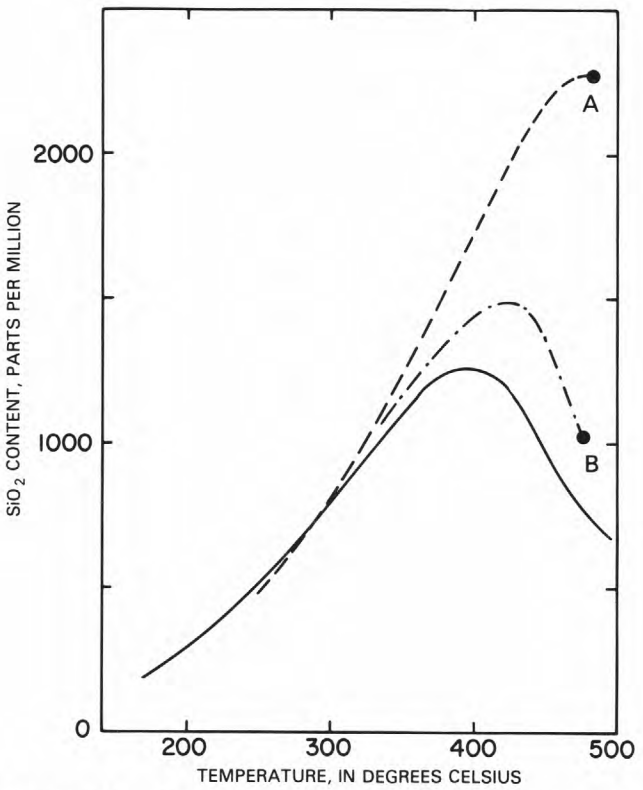

Figure 16. Calculated solubilities of quartz in water and in 5 and 18 weight percent NaCl solutions (dashed curves A and B, respectively) at 50-MPa pressure and various temperatures (using equations of Fournier and Potter, 1982, and Fournier, 1983).

the system. An impermeable barrier of precipitated minerals may form that prevents subsequent direct contact of circulating H_2O (in brine, gas, or supercritical fluid) at hydrostatic pressure with very hot rock or magma (Fournier, 1977). This barrier, in turn, will increase the time required to cool a shallow-intrusive magma and might lead to very steep temperature and pore-pressure gradients across the impermeable barrier. The maximum pore-pressure that can be attained is equal to the least principle stress in the rock. If this impermeable barrier is then ruptured (possibly by seismic activity or increasing pore pressure within the confined, high-pressure side of the system; Phillips, 1973) and permeability on the hydrostatic side of the barrier is large enough to prevent significantly increased pore pressure from developing there, a hydrothermal explosion may occur. This may be a mechanism by which some breccia pipes form (Henley and McNabb, 1978). The sudden decrease in density of the pore fluids, formation of steam, separation of gases, and decrease in temperature accompanying a hydrothermal explosion should cause silica and, to the extent that dissolved aluminum is present, feldspar to precipitate along with sulfides and gold. At high temperatures and low pressures, the feldspar that forms should be very K rich (Fournier, 1976). Note, however, that most hydrothermal brecciation occurs in shallow environments as a result of various mechanisms, including hydraulic fracturing (Grindley and Browne, 1976) or faulting accompanying resurgent doming (Keith and Muffler, 1978) after self-sealing of the outflow part of the system, and sudden changes in the water table (Muffler and others, 1971; Keith and Muffler, 1978). These relatively shallow breccias also may be cemented by quartz+K-feldspar (Grindley and Browne, 1976) or amorphous silica (Keith and Muffler, 1978).

SILICA REPLACEMENT OF LIMESTONE

At high temperatures, in contact-metamorphic environments, calc-silicates generally form where silica and limestone react. In contrast, in carbonate-hosted gold deposits, such as Carlin (Radtke and others, 1980; Rye, this volume) and those in the Jerritt Canyon district (Hawkins, 1982), massive fine-grained silica (now quartz) commonly replaces limestone, with little or no associated calc-silicate. In those deposits, the silicification of limestone forms so-called jasperoid that is most pronounced near faults, along lithologic contacts, and where the limestone was initially most permeable.

Below 300°C, at a constant partial pressure of CO_2, calcite becomes more soluble with decreasing temperature (Ellis, 1959, 1963; Holland and Malinin, 1979), whereas quartz, chalcedony, and amorphous silica become less soluble (fig. 12). Also, at constant temperature, calcite becomes less soluble as the partial pressure of CO_2 decreases (Ellis, 1959). Therefore, slow cooling (without boiling) of a solution at near-neutral pH should promote replacement of limestone by silica. The silica phase that precipitates is likely to be quartz or chalcedony because of the slow cooling; limestone will less likely be replaced by silica where a near-neutral solution boils. Decompressional boiling results in partitioning of dissolved CO_2 into the vapor phase, as well as a rapid decrease in temperature; calcite may precipitate or dissolve, depending on the composition of the hydrothermal solution, the pressure at which boiling is initiated, the drop in pressure, and whether the system is open or closed to loss of volatile materials during that boiling. Loss of volatile materials is likely to cause precipitation of calcite, which would not favor replacement of limestone by silica. Loss of volatile materials (particularly CO_2) could cause quartz to dissolve, because the solubility of quartz is greater in gas-poor than in gas-rich aqueous solutions (Shettel, 1974). Also, the loss of CO_2 could cause a significant increase in the pH of the solution that would increase the solubility of quartz, as mentioned previously. However, the increased solubility of quartz that results from partitioning of gas into the vapor phase is likely to be more than compensated by the increased concentration of silica in the remaining liquid fraction that results from flashing of water to steam. Therefore, the net result of decompressional boiling is likely to be precipitation of silica, except in very gas rich systems.

A mechanism for replacing limestone by massive silica, with little or no cooling of the hydrothermal solution, involves reaction of a silica-rich acidic solution with limestone, generating CO_2. Some or all of

this CO_2 will dissolve in the solution, depending on several factors, including the temperature, partial pressure of CO_2, pH, and salinity. Dissolved CO_2 lowers the activity of water and greatly decreases the ability of a solution to retain high concentrations of dissolved silica (Shettel, 1974). Therefore, silica should precipitate at the interface of solution and limestone, where CO_2 is generated. The local increase in pH of the initially acidic solution, due to reaction with limestone, also will favor silica deposition, as previously discussed. The deposited silica may be quartz, chalcedony, or amorphous, depending on the initial silica concentration in the acidic solution and the temperature. By the above mechanism, silica replacement of limestone at constant temperature would be more likely deeper in a system, where fluid pressures are large enough for significant amounts of CO_2 to dissolve in the solution at the point where that gas is generated. At shallow levels, where little CO_2 can dissolve in the solution, silica replacement of limestone is more likely to occur as a result of neutralization of an ascending acidic solution supersaturated with silica.

Where permeabilities are large enough for hydrostatic pressure to be maintained ($\underline{P}_{total}$ is constant at a given depth), and if the partial pressure of CO_2 becomes large owing to acid attack on the limestone, boiling may be induced because the partial pressure of water is effectively lowered:

$$\underline{P}_{H_2O} = \underline{P}_{total} - \underline{P}_{CO_2}. \quad (3)$$

Where permeabilities are low, hydrostatic pressure may be exceeded by a buildup in total pore pressure as the partial pressure of CO_2 increases. With continued and rapid generation of CO_2, rupturing and brecciation of the overlying rock may occur.

Where limestone is first dissolved and silica+gold are later deposited in the solution cavities, the gold might be carried either as a bisulfide or chloride complex and deposited as a result of boiling (mainly adiabatic cooling) or slow cooling without boiling. If the replacement of limestone by silica and the deposition of gold are the results of related processes that occur simultaneously, constraints may be placeable on those processes. Deposition of gold with silica at constant temperature might be accomplished through various chemical reactions, such as neutralization of an acidic solution by reaction with limestone. The liberated CO_2 could result in deposition of silica, as previously discussed, and the increase in pH would cause any gold initially carried as a chloride complex to precipitate.

In some places, reduction of an oxidized solution by organic matter in the limestone also could be an important factor in precipitating gold as a chloride complex. According to B. R. Berger (oral commun., 1982), the gold-bearing silicified limestone generally was rich in organic matter before hydrothermal alteration, whereas the barren silicified limestone was not. The above observations suggest that reduction of an initially oxidized solution by organic matter may be important for gold deposition in carbonate-hosted deposits. These observations also suggest that decreasing temperature and boiling are not necessarily major factors causing replacement of limestone by massive silica; if they generally were important factors, gold mineralization should be as common in limestone poor in organic matter as in that rich in organic matter.

A decrease in carbon content in limestone should occur where gold, carried in solution as a chloride complex, is deposited as a result of reduction by organic material. However, R. E. Beane (written commun., 1983) noted that carbon appears to have been added by hydrothermal processes to some gold-bearing altered limestone. To account for this observation, he suggested that gold, carried as a bisulfide complex, might be deposited as a result of oxidation of bisulfide by CO_2:

$$HS^- + 2CO_2 = HSO_4^- + 2C. \quad (4)$$

A more complete equation that accounts for the deposition of metallic gold
might involve hydrogen gas:

$$2AuHS + 4CO_2 + H_2 = 2H^+ + 2HSO_4^- + 4C + 2Au. \quad (5)$$

Hydrogen gas may also be generated by reaction of methane with water:

$$CH_4 + 2H_2O = CO_2 + 4H_2. \quad (6)$$

Gold-bisulfide complexes are most important in hydrothermal solutions at near-neutral pH. Therefore, when gold is transported mainly as a bisulfide complex, little reaction of acid with limestone should occur, except for that which results from the formation of H^+ by the oxidation of sulfide. Too little CO_2 probably would be formed as a result of oxidation of sulfide and subsequent reaction with limestone to account for the observed massive replacements of limestone by silica. The simultaneous deposition of silica with gold initially carried as a bisulfide complex seems to require cooling (without boiling) of the solution to account for the dissolution of limestone and deposition of silica.

At present, it appears that some carbonate-hosted gold deposits may have formed as a result of acid-chloride solutions reacting with limestone; others may have formed where neutral sulfide-rich waters cooled as they moved through limestone. Still another possibility is that mixture of waters with different temperatures, salinities, and dissolved-gas concentrations in limestone aquifers caused simultaneous dissolution of carbonate and deposition of gold and silica. Mixing of two waters that were initially at different temperatures generally produces solutions that are supersaturated with silica (fig. 14). However, the mixtures may dissolve or precipitate calcite, depending on the partial pressures of CO_2 in the initial solutions and in the final solution; a high partial pressure of CO_2 in the high-temperature component and a lower partial pressure in the low-temperature component favor a mixture that will dissolve limestone.

CONCLUSIONS

Different varieties of silica form in response to different hydrothermal conditions. The deposition of amorphous silica indicates that high degrees of supersaturation with respect to quartz were attained. This supersaturation generally requires high underground reservoir temperatures and rapid movement of fluids from those reservoirs toward the surface. Solutions that precipitate gold in deposits containing thick siliceous sinter at the Earth's surface probably were neutral to slightly alkaline (by loss of CO_2) chloride-rich waters that rose quickly to the surface from relatively shallow regions where reservoir temperatures were 200° to 250°C. Where gold was deposited with amorphous silica in veins and cavities at depth, the reservoir temperatures in still deeper parts of the system probably exceeded about 240°C. Amorphous silica that is deposited at depth is likely to convert relatively rapidly to chalcedony or quartz, owing to high temperatures and saline environments. Most chalcedonic vein silica probably forms at temperatures lower than about 180°C. Anhedral aggregates of quartz after amorphous silica might form at any temperature within the stability range of quartz, though generally above about 180°C. Sudden decreases in fluid pressure can cause deposition of amorphous silica in veins at high temperature. Gold associated with euhedral quartz crystals probably was deposited at high temperatures (more than 240°C), or from solutions at lower temperatures that cooled less drastically than those that deposited amorphous silica. When hydrothermal explosions occur, brecciating overlying rock, temperatures and pressures decrease quickly and drastically. Simultaneously, nonvolatile dissolved components are enriched in the residual liquid, and partitioning of gases into the steam fraction changes the pH and Eh of the solution. Thus, hydrothermal explosions create ideal conditions for the deposition of silica minerals and gold. The deposition of quartz at temperatures above about 350°C may be a contributing factor to the formation of some deep hydrothermal brecciation and associated gold deposition.

In general, the precipitation of gold is likely to be favored by the same conditions that favor the precipitation of silica minerals. In volcanic rocks, where gold is present with silica minerals in veins and coatings on brecciated material, boiling was probably an important factor controlling mineral deposition. Boiling may be much less important in carbonate-hosted environments, however, where gold deposition may occur as a result of conductive cooling or various oxidation-reduction processes.

REFERENCES CITED

Allen, E. T., and Day, A. L., 1935, Hot springs of the Yellowstone National Park: Carnegie Institution of Washington Publication 466, 525 p.

Barnes, H. L., 1979, Solubilities of ore minerals, in Barnes, H. L., ed., Geochemistry of hydrothermal ore deposits (2d ed.): New York, John Wiley and Sons, p. 404-460.

Bodvarsson, Gunnar, 1964, Utilization of geothermal energy for heating purposes and combined schemes involving power generation, heating and/or by-products: United Nations Conference on New Sources of Energy, Rome, 1961, Proceedings, v. 3, p. 429-436.

Bohlmann, E. G., Mesmer, R. E., and Berlinski, P., 1980, Kinetics of silica deposition from simulated geothermal brines: Society of Petroleum Engineers Journal, v. 20, no. 4, p. 239-248.

Briner, Emile, and Roth, Paul, 1948, Recherches sur l'hydrolyse par la vapeur d'eau de chlorures alcalins seuls ou additionnés de divers adjuvants [Investigations of the water-vapor hydrolysis of alkali chlorides, alone or with the addition of various catalysts]: Helvetica Chimica Acta, v. 31, p. 1352-1360.

Calamai, Adriano, Cataldi, Raffaele, Dall'Aglio, Mario, and Ferrara, G. A., 1976, Preliminary report on the Cesano hot brine deposit (northern Latium, Italy): United Nations Symposium on the Development and Use of Geothermal Resources, 2d, San Francisco, 1975, Proceedings, v. 1, p. 305-313.

Carr, R. M., and Fyfe, W. S., 1958, Some observations on the crystallization of amorphous silica: American Mineralogist, v. 43, no. 9-10, p. 908-916.

Chen, C.-H., 1970, Geology and geothermal power potential of the Tatun volcanic region [Taiwan], in Barbier, Enrico, ed., United Nations Symposium on the Development and Utilization of Geothermal Resources, Pisa, 1970, Proceedings: Geothermics, Special Issue 2, v. 2, pt. 2, p. 1134-1143.

----- 1975, Thermal waters in Taiwan, a preliminary study, in Thermal and chemical problems of thermal waters: International Association of Hydrological Sciences Publication 119, p. 79-88.

Chen, C.-T. A., and Marshall, W. L., 1982, Amorphous silica solubilities IV. Behavior in pure water and aqueous sodium chloride, sodium sulfate, magnesium chloride, and magnesium sulfate up to 350°C: Geochimica et Cosmochimica Acta, v. 46, no. 2, p. 279-287.

Coplen, T. B., Combs, Jim, Elders, W. A., Rex, R. W., Burckhatter, G. C., and Laird, R., 1973, Preliminary findings of an investigation of the Dunes thermal anomaly, Imperial Valley, California: Sacramento, California Department of Water Resources, 48 p.

Crerar, D. A., Axtmann, E. V., and Axtmann, R. C., 1981, Growth and ripening of silica polymers in aqueous solutions: Geochimica et Cosmochimica Acta, v. 45, no. 8, p. 1259-1266.

Dickson, F. W., and Potter, J. M., 1982, Rock-brine chemical interactions: Palo Alto, Calif., Electric Power Research Institute final report for Project 653-2, AP-2258, 89 p.

Ellis, A. J., 1959, The solubility of calcite in carbon dioxide solutions: American Journal of Science, v. 257, no. 5, p. 354-365.

----- 1963, The solubility of calcite in sodium chloride solutions at high temperatures: American Journal of Science, v. 261, no. 3, p. 259-267.

----- 1977, Chemical and isotopic techniques in geothermal investigations, in Barbier, Enrico, ed.,

The application of nuclear techniques to geothermal studies: Geothermics, v. 5, no. 1-4 (special issue), p. 3-12.

----- 1979, Explored geothermal systems, in Barnes, H. L., ed., Geochemistry of hydrothermal ore deposits (2d ed.): New York, John Wiley and Sons, p. 632-683.

Ellis, A. J., and Mahon, W. A. J., 1964, Natural hydrothermal systems and experimental hot-water/rock interactions: Geochimica et Cosmochimica Acta, v. 28, no. 8, p. 1323-1357.

----- 1967, Natural hydrothermal systems and experimental hot water/rock interactions (part 2): Geochimica et Cosmochimica Acta, v. 31, no. 4, p. 519-538.

----- 1977, Chemistry and geothermal systems: New York, Academic Press, 392 p.

Ernst, W. G., and Calvert, S. E., 1969, An experimental study of the recrystallization of porcelanite and its bearing on the origin of some bedded cherts: American Journal of Science, v. 267-A (Schairer volume), p. 114-133.

Facca, G., and Tonani, Franco, 1967, The self-sealing geothermal field: Bulletin Volcanologique, v. 30, p. 271-273.

Fleming, B. A., and Crerar, D. A., 1982, Silicic acid ionization and calculation of silica solubility at elevated temperature and pH. Application to geothermal fluid processing and reinjection: Geothermics, v. 11, no. 1, p. 15-29.

Fournier, R. O., 1973, Silica in thermal waters: Laboratory and field investigations, in International Symposium on Hydrogeochemistry and Biogeochemistry, Tokyo, 1970, Proceedings: Washington, J. W. Clark, v. 1, p. 122-139.

----- 1976, Exchange of Na^+ and K^+ between water vapor and feldspar phases at high temperature and low vapor pressure: Geochimica et Cosmochimica Acta, v. 40, no. 12, p. 1553-1561.

----- 1977, Constraints on the circulation of meteoric water in hydrothermal systems imposed by the solubility of quartz [abs.]: Geological Society of America Abstracts With Programs, v. 9, no. 7, p. 979.

----- 1979, Geochemical and hydrologic considerations and the use of enthalpy-chloride diagrams in the prediction of underground conditions in hot-spring systems: Journal of Volcanology and Geothermal Research, v. 5, no. 1-2, p. 1-16.

----- 1983, A method of calculating quartz solubilities in aqueous sodium chloride solutions: Geochimica et Cosmochimica Acta, v. 47, no. 3, p. 579-586.

Fournier, R. O., and Marshall, W. L., 1983, Calculation of amorphous silica solubilities at 25° to 300°C and apparent cation hydration numbers in aqueous salt solutions using the concept of effective density of water: Geochemica et Cosmochimica Acta, v. 47, no. 3, p. 587-596.

Fournier, R. O., and Potter, R. W. II, 1982, An equation correlating the solubility of quartz in water from 25° to 900°C at pressures up to 10,000 bars: Geochimica et Cosmochimica Acta, v. 46, no. 10, p. 1969-1973.

Fournier, R. O., Rosenbauer, R. J., and Bischoff, J. L., 1982, The solubility of quartz in aqueous sodium chloride solutions at 300°C and 180 to 500 bars: Geochimica et Cosmochimica Acta, v. 46, no. 10, p. 1975-1978.

Fournier, R. O., and Rowe, J. J., 1977, The solubility of amorphous silica in water at high temperatures and high pressures: American Mineralogist, v. 62, no. 9-10, p. 1052-1056.

Fournier, R. O., and Truesdell, A. H., 1970, Chemical indicators of subsurface temperature applied to hot springs of Yellowstone National Park, Wyoming, U. S. A., in Barbier, Enrico, ed., United Nations Symposium on the Development and Utilization of Geothermal Resources, Pisa, 1970, Proceedings: Geothermics, Special Issue 2, v. 2, pt. 1, p. 529-536.

Frondel, Clifford, 1962, The system of mineralogy. Volume III, silica minerals: New York, John Wiley and Sons, 334 p.

Fyfe, W. S., and McKay, D. S., 1962, Hydroxyl ion catalysis of the crystallization of amorphous silica at 330°C and some observations on the hydrolysis of albite solutions: American Mineralogist, v. 47, no. 1-2, p. 83-89.

Galobardes, D. R., Van Hare, D. R., and Rogers, L. B., 1981, Solubility of sodium chloride in dry steam: Journal of Chemical and Engineering Data, v. 26, no. 4, p. 363-366.

Goñi, J. C., Guillemin, Claude, and Sarcia, C., 1967, Géochimie de l'or exogène--étude expérimentale de la formation des dispersions colloïdales d'or et de leur stabilité [The geochemistry of exogenous gold--experimental study of the formation of colloidal dispersions of gold and their stability]: Mineralium Deposita, v. 1, no. 4, p. 259-268.

Gooch, F. A., and Whitfield, J. E., 1888, Analyses of waters of the Yellowstone National Park, with an account of the methods of analysis employed: U.S. Geological Survey Bulletin 47, 84 p.

Grindley, G. W., and Browne, P. R. L., 1976, Structural and hydrologic factors controlling the permeabilities of some hot-water geothermal fields: United Nations Symposium on the Development and use of Geothermal Resources, 2d, San Francisco, 1975, Proceedings, v. 1, p. 377-386.

Harper, R. T., and Arevalo, E. M., 1982, A geoscientific evaluation of the Basley-Danin prospect, Negros Oriental, Philippines: Pacific Geothermal Conference and New Zealand Geothermal Workshop, 4th, Auckland, 1982, Proceedings, pt. 1, p. 235-240.

Hawkins, R. B., 1982, Discovery of the Bell gold mine, Jerritt Canyon district, Elko County, Nevada: Mining Congress Journal, v. 68, no. 2, p. 28-32.

Hein, J. R., and Scholl, D. W., 1978, Diagenesis and distribution of late Cenozoic volcanic sediment in the southern Bering Sea: Geological Society of America Bulletin, v. 89, no. 2, p. 197-210.

Helgeson, H. C., 1969, Thermodynamics of hydrothermal systems at elevated temperatures and pressures: American Journal of Science, v. 267, no. 7, p. 729-804.

Heming, R. F., Hochstein, M. P., and McKenzie, W. F., 1982, Suretimeat geothermal system: An example of a volcanic geothermal system: Pacific

Geothermal Conference and New Zealand Geothermal Workshop, 4th, Auckland, 1982, Proceedings, pt. 1, p. 247-250.

Hemley, J. J., 1959, Some mineralogical equilibria in the system K_2O-Al_2O_3-SiO_2-H_2O: American Journal of Science, v. 257, no. 4, p. 241-270.

Hemley, J. J., and Jones, W. R., 1964, Chemical aspects of hydrothermal alteration with emphasis on hydrogen metasomatism: Economic Geology, v. 59, no. 4, p. 538-569.

Hemley, J. J., Meyer, C., and Richter, D. H., 1961, Some alteration reactions in the system Na_2O-Al_2O_3-SiO_2-H_2O, art. 408 of Short papers in the geologic and hydrologic sciences: U.S. Geological Survey Professional Paper 424-D, p. D338-D340.

Henley, R. W., 1973, Solubility of gold in hydrothermal chloride solutions: Chemical Geology, v. 11, no. 2, p. 73-87.

Henley, R. W., and Ellis, A. J., 1983, Geothermal systems ancient and modern: a geochemical review: Earth-Science Reviews, v. 19, no. 1, p. 1-50.

Henley, R. W., and McNabb, Alex, 1978, Magmatic vapor plumes and ground-water interaction in porphyry copper emplacement: Economic Geology, v. 73, no. 1, p. 1-20.

Heydemann, Annerose, 1964, Untersuchungen über die Bildungsbedingungen von Quarz im Temperaturbereich zwischen 100°C und 250°C [Investigations on the conditions of quartz formation in the temperature range 100°-250°C]: Beiträge zur Mineralogie und Petrographie, v. 10, no. 2, p. 242-259.

Holland, H. D., and Malinin, S. D. 1979, On the solubility and occurrence of non-ore minerals, in Barnes, H. L., ed., Geochemistry of hydrothermal ore deposits (2nd ed.): New York, John Wiley and Sons, p. 461-508.

Ichikuni, Masami, 1968, Uptake of boron by siliceous sinters: Geochemical Journal, v. 2, no. 2, p. 105-109.

Ichikuni, Masumi, and Kobayashi, Shoichi, 1969, Titanium and aluminum in siliceous sinters: Chemical Geology, v. 5, no. 2, p. 131-137.

Iler, R. K., 1979, The chemistry of silica: New York, John Wiley and Sons, 866 p.

Jones, J. B., and Segnit, E. R., 1971, The nature of opal. I. Nomenclature and constituent phases: Geological Society of Australia Journal, v. 18, no. 1, p. 56-68.

Kamiya, Hiroshi, Ozaki, Atsuko, and Imahashi, Masayuki, 1974, Dissolution rate of powdered quartz in acid solution: Geochemical Journal, v. 8, no. 1, p 21-26.

Kano, Kazuhiko, and Taguchi, Kazuo, 1982, Experimental study on the ordering of opal-CT: Geochemical Journal, v. 16, no. 1, p. 33-41.

Kastner, Miriam, Keene, J. B., and Gieskes, J. M., 1977, Diagenesis of siliceous oozes--I. Chemical controls on the rate of opal-A to opal-CT transformation--an experimental study: Geochimica et Cosmochimica Acta, v. 41, no. 8, p. 1041-1059.

Keith, T. E. C., and Muffler, L. J. P., 1978, Minerals produced during cooling and hydrothermal alteration of ash flow tuff from Yellowstone drill hole Y-5: Journal of Volcanology and Geothermal Research, v. 3, no. 3-4, p. 373-402.

Kennedy, G. C., 1950, A portion of the system silica-water: Economic Geology, v. 45, no. 7, p. 629-653.

Lakin, H. W., Curtin, G. C., and Hubert, A. E., 1974, Geochemistry of gold in the weathering cycle: U.S. Geological Survey Bulletin 1330, 80 p.

Lawless, J. V., and Gonzalez, R. C., 1982, Geothermal geology and review of exploration, Biliran Island: Pacific Geothermal Conference and New Zealand Geothermal Workshop, 4th, Auckland, 1982, Proceedings, pt. 1, p. 161-166.

Leach, T. M., and Bogie, I., 1982, Overprinting of hydrothermal regimes in the Palimpinon Geothermal Field, Southern Negros, Philippines: Pacific Geothermal Conference and New Zealand Geothermal Workshop, 4th, Auckland, 1982, Proceedings, pt. 1, p. 179-184.

Mahon, W. A. J., 1966, Silica in hot water discharged from drillholes at Wairakei, New Zealand: New Zealand Journal Science, v. 9, no. 1, p. 135-144.

Marshall, W. L., 1980, Amorphous silica solubilities--III. Activity coefficient relations and predictions of solubility behavior in salt solutions, 0-350°C: Geochimica et Cosmochimica Acta, v. 44, no. 7, p. 925-931.

Marshall, W. L., and Chen, C.-T. A., 1982a, Amorphous silica solubilities--V. Predictions of solubility behavior in aqueous mixed electrolyte solutions to 300° C: Geochimica et Cosmochimica Acta, v. 46, no. 2, p. 289-291.

----- 1982b, Amorphous silica solubilities--VI. Postulated sulfate-silicic acid solution complex: Geochimica et Cosmochimica Acta, v. 46, no. 3, p. 367-370.

Marshall, W. L., and Warakomski, J. M., 1980, Amorphous silica solubilities--II. Effect of aqueous salt solutions at 25°C: Geochimica et Cosmochimica Acta, v. 44, no. 7, p. 915-924.

Martynova, O. I., and Samoilov, Y. F., 1957, [Dissolution of sodium chloride in an atmosphere of water vapor of high parameters]: Zhurnal Neorganisheskoi Khimii, v. 2, no. 12, p. 2829-2833 [in Russian].

Mizutani, Shinjiro, 1970, Silica minerals in the early stage of diagenesis: Sedimentology, v. 15, no. 3-4, p. 419-436.

Muffler, L. J. P., White, D. E., and Truesdell, A. H., 1971, Hydrothermal explosion craters in Yellowstone National Park: Geological Society of America Bulletin, v. 82, no. 3, p. 723-740.

Murata, K. J., and Larson, R. R., 1975, Diagenesis of Miocene siliceous shales, Temblor Range, California: U.S. Geological Survey Journal of Research, v. 3, no. 5, p. 553-566.

Murata, K. J., and Nakata, J. K., 1974, Cristobalitic stage in the diagenesis of diatomaceous shale: Science, v. 184, no. 4136, p. 567-568.

Murata, K. J., and Randall, R. G., 1975, Silica mineralogy and structure of the Monterey Shale, Temblor Range, California: U.S. Geological Survey Journal of Research, v. 3, no. 5, p. 567-572.

Nakamura, Hisayoshi, Sumi, Kiyoshi, Katagiri, K., and

Iwata, Takayuki, 1970, The geological environment of Matsukawa geothermal area [Japan], in Barbier, Enrico, ed., United Nations Symposium on the Development and Utilization of Geothermal Resources, Pisa, 1970, Proceedings: Geothermics, Special Issue 2, v. 2, pt. 1, p. 221-231.

Phillips, W. J., 1973, Mechanical effects of retrograde boiling and its probable importance in the formation of some porphyry ore deposits: Institution of Mining & Metallurgy Transactions, v. 82, sec. B, no. 801, p. B90-B98.

Radtke, A. S., Rye, R. O., and Dickson, F. W., 1980, Geology and stable isotope studies of the Carlin gold deposit, Nevada: Economic Geology, v. 75, no. 5, p. 641-672.

Rimstidt, J. D., and Barnes, H. L., 1980, The kinetics of silica-water reactions: Geochimica et Cosmochimica Acta, v. 44, no. 11, p. 1683-1699.

Romberger, S. B., 1982, Transport and deposition of gold hydrothermal systems at temperatures up to 300°C [abs.]: Geological Society of America Abstracts with Programs, v. 14, no. 7, p. 602.

Rothbaum, H. P., Anderton, B. H., Harrison, R. F., Rohde, A. G., and Slatter, A., 1979, Effect of silica polymerization and pH on geothermal scaling: Geothermics, v. 8, no. 1, p. 1-20.

Rothbaum, H. P., and Rohde, A. G., 1979, Kinetics of silica polymerization and deposition from dilute solutions between 5 and 180°C: Journal of Colloid and Interface Science, v. 71, no. 3, p. 533-559.

Rowe, J. J., Fournier, R. O., and Morey, G. W., 1973, Chemical analysis of thermal waters in Yellowstone National Park, Wyoming, 1960-65: U.S. Geological Survey Bulletin 1303, 31 p.

Sato, Mitsuo, 1962, Tridymite crystals in opaline silica from Kusatsu, Gumma Prefecture [Japan]: Mineralogical Journal, v. 3, no. 5-6, p. 296-305.

Schoen, Robert, and White, D. E., 1965, Hydrothermal alteration in GS-3 and GS-4 drill holes, Main Terrace, Steamboat Springs, Nevada: Economic Geology, v. 60, no. 7, p. 1411-1421.

Seastres, J. S., Jr., 1982, Subsurface geology of the Nasuji-Sogongon sector, Southern Negros Geothermal Field, Philippines: Pacific Geothermal Conference and New Zealand Geothermal Workshop, 4th, Auckland, 1982, Proceedings, pt. 1, p. 173-178.

Seward, T. M., 1973, Thio complexes of gold and the transport of gold in hydrothermal ore solutions: Geochimica et Cosmochimica Acta, v. 37, no. 3, p. 379-399.

----- 1974, Determination of the first ionization constant of silicic acid from quartz solubility in borate buffer solutions at 350°C: Geochimica et Cosmochimica Acta, v. 38, no. 11, p. 1651-1664.

Shettel, D. L., 1974, The solubility of quartz in supercritical H_2O-CO_2 fluids: University Park, Pennsylvania State University, M.S. thesis, 52 p.

Skibsted, L. H., and Bjerrum, Jannik, 1974, Studies on gold complexes. II. The equilibrium between gold(I) and gold(III) in the ammonia system and the standard potentials of the couples involving gold, diamminegold(I), and tetramminegold(III): Acta Chemica Scandinavica, ser. A, v. 28, no. 7, p. 764-770.

Truesdell, A. H., and Fournier, R. O., 1977, Procedure for estimating the temperature of a hot-water component in a mixed water by using a plot of dissolved silica versus enthalpy: U.S. Geological Survey Journal of Research, v. 5, no. 1, p. 49-52.

Weres, Oleh, Yee, Andrew, and Tsao, Leon, 1982, Equations and type curves for predicting the polymerization of amorphous silica in geothermal brines: Society of Petroleum Engineers Journal, v. 22, no. 1, p. 9-16.

White, D. E., Brannock, W. W., and Murata, K. J., 1956, Silica in hot-spring waters: Geochimica et Cosmochimica Acta, v. 10, no. 1-2, p. 27-59.

White, D. E., Muffler, L. J. P., and Truesdell, A. H., 1971, Vapor-dominated hydrothermal systems compared with hot-water systems: Economic Geology, v. 66, no. 1, p. 75-97.

White, D. E., Thompson, G. A., and Sandberg, C. H., 1964, Rocks, structure, and geologic history of Steamboat Springs thermal area, Washoe County, Nevada: U.S. Geological Survey Professional Paper 458-B, p. B1-B62.

Yamada, Eizo, 1976, Geological development of the Onikobe caldera and its hydrothermal system: United Nations Symposium on the Development and Use of Geothermal Resources, 2d, San Francisco, 1975, Proceedings, v. 1, p. 665-672.

Geochemistry of Hydrothermal Transport and Deposition of Gold and Sulfide Minerals in Carlin-Type Gold Deposits

By James J. Rytuba

CONTENTS

INTRODUCTION

The mineralogy of Carlin-type gold deposits is relatively simple, consisting of gold, pyrite, and quartz (Radtke and Dickson, 1974). Pyrite in the ore has high As, Hg, and Sb contents, and realgar and orpiment commonly occur in the deposits; less abundant minerals include cinnabar, stibnite, and various thallium minerals. Thus, hydrothermal transport of gold in Carlin-type deposits must be accompanied by the transport of As, Hg, Sb, Tl, and Fe. Solubility studies of phases which contain these elements provide constraints on the properties of the hydrothermal solution and on the processes which lead to ore deposition. Because of the fine-grained texture of Carlin-type ores and the general absence of veins, the physical and chemical environment of deposition is poorly constrained. Radtke (1981) concluded that most Carlin ores formed in the temperature interval 175°-200°C, from low-salinity (3±1 weight percent NaCl) solutions that were neutral to mildly acid and of low f_{O_2}.

This chapter reviews the solubility data available for the Au, As, Hg, Sb, Tl, and Fe phases present in Carlin-type deposits. I define the physicochemical environment of deposition on the basis of the mineral assemblages present, particularly arsenic minerals, and evaluate the chemical controls on ore deposition.

GOLD SOLUBILITY

Transport of gold in hydrothermal systems requires oxidation of the gold to an ionic species and complexing of it with a ligand. Seward (1982) showed that under all geologic conditions, only the aurous species, Au^+, is important, although its concentration, even at 400°C, is only 3.9×10^{-4} ppb. Complexing of Au^+ with chloride ligands was studied experimentally by Henley (1973) and Rytuba and Dickson (1974), and with sulfide ligands by Seward (1973). Chloride complexing is important only under conditions of low pH, high f_{O_2} and high chloride concentration. At 500°C and 100-MPa pressure in 1 m KCl, Henley measured a gold solubility of 500 ppm under high f_{O_2} established by the magnetite-hematite buffer and low pH established by the feldspar-muscovite-quartz buffer. In contrast, Rytuba and Dickson (1974) measured only 1.5-ppm gold solubility in low-f_{O_2} 1-m NaCl buffered by pyrite-pyrrhotite at 500°C and 100 MPa.

Complexing of Au^+ with sulfide ligands is appreciable. In low-f_{O_2} solutions buffered by pyrite-pyrrhotite, Seward (1973) showed that AuHS dominates in low pH solutions, $Au(HS)_2^-$ in near-neutral solutions, and $Au_2(HS)_2S^{2-}$ in alkaline solutions. Gold solubility increases with increasing pH: At 250,C, the solubility rises from 0.8 ppm Au at pH=4 to a maximum of 62.0 ppm Au at pH=7, and then decreases to a constant concentration of 15.5 ppm Au at pH>9, in solutions containing 0.5 m sulfur. Gold solubility is essentially constant as a function of temperature at pH<6.5, but at pH>6.5, it increases significantly as temperature increases, about a tenfold increase for a 100°C increase in temperature. An increase in pressure decreases the solubility (Seward, 1973).

Because the stability of gold-chloride and gold-sulfide complexes is a function f_{O_2} and pH, a

convenient method for evaluating the relative importance of each is to plot the solubility on an f_{O_2}-pH diagram. Seward (1982) calculated such a diagram at 300° which shows that for f_{O_2} where sulfide sulfur predominates—that is, for f_{O_2} where pyrite is stable—the $Au(HS)_2^-$ complex is the predominant species in solution and the $AuCl_2^-$ complex is of no importance in gold transport (fig. 17). Only in high f_{O_2} low-pH solutions, where sulfur is present dominantly as sulfate, are gold-chloride complexes important.

The close geochemical association of arsenic with gold has led to the speculation that arsenothio, $Au(AsS_2)^0$ and $Au(AsS_3)^{2-}$, complexes may be important in gold transport (Seward, 1973). To evaluate the importance of arsenothio complexes, Rytuba (1977) measured the mutual solubility of orpiment and gold in 1-m NaCl solutions up to 300°C and found the gold solubility to be less than 50 ppb. In the system Na_2S-As_2S_3-H_2O, gold solubility is comparable to that measured by Seward (1973), a result indicating that arsenothio complexes are unimportant in gold transport.

The mutual solubility of gold and orpiment, and of gold and stibnite, in sodium sulfide, polysulfide, and NaOH solutions at 200°C was measured by Grigor'yeva and Sukneva (1981). Although gold solubility was appreciably higher in the presence of orpiment, it is unclear whether arsenic complexing or increasing f_{S_2}, f_{O_2}, or pH caused the increase in gold solubility, because of the complexity of the solutions and the unconstrained f_{O_2}, f_{S_2}, and pH.

PYRITE SOLUBILITY

Pyrite solubility was first measured experimentally by Haas and Barnes (1965) in various systems up to 200°C. Solubility at 200°C was found to be less than 20 ppm in the system H_2S-H_2O and somewhat higher in the system HS^--H_2O at 200°C. Crerar and Barnes (1976) measured the mutual solubility of chalcopyrite, pyrite, and bornite in 0- to 10.38-m NaCl from 200° to 355°C. The high Fe content of the solutions—34.5 ppm at 200°C to 41.5 ppm at 355°C in 1-m NaCl—was attributed to formation of the $FeCl^+$ complex. The mutual solubility of pyrite+pyrrhotite+gold+quartz in the system NaCl-H_2O was measured by Rytuba and Dickson (1974) (fig. 18). In 1-m NaCl at 50 MPa, Fe content increases from 5 ppm at 200°C to 145 ppm at 500°C. The Fe content increases with increasing temperature, and increases sharply at temperatures above 400°C. An increase in

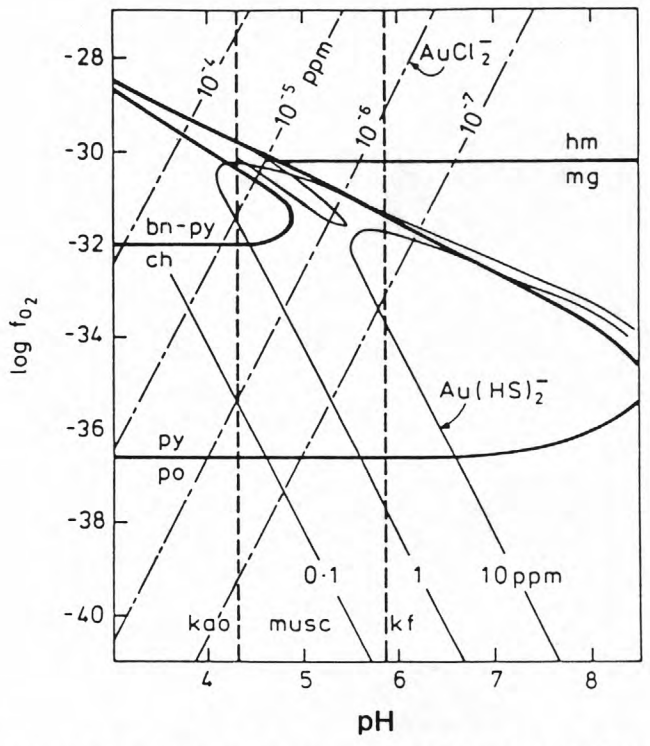

Figure 17. Gold solubility as $AuCl_2^-$ and $Au(HS)_2^-$ in relation to the stability fields of pyrite (py), pyrrhotite (po), magnetite (mg), hematite (hm), bornite (bn), and chalcopyrite (ch) and as a function of f_{O_2} and pH at 300°C in 0.25-m Cl^-, 0.05 m S. From Seward (1982).

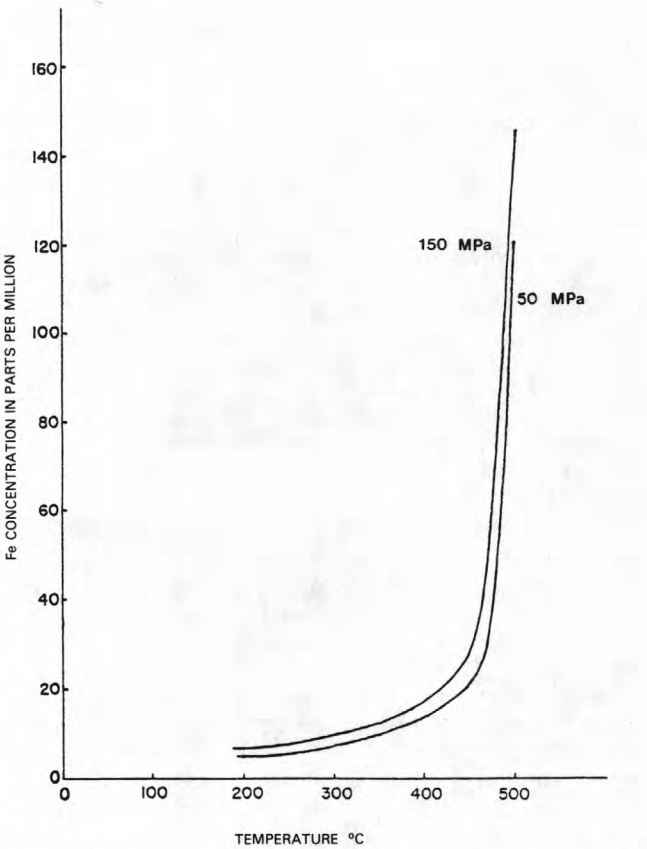

Figure 18. Isobars of Fe concentration in 1-m NaCl for the phases pyrite+pyrrhotite+gold+quartz in the system Fe-S-SiO_2-Au-NaCl-H_2O. From Rytuba (1977).

pressure also increases Fe solubility. The Fe content of solutions, which is a function of NaCl concentration, increases significantly as the NaCl concentration increases (fig. 19). At low NaCl concentrations (less than 0.4 m), the $FeCl^+$ complex predominates; and at higher NaCl concentrations, the $FeCl_3^-$ complex occurs as well. At 500°C, the $FeCl_3^-$ complex predominates at all chloride concentrations.

Extrapolation of Fe content to zero NaCl concentration indicates that solubility of pyrite and pyrrhotite is low, even at high temperatures—for example, 6 ppm at 500°C. Significant transport of pyrite below 350°C requires an NaCl concentration of at least 1 m (5.8 weight percent).

STIBNITE SOLUBILITY

The solubility of stibnite has been studied in a wide variety of systems, but the type of solvation reaction remains uncertain. Querol-Sune (1973) measured the solubility in pure water and in the systems CO_2-H_2O and $CaCO_3$-CO_2-H_2O over the temperature range 150°-250°C and the pressure interval 50-150 MPa. At a pressure of 50 MPa (fig. 20) in pure water, the solubility is appreciable, ranging from 160 ppm at 150°C to 387 ppm at 250°C. The solubility increases sharply above 200°C, at the rate of 4.5 ppm/°C at 50 MPa. The pressure coefficient is negative, and the solubility decreases sharply with an isothermal drop in pressure. In the system CO_2-H_2O, stibnite solubility is less than in pure water: 340 ppm in water containing 3.3×10^{-2} mol CO_2 per kilogram of solution, in comparison with 387 ppm in pure water at 250°C (fig. 20), both at 50 MPa. With the addition of calcite to the system CO_2-H_2O, stibnite solubility is reduced by about 50 percent: 156 ppm with calcite, in comparison with 340 ppm without. The cause of this solubility reduction by calcite is unknown.

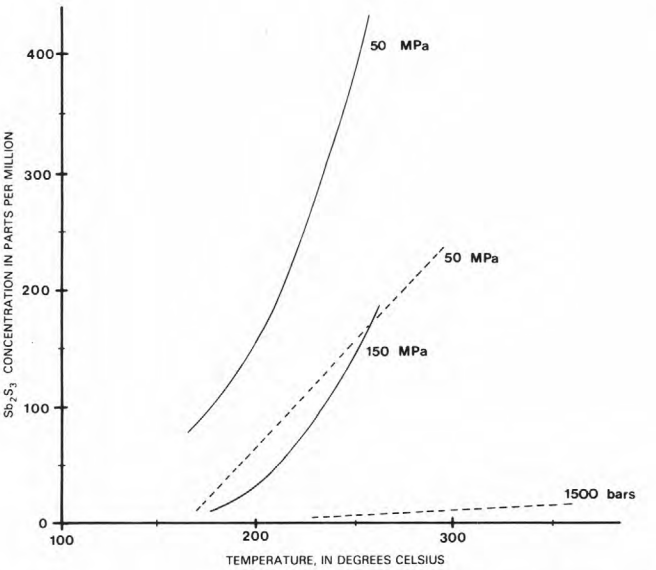

Figure 20. Solubility of stibnite in water (solid curves), and in water and calcite (dashed curves), as a function of temperature. From Querol-Sune (1973).

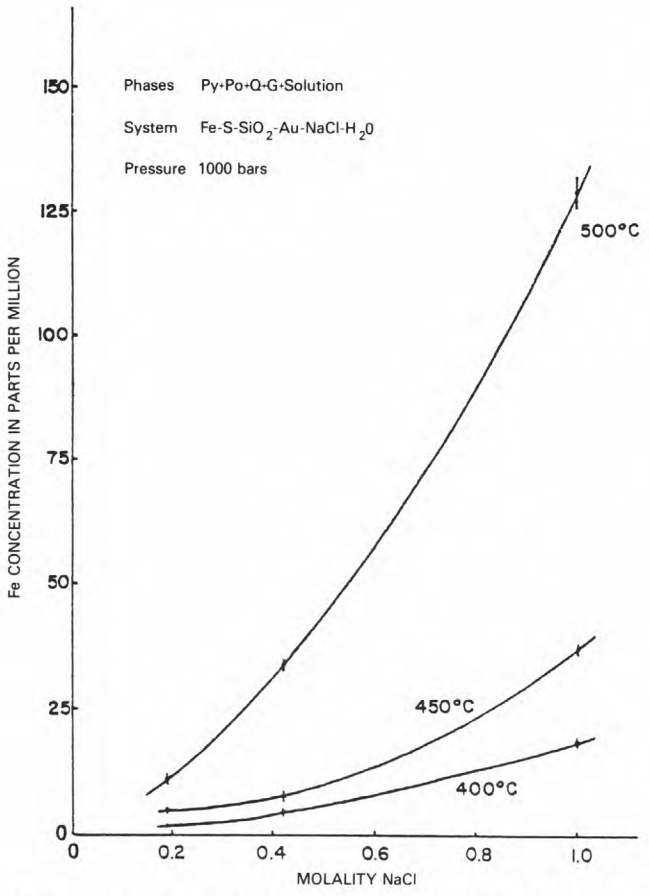

Figure 19. Isotherms of Fe concentration in NaCl solution for the phases pyrite+pyrrhotite+gold+quartz in the system Fe-S-SiO_2-Au-NaCl-H_2O at 100-MPa pressure. From Rytuba and Dickson (1974).

The solubility of stibnite in the system Na_2S-H_2O was measured by Norton (1964), and the mutual solubility of stibnite and cinnabar in the system Na_2S-H_2O was measured by Learned (1966) and Learned and others (1974). In both systems, stibnite solubility is much higher than in pure water: 7,240 ppm in 0.384 weight percent Na_2S, in comparison with 387 ppm in pure water at 250°C. The increase in stibnite solubility with increasing Na_2S concentration indicates the formation of bisulfide complexes. The nature of these complexes is unknown. Raab (1969) demonstrated a similar high stibnite solubility in alkaline solutions in the system KOH-H_2O; measured solubilities are much higher than in pure water but somewhat lower than in the system Na_2S-H_2O. Learned and others (1974) suggested the formation of OH^- complexes, but, again, the nature of these complexes is unknown.

These experimental data demonstrate that stibnite is appreciably soluble at temperatures as low as 150°C in pure water. Solubility is even greater in alkaline solutions, and complexing in Na_2S solutions leads to extremely high solubility. Further experimental work is required to define the solution reaction and to measure the stability constants of the various complexes.

SOLUBILITY OF CINNABAR AND MERCURY

Of all the sulfide minerals, cinnabar is the least soluble in pure water. Krauskopf (1951) calculated its solubility to be 2.0×10^{-17} ppm at 25°C. He determined that deposition of 1 ton of cinnabar would require the passage through a fissure vein of 100 times the volume of water in all the oceans. Thermochemical calculations indicate that hydrothermal transport of cinnabar can occur in only three ways: as the sulfide complex HgS_2^{2-}, as the volatile $HgCl_2$, and as mercury vapor (Krauskopf, 1951).

Several experimental studies have measured the solubility of cinnabar in sulfide solutions. Experimental measurements by Dickson and Tunell (1958) in the system HgS-Na_2S-H_2O at 25°C, and by Dickson (1964, 1966) in the same system up to 250°C and 180 MPa, demonstrated a very high cinnabar solubility as the HgS_2^{2-} complex. Cinnabar solubility in this system decreases from 50° to 120°C, where a solubility minimum occurs, and then increases rapidly with rising temperature. Schwarzenbach and Widmer (1963) measured the solubility of cinnabar in 0.019-m sulfide solutions at 20°C over the pH interval 1-10.74. They found cinnabar solubility to be negligible in acid solutions—0.005 ppm below a pH of 4.57; the solubility increased with increasing pH to more than 0.68 ppm above a pH of 9.7. Barnes and others (1967) measured the solubility of cinnabar in sulfide solutions containing as much as 2.5 m HS^- over the pH interval 3.5-7.8 and the temperature interval 25°-200°C. High solubility occurred in 0.383-m NaHS, ranging from 76 ppm at 25°C to 732 ppm at 201°C; even higher solubility occurred at higher concentrations of HS^-. Four mercury complexes account for the high solubility of cinnabar, and the stability of each complex is a function of pH. The $HgS(H_2S)_2$ complex predominates below a pH of 6.13, the $Hg(HS)_3^-$ complex over the pH interval 6.13-6.89, the $HgS(HS)_2^{2-}$ over the pH interval 6.85-8.5, and the HgS_2^{2-} complex above a pH of 8.5.

The mutual solubilities of cinnabar and stibnite were measured by Learned and others (1974) in the system Na_2S-H_2O from 150°C to 250°C at 10 MPa. The considerable suppression of cinnabar solubility by the presence of stibnite indicates that the solubility of antimony sulfide complexes is considerably higher than that of mercury sulfide complexes. Learned and others (1974) also suggested that transport of mercury in alkaline sulfide solutions is only possible in solutions undersaturated with respect to stibnite.

Kuznetsov and others (1973) demonstrated through thermochemical calculations and experiments that cinnabar ultimately becomes unstable in highly alkaline sulfide solutions and decomposes to native Hg. Moreover, with increasing temperature, cinnabar becomes unstable at progressively lower pH and is unstable at a pH above 11.5 at 100°C, and at a pH of 10 at 300°C, at a sulfur activity of 10^{-6} m.

In summary, experimental work on sulfide solutions indicates that cinnabar is highly soluble in alkaline solutions, even at relatively low temperatures. Although its solubility decreases with decreasing pH, cinnabar is still appreciably soluble in weakly alkaline to near-neutral solutions. Cinnabar solubility increases strongly with increasing temperature at high concentrations of sulfide but, at low concentrations, is nearly independent of temperature. In strongly alkaline solutions, cinnabar instability requires transport of native mercury.

The solubility of native mercury, as the zero-valent atom (Hg^0), is appreciable in pure water, ranging from 0.1 ppm at 50°C to 0.95 ppm at 120°C (Glew and Hames, 1971). At higher temperatures, the solubility is relatively high, ranging from 290 ppm at 300°C to 2,400 ppm at 500°C (Sorokin, 1973). Although the presence of cinnabar decreases Hg^0 solubility, Varekamp and Buseck (1982) calculated that between 100° and 250°C and at a pH of 6, Hg^0 is the dominant species in solution, and its concentration is adequate to account for transport in dilute hydrothermal systems that are strongly reducing, with f_{O_2} from 10^{-55} to 10^{-37}, and sulfide poor. In strongly saline systems, Hg^0 solubility is lower, and transport probably occurs as mercury-chloride complexes. During boiling, vapor transport of mercury becomes important (Varekamp and Buseck, 1982).

SOLUBILITY OF THALLIUM MINERALS

A wide variety of thallium minerals occurs in the Carlin deposit, including carlinite (Tl_2S), ellisite (Tl_3AsS_3), weissbergite ($TlSbS_2$), christite ($TlHgAsS_3$), lorandite ($TlAsS_2$), galkhaite, and jordanite. Of all the sulfide minerals, carlinite has the highest solubility in pure water—215 ppm at 20°C (Radtke and Dickson, 1975); its solubility is even higher in acidic solutions. Tl_2S oxidizes rapidly to Tl_2O_3 (avicennite), and in the process Tl_2SO_4 is formed, which is even more soluble than Tl_2O_3. Because of the high solubility of some thallium minerals, thallium probably has been repeatedly mobilized in the Carlin deposit (Radtke and Dickson, 1975).

SOLUBILITY OF ORPIMENT AND REALGAR

Experimental studies of arsenic sulfides have concentrated on the solubility of orpiment, and only reconnaissance studies of realgar have been made. The solubility of orpiment in pure water and in the system Na_2S-H_2O was measured by Weissberg and others (1966). In pure water, orpiment is highly soluble: 124 ppm at 98°C and 160 ppm at 151°C, at 75 MPa. In the system Na_2S-H_2O, the solubility is greatly enhanced over that in pure water, ranging from 16,200 ppm at 100°C to 18,100 ppm at 203°C, 75 MPa, and 0.55 weight percent H_2S. Orpiment solubility increases rapidly as the temperature rises, to extremely high values above 200°C. At low temperatures, the solubility passes through a minimum at 100°C. Mironova and Zotov (1980) demonstrated that binuclear sulfide complexes account for the high solubility of orpiment in sulfide solutions. They measured its solubility as a function of pH at 90°C and found that in acidic solutions (pH<4.0), the $H_2As_2S_4^0$ complex predominates; from a pH of 4.0 to 6.3, the $H_2As_2S_4^-$ complex predominates; and above a pH of 6.3 the $As_2S_4^{2-}$ complex predominates. Orpiment solubility is independent of pH in acidic solutions but increases significantly above a pH of 4.

The solubility of realgar at low temperatures was measured by Raab (1969). At 105.5 mmol of $Na_2B_4O_7$ per kilogram of solution, the solubility is 0.6 mmol at 50°C and 0.1 MPa; and at 99.4 mmol Na_2CO_3 per kilogram of solution, the solubility is 11.4 mmol at 75°C and 0.1 MPa. Realgar also is appreciably soluble in alkaline solutions, even at low temperatures.

Experimental data indicate that the solubility of orpiment is appreciable in pure water at elevated temperatures. Although sulfide complexing enhances the solubility, excess sulfide is not necessary for significant transport of orpiment or realgar. No data are available for the solubility of arsenopyrite or native arsenic.

ARSENIC MINERALS AS INDICATORS OF f_{S_2}

Arsenic minerals commonly present in Carlin-type gold deposits include orpiment, realgar, and arsenic-rich pyrite; arsenopyrite is generally rare or absent. The relative stability of the arsenic minerals is a function of the sulfur fugacity (f_{S_2}) and can be conveniently shown on an f_{S_2}-f_{O_2} diagram (fig. 21). At high f_{S_2}, orpiment is the stable arsenic sulfide, but it becomes unstable at very high f_{S_2}, where As-S liquid forms. At lower f_{S_2}, orpiment becomes unstable, and realgar forms. Further decrease in f_{S_2} results in the formation of more sulfur deficient arsenic minerals and the progressive formation of native arsenic, arsenopyrite, and, finally, loellingite. The relative stability of these minerals is independent of f_{O_2}. At high f_{O_2}, the arsenic minerals are oxidized to iron arsenates, but the absence of thermochemical data precludes calculation of the stability fields of these arsenate minerals. The stability fields of the non-iron-containing arsenic minerals in figure 21 have been extended to the f_{O_2} established by oxidation of the arsenic phase to As_2O_3, for which thermochemical data are available. For iron-bearing arsenic minerals, the stability fields have been terminated along the iron sulfide/magnetite boundary.

The stability of the iron sulfides and oxides are plotted on figure 21 for reference. Within the pyrite stability field, four arsenic minerals are stable and may coexist with pyrite: realgar, orpiment, arsenic, and arsenopyrite. Arsenopyrite may coexist with pyrrhotite, but loellingite is stable only with pyrrhotite. In the epithermal environment, at 100° to 250°C, the relative stability fields of the arsenic and iron sulfides remain as shown on the f_{S_2}-f_{O_2} diagram constructed for 200°C (fig. 21).

The univariant equilibrium assemblages of orpiment+realgar, realgar+native arsenic, and native arsenic+arsenopyrite establish sulfur-fugacity buffers. In mineral deposits containing one of these assemblages in sufficient quantity, the sulfur fugacity will be fixed. The narrow stability fields of the arsenic minerals as a function of f_{S_2} also provide a useful indication of the f_{S_2} within mineral deposits containing any one of these phases.

In the Carlin gold deposit, Radtke (1981) reported that the main stage of gold deposition occurred without

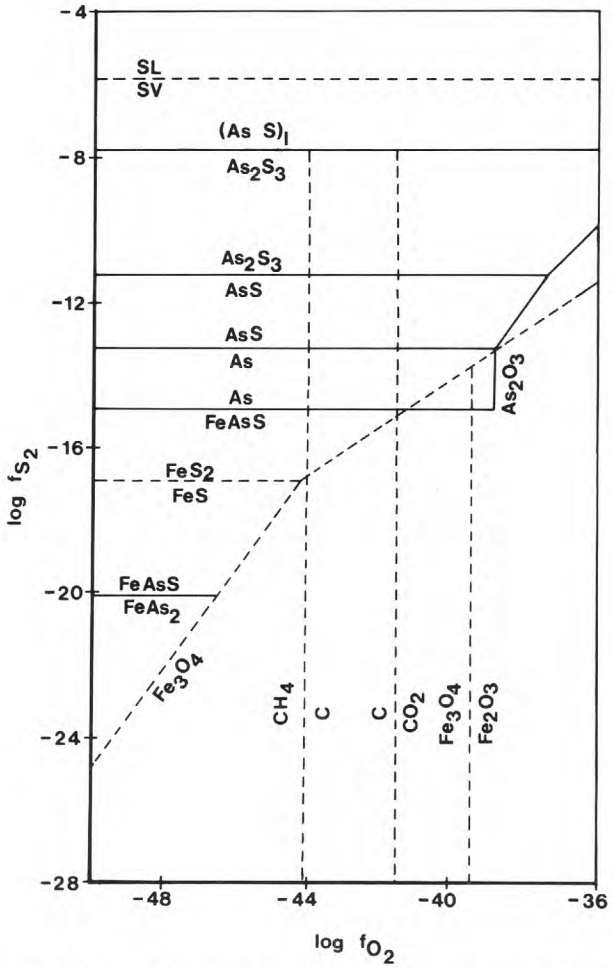

Figure 21. Stability of arsenic minerals at 200°C as a function of f_{S_2} and f_{O_2}. Stability fields of iron minerals are enclosed by dashed lines. f_{O_2} established by C-CO_2 and C-CH_4 buffers for f_{CO_2}=10 MPa is shown by dashed lines. SL, sulfur liquid, SV, sulfur vapor.

deposition of arsenic sulfides. Instead, arsenic was deposited as coatings on pyrite and coprecipitated with pyrite to form arsenic-rich pyrite. This assemblage indicates that during the main stage of deposition, the f_{S_2} was low enough for native arsenic to be stable but high enough to prevent the formation of arsenopyrite (fig. 22). Native arsenic has been found in the Carlin ores in association with organic material (Radtke, 1981). Because deposition of the ores occurred in carbonaceous limestone, the f_{O_2} would have been fixed by the C-CO_2 buffer. The C-CO_2 boundary plotted in figure 21 assumes an f_{CO_2} of 10 MPa. If $\Sigma C<0.2$, then the graphite field disappears, and the f_{O_2} will be established by the CH_4-CO_2 buffer. Figure 22 plots the f_{O_2}-f_{S_2} field of deposition of main-stage Carlin ores. Late-stage realgar, which makes up 90 percent of the arsenic sulfides in the Carlin ore body, was deposited at 180° to 210°C (Radtke, 1981). The realgar occurs as

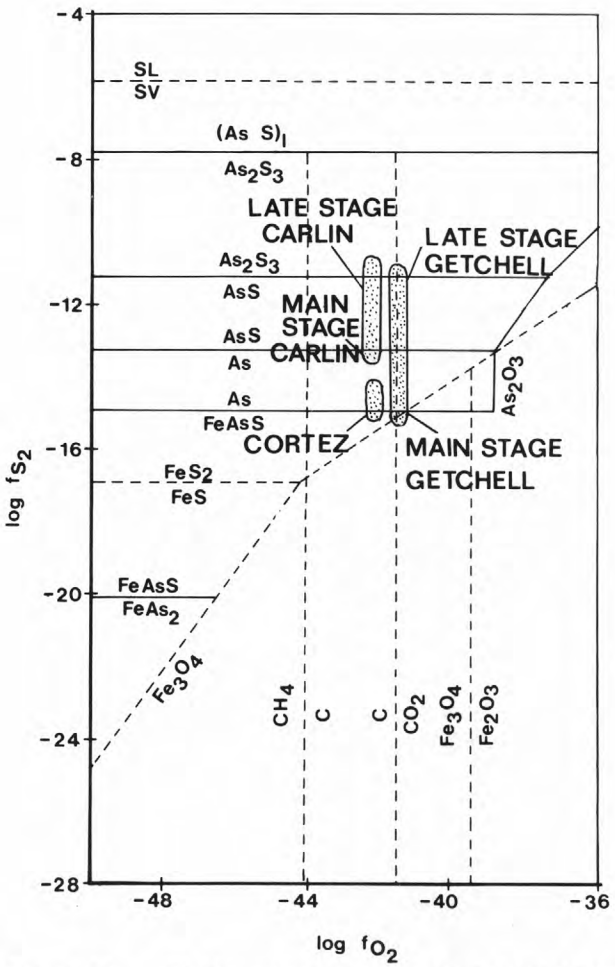

Figure 22. Fields of ore deposition (stippled) as indicated by arsenic mineral assemblages at Carlin, Cortez, and Getchell.

fracture coatings, as seams in carbonaceous ores, in vugs, and in calcite veins, all of which cut the ore (Radtke, 1981). The presence of postore realgar indicates that the f_{S_2} increased in the late-stage hydrothermal fluids. At high levels in the Main and East ore zones, orpiment and realgar are present, defining the highest f_{S_2} environment in the deposit. Arsenic minerals at Carlin reflect changes in f_{S_2} over time. Fluids responsible for main-stage gold deposition had an initially low f_{S_2} but developed a progressively higher f_{S_2}, culminating in late-stage deposition of realgar and orpiment (fig. 22).

Although the Getchell gold deposit is noted for its abundant arsenic sulfides, Joraleman (1951) reported that the high-grade gold ores ("gumbo") consisted only of carbon, gold, quartz, and magnetite, with no arsenic sulfides. The widespread occurrence of arsenic in Getchell ores suggests that these high-grade ores likely also contain arsenic. In the restricted field of magnetite and carbon (fig. 21), native arsenic can be a stable phase. Because the stable phase is native arsenic, which is commonly coated black, the mineral probably has not been recognized in these dark carbonaceous ores. Arsenopyrite is reported to occur in and coating pyrite, indicating a low f_{S_2} near the As-FeAsS boundary. Joralemon (1951) observed that both realgar and orpiment are present; veining and coating of realgar by orpiment indicate that the orpiment is later than the realgar. Berger (1975) reported that although arsenic is closely associated with gold mineralization, realgar and orpiment are late-stage minerals and occur as veins, in fractures, and on bedding planes that cut the ore and gangue minerals. The arsenic-mineral paragenesis at Getchell, which is similar to that at Carlin, indicates that main-stage gold fluids had a low f_{S_2} but became progressively higher in f_{S_2} with late-stage deposition of realgar and orpiment (fig. 22).

In the Cortez deposit, Wells and Mullens (1973) reported that the carbonaceous ore contained arsenic in association with gold as rims on pyrite, in "arsenian pyrite," and as gold-bearing arsenopyrite. Microprobe analyses reported by Wells and Mullens indicate that the carbonaceous material contained as much as to 0.5 weight percent As, and they speculated that the gold and arsenic were associated with submicron-size pyrite "inadvertently included in the analyzed spot" (Wells and Mullens, 1973, p. 197). A more likely interpretation is that the gold occurred in association with native arsenic in the carbonaceous ore. Thus, the f_{O_2}-f_{S_2} field of deposition for Cortez ores can be placed near the As-FeAsS boundary (fig. 22).

ENVIRONMENT OF DEPOSITION

The presence of native arsenic in Carlin-type deposits indicates that main-stage gold deposition occurred at low f_{S_2}. Arsenic occurs as coatings on pyrite, coprecipitated with pyrite (arsenian pyrite), and as the native element. Although native arsenic is white, it commonly tarnishes to dark gray and would be easily overlooked in carbonaceous ores. The presence of abundant carbonaceous material indicates that the f_{O_2} was low, probably fixed by the C-CO_2 buffer. At low f_{O_2} and f_{S_2}, significant amounts of gold can be transported only as a gold-sulfide complex (Seward, 1973, 1982). The solubility of native arsenic at elevated temperatures is unknown. The concentration of mercury in the hydrothermal solution would have been high, and it would have been present as the native element. The solubility of stibnite would also have been appreciable. Transport of pyrite would require a total chloride concentration sufficient to form the $FeCl^+$ complex, equivalent to about 5 weight percent NaCl.

After main-stage gold deposition, the f_{S_2} of the fluids increased, so that realgar became the stable arsenic phase. In some deposits, the f_{S_2} increased sufficiently for orpiment to form. Because the f_{O_2} would still be fixed by the C-CO_2 buffer, any increase in f_{S_2} would reflect changes in ΣS. Assuming that the pH in the carbonate-host-rock environment was

maintained by $CaCO_3$-CO_2 equilibria, the pH would have been below the first ionization constant of H_2S(aq), and so ΣS may be approximated by H_2S(aq). For univariant arsenic-mineral assemblages, such as in equation (1), below, f_{S_2} is related to ΣS and f_{O_2} by the following equilibria:

$$2As+S_2(g)=2AsS \quad (1)$$

$$2H_2S(aq)+O_2(g)=2H_2O(l)+S_2(g) \quad (2)$$

An increase in the activity of H_2S(aq), at constant f_{O_2} and temperature, will lead to the formation of more sulfur enriched arsenic phases. The increase in the activity of H_2S(aq) indicated by the change from arsenic-stable to orpiment-stable conditions at constant f_{O_2} and temperature would be by a factor of about 100. In Carlin-type deposits, the more sulfur enriched arsenic phases occur late in the ore-forming stage, when ΣS would be expected to have decreased owing to dilution. The temperature also was probably lower in late-stage realgar veins than during the main stage of gold deposition. Figure 23 plots the temperature dependence of the univariant arsenic-phase assemblages, such as in equation 1 above. The curves were constructed by assuming that f_{O_2} is fixed by the C-CO_2 buffer, that f_{CO_2}=10 MPa, and that the pH is low enough that $\Sigma S=H_2S$(aq). The effects of changes in temperature and in the activity of H_2S(aq) on the stability of arsenic phases are shown in figure 23 for two cases: (1) Temperature decrease accompanied by no change in the activity of H_2S(aq), and (2) temperature decrease accompanied by a decrease in the activity of H_2S(aq). In path 1, the deposition begins in the arsenic stability field, and moves into the realgar stability field with decreasing temperature. Further temperature decrease leads to deposition of orpiment. Path 2 is similar, but because ΣS decreases, a larger temperature decrease is required for a change from the arsenic stability field to the orpiment stability field. Either path 1 or 2 would lead to gold deposition because the stability of the gold-sulfide complex is temperature dependent. Gold deposition would be enhanced further if temperature decrease were accompanied by a decrease in ΣS, because the stability of the gold-sulfide complex ($Au(HS)_2^-$) is also a function of ΣS.

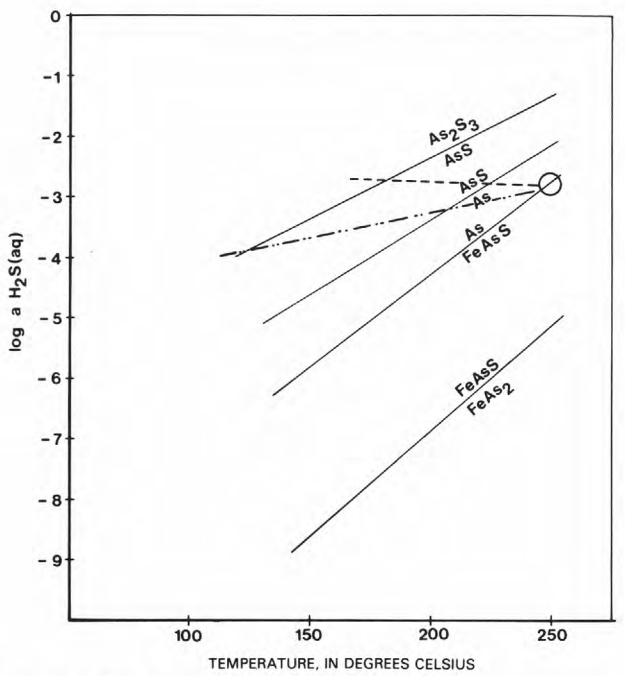

Figure 23. Sulfide-sulfur concentration established by univariant arsenic-mineral assemblages, as a function of temperature. f_{O_2} is fixed by C-CO_2 buffer and f_{CO_2}=100 MPa. Path 1 (dashed line), constant ΣS; path 2 (dotted line), decreasing ΣS.

If main-stage gold deposition began in the arsenic stability field, as in the Carlin deposit, or at the As-FeAsS boundary at Cortez, a decrease in temperature would eventually have resulted in the formation of realgar and the deposition of gold. The close spatial association of gold and realgar in the Carlin deposit may reflect temperature decreases, which moved the depositional path from the arsenic to the realgar stability field and caused the deposition of gold. A relatively large temperature decrease is required for orpiment to become stable. Such a decrease would probably cause deposition of most gold in solution, and so the poor spatial correlation of orpiment with gold in Carlin-type deposits would be expected. Note that at temperatures below 100°C and at low f_{O_2}, orpiment is the only stable phase at any geologically reasonable concentration of H_2S. Thus, in carbonaceous ores where f_{O_2} is low, all arsenic phases will alter to orpiment.

Mineral assemblages and fluid-inclusion data indicate that the hydrothermal solutions which formed Carlin-type gold deposits were of low temperature (150°-250°C), low ionic strength (3-5 weight percent NaCl equivalent), low total sulfide content (0.0001-0.001 m), and low f_{O_2} and f_{S_2}. Under these conditions, a hydrothermal solution can transport significant amounts of gold only as the $Au(HS)_2^-$ complex, of iron as the $FeCl^+$ complex, and of mercury as the native element, Hg^0. The Sb content of the solution will be high and controlled by simple stibnite solvation because the sulfide concentration is low. Native arsenic controls the As content of the solution, but the nature of the arsenic species in solution is unknown. The observed change in arsenic phases in the deposits indicates a decrease in the temperature of the hydrothermal solution over time, resulting in deposition of gold and associated elements.

REFERENCES CITED

Barnes, H. L., Romberger, S. B., and Stemprok, Miroslav., 1967, Ore solution chemistry II. Solubility of HgS in sulfide solutions: Economic Geology, v. 62, no. 7, p. 957-982.

Berger, Byron, 1975, Geology and geochemistry of the Getchell disseminated gold deposit, Humboldt

County, Nevada: Society of Mining Engineers of AIME Preprint 75-1-305, 26 p.

Crerar, D. A., and Barnes, H. L., 1976, Ore solution chemistry: V. Solubilities of chalcopyrite and chalcocite assemblages in hydrothermal solution at 200° to 350°C: Economic Geology, v. 71, no. 4, p. 772-794.

Dickson, F. W., 1964, Solubility of cinnabar in Na_2S solutions at 50-250° C and 1-1,800 bars, with geologic implications: Economic Geology, v. 59, no. 4, p. 625-635.

----- 1966, Solubilities of metallic sulfides and quartz in hydrothermal sulfide solutions: Bulletin Volcanologique, v. 29, p. 605-628.

Dickson, F. W., and Tunell, George, 1958, Equilibria of red HgS (cinnabar) and black HgS (metacinnabar) and their saturated solutions in the systems HgS-Na_2S-H_2O and HgS-Na_2S-Na_2O-H_2O from 25°C to 75°C at 1 atmosphere pressure: American Journal of Science, v. 256, no. 9, p. 654-679.

Glew, D. N., and Hames, D. A., 1971, Aqueous nonelectrolyte solutions. Part X. Mercury solubility in water: Canadian Journal of Chemistry, v. 49, no. 19, p. 3114-3118.

Grigor'yeva, T. A., and Sukneva, L. S., 1981, Effects of sulfur and of antimony and arsenic sulfides on the solubility of gold: Geochemistry International, v. 18, no. 5, p. 153-158.

Haas, J. L., and Barnes, H. L., 1965, Ore solution transport of pyrite [abs.]: American Geophysical Union Transactions, v. 46, no. 1, p. 183.

Henley, R. W., 1973, Solubility of gold in hydrothermal chloride solutions: Chemical Geology, v. 11, no. 2, p. 73-87.

Joralemon, Peter, 1951, The occurrence of gold at the Getchell mine, Nevada: Economic Geology, v. 46, no. 3, p. 267-310.

Krauskopf, K. B., 1951, Physical chemistry of quicksilver transportation in vein fluids: Economic Geology, v. 46, no. 5, p. 498-523.

Kuznetsov, V. A., Efremora, E. P., and Kolonin, G. R., 1973, On the stability of cinnabar in high temperature solutions: Geochemistry International, v. 10, no. 3, p. 498-507.

Learned, R. E., 1966, The solubility of quartz, quartz-cinnabar and cinnabar-stibnite in sodium sulfide solutions and their implications for ore genesis: Riverside, University of California, Ph. D. thesis, 161 p.

Learned, R. E., Tunell, G., and Dickson, F. W., 1974, Equilibria of cinnabar, stibnite, and saturated solutions in the system HgS-Sb_2S_3-Na_2S-H_2O from 150° to 250°C at 100 bars, with implications concerning ore genesis: U.S. Geological Survey Journal of Research, v. 2, no. 4, p. 457-466.

Mironova, G. D., and Zotov, A. V., 1980, Solubility studies of the stability of As(III) sulfide complexes at 90°C: Geochemistry International, v. 17, no. 2, p. 46-54.

Norton, D. L., 1964, Geological and geochemical investigations of stibnite deposits: Riverside, University of California, Ph. D. thesis, 116 p.

Querol-Sune, Francisco, 1973, The genesis of the antimony deposits at Wadley, San Luis Potosi, Mexico: Field investigations and stibnite solubility studies: Stanford, Calif., Stanford University, Ph. D. thesis, 180 p.

Raab, W. J., 1969, Solubilities of stibnite, orpiment and realgar in borate, carbonate, and hydroxide solutions as functions of temperature, pressure, and their implications as applied to the borax deposits at Boron, California: Riverside, University of California, Ph. D. thesis, 228 p.

Radtke, A. S., 1981, Geology of the Carlin Gold deposit, Nevada: U.S. Geological Survey Open-File Report 81-97, 154 p.

Radtke, A. S., and Dickson, F. W., 1974, Genesis and vertical position of fine-grained disseminated replacement-type gold deposits in Nevada and Utah, U.S.A.: International Association on the Genesis of Ore Deposits Symposium, 4th, Varna, Bulgaria, 1974, Proceedings, v. 1, p. 71-78.

----- 1975, Carlinite, Tl_2S, a new mineral from Nevada: American Mineralogist, v. 60, no. 7-8, p. 559-565.

Rytuba, J. J., 1977, Mutual solubilities of pyrite, pyrrhotite, quartz and gold in aqueous NaCl solutions from 200° to 500° C, and 500 to 1,500 bars and genesis of the Cortez gold deposit, Nevada: Stanford, Calif., Stanford University, Ph. D. thesis, 122 p.

Rytuba, J. J., and Dickson, F. W., 1974, Reaction of pyrite+pyrrhotite+quartz+gold with NaCl-H_2O solutions, 300-500° C, 500-1,500 bars and genetic implications: International Association on the Genesis of Ore Deposits Symposium, 4th, Varna, Bulgaria, 1974, Proceedings, v. 1, p. 320-326.

Schwartzenback, Gerold, and Widmer, Michael, 1963, Die Löschlichkeit von Metallsulfiden I. Schwarzes Quecksilbersulfid [The solubility of metallic sulfides. I. Black mercury sulfide]: Helvetica Chimica Acta, v. 46, p. 2613-2628.

Seward, T. M., 1973, Thio complexes of gold and the transport of gold in hydrothermal ore solutions: Geochimica et Cosmochimica Acta, v. 37, no. 3, p. 379-399.

----- 1982, Hydrothermal transport and deposition of gold, in Glover, J. E., and Groves, D. I., eds., Gold mineralization: University of West Australia, Geology Department and Extension Service Publications, p. 45-55.

Sorokin, V. I., 1973, Solubility of mercury in water at temperatures from 300° to 500° C and pressures from 500 to 1,000 atm: Akademia Nauk S.S.S.R. Doklady, v. 213, p. 852-855.

Varekamp, J. C., and Buseck, P. R., 1982, Transport and deposition of Hg in hydrothermal systems [abs.]: Eos (American Geophysical Union Transactions), v. 63, no. 45, p. 1127-1128.

Weissberg, B. G., Dickson, F. W., and Tunell, George, 1966, Solubility of orpiment (As_2S_3) in Na_2S-H_2O at 50-200°C and 100-1,500 bars, with geological applications: Geochimica et Cosmochimica Acta, v. 30, no. 8, p. 815-827.

Wells, J. D., and Mullens, T. E., 1973, Gold-bearing arsenian pyrite determined by microprobe analysis, Cortez and Carlin gold mines, Nevada: Economic Geology, v. 68, no. 2, p. 187-201.

A Model for the Formation of Carbonate-Hosted Disseminated Gold Deposits Based on Geologic, Fluid-Inclusion, Geochemical, and Stable-Isotope Studies of the Carlin and Cortez Deposits, Nevada

By Robert O. Rye

CONTENTS

INTRODUCTION

Integrated geologic, mineralogic, fluid-inclusion, geochemical, and stable-isotope studies of the Carlin, Nev., carbonate-hosted disseminated gold deposit (Radtke and others, 1980) indicate that mineralization and, probably, much of subsequent oxidation were related to events that occurred in the shallow levels of a meteoric-water hydrothermal system, which was probably set in motion by underlying Tertiary igneous activity. Earlier and less detailed studies on the Cortez, Nev., deposit (Wells and others, 1969; Rye and others, 1974) indicated that mineralization was the result of essentially the same processes as those at Carlin, in spite of differences in age, structural setting, and geochemical details.

The broad-scale geochemical similarities of these two deposits suggest that carbonate-hosted disseminated gold deposits in Nevada may be a result of a general set of processes that have operated repeatedly in various places. These detailed studies of the Carlin and Cortez deposits can serve as the basis for a conceptual model, which can be revised and refined as additional studies of similar deposits give a better understanding of the fundamental processes and of how these processes may have been expressed in individual deposits. This chapter also presents new data and observations on other carbonate-hosted disseminated gold deposits in Nevada and proposes some slight modifications and extensions to previously published conclusions on the Carlin and Cortez deposits.

GENERAL GEOLOGIC RELATIONS

Both the Carlin and Cortez deposits occur in lower-plate lower Paleozoic rocks that are exposed in windows through the Roberts Mountains thrust. Although the ages of mineralization are difficult to determine with certainty, both deposits occur in areas of Tertiary volcanism. The mineralization at the Cortez deposit is believed to date from 34 m.y. B.P., whereas that at Carlin may be as recent as 14 m.y. B.P. on the basis of the ages of closely associated igneous rocks.

Figure 24A shows a schematic cross section through the main ore zone at Carlin that illustrates the gross spatial relations of important features of the deposit. Although mineralization was related to high-angle faults, it was confined to replacement of the calcite component of a certain favorable (permeable) facies within the Roberts Mountains Formation, resulting in conformable-tabular ore bodies. The upper part of the ore zone has been oxidized, and conformability of the bottom of the oxidized zone to the present topography suggests that this zone must be partly a late or supergene feature of the deposit. Within the oxidized zone is a zone of leaching from which enormous amounts of carbonate have been removed by acidic solutions.

Jasperoid bodies, which extend outward from faults as much as 30 m and generally are concentrated in the upper part of the deposit, are a conspicuous feature at Carlin. Additional features are barite veins

and veinlets that are well developed within the leached zone but pinch out in the upper 15 to 20 m of the underlying unoxidized ores, where they commonly contain base-metal sulfides. Some quartz veinlets, which are critical for geochemical studies, occur deep in the unoxidized ores and in association with barite in the oxidized-leached zone. Finally, calcite veins are abundant both above and below the leached zone in the oxidized part of the deposit and occur to a minor extent deep within the unoxidized ores.

At Cortez, mineralization is largely discordant and occurs in brecciated and microfractured carbonate host rock near a 34-m.y.-old altered quartz porphyry (fig. 24B). Farther from this intrusive body, mineralization tends to be restricted to certain altered beds, just as at Carlin. Replacement jasperoid bodies are also present in the mineralized area. Barite and quartz veinlets are very rare, but calcite veins are very abundant. Oxidation of almost the entire ore body to the deepest levels exposed by mining makes it difficult to recognize primary mineralogy. On the basis of $\delta^{18}O$ data, the oxidation at Cortez seems to be a secondary feature of the deposit and to be related at least in part to supergene processes. Although no leached zone occurs at Cortez, the abundance of late calcite veins and their $\delta^{18}O$ data suggest the former presence of an overlying leached zone that has been removed by erosion.

GENERAL PARAGENETIC RELATIONS

The fine-grained texture of the ores and the general absence of clearly defined crosscutting relations between many important geologic features in carbonate-hosted disseminated gold deposits make a definitive determination of the sequence of events very difficult. Although exceptions in application will always occur at any specific deposit, a generalized paragenesis can probably best be constructed by combining the definitive paragenetic features of different deposits.

Main-stage mineralization in the unoxidized ores at Carlin was characterized by the formation of quartz, pyrite, kaolinite, and sericite, along with the introduction of gold, mercury, arsenic, antimony, and thallium—largely at the expense of the calcite component of the carbonate host rock (fig. 25A). One conspicuous feature of the deposit was the introduction or concentration of large masses of hydrothermal carbonaceous matter near faults. Most of the mineralization consists of free gold in association with pyrite; however, about 20 percent of the gold occurs dispersed in carbonaceous material and in association with arsenic minerals.

Late-stage mineralization in the upper parts of the ore bodies at Carlin was characterized by the introduction of barite veins and the precipitation of calcite veins and anhydrite outside the leached zone, the oxidation of pyrite and organic matter, and the removal of carbonate from the leached zone. The anhydrite was largely removed by later supergene processes. The exact paragenetic position of the jasperoid bodies at Carlin was unclear from previous studies. At Jerritt Canyon, however, the jasperoid bodies are severely deformed and are clearly cut by barite and coarse quartz veins, suggesting that these bodies are an early feature of the hydrothermal system. A similar paragenetic position for the jasperoids at both Carlin and Cortez is supported by $\delta^{18}O$ data.

From the time-space features of the Carlin deposits, the following scenario may be developed. Ore deposition was related to fluids that migrated upward along high-angle faults and outward along favorable permeable facies. Eventually, as indicated by fluid-inclusion data, the fluids boiled in the upper levels of the deposit. Condensation of acidic volatile materials in the upper levels of the deposit resulted in widespread acid leaching and, presumably, oxidation of the host rocks. After the hydrothermal system subsided, ground waters invaded the area and enlarged the oxidized zone to its present size. This scenario suggests that at Carlin the oxidation of the upper part of the deposit was both hypogene and supergene and has probably been going on since the boiling episode of the hydrothermal fluids. At other deposits, the degree of hypogene (versus supergene) oxidation probably depended on the timing and relative intensity of similar boiling episodes in their respective hydrothermal systems.

PHYSICOCHEMICAL ENVIRONMENT OF ORE DEPOSITION

Although materials suitable for fluid-inclusion studies were unavailable from the Cortez deposit, enough material was obtainable from the Carlin deposit to trace the temperature and salinity history of the hydrothermal fluids during main-stage mineralization and subsequent leaching and oxidation of the upper levels of the deposit. Figure 25B summarizes the temperature and salinity data for Carlin.

From measurements of the fluid-inclusion temperatures in quartz, realgar, and calcite from the unoxidized ores, Radtke and others (1980) concluded that most main-stage gold deposition occurred between 175° and 200°C, from fluids whose salinities were typically 3±1 weight percent NaCl equivalent. They observed no evidence of boiling in the main-stage ore fluids. This fluid-inclusion evidence suggests that the temperature of the fluids increased and that the fluids boiled sometime near the end of gold deposition. This boiling signaled an end to ore deposition and the beginning of leaching and oxidation in the uppermost parts of the ore deposit. Data from fluid inclusions in quartz, barite, realgar, sphalerite, and calcite in the oxidized-leached zone indicate that the temperature may have exceeded 200°C during boiling, and that the salinities of the fluids ranged as high as 18 weight percent NaCl equivalent in response to boiling and the dissolution of enormous amounts of carbonate in the upper part of the ore body. Evidence from fluid inclusions in late-stage calcite and quartz indicate that at the conclusion of the boiling phase, the hydrothermal system collapsed and low-temperature low-salinity ground waters invaded the system.

Assuming equilibrium conditions, other physicochemical parameters of the hydrothermal fluids can be approximated from the mineral assemblages. The

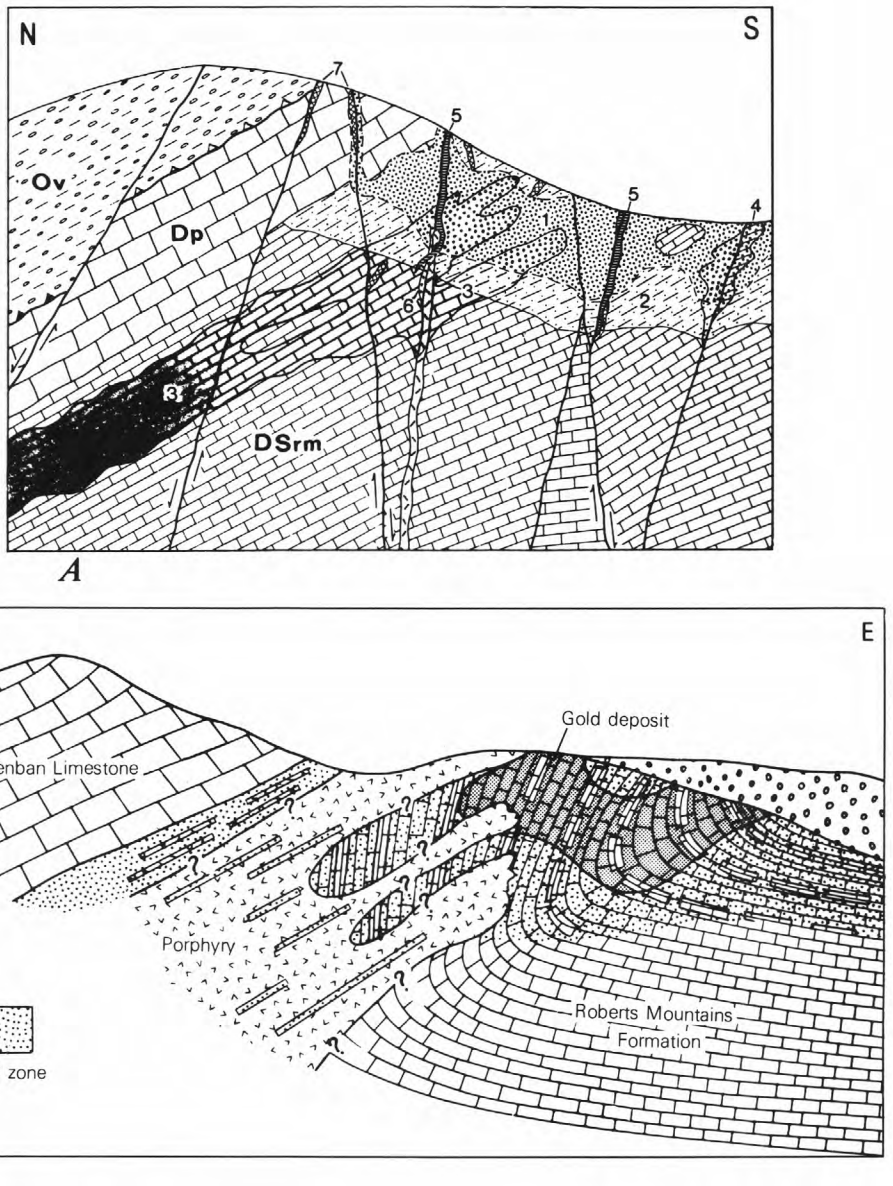

Figure 24. Important features of the Carlin and Cortez deposits. A, Schematic north-south cross section through main ore zone and Popovich Hill, Carlin district, showing important geologic features. Lithologic units include the Ordovician Vinini Formation (Ov), the Silurian-Devonian Roberts Mountains Formation (DSrm), and the Devonian Popovich Formation (Dp). 1, zone of leaching-alteration (stippled); 2, zone of late supergene alteration (dots and dashes), extending from surface downward through and below acid-leached zones; 3, main ore zone, including lower unoxidized ores (dark gray) and upper oxidized ores (light gray); 4, jasperoid bodies (solid-black-dot-and-line pattern)—note igneous dike emplaced along fault near center; 5, barite veins (horizontal-bar pattern) 6, quartz veins (dots); 7, calcite veins (crosshatched pattern). From Radtke and others (1980, fig. 7). Not to scale. B, Idealized east-west cross section through the Cortez gold deposit, showing rock units, gold deposit, alteration zone (lower extent of which is known), and overlying gravel. Slightly modified from Wells and others (1969, fig. 6). Not to scale.

pH of the main-stage preboiling solutions was neutral to mildly acidic, as indicated by the assemblage kaolinite-sericite-quartz in the unoxidized ores. The f_{O_2} was probably low from equilibration with organic matter in the country rocks and may have been close to the C-CO_2 buffer. Under these conditions, H_2S would have been the dominant sulfur species in the hydrothermal fluids. During the late-stage acid-leaching/oxidation

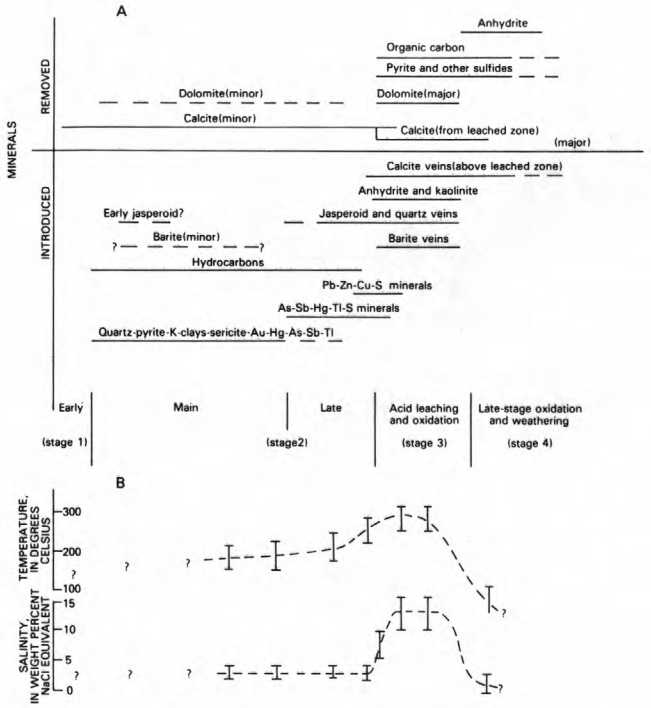

Figure 25. Mineral paragenesis, temperature, and salinity history of hydrothermal fluids in the Carlin gold deposit. A, Paragenesis of introduced and removed minerals. Acid leaching and accompanying oxidation (stage 3) were superimposed on late hydrothermal (stage 2) events in upper part of deposit. Extent to which main- and late-stage events, including mineralization, continued at depth during acid leaching in the upper levels is not known. B, Average temperature and salinity trends of hydrothermal fluids, as indicated by fluid-inclusion data, from Radtke and others (1980, fig. 8); curves are highly schematic.

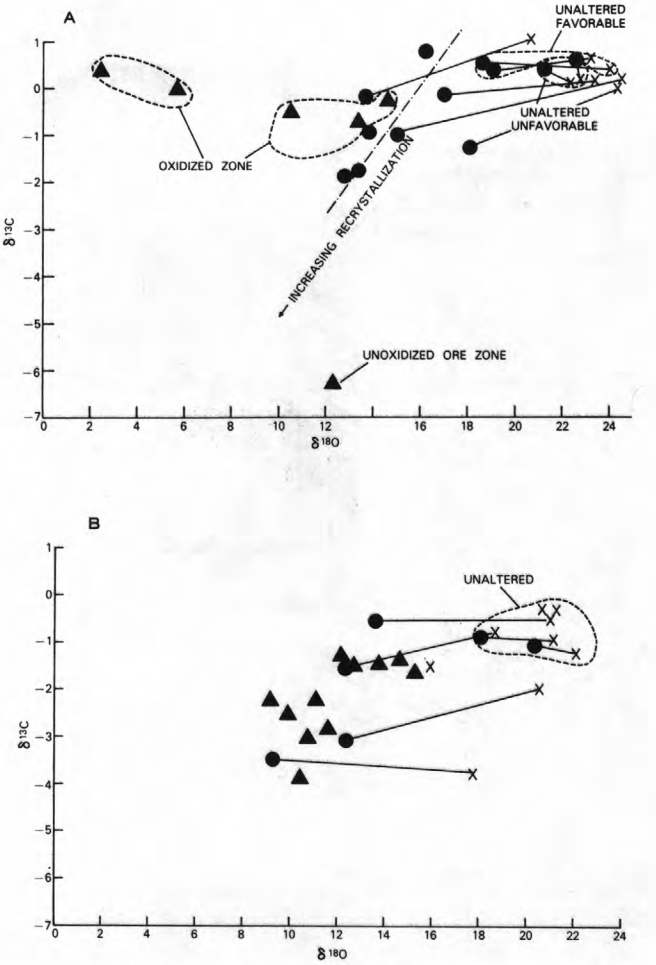

Figure 26. Summary of carbon- and oxygen-isotope data on altered and unaltered Roberts Mountains Formation, host rocks, and calcite veins at the Carlin (A) and Cortez (B) deposits, showing range of isotopic compositions of calcite (dots) and dolomite (X's) of unaltered favorable and unfavorable facies (tielines connect coexisting calcite and dolomite), altered host rocks, and calcite veins (triangles) in oxidized and unoxidized zones. Data from Rye and others (1974) and Radtke and others (1980).

episode in the upper levels of the deposit, the pH of the fluids was much lower, whereas the f_{O_2} was much higher, and SO_4^{2-} was the dominant sulfur species in the fluids. The sulfur-isotope data, however, indicate the SO_4^{2-} and H_2S were not in isotopic equilibrium, and by inference these species were probably not in chemical equilibrium throughout most of hydrothermal activity.

CARBON- AND OXYGEN-ISOTOPE DATA ON CARBONATES

Figure 26 plots the carbon- and oxygen-isotopic compositions of altered and unaltered Roberts Mountains host rocks and calcite veins in the Carlin and Cortez deposits. In the unaltered, unfavorable facies at Carlin (fig. 26), the isotopic compositions of the calcite and dolomite components are similar. In the unaltered, favorable facies, however, the calcite component is depleted in $\delta^{18}O$. This depletion probably occurred during diagenesis and may reflect the fact that the favorable facies is highly permeable and that its calcite component has long been susceptible to recrystallization and exchange with external fluids. Similar $\delta^{18}O$ depletions may be useful to locate favorable facies in other parts of the sedimentary section.

In the altered host rocks at Carlin, the carbonate component has undergone considerable ^{18}O depletion, whereas the isotopic composition of the dolomite component is virtually unchanged in both deposits. The degree of isotopic exchange in these components reflects the degree of recrystallization of the calcite component of the rock. The dolomite component is rarely mineralized or recrystallized, and so it has undergone only slight isotopic exchange.

The isotopic compositions of the calcite veins fall into three categories, only one of which is present in the Cortez deposit. One group of calcite veins from the oxidized zone at Carlin and all the veins at Cortez have oxygen-isotope compositions similar to that of the calcite component in the altered host rock. These veins

were probably derived from the acid-leached zone at Carlin and from an eroded overlying acid-leached zone at Cortez. Other calcite veins in the oxidized zone with low $\delta^{18}O$ values at Carlin were derived from low-temperature ground waters. The single calcite sample from the unoxidized ores at Carlin probably was derived by reprecipitation of the host-rock calcite, which was replaced during mineralization. The shift to lower $\delta^{13}C$ values in some calcite veins probably reflects a contribution of isotopically light organic carbon from the country rocks.

HYDROGEN- AND OXYGEN-ISOTOPE DATA ON FLUIDS

Figure 27 plots the hydrogen- and oxygen-isotopic compositions of the various fluids at Carlin and Cortez. These fluid compositions were determined directly from analyses of inclusion fluids and indirectly from calculations based on temperatures and the $\delta^{18}O$ and δD values of mineral separates, jasperoid bodies, and altered host rocks.

The very large negative δD values (-140±12 permil) indicate that the fluids in both deposits were largely, if not entirely, meteoric waters. The large $\delta^{18}O$ values (4±2 permil) for the main-stage fluids in both deposits indicate that during mineralization, the fluids underwent substantial exchange with carbonate or igneous rocks in the plumbing system, and that water/rock ratios in the systems were low. During the acid-leaching episode at Carlin, the $\delta^{18}O$ of the fluids increased owing to boiling and the dissolution of large amounts of ^{18}O-enriched carbonate. The earlier jasperoid masses precipitated from less exchanged and, probably, lower temperature ground water. Finally, late-stage carbonate deposition and oxidation of pyrite at both deposits resulted from relatively unexchanged low-temperature ground waters which invaded the deposit after the collapse of the hydrothermal system. Even more important than the details of the individual systems may be the fact that both these deposits, which may be 20 m.y. apart in age, formed from hydrothermal systems that had almost identical water-rock histories and that gold mineralization occurred when water/rock ratios were relatively low. The different generations shown in figure 27A for the Carlin deposit approximately coincide with the paragenetic stages in figure 25A.

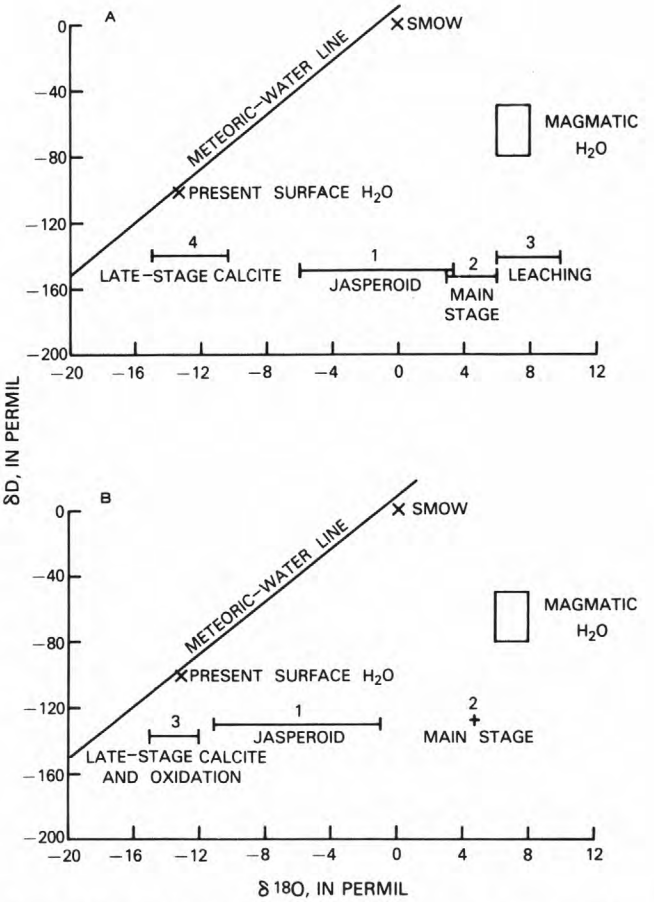

Figure 27. Hydrogen- and oxygen-isotopic compositions of water in fluids in the Carlin (A) and Cortez (B) deposits. Numbers 1 through 4 denote positions in paragenesis and approximately coincide with those in figure 25A. SMOW, standard mean ocean water. Data from Rye and others (1974) and Radtke and others (1980).

SULFUR-ISOTOPE DATA

Figure 28 summarizes sulfur-isotope data on the Carlin and Cortez deposits, as well as available data for other carbonate-hosted disseminated gold deposits in Nevada. The sulfides in both deposits are isotopically heavy; $\delta^{34}S$ values range from 4.2 to 16.1 permil. Except for Getchell, the sulfides in the other deposits also have $\delta^{34}S$ values that fall within this range. Barites from all the deposits, including Cortez and Carlin, range in $\delta^{34}S$ value from 27.5 to 31.7 permil. Although more data are needed, most deposits evidently have similar sulfur-isotope systematics. This result is highly significant because it implies a common geochemical history for most of the deposits.

Recent studies indicate that in low-temperature geothermal systems, sulfate and sulfide isotopic systematics are commonly governed by disequilibrium relations and that sulfate and sulfide can be viewed as independent components which did not interact in response to changing chemical conditions (Ohmoto and Rye, 1979). This noninteraction, in turn, implies that the sulfate and sulfide in the hydrothermal fluids had independent sources whose isotopic compositions determined those of the resulting sulfate and sulfide minerals.

The lower part of figure 28 shows the range in isotopic compositions for possible sulfur sources, of which igneous sulfur is insignificant. The most likely sources for the sulfide sulfur were sedimentary pyrite and (or) sulfur in organic matter within the sedimentary rocks. The $\delta^{34}S$ values of nearly 30 permil for barite in the deposits fall in the range typical for lower Paleozoic sedimentary barite deposits in Nevada (Rye and others,

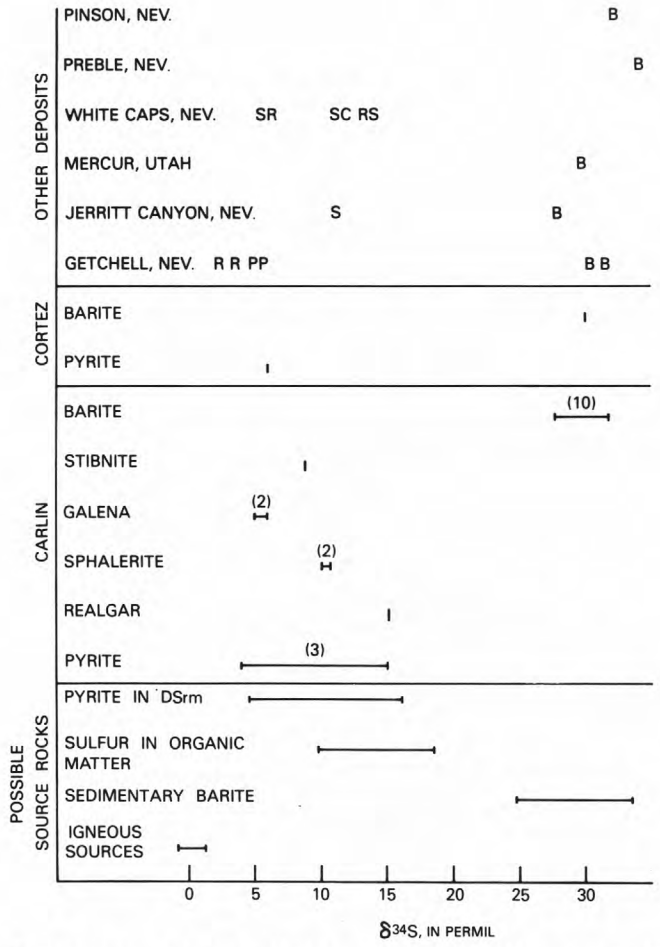

Figure 28. Sulphur-isotope data on sulfides in barite from Carlin, Cortez, and other disseminated gold deposits in Nevada. Minerals for other deposits include barite (B), cinnabar (C), pyrite (P), realgar (R), and stibnite (S). Lower part of diagram shows range of $\delta^{34}S$ values for possible sulfur sources. Range of $\delta^{34}S$ values for sedimentary barite in Nevada from R. O. Rye (unpub. data, 1980); ranges for sulfur in organic matter and igneous sources from Ohmoto and Rye (1979); other data from Rye and others (1974) and Radtke and others (1980).

1978), and so dispersed sedimentary barite was probably the source of the hydrothermal sulfate.

As mentioned above, the deposition of barite at Carlin seems to have been related to the boiling episode in the hydrothermal fluids. As illustrated in figure 29, this boiling event significantly affected the sulfur-isotope system. Because of the abundance of organic matter in the country rocks, the initial hydrothermal fluids were probably highly reduced and had a large H_2S/SO_4^{2-} ratio, although the H_2S and SO_4^{2-} were not in isotopic equilibrium and probably not in chemical equilibrium. The average approximate sulfur-isotopic compositions of the H_2S and SO_4^{2-} were about 10 and 30 permil, respectively. Sulfides with an average $\delta^{34}S$ value of 10 permil were precipitated from the initial solutions. During boiling of the hydrothermal fluids, H_2S and SO_4^{2-} were separated without significant changes in their isotopic compositions, and barites averaging about 30 permil in $\delta^{34}S$ value were precipitated, while H_2S with a $\delta^{34}S$ value of 10 permil was oxidized to sulfate. This separation led to the development of highly acidic solutions and the eventual precipitation of now largely removed anhydrite in the upper part of the ore body. Any alunite that may have formed during the boiling episode also would probably have had a $\delta^{34}S$ value of about 10 permil.

SUMMARY AND RECOMMENDATIONS FOR FUTURE RESEARCH

The geologic, chemical, and isotopic data permit at least a qualitative summary of the ore-forming process at Cortez and Carlin. Figure 30 shows an idealized cross section of the Carlin area, illustrating the proposed hydrothermal system for the deposit and its relation to structure, stratigraphy, and the presumed underlying intrusion. Recharge for the hydrothermal system was probably controlled by topographic highs formed by the highly brecciated Eureka Quartzite and by steep faults.

All the components introduced into Carlin-type deposits are abundant in the Roberts Mountains Formation and, presumably, in the other argillaceous and arenaceous carbonate units that compose most of the underlying sedimentary-rock suite. Experimental studies have shown that these introduced components could easily have been leached from the Paleozoic sedimentary rocks by hydrothermal fluids (Dickson and others, 1979). Thus, the source of components is not a problem for these systems. In fact, all the elements that were introduced into the Carlin and Cortez deposits are mobile in shallow hydrothermal systems (White, 1981), and so probably any rock could serve as a source of these elements, given enough area through which to pass heated fluid.

Gold transport and depositional mechanisms are currently not fully understood for the Carlin and Cortez deposits. Future research on disseminated gold deposits must be accompanied by experimental studies on gold solubility in systems chemically approximating the ore-forming fluids, to understand the full range of possibilities for gold deposition. Gold may have been transported as a chloride complex and precipitated by an increase in pH during the dissolution of calcite in the host rocks (Casadevall, 1976); this increase would also have precipitated pyrite and thus would account for the close association of gold and pyrite. Gold may also have been carried as an HS^- complex and precipitated when a decrease in sulfur concentration occurred during the formation of pyrite (Seward, 1973). At Carlin, gold may have been transported as arsenic and organic complexes, especially where large masses of introduced or remobilized hydrocarbons formed. Boiling or mixing of the hydrothermal fluids with low-temperature ground waters apparently was unimportant in the deposition of gold, even though the deposits were presumably emplaced at shallow depths and even though boiling was widespread after main-stage gold deposition. Both

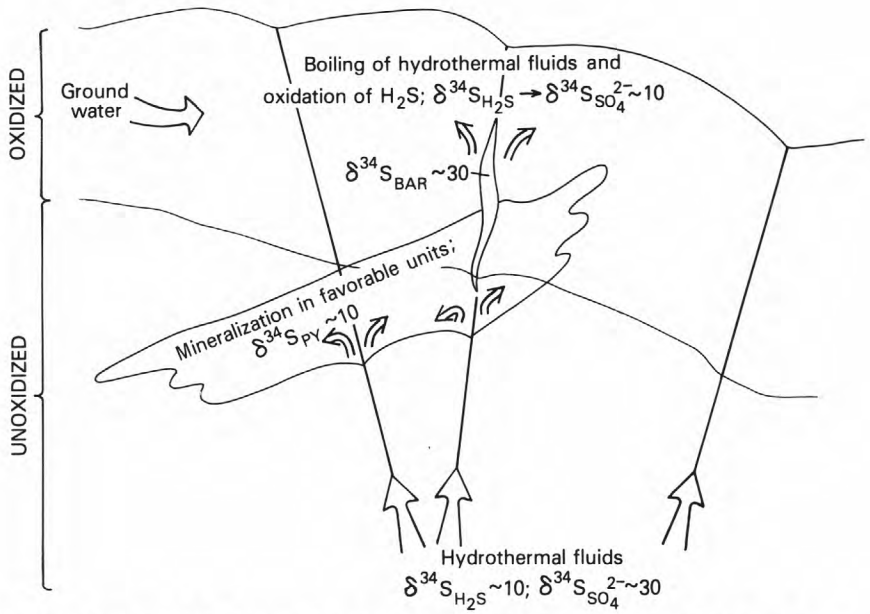

Figure 29. Model for sulfur-isotope distribution in the Carlin deposit, showing conformable ore zone with reduced and oxidized parts and crosscutting barite vein. Arrows show general direction of hydrothermal-fluid movement up steep faults and laterally along permeable facies; fluids eventually boiled in upper levels of deposit. Boiling event is superimposed on primary gold mineralization and probably coincides with barite (BAR) deposition. Deep in the unoxidized zone, sulfur was present as H_2S and SO_4^{2-} with $\delta^{34}S$ values of about 10 and 30 permil, respectively. Sulfur species were not in isotopic equilibrium and probably not in chemical equilibrium. During gold mineralization, pyrite (PYR) with a $\delta^{34}S$ value of 10 permil precipitated from the H_2S; later, barite with a $\delta^{34}S$ value of 30 permil precipitated from the SO_4^{2-}. During boiling, oxidation of the H_2S to SO_4^{2-} led to acid leaching by ground water in upper part of deposit.

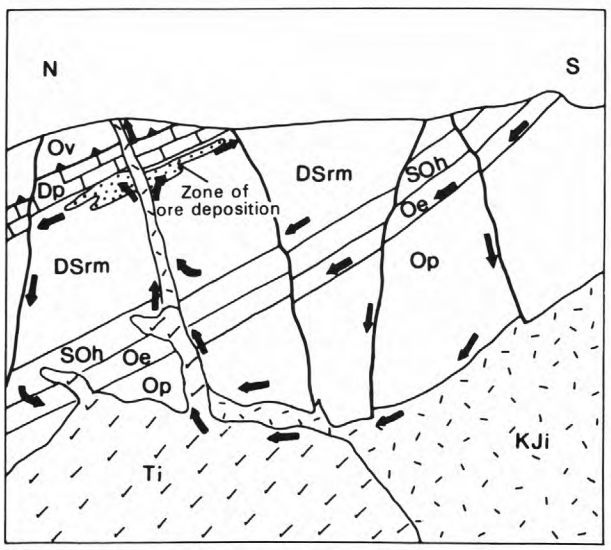

Figure 30. Schematic cross section illustrating hydrothermal systems and possible solution paths inferred for the Carlin gold deposit. Dp, Devonian Popovich Formation; Dsrm, Devonian and Silurian Roberts Mountains Formation; KJi, intrusive Cretaceous-Jurassic rocks; Oe, Ordovician Eureka Quartzite; Op, Ordovician Pogonip Group; Ov, Ordovician Vinini Formation; SOh, Silurian and Ordovician Hanson Creek Formation; Ti, Tertiary intrusive rocks. Modified from Radtke and others (1980, fig. 9).

these mechanisms may have been important at other deposits with different structural settings.

Additional integrated geologic-geochemical investigations should be made on other carbonate-hosted disseminated gold deposits as they become available for detailed study. In particular, better understanding of the origin of the jasperoid bodies and carbonaceous ores is needed. Future studies should concentrate on a more quantitative understanding of the hydrothermal system and its relation to the presumed underlying igneous system, as well as on the geochemistry of ore and gangue material transport and deposition. Eventually, the entire process could be subject to computer-based modeling. These studies could considerably affect the exploration for disseminated gold deposits. The argillaceous carbonates in the lower Paleozoic section of Nevada provided both a suitable source of ore-forming elements and a chemical trap for their deposition. The processes which created the Carlin and Cortez deposits are probably so fundamental that similar types of deposits may be expected anywhere igneous activity has developed a hydrothermal system in thick sections of carbonate rocks similar to those in the Carlin and Cortez areas.

REFERENCES CITED

Casadevall, T. J., 1976, Gold geochemistry: Transport and deposition in various hydrothermal systems: University Park, Pennsylvania State University, Ph. D. thesis, 22 p.

Dickson, F. W., Rye, R. O., and Radtke, A. S., 1979, The Carlin gold deposit as a product of rock-water interactions, in Ridge, J. D., ed., Papers on mineral deposits of western North America: Nevada Bureau of Mines and Geology Report 33, p. 101-108.

Ohmoto, Hiroshi, and Rye, R. O., 1979, Carbon and sulfur isotopes, in Barnes, H. L., ed., Geochemistry of hydrothermal ore deposits: New York, John Wiley and Sons, p. 509-567.

Radtke, A. S., Rye, R. O., and Dickson, F. W., 1980, Geology and stable isotope studies of the Carlin gold deposit, Nevada: Economic Geology, v. 75, no. 5, p. 641-672.

Rye, R. O., Doe, B. R., and Wells, J. D., 1974, Stable isotope and lead isotope studies of the Cortez, Nevada, gold deposit and surrounding area: U.S. Geological Survey Journal of Research, v. 2, no. 1, p. 13-23.

Rye, R. O., Shawe, D. R., and Poole, F. G., 1978, Stable isotope studies of bedded barite at East Northumberland Canyon in Toquima Range, central Nevada: U.S. Geological Survey Journal of Research, v. 6, no. 2, p. 221-229.

Seward, T. M., 1973, Thio complexes of gold and the transport of gold in hydrothermal ore solutions: Geochimica et Cosmochimica Acta, v. 37, no. 3, p. 379-399.

Wells, J. D., Stoiser, L. R., and Elliott, J. E., 1969, Geology and geochemistry of the Cortez gold deposit, Nevada: Economic Geology, v. 64, no. 5, p. 526-537.

White, D. E., 1981, Active geothermal systems and hydrothermal ore deposits: Economic Geology, 75th anniversary volume, p. 392-423.

Characteristics of Boiling-Water-Table and Carbon Dioxide Models for Epithermal Gold Deposition

By Charles G. Cunningham

CONTENTS

INTRODUCTION

Hydrothermal ore fluids are multicomponent fluids in which many complex and interrelated factors influence the actual deposition of metals. Some of the more significant of these factors include cooling, changes in pH, interaction with the wallrocks, oxidation by mixing with oxygenated ground water or by contact with the atmosphere, and physicochemical reactions that modify the complexing species. In addition to these factors, boiling or effervescence of a hydrothermal fluid can cool or alter the chemistry of the fluid and lead directly or indirectly to the deposition of metals. The relation between boiling and ore deposition has been emphasized recently by many authors (Ewers and Keays, 1977; Kamilli and Ohmoto, 1977; Cunningham, 1978; Buchanan, 1980; Clifton and others, 1980; Bodnar, 1981; Drummond, 1981; Berger and Eimon, 1982; Romberger, 1982; Heald-Wetlaufer and others, 1983), but the interdependence of boiling and gold deposition has not been conclusively demonstrated. In this chapter I propose two models that illustrate specific aspects of this complex process. These models are intended to explain two ways in which boiling can cause deposition of gold and to suggest fluid-inclusion and mineral-paragenetic criteria that may be useful in precious-metal exploration.

Acknowledgment.—The manuscript was greatly improved by helpful suggestions and perceptive reviews by T. A. Steven, R. O. Rye, R. J. Bodnar, B. R. Berger, and G. W. Nieman. One purpose of this chapter has been to propose ideas, generate discussion, and develop criteria to test models, and thus far it has been very successful in this endeavor.

BOILING-WATER-TABLE MODEL

Gold can be deposited at or near the water table by boiling, as a result of certain relatively simple geologic and geochemical processes. Gold is soluble to varying degrees in aqueous sulfide solutions, in which the solubility depends on pressure, temperature, and sulfur concentration. Gold is most soluble when the pH is nearly neutral or slightly alkaline (Seward, 1973; Casadevall, 1976; Romberger, 1982). If a rising hydrothermal solution containing gold in a bisulfide complex, such as $Au(HS)_2^-$, were to reach a water table in which boiling was occurring (fig. 31), H_2S would be selectively partitioned into the vapor phase (steam) above the water table. There, the H_2S could readily be oxidized by atmospheric oxygen and ultimately form H_2SO_4 in the condensate, which, in turn, could react with the host rocks to form an argillic-alteration mineral assemblage. Loss of H_2S by boiling would destabilize the gold-sulfide complex, and native gold would be precipitated. In addition, the top of the water table would be oxidized by mixing back of the barren, but oxidized, condensate; and native gold, which is relatively insoluble in an oxidized acidic solution, would precipitate. Silica also is less soluble in an oxidized acidic solution than under the conditions at greater depth and should precipitate. Any barium in solution would combine with the sulfate to form barite. In this model, gold, barite, and quartz would be precipitated within a relatively narrow vertical zone controlled by the position of the top of the paleowater table. This position would fluctuate up and down with changes in

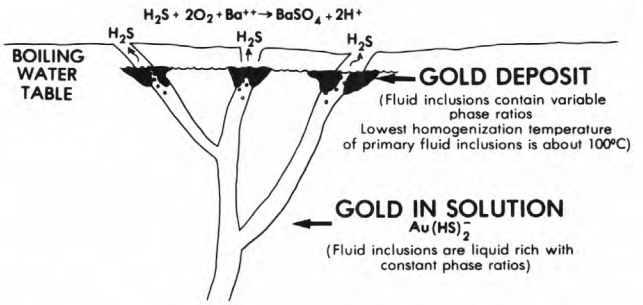

Figure 31. Boiling-water-table model for epithermal gold deposition.

the permeability, heat flow, and hydrology of the recharge areas, but still within a limited vertical range.

Fluid-inclusion data, as well as mineralogic and paragenetic relations, may be useful in recognizing the conditions illustrated in the boiling-water-table model (fig. 31). Native gold would be expected to coprecipitate with barite, and the host rock would be intensely argillized. Samples of the boiling solution trapped as fluid inclusions in the precipitating minerals, especially in quartz and barite, are amenable to study to determine the pressures, temperatures, and compositions of the hydrothermal fluids. The barite crystal lattice, however, is susceptible to stretching from increases in pressure within fluid inclusions during heating runs and during sample preparation (R. J. Bodnar, oral commun., 1981), and so measured temperatures may not be reliable, especially above about 100°C. Although fluid inclusions in the barite would probably have varying phase ratios, the lowest homogenization temperature of either the liquid or vapor phase would be the boiling temperature, which would depend on elevation, depth below the water table, fluid composition, and the presence of other gases in solution. The highest homogenization temperature in an $NaCl-H_2O$ system would be the critical temperature for the fluid composition. Theoretically, any temperature between these limits is obtainable by trapping various combinations of liquid and vapor. Although boiling can occur deeper in a system if the necessary pressure-temperature-composition conditions are met, higher pressures would be reflected by higher homogenization temperatures.

The boiling-water-table model was suggested by paragenetic and preliminary fluid-inclusion data from the Summitville district, in the southeastern part of the mid-Tertiary San Juan volcanic field of southern Colorado. Geologic mapping by Steven and Ratté (1960) showed that mineralization was related to a late-stage volcanic dome (the South Mountain dome) emplaced along the west margin of Summitville caldera (Lipman, 1975; Steven and Lipman, 1976). That part of the South Mountain dome containing most of the mines is currently being studied in detail (Perkins and Nieman, 1983).

The ore in the Summitville district occurs in several geologic environments. Much of the ore is concentrated in a near-surface oxidized zone, where native gold, barite, and goethitic vuggy silica are present in pipes, pods, and tabular masses (Perkins and Nieman, 1983). Deeper in the system, gold occurs in association with iron and copper sulfides and sulfosalts (Perkins and Nieman, 1983), and the transition zone may have been the position of a boiling water table.

A remarkable boulder weighing 51.7 kg, apparently containing the largest amount of native gold in any single equivalent-sized specimen yet found in Colorado, was discovered in talus on the slopes of the South Mountain dome in 1975. It is currently on display at the Denver Museum of Natural History and is called the Gold Boulder of Summitville. This boulder (fig. 32) contains intergrown native gold, coarse-crystalline barite, and some quartz, forming a matrix surrounding argillically altered quartz latite breccia fragments (Charles Beverly, written commun., 1978). Textural relations suggest that the native gold, barite, and quartz were coprecipitated and that the quartz latite could have been altered by the same fluids. A preliminary study of the fluid inclusions in two samples of barite from this boulder indicates that the barite and gold were deposited from an aqueous solution that was boiling at about 100°C. No CO_2 or daughter minerals were observed in the fluid inclusions. The Summitville gold deposit has a complex history of gold deposition (Perkins and Nieman, 1983), and the Gold Boulder of Summitville represents only one part of this system. Nonetheless, much gold was concentrated in a small part of the system which may have been situated at the paleowater table.

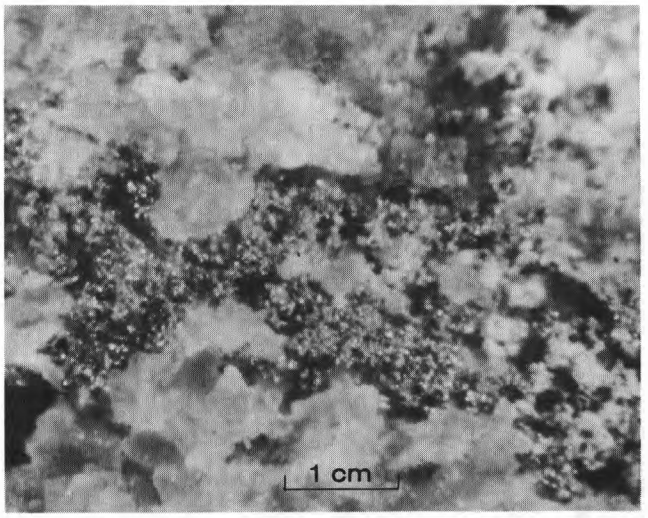

Figure 32. Gold Boulder of Summitville, showing codeposited gold (dark) and barite (white). Photographed area is about 6 cm wide. The boulder is presently located in the Denver Museum of Natural History. Photograph courtesy of Denver Museum of Natural History.

CARBON DIOXIDE MODEL

Gold can be deposited within a hydrothermal system below the water table in response to several factors, including local boiling or effervescence of a saline carbonate solution. Such effervescence creates a mildly saline aqueous phase and an effectively immiscible CO_2-vapor phase. Carbon dioxide is a common constituent of hydrothermal fluids in gold districts (Nash and Cunningham, 1973; Luce and others, 1979; Buchanan, 1980; Harris, 1980), and when boiling or effervescence occurs, the CO_2 partitions itself between the phases according to local pressure-temperature-composition conditions.

Although carbon dioxide apparently does not combine directly with gold to form significantly soluble complexes, it can influence gold solubility indirectly by its effect on other gold complexes. Gold is soluble as a chloride complex under conditions of low pH, intense oxidation, high chloride activity (Romberger, 1982), and low total sulfur content (R. J. Bodnar, written commun., 1982). Gold in a chloride complex at higher temperatures can be deposited simply by a decrease in temperature (Henley, 1973), reduction, an increase in the pH, or dilution (Romberger, 1982). When a

hydrothermal fluid containing CO_2 moves upward into regions of lower pressure and temperature, boiling begins, and CO_2 is partitioned into the vapor phase. As the CO_2 content of the coexisting aqueous phase decreased, the pH of the solution increases. Such an increase in the pH lowers the solubility of gold as a chloride complex (Romberger, 1982) and may result in deposition of the gold (fig. 33).

A direct implication of this model is that gold would be deposited where a hydrothermal fluid begins to boil or effervesce. Because hydrothermal fluids in an epithermal environment are commonly contained in fractures under hydrostatic pressure, the elevation of the ground-water table is a major factor in controlling pressure and, consequently, the depth of boiling. Depending on local factors, gold can be deposited at a relatively constant depth (that is, elevation; Kamilli and Ohmoto, 1977; Buchanan, 1980) beneath that water table.

In certain deposits, fluid inclusions may be useful (Nash, 1972; Roedder, 1977) in determining the position of a given point within a vein system relative to the gold-bearing zone (Bodnar, 1981). As shown on figure 33, fluid inclusions from beneath the gold-bearing zone would be trapped from a homogeneous aqueous fluid and thus would have uniform H_2O–CO_2-vapor phase ratios (Roedder, 1979). Inclusions trapped in the gold-bearing zone would have varying phase ratios in association with gold, whereas those above would have varying phase ratios in association with relatively barren gangue. Carbon dioxide may be visible in fluid inclusions as an immiscible fluid phase forming an annular ring around the vapor bubble if the proper pressure-temperature-composition conditions prevailed at the time of trapping (Nash and Cunningham, 1973); otherwise, a crushing stage (Roedder, 1970) or other quantitative analytical equipment is needed to determine its presence. Some quantitative information about the miscibility gap in the system H_2O–CO_2-NaCl has been published (Takenouchi and Kennedy, 1964, 1965), but complete data are not yet available. A detailed systematic study to fill this gap is currently in progress (R. J. Bodnar, oral commun., 1982).

The carbon dioxide model was suggested by paragenetic and preliminary fluid-inclusion data from the Mahd adh Dahab gold deposit in Saudi Arabia. This deposit was the largest and most productive mine in Saudi Arabia in ancient and modern times (Luce and others, 1979). Both the ancient and recent workings and a new deposit recently discovered immediately to the south are mostly in north-south-trending gold-bearing quartz veins (Worl, 1979). Recent geologic studies (Rye and others, 1983) indicate that these veins are related to a Precambrian rhyolite stock. Preliminary studies of the quartz veins indicated that the fluid inclusions in barren veins are all liquid rich and homogenize between 110° and 125°C, whereas those in the gold-bearing veins are characterized both by abundant vapor-rich phases and by contents that homogenize to a liquid between 125° and 154°C (Rye and others, 1983). Although carbon dioxide is known to be present in the hydrothermal system (Luce and others, 1979), the detailed time-space-composition relations between the barren and gold-bearing veins have not yet been established. Thus, in such an area where both mineralized and barren quartz veins are present, fluid inclusions may be a useful tool for determining which hydrothermal systems are potentially productive.

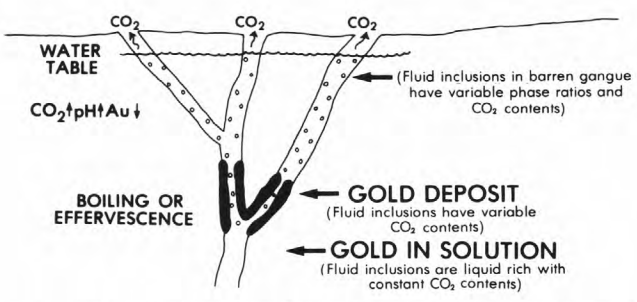

Figure 33. Carbon dioxide model for epithermal gold deposition.

REFERENCES CITED

Berger, B. R., and Eimon, Paul, 1982, Comparative genetic model characteristics of epithermal gold-silver deposits: American Institute of Mining and Metallurgical Engineers Preprint 82-13, 25 p.

Bodnar, R. J., 1981, Use of fluid inclusions in mineral exploration: Comparison of observed features with theoretical and experimental data on ore genesis [abs.]: Geological Society of America Abstracts with Programs, v. 13, no. 7, p. 412.

Buchanan, L. J., 1980, Ore controls of vertically stacked deposits, Guanajuato, Mexico: American Institute of Mining and Metallurgical Engineers Preprint 80-82, 26 p.

Casadevall, T. J., 1976, Sunnyside mine, Eureka mining district, San Juan County, Colorado: Geochemistry of gold and base metal ore formation in the volcanic environment: University Park, Pennsylvania State University, Ph. D. thesis, 146 p.

Clifton, C. G., Buchanan, L. J., and Durning, W. P., 1980, Exploration procedure and controls of mineralization in the Oatman mining district, Oatman, Arizona: American Institute of Mining and Metallurgical Engineers Preprint 80-143, 45 p.

Cunningham, C. G., 1978, Pressure gradients and boiling as mechanism for localizing ore in porphyry systems: U.S. Geological Survey Journal of Research, v. 6, no. 6, p. 745-754.

Drummond, S. E., Jr., 1981, Boiling and mixing of hydrothermal fluids; Chemical effects on mineral precipitation: University Park, Pennsylvania State University, Ph. D. thesis, 380 p.

Ewers, G. R., and Keays, R. R., 1977, Volatile and precious metal zoning in the Broadlands geothermal field, New Zealand: Economic Geology, v. 72, no. 7, p. 1337-1354.

Harris, M., 1980, Gold mineralization at the Salave gold prospect, northwest Spain: Institute of Mining and Metallurgy Transactions, v. 89, sec. B, p. B1-B4.

Heald-Wetlaufer, Pamela, Hayba, D. O., Foley, N. K., and Goss, J. A., 1983, Comparative anatomy of epithermal precious- and base-metal districts hosted by volcanic rocks: A talk presented at the

GAC/MAC/GGU Joint Annual Meeting, May 11-13, 1983, Victoria, British Columbia [Canada]: U.S. Geological Survey Open-File Report 83-710, 16 p.

Henley, R. W., 1973, Solubility of gold in hydrothermal chloride solutions: Chemical Geology, v. 11, no. 2, p. 73-87.

Kamilli, R. J., and Ohmoto, Hiroshi, 1977, Paragenesis, zoning, fluid inclusion, and isotopic studies of the Finnlandia vein, Colqui District, Central Peru: Economic Geology, v. 72, no. 6, p. 950-982.

Lipman, P. W., 1975, Evolution of the Platoro caldera complex and related volcanic rocks, southeastern San Juan Mountains, Colorado: U.S. Geological Survey Professional Paper 852, 128 p.

Luce, R. W., O'Neil, J. R., and Rye, R. O., 1979, Mahd adh Dhahab: Precambrian epithermal gold deposit, Kingdom of Saudi Arabia: U.S. Geological Survey Open-File Report 79-1190 (Saudi Arabian Project Report 256), 33 p.

Nash, J. T., 1972, Fluid-inclusion studies of some gold deposits in Nevada, in Geological Survey research, 1972: U.S. Geological Survey Professional Paper 800-C, p. C15-C19.

Nash, J. T., and Cunningham, C. G., Jr., 1973, Fluid-inclusion studies of the fluorspar and gold deposits, Jamestown District, Colorado: Economic Geology, v. 68, no. 8, p. 1247-1262.

Perkins, R. M., and Nieman, G. W., 1983, Epithermal gold mineralization in the South Mountain volcanic dome, Summitville, Colorado, in The genesis of Rocky Mountain ore deposits: Changes with time and tectonics: Denver, Colo., Denver Region Exploration Geologists' Society, p. 165-171.

Roedder, Edwin, 1970, Application of an improved crushing microscope stage to studies of the gases in fluid inclusions: Schweizerische Mineralogische und Petrographische Mitteilungen, v. 50, no. 1, p. 41-58.

----- 1977, Fluid inclusions as tools in mineral exploration: Economic Geology, v. 72, no. 3, p. 503-525.

----- 1979, Fluid inclusions as samples of ore fluids, chap. 14 of Barnes, H. L., ed., Geochemistry of hydrothermal ore deposits (2d ed.): New York, John Wiley & Sons, p. 684-737.

Romberger, S. B., 1982, Transport and deposition of gold hydrothermal systems at temperatures up to 300,C [abs.]: Geological Society of America Abstracts with Programs, v. 14, no. 7, p. 602.

Rye, R. O., Hall, W. E., Cunningham, C. G., Czamanske, G. K., Afifi, A. K., and Stacey, J. S., 1983, Preliminary mineralogic, fluid inclusion, and stable isotope study of the Mahd adh Dhahab gold mine, Kingdom of Saudi Arabia: Saudi Arabian Deputy Ministry for Mineral Resources Report: U.S. Geological Survey Open-File Report 83-291, 26 p.

Seward, T. M., 1973, Thio complexes of gold and the transport of gold in hydrothermal ore solutions: Geochimica et Cosmochimica Acta, v. 37, no. 3, p. 379-399.

Steven, T. A., and Lipman, P. W., 1976, Calderas of the U.S. Geological Survey Professional Paper 958, 35 p.

Steven, T. A., and Ratté, J. C., 1960, Geology and ore deposits of the Summitville district, San Juan Mountains, Colorado: U.S. Geological Survey Professional Paper 343, 70 p.

Takenouchi, Sukune, and Kennedy, G. C., 1964, The binary system H_2O-CO_2 at high temperatures and pressures: American Journal of Science, v. 262, no. 9, p. 1055-1074.

----- 1965, The solubility of carbon dioxide in NaCl solutions at high temperatures and pressures: American Journal of Science, v. 263, no. 5, p. 445-454.

Worl, R. G., 1979, Ore controls of the Mahd adh Dhahab gold mine, Kingdom of Saudi Arabia, in Evolution and mineralization of the Arabian-Nubian Shield: Oxford, Pergamon (Jeddah, Saudi Arabia, King Abdulaziz University, Institute of Applied Geology Bulletin 3), v. 2, p. 93-106.

Geologic-Geochemical Features of Hot-Spring Precious-Metal Deposits

By Byron R. Berger

CONTENTS

INTRODUCTION

Recent geologic studies of epithermal precious-metal deposits in the Western United States have increased our understanding of the physical and chemical properties of deposits formed in the near surface of hot springs. These deposits have become known as hot-spring precious-metal occurrences (Berger and Eimon, 1982; Silberman, 1982). Ore deposits of this type contain both bonanza ores and lower grade, bulk-minable ores. Typical examples are the McLaughlin (Knoxville) district, Calif. (for example, the Manhattan mine; Becker, 1888; Averitt, 1945), Round Mountain, Nev. (Berger and Tingley, 1980), the Hasbrouck Peak (Divide) district, Nev. (Silberman, 1982), the DeLamar mine, Idaho (William Strowd, commun., 1982), and Sulphur, Nev. (Wallace, 1980). This chapter describes the geologic features and trace-element associations in hot-spring precious-metal deposits and briefly compares the geochemistry of this deposit type with that of other types of precious-metal occurrences. The geologic model presented here is largely that of Berger and Eimon (1982), which was based on those of Berger and Tingley (1980), Berger and others (1981), and Silberman (1982).

GEOLOGIC CHARACTERISTICS OF HOT-SPRING PRECIOUS-METAL DEPOSITS

Most epithermal precious-metal mineral deposits were probably formed by hydrothermal systems that vented thermal waters to the surface in some manner. However, deposition from very hot fluids at or very near the Earth's surface results in a set of geologic characteristics that set hot-spring deposits somewhat apart from those epithermal deposits formed at greater depths. These characteristics include extensive surficial and near-surface silicification and widespread hydrothermal brecciation.

Figure 34 shows a schematic cross section of the geologic features found in hot-spring deposits. The generalized sequence of alteration and structure becomes increasingly complex upward in the system but generally follows a vertical sequence downward from the surface: silicification—quartz+adularia+hydromica—quartz+chlorite. The actual spatial and temporal

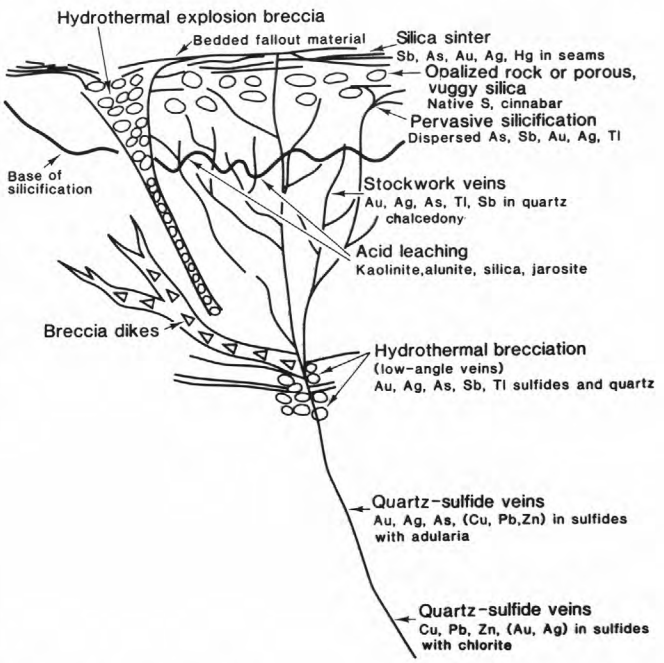

Figure 34. Schematic cross section illustrating geologic features found in hot-spring precious-metal deposits, showing generalized vertical geochemical zoning (from Berger and Eimon, 1982, fig. 11a). Actual spatial and temporal relations between geologic features may vary significantly from deposit to deposit.

relations between the geologic features may vary significantly from deposit to deposit.

Hot-spring deposits are associated with the formation of silica sinter on the surface. Sinter is deposited intermittently during the course of mineralization at depth, and Ag, As, Au, Hg, Sb, and Tl values occur sporadically within the sinter. The highest trace-element concentrations generally occur in closest proximity to the vents, and their occurrence in bedded zones in the sinter reflects multiple periods of precious-metal transport in hydrothermal fluids. Fluids expelled onto flat or sloping surfaces or in bodies of water exhibit stratiform chemical enrichments. Examples of sinter are observable at Hasbrouck Peak and Sulphur, Nev., at McLaughlin, Calif., and in a collapse breccia at Round Mountain, Nev.

The sinter is underlain by a zone of intense silicification of the country rock. The silicified zone forms a seal or capping over the hydrothermal system and is characterized in ore-bearing deposits (for example, Round Mountain, Hasbrouck Peak) by repeated episodes of brecciation. Each episode of fracturing of the capping is followed by self-sealing with silica. The brecciated zones are interpreted as representing the main hydrothermal flues, and clasts in the breccia may be remnants of earlier periods of brecciation and self-sealing, indicating that repeated activity was focused in the same hydrothermal conduits. Sinter is deposited intermittently above the capping during periods that follow rupturing of the cap and before complete self-sealing. The number of episodes of brecciation is difficult to document; repeated rupturing seems to be important in the development of high concentrations of precious metals, although multiple brecciation does not assure the presence of ore. Berger and Tingley (1980) found the most extensive underground mining at Round Mountain to have taken place beneath those areas within the silicified capping that showed evidence of multiple brecciation events. The thickness of the silicified zone may be as much as several hundred meters, depending on the host-rock composition and permeability, the amount of silica being transported in the system, and the duration of the thermal activity. If the host rock is impermeable and brittle, the silica cap may consist essentially of numerous crosscutting quartz veins that act as a seal.

The breccia zones in the silica cap generally may be followed downward beneath the silica cap into stockwork veining, as can be seen at DeLamar, Idaho, and Round Mountain, Nev. The veins commonly consist of either quartz or quartz-adularia gangue, with narrow selvages of hydromica alteration of mafic minerals adjacent to the veins. The veins, which contain sporadic precious-metal and sulfide ore in veinlets, may extend upward into the silica cap, such as at Round Mountain and Hasbrouck Peak. Some of the veins display a chambered structure, and normally they have sharp contacts with the wallrock. The veins also are generally narrow, and only a few exceed a few centimeters in total thickness. Those at Round Mountain are generally less than 5 cm thick, whereas many veins at DeLamar are as much as 15.2 to 20.3 cm thick. The abundance of veining depends on the structural controls of the hydrothermal system and on the brittleness of the host rocks, as do the vertical and horizontal extent of individual veins. At Round Mountain, the quartz-adularia veins are controlled largely by sets of closely spaced vertical fractures, whereas faulting and brittle fracture seem to be more important features at DeLamar. I believe that the veins represent a deeper part of the conduits feeding the cap and sinter, and that the brecciated parts of the cap are spatially related to the veining.

Explosive brecciation also is commonly evident beneath the silicified cap in the form of veins, pipes, and dikes. Some of these breccias consist wholly of uncemented rubbly host rock, with clast sizes ranging from sand to large boulders; aggregates of the finer particles generally wrap around the larger fragments. These uncemented breccias commonly break through to the surface, as implied at Round Mountain by the presence of sinter or surface silica deposits in adjacent cemented breccia pipes. The breccias may disrupt the sinter, form explosion craters (maars), and create "fallout" aprons. The fallout deposits appear as sedimentary breccias and consist of poorly sorted fragments of the silica cap or other parts of the alteration sequence. Any condensate carried in the explosive event may precipitate metals when trapped in the bedded material. At Round Mountain, the uncemented breccias show little evidence of large-scale vertical transport of rock fragments. Stratigraphic continuity is common through the breccia from wall to wall, and little exotic material is present. This continuity is particularly well observed at Hasbrouck Peak, where fine-laminated sediment is traceable across the jumbled breccia zones. Most of the uncemented breccia fragments are highly angular. The brecciated zones may range from a few centimeters to many meters across and may extend for several hundred meters in the vertical dimension; at Round Mountain, one breccia pipe is at least 150 m high. The absence of cementing in the breccias suggests that the hydrothermal fluids were not able to recharge after the hydrothermal expansion into the brecciated zone. I believe that these breccias formed by predominantly gaseous discharges and that the aqueous fluids may have been prevented from flooding the breccias either by sealing due to rapid mineral deposition at the focus of the brecciation or because the breccias may have formed during a late-stage period of steam dominance in the geothermal system. At DeLamar, some uncemented breccias disrupt earlier siliceous ores. In such places, these breccias probably formed at different times during the lifetime of the geothermal system. The open breccias appear to constitute ore only where the rock was mineralized before brecciation.

Another type of hydrothermal breccia beneath the silica cap is a cemented breccia. The cement is predominantly silica, with or without accompanying sulfides and precious metals. These breccias are an important source of the "bonanza" ore at Round Mountain and Hasbrouck Peak. At all of the type deposits, many of the cemented breccias show the same evidence of repeated brecciation and cementation that is evident in the silicified cappings. This repeated brecciation indicates that the hydrothermal fluids were continually focused in certain conduits. The cemented breccias may be pipes, podlike bodies, or veins with sand-size rock fragments in the silica matrix. At Round Mountain, vuggy areas commonly occur between the breccia fragments in large breccias exposed in the

underground workings; some of these vugs are filled with euhedral quartz and sulfides containing visible free gold. Quartz-adularia veins either crosscut the cemented breccias at Round Mountain or occur as clasts in the breccias. At all of the type deposits, there is a considerable variety of cemented breccias that were probably formed by diverse genetic processes; however, further research is needed to fully understand these features and to relate them to other aspects of ore-bearing hot-spring systems.

Where preexisting low-angle weaknesses are present in the host rock, such as joints in bedding planes, lateral extension of the hydrothermal brecciation can result in "flat veins." Low-angle cooling joints in welded tuff at Round Mountain form such a zone of weakness, and cemented breccias and multiple injections of quartz veins or siliceous breccias containing sulfides and precious metals make up flat veins (for example, the Los Gazabo and Mariposa veins). These low-angle veins tend to dip into the centers of massive brecciation (fig. 35). Multiple episodes of brecciation at one center may result in a substantial dilation of the low-angle-vein zone, such that it thickens to several meters adjacent to the breccia and decreases in thickness away from the breccias. Stockwork quartz veins can occur in the hanging walls of the low-angle veins.

Explosive brecciation of all types that either is near to or has breached the surface indicates that hot-spring precious-metal systems become overpressured, with a consequent violent and sudden release of energy. Thus, the formation of a seal or cap on the system seems to be a necessary requisite for the development of the rest of the system.

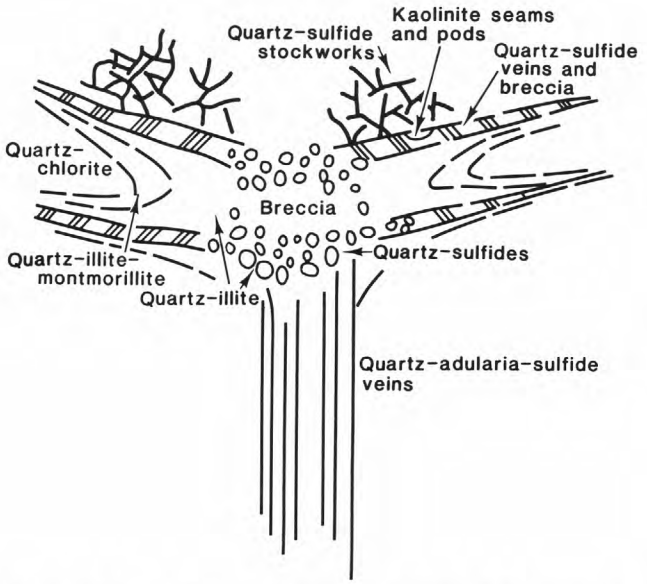

Figure 35. Idealized cross section of center of hydrothermal brecciation, showing alteration and veining features (from Berger and Eimon, 1982, fig. 11b). Flat veins develop where there is a prebrecciation and prevein low-angle structure already present; high-angle fractures would result in high-angle breccia veins.

The geologic evidence at Round Mountain, Hasbrouck Peak, McLaughlin, and DeLamar is best explained as a process of sealing followed by brecciation that occurs in more than one cycle. Corroborative geologic evidence for self-sealing and sudden pressure release at Round Mountain is found in fluid-inclusion-filling temperatures in a vein interpreted to have formed over a short period. Near the top of Round Mountain, two generations of quartz occur in a single quartz-adularia vein that is approximately 30 to 45 m below the paleosurface (interbedded lake sediment and sinter indicate that a lake of unknown depth may have overlain the hydrothermal system). Quartz intergrown with adularia has filling temperatures of approximately 245°C, whereas euhedral quartz interstitial to the quartz-adularia has filling temperatures of approximately 210°C (B. R. Berger, unpub. data, 1982). A vein about 90 to 120 m deeper in the system contains quartz that yields a filling temperature of approximately 268°C. Varying vapor/liquid ratios in the 245°C inclusions from the top of Round Mountain are interpreted to indicate that the hydrothermal system was boiling during quartz-adularia deposition. At constant NaCl and CO_2 contents, a temperature increase from 210° to 245°C would result in a significant pressure increase, probably enough to fracture the rock.

When the silica seal is ruptured, a sudden pressure drop occurs, and the hydrothermal fluid boils. Chemical and temperature changes accompanying this rapid boiling may cause the deposition to quartz, sulfides, and precious metals (Drummond, 1981). Brecciation is caused by a simultaneous volume expansion. The gases evolved during boiling may recondense in cooler aquifers near or at the surface, and when these gases include H_2S and CO_2, an acid-sulfate solution results that may pervasively acid-leach the host rock through downward percolation. The intensity of this acid leaching depends on the amount of condensate, its acidity, and the level of the water table. A lowered water table may also result in acid leaching through generation of a steam column beneath the silica cap and above the boiling water table. Recondensation of acidic vapors derived from any process along the underside of the silica cap results in patchy, localized acid leaching.

Minerals commonly found in the acid-leached parts of hot-spring precious-metal systems formed by water-rock interactions include kaolinite, alunite, jarosite, and iron oxides. Immediately adjacent to the silicified breccia, the host rock may be pervasively argillically altered; at Round Mountain, seams and pods of massive kaolinite or illite are strung out along low-angle fractures.

TRACE-ELEMENT SUITES IN EPITHERMAL SYSTEMS

Hot-spring deposits

The trace-element geochemistry of hot-spring precious-metal deposits has been studied at only a few localities. Table 2 lists analytical results for selected representative samples from Round Mountain and Hasbrouck Peak. The sinter deposits at Hasbrouck Peak contain a suite of trace elements that reflect the

Table 2. Trace-element data on selected samples from hot-spring precious-metal deposits in Nevada

[All values in parts per million. <, below level of detection; ≤, below level of determination but not below level of detection; --, no analysis done or no data reported]

Sample	Description	Au	Ag	As	Sb	Hg	Tl	W	Cu	Pb	Zn
					Hasbrouck Mountain						
[1]H-7	Chalcedonic sinter-----	<0.05	3	5	6	0.30	0.8	<50	5	<10	<5
BPP-024	do-----------	<.05	<.5	20	6	.28	<.2	11	<5	<10	<5
BPP-022	Silicified sediment----	.15	1	60	3	.06	2.8	3	50	<10	15
[2]MLS-1	do-----------	<.02	2	800	10	5	--	--	--	--	--
[3]TND-00263	do-----------	15	1,500	≤200	100	--	--	<50	100	20	<200
BPP-023	Banded quartz vein-----	.45	20	180	6	.16	4.2	12	15	<10	15
[1]H-3X	do-----------	2.4	150	230	9	.30	.8	<50	30	<10	5
[1]H-6	Hydrothermal breccia---	6.5	2,000	200	43	.06	4.2	<50	50	70	5
[2]MLS-2	do-----------	1.0	70	80	6	2.0	--	--	--	--	--
[3]TNR-00265	do-----------	<10	500	≤200	≤100	--	--	<50	20	20	<200
					Round Mountain						
RMB-1005	Silicified tuff--------	0.2	5	150	15	0.12	9.4	10	<5	15	<200
RMB-1006	do-----------	.1	3	100	5	.06	14.0	5	5	10	<200
RMB-3009	Quartz vein----------	10.0	23	2,000	45	--	3.5	<1	5	10	100
RMB-3028	do-----------	110.0	7	650	4	--	5.5	10	5	20	5
RMB-3007	Hydrothermal breccia---	3.0	2	>1,000	150	--	6	--	10	15	70
RMB-3012	do-----------	.25	3.8	300	4	--	13	20	10	30	35
9722	Nonwelded tuff---------	1.5	5	65	3	.02	5.9	10	≤5	15	<200

[1]M. L. Silberman (unpub. data, 1983).
[2]Silberman (1982).
[3]J. T. Nash (unpub. data, 1982).

former presence in the underlying rocks of metal-bearing fluids. Ag, Hg, Sb, Tl, and W, which occur in anomalous concentrations, make up the main trace-element suite. In the sinter, the anomalous concentrations are erratically distributed. For the purposes of comparison, table 3 lists data for sinter collected from Sinter Hill and the Main Terrace at Steamboat Springs, Nev. Beneath the sinter at Hasbrouck Peak is a zone of silicification. Both this silica zone and the one at Round Mountain contain Ag, As, Au, Hg, Sb, Tl, and W (table 2). Cu, Pb, and Zn are generally present in low concentrations and do not seem to have been important components in the hydrothermal fluids, at least at near-surface depths. The highest concentrations of the anomalous trace elements mentioned above occur in veins and hydrothermal breccias. There is some indication from detailed geologic studies at Hasbrouck Peak by Joseph Graney (unpub. data, 1983) that the vein and breccia zones are both structurally and stratigraphically controlled; the result is a host-rock control on the geochemical zoning, in addition to an overall vertical zonation.

Berger and others (1981) defined the generalized trace-element zoning patterns at Round Mountain. Figure 36 shows a plan-view summary of the zoning pattern for As, Sb, and Tl at Round Mountain. The highest concentrations of these elements coincide with the area beneath which explosion breccias occur, in

Table 3. Trace-element data on selected samples from Steamboat Springs, Nevada

[All values in parts per million. <, below level of detection; ≤, below level of determination but not below level of detection. Data from M. L. Silberman (unpub. data, 1983)]

Locality	Description	Au	Ag	As	Sb	Hg	Tl	Cu	Pb	Zn
Sinter Hill----	Chalcedonic sinter---	0.10	<0.5	<5	500	>13	<0.2	≤5	<10	<5
Main Terrace---	Opaline sinter-------	.10	1.5	35	1,000	6.5	54	5	<10	10

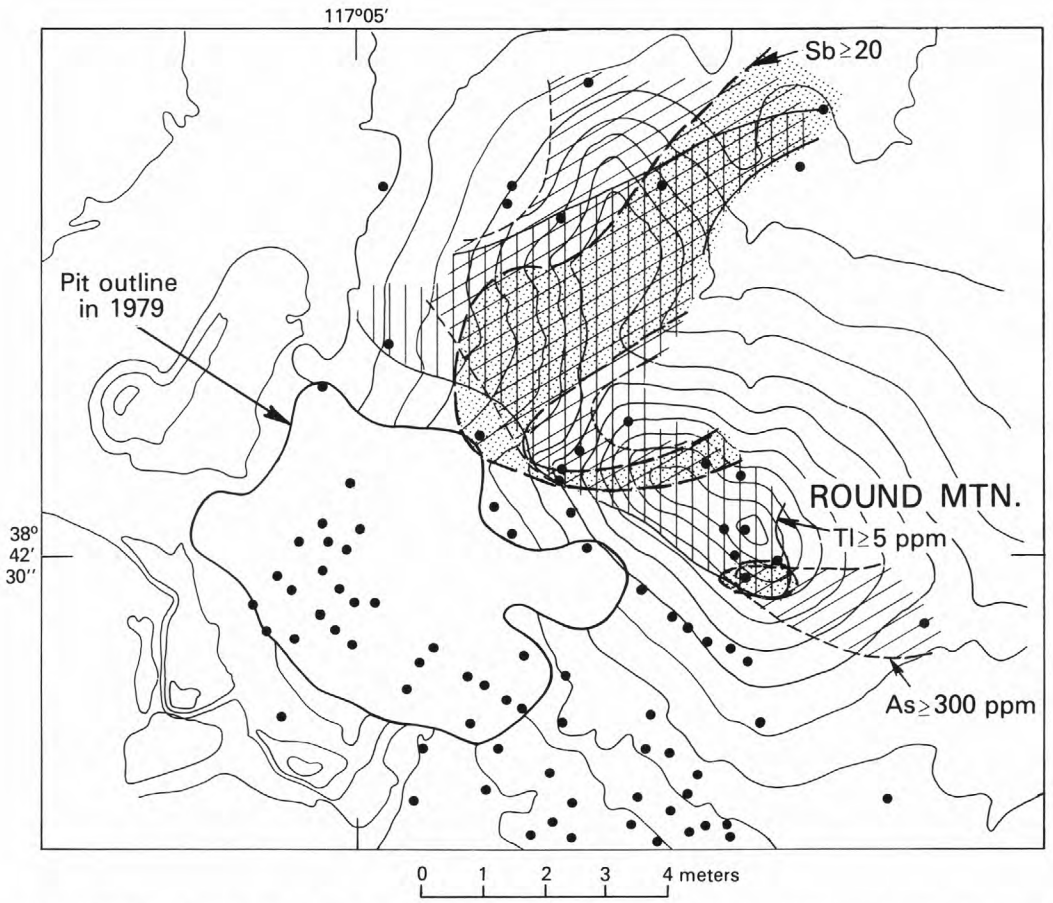

Figure 36. Round Mountain deposit, Nev., showing distribution of arsenic (min 300 ppm), antimony (more than 20 ppm), and thallium (min 5 ppm) in rock samples. Dots denote sample localities.

which the alteration consists of pervasive silicification (illite after biotite) in the presence of quartz-adularia veins, as shown in the schematic portrayal of the vertical zoning in hot-spring deposits in figure 34.

Other types of epithermal deposits

The trace-element suite defined at present from hot-spring precious-metal deposits is nearly identical to the suite found in carbonate-hosted precious-metal deposits (for example, Carlin, Nev., and Mercur, Utah) but generally different from those found in fissure-vein deposits. Tables 4 and 5 list data for several carbonate-hosted deposits, and table 6 for two major classes of fissure-vein deposits.

The similarity of the trace-element suites in hot-spring and carbonate-hosted deposits suggests a commonality of some, though clearly not all, of the genetic, geologic, and geochemical processes important to the formation of these two deposit types. At Round Mountain, a small carbonate-hosted gold deposit known as the Shale Pit may be temporally related to the formation of the main Round Mountain volcanic-hosted deposits. Table 5 lists the results of chemical analyses from the Shale Pit and vicinity; these results are comparable to those at Round Mountain listed in table 2. As a generalization, both the hot-spring and carbonate-hosted deposits appear to have a higher Au/Ag ratio than do fissure-vein deposits, as well as accompanying high concentrations of As, Hg, Sb, Tl, and W, and sparse Cu, Pb, and Zn.

The most significant geochemical differences between the ores in hot-spring precious-metal deposits and open-fissure-vein deposits are the lower Au/Ag ratios and the higher concentrations of Cu, Pb, and Zn in the fissure veins. The mineralogic differences also indicate fluid-chemistry differences. Empirically, the fissure-vein deposits, such as the Comstock Lode, Tonopah, and Bodie districts, Nev., are all related to dacitic, quartz latitic, and (or) rhyodacite volcanism. At Round Mountain, Hasbrouck Peak, and Sulphur, mineralization is spatially associated with rhyolitic volcanism.

SUMMARY

Hot-spring precious-metal ore deposits are related to surficial and near-surface processes that result in extensive silicification, hydrothermal brecciation, and veining. The highest grade ores are in veins and (or)

Table 4. Trace-element data on selected samples from carbonate-hosted disseminated precious-metal deposits in Nevada

[All values in parts per million. <, below level of detection; ≤, below level of determination but not below level of detection; --, no analysis done or none reported. Data for Cortez from Erickson and others (1964); data for Carlin, Atlanta, and Mercur from T. G. Lovering (unpub. data, 1983)]

Sample	Description	Au	Ag	As	Sb	Hg	Tl	W	Cu	Pb	Zn
					Cortez						
722	Silicified limestone-----	59	2.7	1,500	<100	0.85	--	<50	--	--	--
749	Jasperoid----------	.6	--	700	200	.08	--	<50	--	--	--
					Carlin						
5A	Silicified limestone-----	0.7	0.7	<200	1,500	0.42	--	--	15	50	300
5B	do----------	2.8	.7	<200	1,000	5.0	--	--	70	10	300
					Atlanta						
1A	Silicified dolomite------	0.8	40	<200	300	11.0	1.1	--	5	15	--
1B	do----------	2.9	20	<200	300	3.8	3.6	--	10	30	--
					Alligator Ridge						
BPP-026	Argillized limestone-----	≤0.05	≤0.5	120	38	0.98	1.2	8	20	10	60
BPP-029	Carbonaceous limestone---	≤.05	≤.5	360	3	.20	.8	5.5	20	20	45
					Mercur						
6A	Silicified limestone-----	0.3	1.5	3,000	7,000	25	--	--	70	<10	<200
2A	do----------	1.1	30	--	300	10	--	--	30	<10	<200

Table 5. Trace-element data on selected samples from the Shale Pit and vicinity, Round Mountain, Nevada

[All values in parts per million. <, below level of detection; ≤, below level of determination but not below level of detection]

Sample	Description	Au	Ag	As	Sb	Hg	Tl	W	Cu	Pb	Zn
RMB-3078	Silicified limestone---	≤0.05	0.45	150	7	0.5	1.0	5	20	15	140
RMB-3079	do----------	.15	.7	200	5	.04	1.2	3	15	20	55
[1]RMB-3076	Pumiceous tuff---------	≤.05	.5	350	9	≤.02	1.4	2	<5	50	70
[2]RMB-4218	do----------	.30	2.0	200	10	.04	32.0	20	50	100	40

[1]Tuff sample in stratigraphic contact with mineralized carbonate adjacent to open pit.
[2]Tuff sample from flats to south and from western open pit.

Table 6. Trace-element data on selected samples from quartz veins in the Comstock Lode and Tonopah mining districts, Nevada

[All values in parts per million. <, below level of detection; --, not determined. Data from Whitebread (1976) and Bonham and Garside (1982)]

Sample	Au	Ag	As	Sb	Hg	Cu	Pb	Zn
Comstock Lode (Virginia City)								
6-89C	<0.02	3	10	--	0.12	1,000	1,000	1,000
6-90B	<.02	30	5	--	.45	50	100	<200
6-93K	.7	30	--	--	.26	20	100	<200
Tonopah								
T7gc	0.7	97	6	16	0.59	2,200	6,200	1,420
T7gd	4.1	633	12	70	--	92	62	1,360
GC109	.2	231	89	149	.66	111	3,920	98
Gc93	1.4	982	9	811	.06	1,660	2,770	257

breccias. The ores have higher Au/Ag ratios and lower concentrations of Cu, Pb, and Zn than in epithermal open-fissure-vein deposits. Accompanying the ores in the veins and breccias are trace to minor concentrations of As, Hb, Sb, Tl, and W. The abundance of these elements varies from deposit to deposit, depending on primary-fluid composition and temperature, mechanisms of mineral deposition, and host-rock compositions.

REFERENCES CITED

Averitt, Paul, 1945, Quicksilver deposits of the Knoxville district, Napa, Yolo, and Lake Counties, California: California Journal of Mines and Geology, v. 41, no. 2, p. 65-89.

Becker, G. F., 1888, Geology of the Quicksilver deposits of the Pacific slope, with an atlas: U.S. Geological Survey Monograph 13, 486 p.

Berger, B. R., and Eimon, P. I., 1982, Comparative models of epithermal precious-metal deposits: American Insitute of Mining Engineers Preprint 82-13, 36 p.

Berger, B. R., and Tingley, J. V., 1980, Geology and geochemistry of the Round Mountain gold deposit, Nye County, Nevada [abs.]: Nevada Bureau of Mines and Geology Precious Metals Symposium, Reno, 1980, Abstracts, p. 18c.

Berger, B. R., Tingley, J. V., Filipek, L. H., and Neighbor, J., 1981, Origin of pathfinder trace-element patterns associated with gold-silver mineralization in late Oligocene volcanic rocks, Round Mountain, Nye County, Nevada [abs.]: Association of Exploration Geochemists Precious Metals Symposium, Vancouver, British Columbia, Canada, 1981, Abstracts, p. 207.

Bonham, H. F., Jr., and Garside, L. J., 1982, Geochemical reconnaissance of the Tonopah, Lone Mountain, Klondike, and northern Mud Lake quadrangles, Nevada: Nevada Bureau of Mines and Geology Bulletin 96, 68 p.

Drummond, S. E., Jr., 1981, Boiling and mixing of hydrothermal fluids: Chemical effects on mineral precipitation: University Park, Pennsylvania State University, Ph. D. thesis, 380 p.

Erickson, R. L., Marranzino, A. P., Oda, Uteana, and Janes, W. W., 1964, Geochemical exploration near the Getchell mine, Humboldt County, Nevada: U.S. Geological Survey Bulletin 1198-A, p. A1-A26.

Silberman, M. L., 1982, Hot-spring type, large tonnage, low-grade gold deposits, in Erickson, R. L., compiler, Characteristics of mineral deposit occurrences: U.S. Geological Survey Open-File Report 82-795, p. 131-143.

Wallace, A. B., 1980, Geology of the Sulphur district, southwestern Humboldt County, Nevada: Society of Economic Geologists Field Conference on Epithermal Deposits Guidebook, 1980, p. 80-91.

Whitebread, D. H., 1976, Alteration and geochemistry of Tertiary volcanic rocks in parts of the Virginia City quadrangle, Nevada: U.S. Geological Survey Professional Paper 936, 43 p.

Geochronology of Hydrothermal Alteration and Mineralization: Tertiary Epithermal Precious-Metal Deposits in the Great Basin

By Miles L. Silberman

CONTENTS

INTRODUCTION

The timing of hydrothermal alteration and mineralization is important to investigate for several theoretical and practical reasons, as follows:

1. How is the time of hydrothermal activity related to volcanism and plutonism? Geochronologic studies of epithermal precious-metal deposits and porphyry copper deposits have shown that alteration and mineralization are relatable to specific localized stages of igneous activity (Silberman and others, 1972; Ashley and Silberman, 1976; Chivas and McDougall, 1978; Whalen and others, 1982). In epithermal precious-metal deposits, a consistent relation between hydrothermal alteration and later stages of volcanic activity within a given cycle can be demonstrated (Silberman and others, 1972; Ashley and Silberman, 1976).
2. What is the duration of hydrothermal activity, including both alteration and mineralization? Estimates of the duration of hydrothermal activity in ore deposits or thermal-spring systems range from considerably less than 1 m.y. (Whalen and others, 1982; Noble and Silberman, 1984) to nearly 3 m.y. (Silberman and others, 1979b). The time interval required for ore deposition within overall hydrothermal phases of activity is still uncertain. Studies of the physical characteristics of hot-spring and vein-type Au-Ag deposits (Buchanan, 1981; Silberman, 1982b; Berger and Eimon, 1983), and attempts at detailed geochronology in complex alteration-mineralization systems (Noble and Silberman, 1984), suggest that the ore-depositing episodes are short lived. Some geochronologic data, however, suggest that productive precious-metal deposits form in conjunction with hydrothermal systems where the overall period of activity is relatively lengthy—at least 1 m.y. and, possibly, longer than 3 m.y. (Silberman and others, 1972; Ashley and Silberman, 1976; M. L. Silberman, unpub. data, 1983)—and are characterized by repetitive and episodic, short-lived hydrothermal processes (Silberman, 1982a, b; Berger and Eimon, 1983).
3. What are the regional age relations of ore deposits within the context of the tectonic framework, including structural evolution, igneous activity, and metamorphism? Age determinations of hydrothermal alteration and mineralization have been successful in relating mineral deposits to a tectonic framework. For example, in the Great Basin, Silberman and others (1976) and Rowen and others (1984); in southern Alaska, Silberman and others (1980), Wilson (1980), and Mitchell and others (1981); and in Mexico, Clark and others (1982) and Damon and others (1984) related the timing of mineralization to tectonic processes within the areas in question.

The most significant hydrothermal deposit type that has not yet been studied conclusively as to its age of mineralization and timing of hydrothermal activity is the carbonate-sediment-hosted (Carlin type) disseminated gold deposit. Silberman and others (1974) determined the age of mineralization at the Getchell deposit, Nev., and reported ages from a similar deposit at Gold Acres, Nev. Although data exist for similar deposits at Northumberland and Pinson, Nev. (M. L. Silberman and others, unpub. data, 1973-82), attempts to unequivocally interpret the age relations in these deposits have generally been unsuccessful. Geochronologic technology, particularly the widespread application of spectrum Ar-Ar dating, is adequate to determine the timing of hydrothermal alteration and mineralization in these important deposits, and so an attempt to carry out such studies should be made.

Acknowledgements.—Many of the data presented here were produced or gathered during U.S. Geological Survey-sponsored research between 1967 and 1982. The ideas crystallized during my work with the Anaconda Minerals Co. in 1982 and 1983. I appreciate the assistance of many colleagues and the coauthors of previous reports at the Survey, the Nevada Bureau of Mines and Geology, the California Division of Mines and Geology, the Mackay School of Mines of the University of Nevada, and many mining companies whose properties I worked on, on which this chapter is based. I am particularly indebted to Paul Damon and Donald White for their pioneering work on the geochronology of ore deposits and on the relation of thermal-spring systems and epithermal ore deposits, respectively.

METHODS AND MATERIALS—EPITHERMAL PRECIOUS-METAL DEPOSITS

Although several different methods of isotopic-age determination are applicable to dating hydrothermal alteration, the most widely applied method has been conventional K-Ar analyses. Hydrothermal fluids that deposit metallic ores also deposit K-bearing gangue and wallrock-alteration minerals that are datable by this method. The alteration mineralogy in any hydrothermal system depends on various factors, including original host-rock mineralogy, hydrothermal-fluid temperature, composition, pH, and Eh (Meyer and Hemley, 1967; Rose and Burt, 1979).

The K-bearing minerals used to determine the age of hydrothermal alteration include hydrothermal K-feldspars (adularia; Silberman and others, 1972; Koski and others, 1978); sericite (Silberman and others, 1974); muscovite; alunite and natroalunite (Mehnert and others, 1973; Ashley and Silberman, 1976); and jarosite (Erickson and others, 1978). All these K-bearing minerals are common gangue and wallrock-alteration minerals in epithermal vein and disseminated Au-Ag deposits. Adularia, sericite, and alunite are the most commonly dated alteration phases in epithermal deposits. Other minerals that have been used to date alteration directly are hydrothermal biotite and phlogopite (Moore and Lanphere, 1971), hydrothermal amphibole (Silberman and others, 1977), chlorite (Silberman and others, 1977), and mariposite (M. L. Silberman and F. C. Dodge, unpub. data, 1979), as well as whole-rock samples containing combinations of K-bearing phases (Silberman and others, 1972; Morton and others, 1977; Silberman and others, 1979a).

The second most widely applied method of alteration geochronology is fission-track dating. Apatite, zircon, and sphene have been used successfully to study age relations in alteration systems (Ashley and Silberman, 1976; Lipman and others, 1976). The combination of K-Ar and fission-track techniques has been particularly useful because the temperature of annealing of fission tracks in minerals is better known than that of diffusional loss of argon (Naeser and Faul, 1969). Combined K-Ar fission-track data allow a more nearly complete thermal history of an alteration system to be constructed.

EXAMPLES OF ORE-DEPOSIT GEOCHRONOLOGY

Numerous examples of detailed geochronologic studies of hydrothermal alteration and mineralization have been described in the literature. I have chosen to summarize two such studies here because of the numerous isotopic ages reported therein and because these studies were specifically designed to answer parts of questions 1 and 2 above. Silberman and others (1972) reported on the age of mineralization at Bodie, Calif., in their summary of the results of 40 K-Ar analyses of rocks and veins from within and near the district. Silberman and Ashley (1970) and Ashley and Silberman (1976) summarized the results of determinations of 55 K-Ar and fission-track ages from the Goldfield district, Nev.

Bodie mining district

Geology

The Bodie mining district, which has produced more than $34 million in gold and silver from fissure veins in volcanic rocks of intermediate composition, is near the east margin of the Bodie Hills, Calif., a volcanic massif approximately 35 km^3 in volume and as much as 400 m thick. The area surrounding the Bodie Hills constitutes a major volcanic province (fig. 37) which has been subdivided on the basis of dominant overall lithology and age of activity (Chesterman, 1968; Gilbert and others, 1968; Kleinhampl and others, 1975).

Chesterman (1968) and Chesterman and Gray (1975) defined five volcanic formations of Tertiary age in the Bodie Hills, on the basis of proximity to eruptive centers which are characterized by complex structure and intrusive plugs. Many of these formations overlap each other in age because the eruptive centers commonly were active contemporaneously. Hydrothermal alteration and mineral prospects are common in the Bodie Hills, but the only major deposit located to date has been at Bodie. Although volcanic activity in the hills spanned the time interval 13.3-5.7 m.y. B.P., most of the eruptive material was emplaced between about 9.5 and 7.8 m.y. B.P.

The Bodie mining district is localized in dacite flows, tuff breccias, and small intrusive plugs of the Silver Hill Volcanic Series of Chesterman and Gray

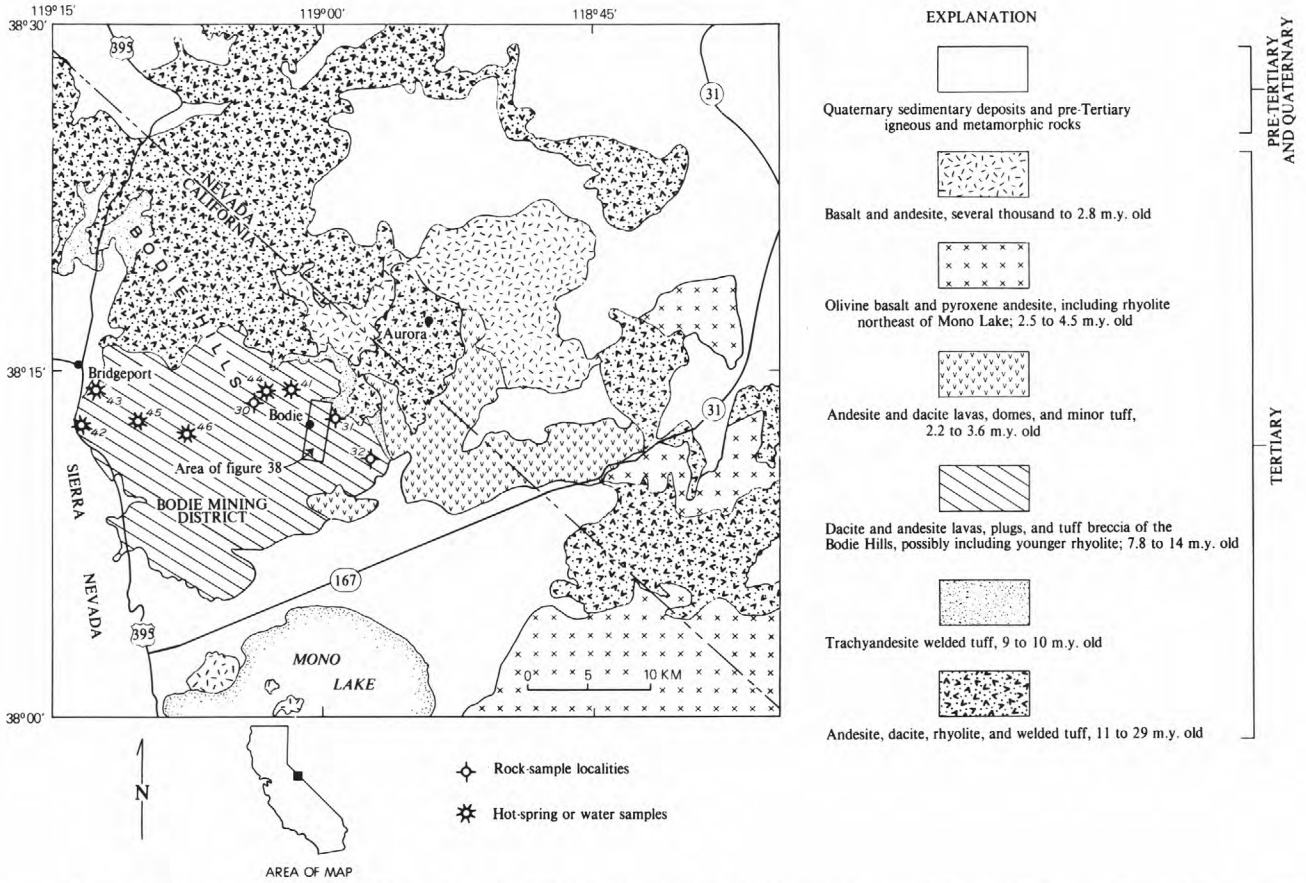

Figure 37. Regional geologic setting of the Bodie Hills and vicinity, California and Nevada, showing ages and dominant compositions of the Tertiary volcanic rocks (modified from Kleinhampl and others, 1975, fig. 2).

(1975), one of the volcanic formations of the Bodie Hills. The district itself is an eruptive center. The structure consists of an irregular faulted north-south-trending anticline (fig. 38) formed by intrusion and doming of the flows and tuff breccia by small plugs; the plugs occupy vents from which the extrusive volcanic rocks were erupted. Several sets of steeply dipping faults cut all the units, including the plugs. One predominant set strikes north-south to northeast, and another set is normal to this strike (fig. 38). The major vein and fractures at Bodie also strike north-south to northeast, parallel to one of the fault sets. Most production from the district has come from the vicinity of Bodie Bluff and Standard Hill in the north, in the vicinity of the graben of tuff breccia that was downfaulted into the intrusive dacite during or shortly after its emplacement (fig. 38).

The productive quartz veins cut both the tuff breccia and intrusive rock. Several sets of quartz veins, which range in thickness from about 0.3 to 27 m, are present, although most veins are no more than a few meters thick (Chesterman and others, 1984). Adularia, a common constituent of the veins, in some places forms crystals as much as 3 cm long coating open fractures. Ore minerals are principally native gold and silver, but argentite, pyrite, and sphalerite also occur. The abundance of sphalerite increases with depth as the tenor of gold decreases. In the main productive zone near the graben, old records quoted by Chesterman and others (1984) indicate that the ore averaged 1.7 troy oz Au per ton (58 g Au/t) and 3.1 troy oz Ag per ton (106 g Ag/t).

Alteration zoning at Bodie has not yet been studied in detail, although O'Neil and others (1973) reported on the isotopic and chemical effects of hydrothermal K-silicate alteration at Bodie Bluff. Chesterman and others (1984) indicated that zoning occurs both laterally and vertically. In the north, at Bodie Bluff, both the intrusive dacite and tuff breccia and flows are strongly silicified at the surface. Silberman (1982b) suggested that this silicified zone, a part of which has chalcedonic quartz-vein stockworking, represents a very shallow level in the system, probably just subsurface. Below this near-surface alteration, the rocks of the Bodie Bluff area are strongly K-silicate altered, largely recrystallized to the assemblage K-feldspar (adularia), K-mica (sericite), and quartz. This alteration also characterizes the wallrocks of the productive-vein zone. To the south, argillic alteration occurs, as well as at least some zones of sericitic alteration. Outside of the central part of the district, most of the volcanic rocks are strongly propylitized. At the lowest level of the workings at Bodie Bluff that was accessible in recent years, about 210 m beneath the top,

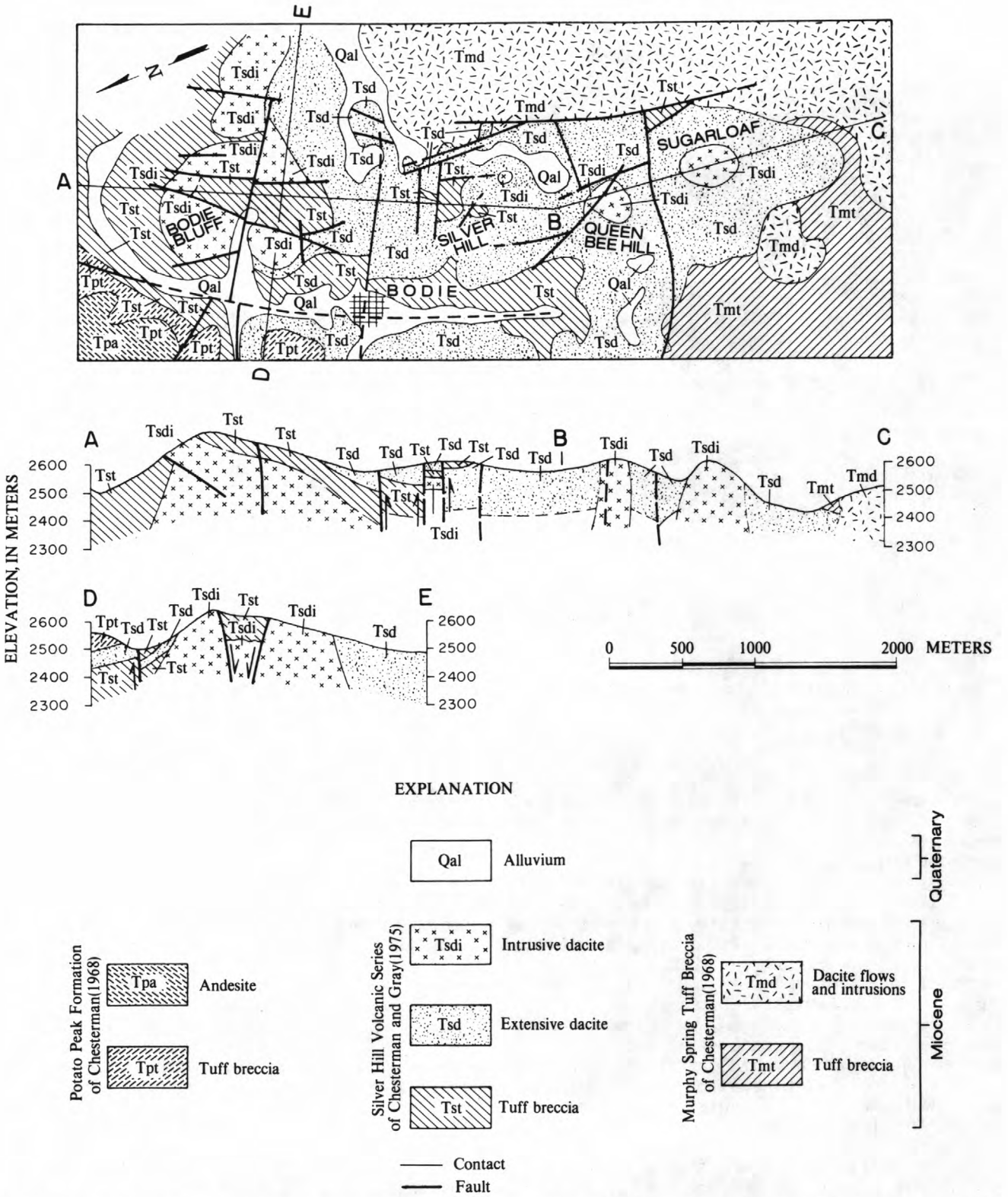

Figure 38. Generalized geologic map and cross sections of the Bodie mining district, Mono County, Calif. (modified from Chesterman and others, 1984, plate 2). See figure 37 for location.

the altered rocks still contain K-feldspar, although sericite and kaolinite are more abundant.

Age relations

Figure 39 summarizes the age determinations at Bodie and vicinity, as reported by Silberman and Chesterman (1972), Silberman and others (1972), and Kleinhampl and others (1975). The ranges in the dates of formation of veins and volcanic rocks in and near the Bodie mining district are as follows:

Unit or event	Date (m.y. B.P.)
Younger postore sequence, east of the Bodie mining district.	3.6-0.25
Younger rhyolitic rocks, western Bodie Hills.	5.7-5.3
Veins, Bodie mining district--------	8.0-7.1
Hydrothermal activity----------	8.6-7.1
Dacite intrusive rocks, Bodie mining district.	9.2-8.6
Silver Hill Volcanic Series of Chesterman and Gray (1966), Bodie mining district.	9.4-8.8
[1]Murphy Spring Tuff Breccia of Chesterman (1968).	8.9-8.7
[1]Potato Peak Formation of Chesterman (1968).	9.1-8.4
[1]Other basalt-andesite-dacite-rhyolite, western Bodie Hills.	13.3-7.8

[1]Volcanic rocks of the Bodie Hills outside the Bodie mining district; modified from Silberman and others (1972).

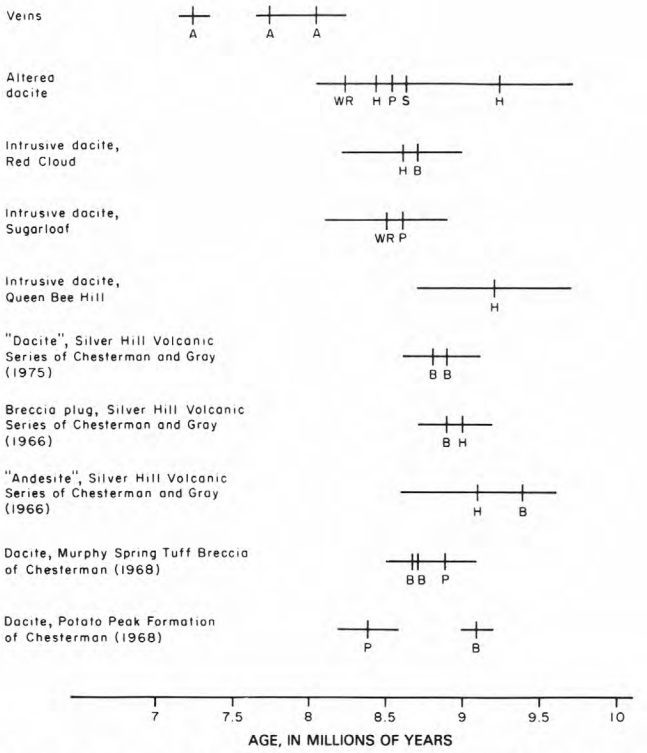

Figure 39. K-Ar ages of volcanic rocks, altered volcanic rocks, and quartz-adularia veins in the Bodie mining district and vicinity, Mono County, Calif. (modified from Silberman and others, 1972, fig. 3). Horizontal lines represent analytical uncertainty in age determination. A, adularia; B, biotite; H, hornblende; P, plagioclase; S, sericite; WR, whole rock. Plagioclase ages from Gilbert and others (1968).

The extrusive rocks of the Silver Hill volcanic series were emplaced between 9.4 and 8.8 m.y. B.P., and the comagmatic plugs were intruded between 9.4 and 8.6 m.y. B.P. Hydrothermal activity, as dated by the K-Ar ages of sericite from altered tuff breccia in the southern part of the Bodie district, and of K-silicate-altered Bodie Bluff intrusive dacite, began at 8.6 m.y. B.P. just about at the end stage of volcanic activity in the district. Three K-Ar ages from adularia separated from mineralized quartz veins fall in the range 7.1 to 8.0 m.y.; the youngest age is from a vein occupying a structure that cuts others which hosted veins in the northern part of the district.

Volcanic rocks were emplaced within the volcanic center between 9.4 and 8.6 m.y. B.P.—about a 1-m.y. duration of volcanic activity. Hydrothermal alteration commenced at the end of or immediately after volcanism and continued for 1.5 m.y., during which periods several sets of veins that show crosscutting relations (Chesterman and others, 1984) were emplaced, and a major precious-metal deposit was formed. The alteration-mineralization at Bodie was nearly the last stage of igneous-hydrothermal activity associated with the development of the Bodie Hills volcanic field. Not until nearly 2.5 m.y. later did minor volcanism again occur, west of the district. To the east, major volcanic activity commenced again at 3.6 m.y. B.P. (fig. 37).

Goldfield mining district, Nevada

Geology

The Goldfield mining district (fig. 40) in the Goldfield Hills of western Nevada is underlain by a complex sequence of Oligocene and Miocene volcanic rocks which cover a pre-Tertiary basement composed of Ordovician sedimentary rocks and Jurassic granitic rocks. The older Oligocene volcanic rocks consist of silicic flows and tuff of local origin from a caldera whose ring-fracture zone is outlined by the faulting and alteration patterns. The pre-Tertiary rocks are exposed in the core of this caldera. Approximately 4 to 8 m.y. years after cessation of the silicic volcanic activity, a new series of dominantly intermediate flows, tuff, breccia, and domes were emplaced during the early Miocene from vents within and near the mining district (Ashley, 1974; Ashley and Silberman, 1976). Middle and upper Miocene sedimentary and volcanic rocks that unconformably overlie the lower Miocene volcanic rocks are largely from sources some distance away from the mining district, although some of the basalt in this younger sequence was erupted from local vents.

Hydrothermal alteration and mineralization at Goldfield are spatially and temporally associated with

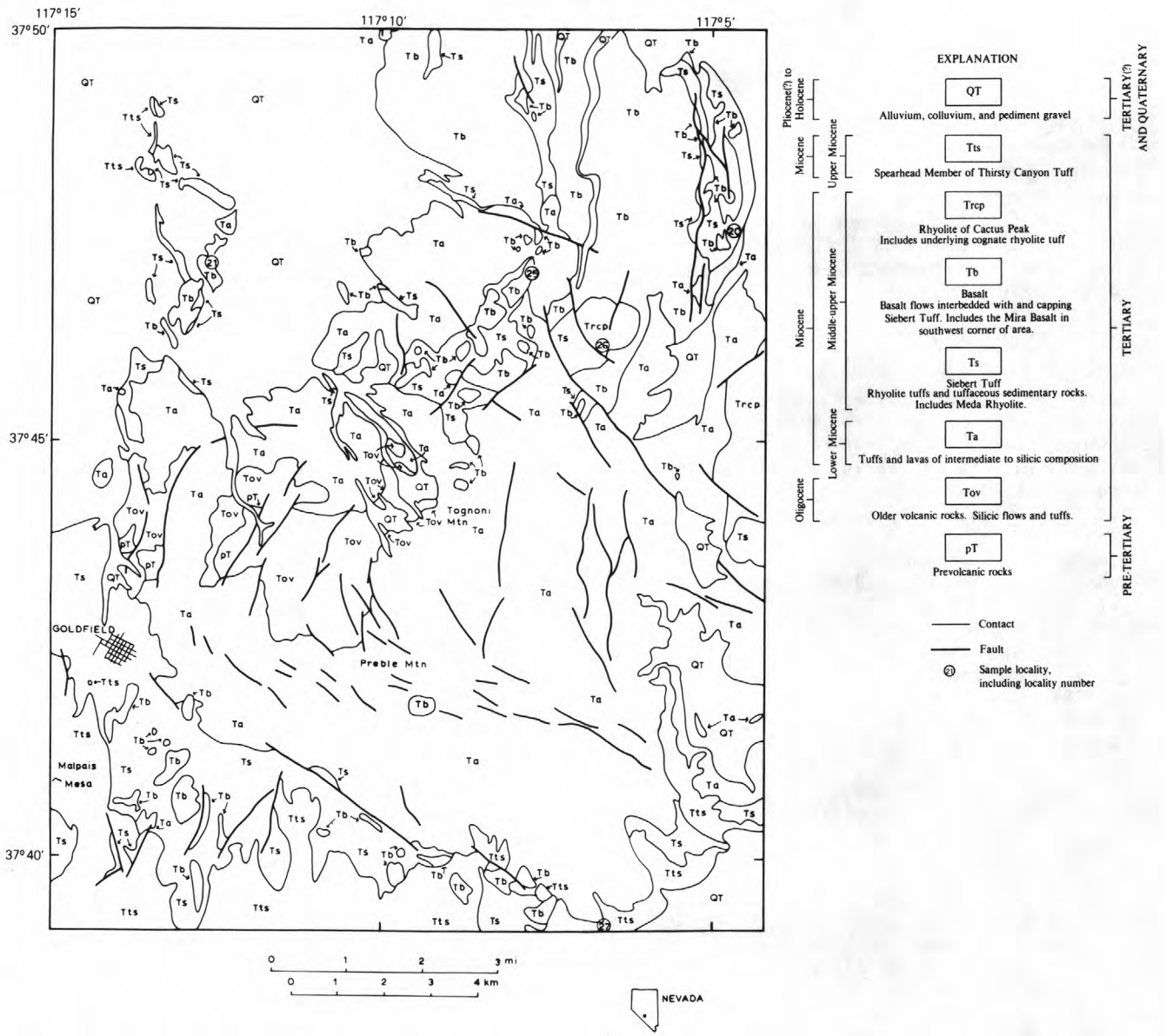

Figure 40. Simplified geologic map of the Goldfield mining district, Esmeralda and Nye Counties, Nev. (modified from Ashley and Silberman, 1976, fig. 2). Geology generalized from mapping by R. P. Ashley (unpub. data, 1972). Base from U.S. Geological Survey, scale 1:62,500, Goldfield and Mud Lake quadrangles, 1952. The Spearhead Member has recently been reassigned from the Thirsty Canyon Tuff to the Stonewall Flat Tuff (Noble and others, 1984).

the dominantly intermediate lower Miocene tuff and lava. Some rocks of this unit were emplaced after the onset of hydrothermal alteration, but outside of the mineralized part of the district (fig. 40). Mineralization at Goldfield occurs in silicified ledges, consisting of prominent outcrops of fine-grained quartz which occur throughout a 40-km^2 area of poorly exposed argillic and propylitic rocks. These ledges, which formed as replacement bodies along faults and fractures, may contain alunite, kaolinite, pyrophyllite and diaspore along with quartz. Limonite and pyrite (in the unoxidized rocks) occur in all the silicified zones. Productive mineralization in the ledges is restricted to a small (1.3 km^2) area just north of Goldfield (fig. 40). Unoxidized ore, which formed open cavity fillings in brecciated ledge material, consisted of varying proportions of native gold and sulfide and sulfosalt minerals (Ashley, 1974). The overall average grade of ore at Goldfield was 18.5 g Au/t (Albers and Stewart, 1972), but grades as high as 21 kg Au/t were reported (Ransome, 1909).

Alunite was an important hypogene constituent of the silicified ledges, including those hosting mineralization. The alunite occurred as replacements of feldspar phenocrysts and pumice and as coarse hypogene veins cutting the silicified zones. Alunite deposition in the ledges persisted into the early stages of mineralization (Ashley and Silberman, 1976). Supergene alunite occurs as fine-grained veins cutting both oxidized silicified and argillized rocks. The zones

peripheral to the quartz-alunite ledges were commonly argillized, but, at least in some areas, including the productive zone, quartz-sericite alteration mantles the ledges (Ashley and Silberman, 1976). The occurrences of the advanced argillic, alunite-containing alteration and the quartz-sericite alteration allowed the K-Ar ages of two alteration minerals to be determined.

Age relations

K-Ar ages of minerals from unaltered volcanic rocks, and from alunite and K-mica (sericite, $2M_1$ polymorph), were determined. In addition, fission-track ages on several units, including the pre-Tertiary and older volcanic rocks, were obtained. Figure 41 summarizes the isotopic ages of these rocks, as reported by Ashley and Silberman (1976). The older silicic units were propylitized and so could not be dated by the K-Ar method. Zircon and apatites in these rocks, however, were not affected by that alteration and indicate emplacement ages of from 28 to 34 m.y. The early Miocene host rocks were emplaced starting at about 22 m.y. B.P. and volcanism continued for about 1 to 2 m.y. Concordant K-Ar mineral ages and fission-track ages were obtained for units of the early Miocene sequence (fig. 41). The postmineralization volcanic and sedimentary units formed from about 18 to 7 m.y. B.P. Mineralization thus occurred between 22 and 18 m.y. B.P.

K-Ar ages of replacement and hypogene vein alunites range from 20 and 21 m.y. Concordant results were obtained on the sericite samples from quartz-sericite zones near the ledges. Apatite fission-track ages from pre-early Miocene units near altered zones gave ages of 21.0 and 19.6 m.y., concordant with the K-Ar results. The isotopic ages of alunite and apatite from Goldfield indicate that alunite provides accurate ages of mineralization in hydrothermal systems and that the apatite ages of rocks near (within several meters of) strongly altered zones also determine the ages of alteration. These results have been confirmed in other

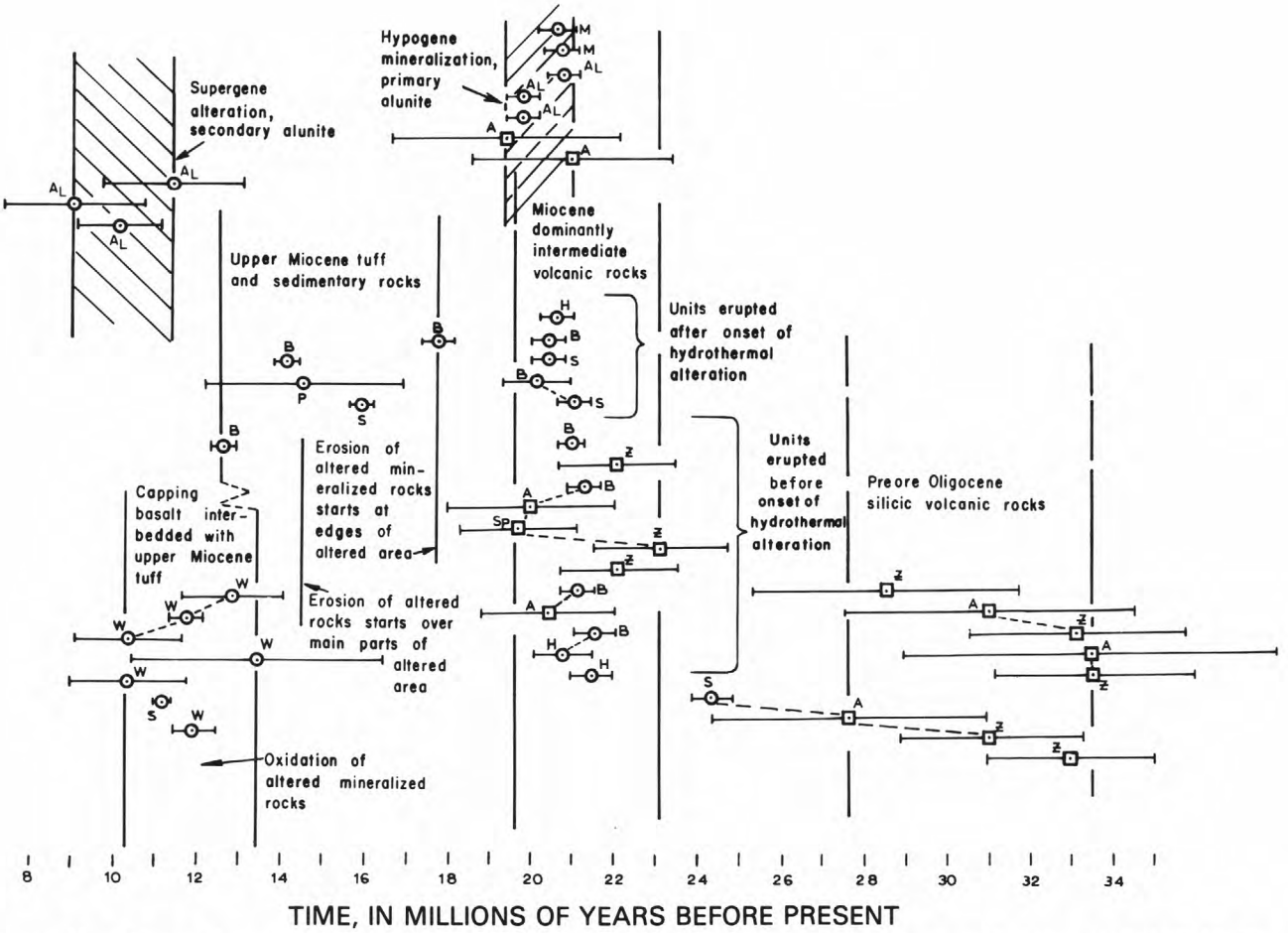

Figure 41. Schematic summary of volcanic history and timing of alteration and mineralization at Goldfield, Nev. (modified from Ashley and Silberman, 1976, fig. 4). Squares, fission-track age; circles, K-Ar age. Error bars represent analytical uncertainty in age determination. Dotted lines connect multiple minerals from a single sample: A, apatite; Al, alunite; B, biotite; H, hornblende; M, K-mica; P, plagioclase; S, sanidine; Sp, sphene; W, whole-rock basalt; Z, zircon.

mineralized areas in epithermal systems (Lipman and others, 1976; Morton and others, 1977). In contrast, zircon and sphene fission-track ages (some of which were obtained from the same units as the apatite ages that were reset) are unaffected by proximity to this type of alteration (Ashley and Silberman, 1976).

The three supergene alunite K-Ar ages of about 10 m.y. represent oxidation of the sulfide-bearing altered rocks some 10 m.y. after the hypogene mineralization. Fission-track apatite ages demonstrate that no major thermal events affected the mineralized area after the early Miocene hydrothermal event. Thus, the middle and lower Miocene volcanic activity apparently had no strong thermal effect. Structural and stratigraphic data accord with the beginning of erosion and oxidation in the mineralized area at about the time indicated by the supergene alunite ages. Thus, at Goldfield, both hypogene hydrothermal alteration and supergene oxidation are dated by application of K-Ar analyses to alunites. The age relations of volcanic activity and alteration-mineralization at Goldfield are similar to those at Bodie.

Several generalized conclusions can be drawn about the timing of igneous-hydrothermal activity from these studies.

1. Hydrothermal alteration and mineralization starts late and generally continues for some time after some significant local stage of volcanic activity. Prealteration and synalteration volcanism lasts about 1 m.y. or longer.
2. The overall duration of hydrothermal activity indicated by the data at Bodie and Goldfield is 1 to 1.5 m.y., close to the average age of the hydrothermal systems related to mineralization, as shown below.
3. Volcanic activity can and does take place during and after hydrothermal mineralization, through generally outside the zone of mineralization.

These three generalizations have been confirmed by detailed study of other epithermal systems (Silberman and others, 1979a; Noble and Silberman, 1984).

DATA ON THE LIFETIMES OF HYDROTHERMAL SYSTEMS

Numerous radiometric-age data have become available on mineral deposits since the pioneering studies of Paul Damon and coworkers (Damon and Mauger, 1966) on porphyry copper deposits, and the spans of hydrothermal activity at Bodie and Goldfield and their temporal relations to spatially associated igneous rocks can be compared with data from other hydrothermal mineral deposits and thermal spring systems. However, few detailed studies have been done on the chronology of hydrothermal systems, and even fewer that provide unequivocal estimates of the duration of hydrothermal activity.

Figure 42 summarizes data from a tabulation of isotopic age studies of hydrothermal systems, including porphyry copper deposits, epithermal precious-metal deposits, polymetallic vein deposits, and thermal hot-spring systems (M. L. Silberman, unpub. data, 1982).

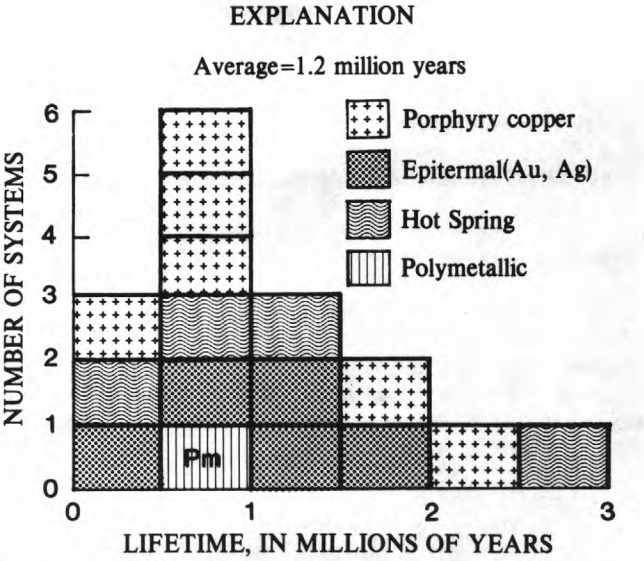

Figure 42. Radiometric lifetimes of hydrothermal alteration-mineralization systems.

Hydrothermal activity in porphyry copper deposits is generally found to have lasted about 1 m.y. or less, except in the Bingham, Utah (Warnaars and others, 1978), and El Salvador, Chile (Gustafson and Hunt, 1975), systems, where I interpret the data to indicate lifetimes of about 2 m.y.

The few detailed studies of precious- and base-metal vein systems available suggest that hydrothermal activity commonly extends over periods of about 0.5 to 1.5 m.y. The longest lived documented system is at Bodie, Calif. (Silberman and others, 1972). The estimate of about 1.5-m.y. duration is relatively accurate because the youngest age was obtained on vein material from a structure that cuts other mineralized structures and veins (Silberman and others, 1972). A similar lifetime is suggested for the Tui mine, New Zealand (Adams and others, 1974). Lifetimes of about 1, 0.7, and 0.5 are indicated for Goldfield and Divide, Nev. (Silberman and others, 1979a), and Summitville, Colo. (Mehnert and others, 1973), respectively. Data on other epithermal districts generally indicate a close association of igneous and hydrothermal activity, but are inadequate to infer the interval over which hydrothermal activity was taking place.

White (1955, 1974) stressed the close similarity of many thermal springs and epithermal Au-Ag systems, and it now appears that several low-grade large-tonnage disseminated Au-Ag deposits and prospects in Nevada, such as Round Mountain (Berger and Tingley, 1980), Borealis (Strachan and others, 1982), Sulfur (Wallace, 1980), and Hasbrouck Peak (Bonham and Garside, 1979), are fossil, at least partly surficial thermal-spring systems. The age ranges for most thermal-spring systems are identical to those of porphyry and vein deposits except at Steamboat Springs, for which episodic activity appears to be unusually long lived.

There seem to be no significant differences in the lifetimes of these three types of systems, although the

available data base is sparse. The average lifetime of hydrothermal activity based on this summary is 1.2 m.y., approximately the age of activity determined for Bodie and Goldfield.

PATTERNS OF GREAT BASIN MINERALIZATION

The relation between the tectonic evolution of the Great Basin and the distribution of epithermal mineral deposits is well documented (Silberman and others, 1976). Precious-metal deposits are associated in space and time with several suites of volcanic rocks that were erupted in the Great Basin from mid to late Tertiary time in response to interactions of the North American plate with various Pacific plates. The patterns of volcanic activity are thought to be related to variations in the dip and rate of convergence of the plates, and to transform faulting and migration of triple junctions (Atwater, 1970; Chistiansen and Lipman, 1972; Lipman and others, 1972; Snyder and others, 1976). The distribution of volcanic rocks in the Great Basin in space and time was summarized by Stewart and Carlson (1976). Figures 43 through 46 show simplified versions of the maps of Stewart and Carlson along with the locations of dated epithermal precious-metal deposits (Silberman and others, 1976).

The entire pattern represented in figures 43 through 46 shows a generally outward arcuate progression of volcanic activity over time from the central Great Basin toward its margin. The maps also illustrate a similar pattern in outward migration of hydrothermal mineral deposits. Figure 47 shows the overall distribution of hydrothermal Au-Ag deposits in the Great Basin whose ages have been determined. When these distribution and ages are considered in greater detail, several patterns and associations of interest are evident. Because patterns differ in the northern and central Great Basin and in the Walker Lane (western Great Basin), I discuss these areas separately below.

Northern and central Great Basin

Figures 48 and 49 plot the ages of dated ore deposits and their host rocks and illustrate the style of volcanism in the northern and central Great Basin. The pattern for this region shows epithermal deposits

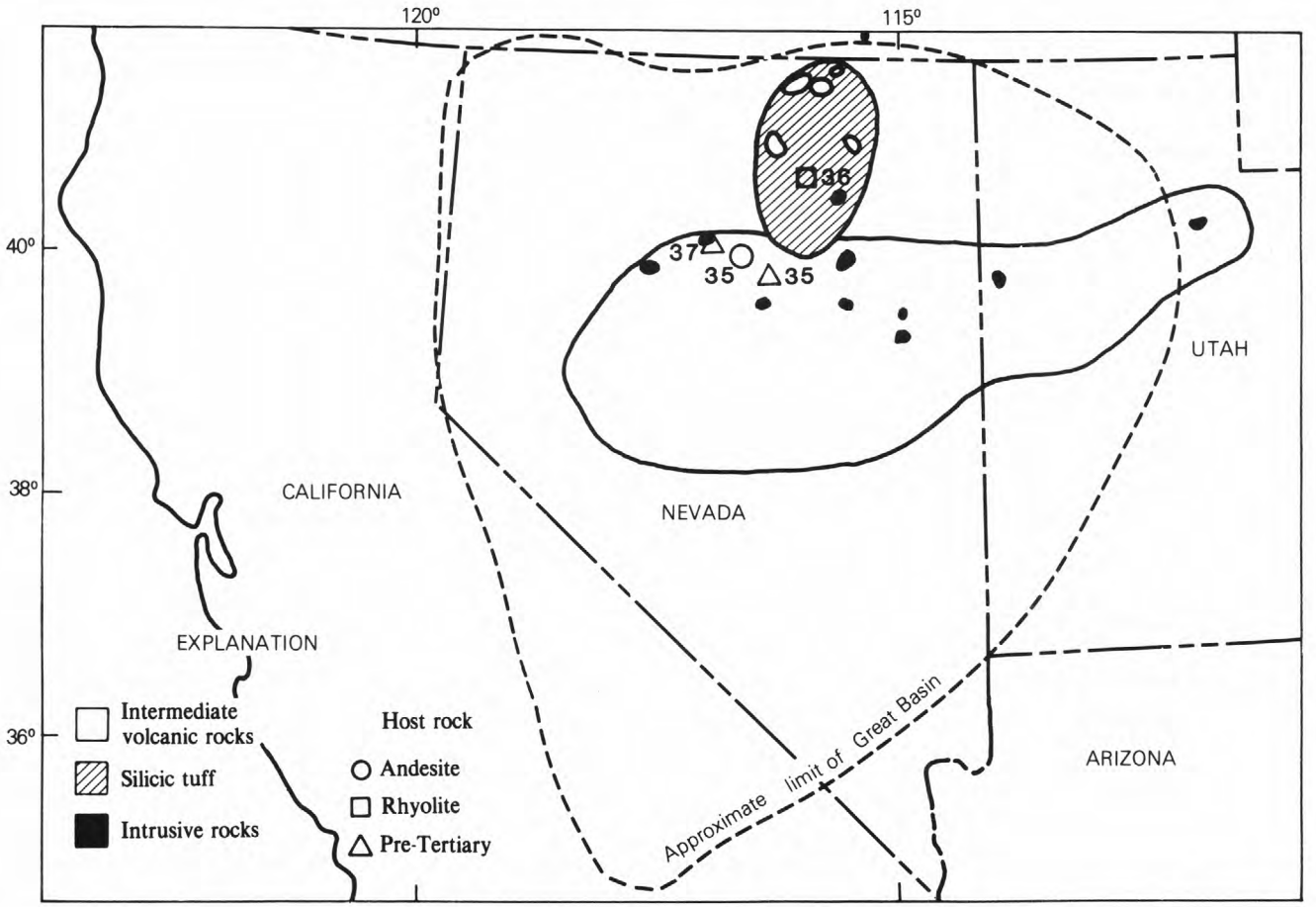

Figure 43. Nevada and adjacent States, showing distribution of volcanic rocks 34 to 43 m.y. old in the Great Basin and surrounding regions (modified from Stewart and Carlson, 1976, sheet 1), and locations and ages of ore deposits and host-rock lithologies.

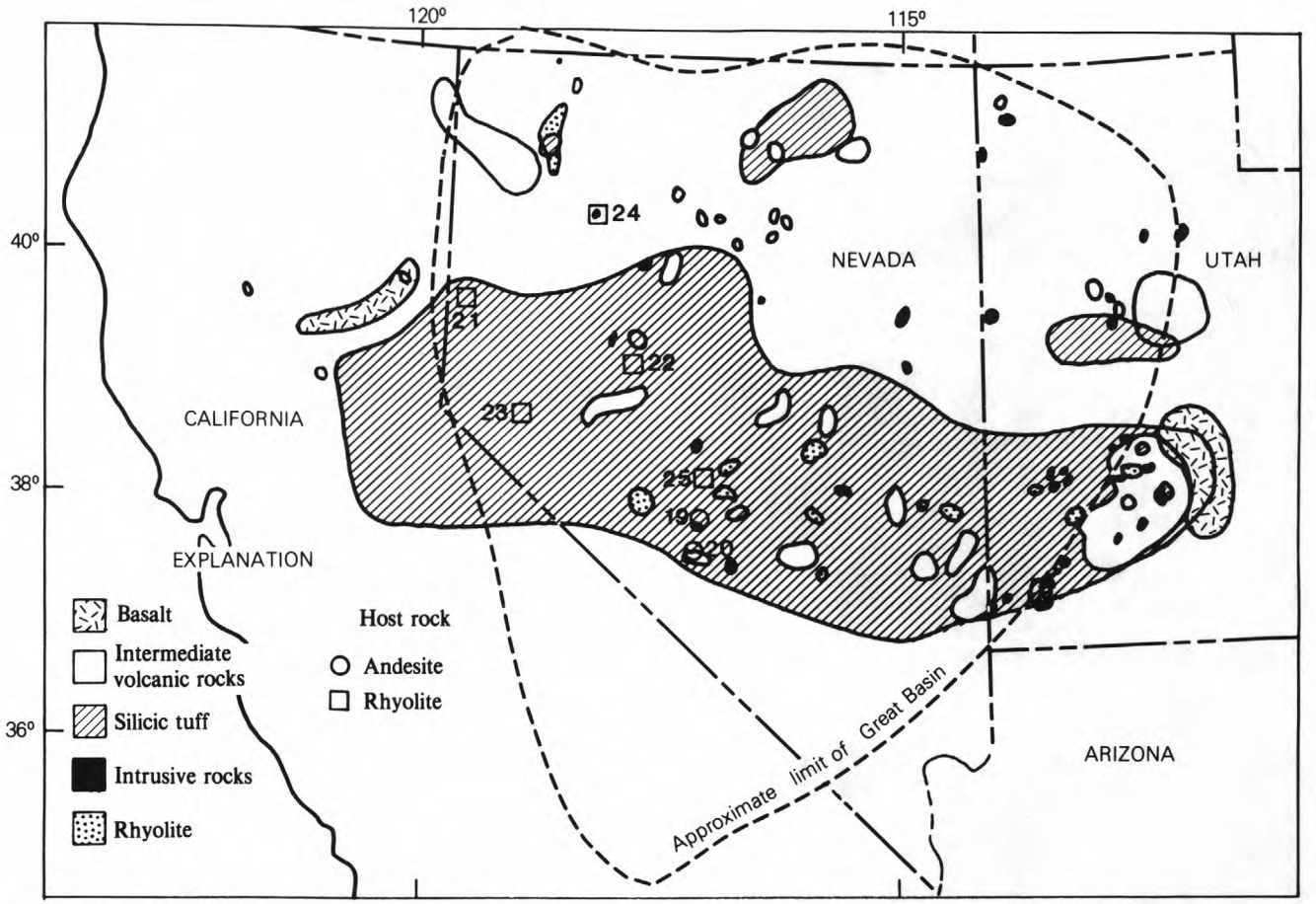

Figure 44. Nevada and adjacent States, showing distribution of volcanic rocks 17 to 34 m.y. old in the Great Basin and surrounding regions (modified from Stewart and Carlson, 1976, sheet 2), and locations and ages of ore deposits and host-rock lithologies.

associated with all stages of volcanic activity, particularly vigorous hydrothermal activity immediately following the onset of crustal extension, and no predominant host-rock lithology. The region is characterized by a grouping of deposits over time, rather than by a host-rock association. Of the 16 dated deposits in the northern and central Great Basin (figs. 47, 48) 4 were formed during an early stage of intermediate volcanic activity, and 3 during a period of dominant ash-flow-tuff eruption. All these deposits are related to local intrusive or volcanic activity, and many are significant, with production and (or) reserves of greater than 3,400 kg Au, and some with greater than 34,000 kg Au (for example, Round Mountain and Cortez). A significant grouping of fissure-vein deposits occurs between 16 and 12 m.y. B.P., in association with the 17- and 6-m.y.-B.P. mixed volcanic episodes. Many of these are small deposits (less than 3,400 kg Au) and occur in faults or shear zones related to basin-and-range faulting, which followed the onset of crustal extension at 20-17 m.y. B.P. The deposits are relatively independent of host-rock type and are not demonstrably related to local volcanic activity. Exceptions occur at Jarbidge and McDermitt, Nev., where the deposits occur within voluminous volcanic sequences near the margins of the Great Basin. The age on figure 46 and 47 from the Sulfur prospect in northwestern Nevada (M. L. Silberman and A. B. Wallace, unpub. data, 1980), represents the youngest known Au-containing system in the central Great Basin.

Walker Lane (western Great Basin)

The pattern of distribution of deposits along the Walker Lane differs considerably from that in the northern and central Great Basin (fig. 49). No clear grouping over time is evident; instead, mineral deposits occur throughout most of the time interval shown. Of 20 dated deposits, 9 are in andesitic host rocks, and 4 are in volcanic sequences that contain andesite as part of the host-rock association. The major producers (greater than 34,000 kg Au) are all in andesite and include the Comstock Lode, Bodie, Aurora, Goldfield, and Tonopah. Production figures, as summarized in Silberman and others (1976), bear out the importance of

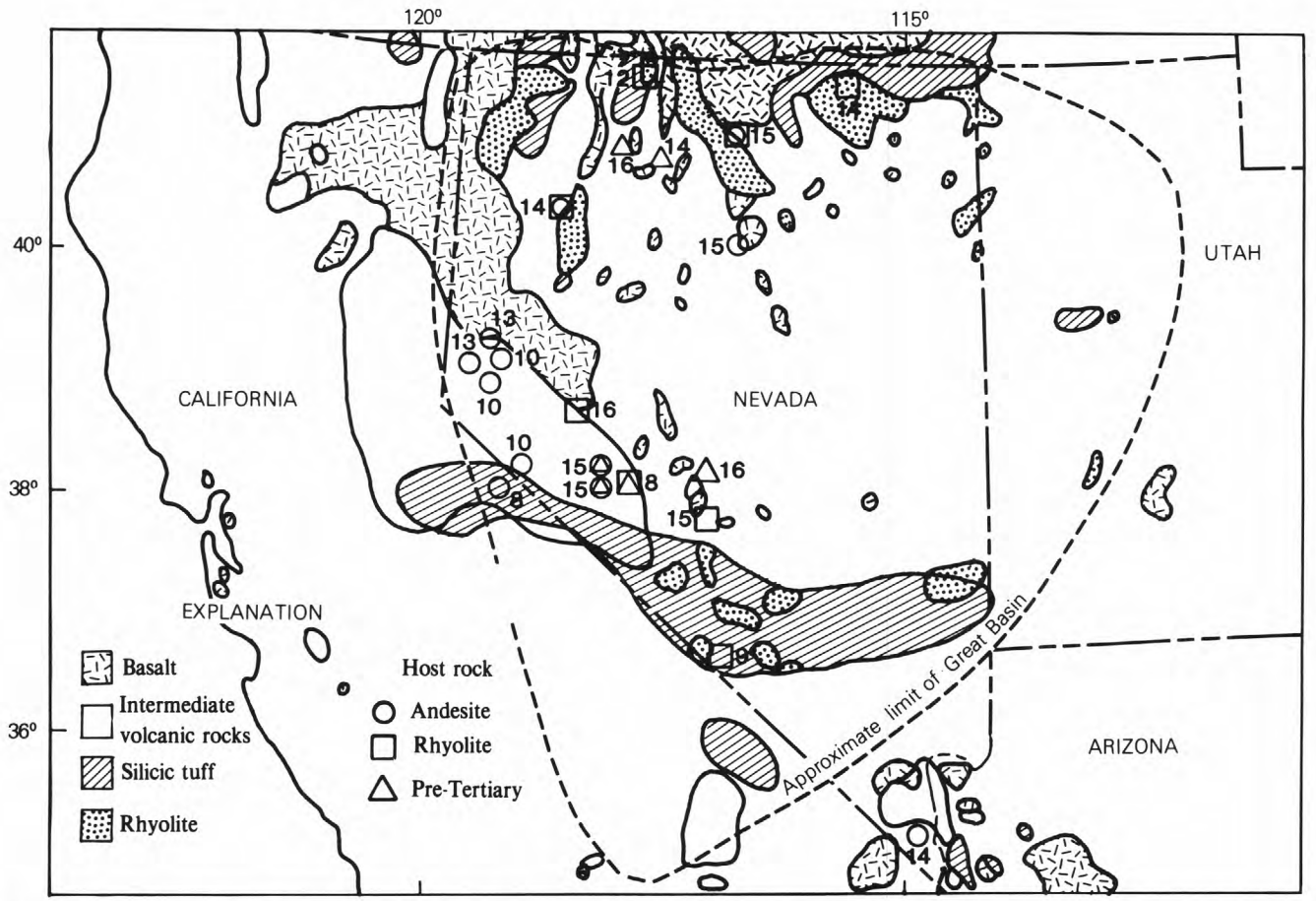

Figure 45. Nevada and adjacent States, showing distribution of volcanic rocks 6 to 17 m.y. old in the Great Basin and surrounding regions (modified from Stewart and Carlson, 1976, sheet 3), and locations and ages of ore deposits and host-rock lithologies.

andesite as a host rock for precious-metal deposits in the Walker Lane. Most of these deposits are associated with local stages of volcanic or intrusive activity. Thus, the pattern for the Walker Lane shows no essential grouping over time but a very strong association with a particular host-rock lithology.

I note that five deposits 5 m.y. old or younger occur in the Walker Lane. The 2-m.y.-old Sulfur deposit, though in the northern and central parts of the Great Basin, is close to the Walker Lane. Mineralization in the Great Basin has continued until nearly recent time, even though subduction affecting the region ended between 10 and 5 m.y. B.P. (Atwater and Molnar, 1973; Silberman and others, 1975).

TIMING OF STAGES OF ALTERATION-MINERALIZATION

None of the geochronologic studies mentioned above attempted to define the duration of a single stage of hydrothermal activity or a mineralizing event within an overall period of hydrothermal activity. Nonetheless, a consensus appears to be developing among workers in epithermal systems that mineralizing events are short-lived, transitory, and repetitive events within a context of longer lived hydrothermal activity (Silberman, 1982a). Some of the evidence of this interpretation is as follows.

1. Multiple stages of hydrothermal brecciation and stockwork veining have occurred, only some of which are associated with sulfide deposition and mineralization in bulk-tonnage precious-metal systems (Silberman, 1982a, b; Berger and Eimon, 1984).
2. Banding of epithermal quartz veins occurs in bonanza systems, and only a few of the bands contain sulfides. Both the banding and the brecciation are believed to be related to boiling, which occurs episodically in most systems (Buchanan, 1981).
3. Several alteration assemblages succeed each other within a restricted area. In some systems, such as Bodie (Silberman and others, 1972; O'Neil and others, 1973) and Julcani (Peterson and others, 1977; Noble and Silberman, 1984), mineralization occurs in association with one particular assemblage, but not with others.

Epithermal mineral deposits commonly occur in close association with intrusive phases, where the heat of the crystallizing magma generates a convective

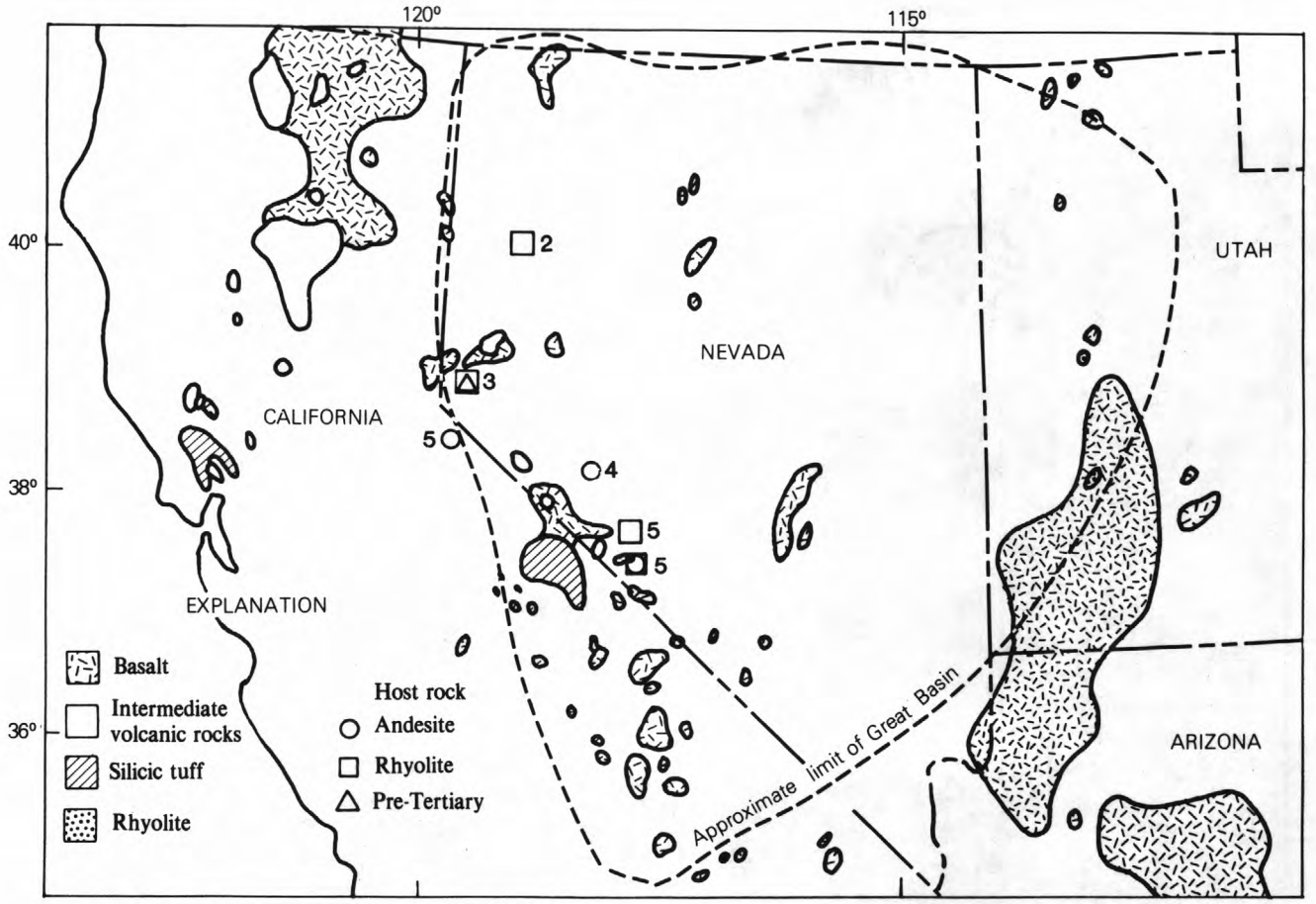

Figure 46. Nevada and adjacent States, showing distribution of volcanic rocks 0 to 6 m.y. old in the Great Basin and surrounding regions (modified from Stewart and Carlson, 1976, sheet 4), and locations and ages of ore deposits and host-rock lithologies.

hydrothermal system (White, 1974, 1981; Norton and Cathles, 1979). Cooling of the magma by conduction and convection, unless new sources of heat (magma) are provided, will limit the period during which circulation can occur in a hydrothermal system. Such factors as permeability, salinity of the fluid, and recharge conditions (amount of fluid) will also affect the length of this period. In general, hydrothermal systems are permeable owing to fracturing, and cooling can be considered in a convective-circulation model (Norton and Cathles, 1979). Models of cooling plutons approximately 2 km wide suggest decay of a hydrothermal-circulation cell well within about 100,000 years. This period is short in relation to the estimates discussed previously for overall hydrothermal lifetimes in epithermal systems. These observations suggest either that the magmatic bodies related to the generation of epithermal ore deposits are much larger than the 1- to 3-km bodies commonly found at the present-day surface near such deposits (for example, Bodie Bluff at Bodie; Mount Davidson at the Comstock Lode; the rhyolite domes at Steamboat Springs, Nev.) or that successive closely spaced pulses of magmatic influx must occur that renew the sources of heat for the convective systems. In at least two areas—Steamboat Springs, Nev. (Silberman and others, 1979b), and Tonopah, Nev. (Silberman and others, 1979a)—the presence of a regional batholith and the occurrence of several pulses of magma influx have been invoked to explain long-lived, complex hydrothermal systems.

K-Ar data from the Julcani polymetallic-vein district of Peru (Noble and Silberman, 1984) support the interpretation that individual pulses of alteration and mineralization are only short lived. K-Ar ages and geologic relations at Julcani suggest that eight stages of interspersed volcanic and hydrothermal activity, including a pulse of sulfide mineralization, occurred over a timespan of 700,000 years. Although not all of these stages could be definitively dated, estimates of the duration of the hydrothermal episodes range from 100,000 to 200,000 years. These time intervals are interestingly similar to the convective-cooling periods for small plutons suggested by the Norton and Cathles (1979).

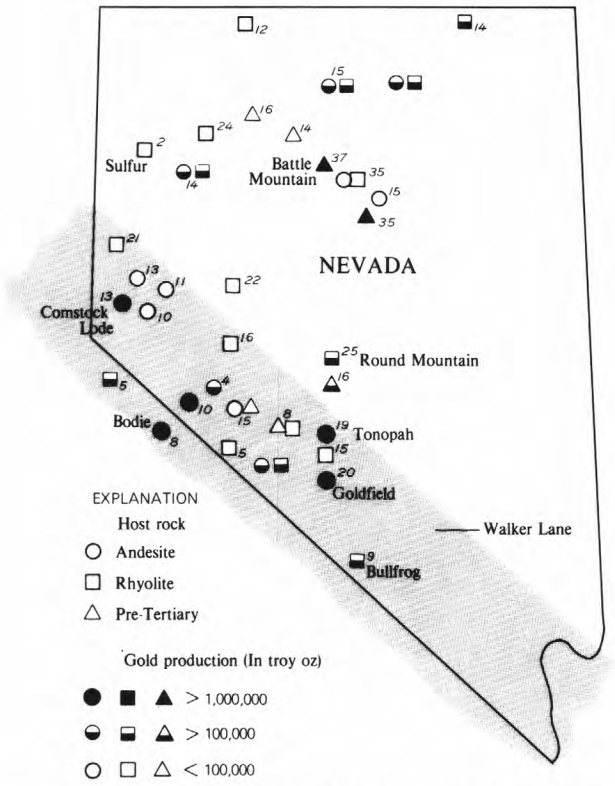

Figure 47. Nevada, showing distribution of ore deposits dated by the K-Ar method in the Great Basin, showing host-rock lithology and approximate production of gold (modified from Silberman and others, 1976, fig. 8).

SUMMARY

This discussion of the geochronology of hydrothermal alteration and mineralization, particularly of epithermal precious-metal systems, has demonstrated the temporal relations of hydrothermal processes to volcanic activity and has suggested a range in the timing of overall hydrothermal activity of 0.5 to 3 m.y. for many systems. I have also shown that regional patterns of hydrothermal mineralization occur and that these patterns are relatable to the timing of tectonic and volcanic evolution, though not always in a simple fashion. Finally, a start has been made in interpreting the timing of pulses of alteration and mineralization within a broader frame of overall hydrothermal activity—a topic that needs further investigation. The methods for isotopically determining the period of activity of alteration pulses and mineral deposition have yet to be refined, and the question whether this fine-scale tuning of the timing relations has any correlation with the degree of mineralization (that is, any economic significance) has not yet been answered.

REFERENCES CITED

Adams, C. J. D., Wodzicki, Antoni, and Weissberg, B. G., 1974, K-Ar dating of hydrothermal alteration at the Tui Mine, Te Aroha, New Zealand: New Zealand Journal of Science, no. 2, v. 17, p. 193-199.

Albers, J. P., and Stewart, J. H., 1972, Geology and mineral deposits of Esmeralda Co., Nevada: Nevada Bureau of Mines Bulletin, 78, 80 p.

Ashley, R. P., 1974, Goldfield mining district, in Guidebook to the geology of four Tertiary volcanic centers in central Nevada: Nevada Bureau of Mines and Geology Report 19, p. 49-66.

Ashley, R. P., and Silberman, M. L., 1976, Direct dating of mineralization at Goldfield, Nevada, by potassium-argon and fission-track methods: Economic Geology, v. 71, no. 5, p. 904-924.

Atwater, Tanya, 1970, Implications of plate tectonics for the Cenozoic tectonic evolution of western

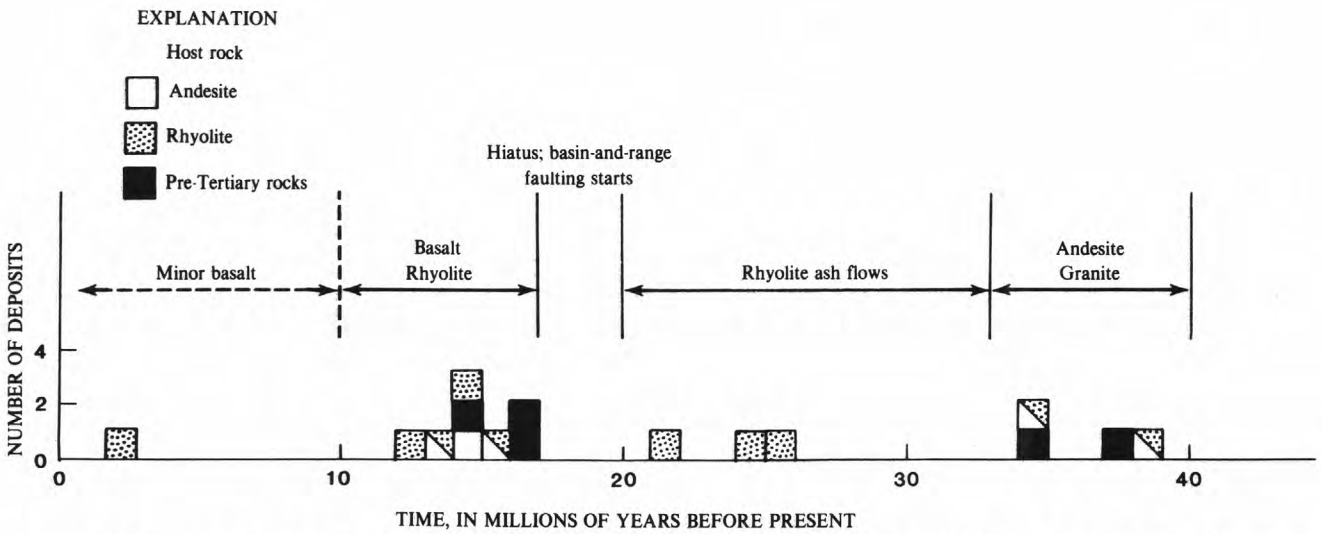

Figure 48. Dates of formation of ore deposits and host-rock lithology in the central and northern Great Basin.

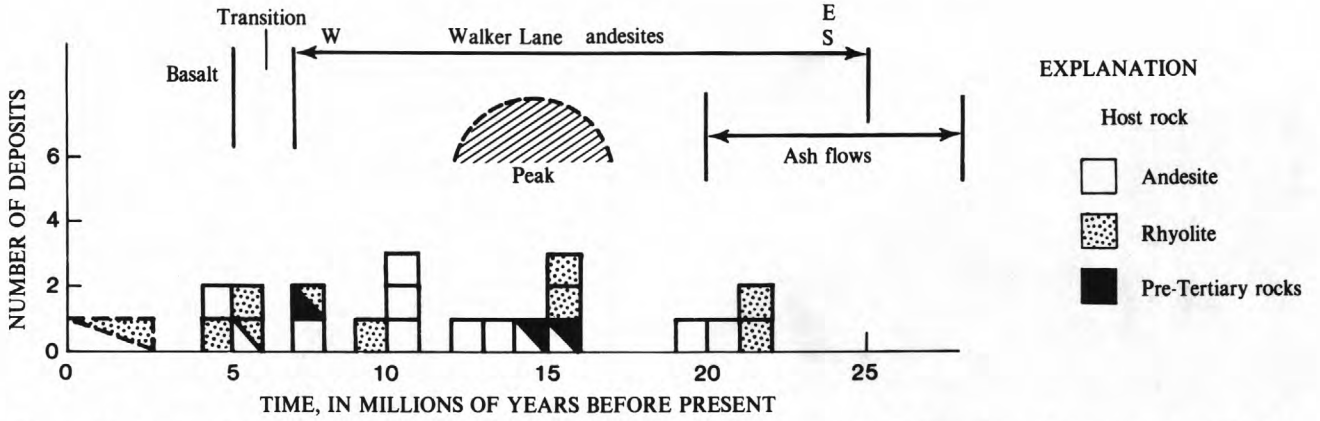

Figure 49. Dates of formation of ore deposits and host-rock lithology in the Walker Lane (western Great Basin).

North America: Geological Society of America Bulletin, v. 81, no. 12, p. 3513-3536.

Atwater, Tanya, and Molnar, Peter, 1973, Relative motions of the Pacific and North American plates deduced from sea-floor spreading in the Atlantic, Indian, and south Pacific oceans, in Kovach, R. L., and Nur, Amos, eds., Proceedings of the conference on tectonic problems of the San Andreas fault system: Stanford University Publication in the Geological Sciences, v. 13, p. 136-148.

Berger, B. R., and Eimon, P. I., 1983, Conceptual models of epithermal precious-metal deposits in Shanks, W. C., ed., Cameron Volum on unconventional mineral deposits: American Institute of Mining, Metallurgical and Petroleum Engineers, New York, p. 191-205.

Berger, B. R., and Tingley, J. V., 1980, Geochemistry of the Round Mountain gold deposit, Nye Co., Nevada [abs.]: Society of Mining Engineers of AIME, Northern Nevada Section Precious Metals Symposium, Sparks, Nev., 1980, Abstracts, p. 18c.

Bonham, H. F., Jr., and Garside, L. R., 1979, Geologic map of the Tonopah, Lone Mountain, Klondike, and Northern Mud Lake quadrangles, Nevada: Nevada Bureau of Mines and Geology Bulletin 92, 142 p.

Buchanan, L. J., 1981, Precious metal deposits associated with volcanic environments in the southwest, in Dickinson, W. R., and Payne, W. D., eds., Relations of tectonics to ore deposits in the Southern Cordillera: Arizona Geological Society Digest, Vol. 14, p. 237-262.

Chesterman, C. W., 1968, Volcanic geology of the Bodie Hills, Mono County, California, in Coats, R. R., Hay, R. L., and Anderson, C. A., eds., Studies in volcanology: A memoir in honor of Howell Williams: Geological Society of America Memoir 116, p. 45-68.

Chesterman, C. W., and Gray, C. H., Jr., 1975, Geology of the Bodie 15-minute quadrangle: California Division of Mines and Geology Map Sheet 21, scale 1:48,000.

Chesterman, C. W., Chapman, R. H., and Gray, C. H., 1984, Geology and ore deposits of the Bodie mining district, Mono County, California: California Division of Mines and Geology Bulletin [in press].

Chivas, A. R., and McDougall, Ian, 1978, Geochronology of the Koloula porphyry copper prospect, Guadalcanal, Solomon Islands: Economic Geology, v. 73, no. 5, p. 678-689.

Christiansen, R. L., and Lipman, P. W., 1972, Cenozoic volcanism and plate tectonic evolution of the western United States. II, Late Cenozoic: Royal Society of London Philosophical Transactions, ser. A, v. 271, no. 1213, p. 249-284.

Clark, K. F., Foster, C. T., and Damon, P. E., 1982, Cenozoic mineral deposits and subduction-related magmatic arcs in Mexico: Geological Society of America Bulletin, v. 93, no. 6, p. 533-544.

Damon, Paul, and Mauger, R. L., 1966, Epeirogeny-orogeny viewed from the Basin and Range province: Americam Institute of Mining, Metallurgical and Petroleum Engineers Transactions, v. 235, p. 99-112.

Damon, P. E., Shafiquallah, Muhammad, and Clark, K. F., 1984, Geochronology of the porphyry copper deposits and related mineralization of Mexico: Canadian Journal of Earth Sciences [in press].

Erickson, R. L., Silberman, M. L., and Marsh, S. P., 1978, Age and composition of igneous rocks, Edna Mountain quadrangle, Humboldt County, Nevada: U.S. Geological Survey Journal of Research, v. 6, no. 6, p. 727-743.

Gilbert, C. M., Christensen, J. N., Al-Rawi, Yehya, and Lajoie, K. R., 1968, Structural and volcanic history of Mono Basin, California-Nevada, in Coats, R. R., Hay, R. L., and Anderson, C. A., eds., Studies in volcanology: A memoir in honor of Howell Williams: Geological Society of America Memoir 116, p. 275-329.

Gustafson, L. B., and Hunt, J. P., 1975, The porphyry copper deposit at El Salvador, Chile: Economic Geology, v. 70, no. 5, p. 857-912.

Kleinhampl, F. J., Silberman, M. L., Chesterman, C. L., Chapman, R. H., and Gray, C. H., Jr., 1975,

Aeromagnetic and limited gravity studies and generalized geology of the Bodie Hills region, Nevada and California: U.S. Geological Survey Bulletin 1384, 38 p.

Koski, R. A., Chesterman, C. W., Silberman, M. L., and Fabbi, B. P., 1978, Hydrothermal adularia at Bodie, Mono County, California: U.S. Geological Survey Open-File Report 78-942, 24 p.

Lipman, P. W., Fisher, F. S., Mehnert, H. H., Naeser, C. W., Luedke, R. G., and Steven, T. A., 1976, Multiple ages of mid-Tertiary mineralization and alteration in the western San Juan Mountains, Colorado: Economic Geology, v. 71, no. 3, p. 571-588.

Lipman, P. W., Prostka, H. J., and Christiansen, R. L., 1972, Cenozoic volcanism and plate tectonic evolution of the western United States. I. Early and Middle Cenozoic: Royal Society of London Philosophical Transactions, ser. A, v. 271, no. 1213, p. 217-248.

Mehnert, H. H., Lipman, P. W., and Steven, T. A., 1973, Age of mineralization at Summitville, Colorado, as indicated by K-Ar dating of alunite: Economic Geology, v. 68, no. 3, p. 399-401.

Meyer, Charles, and Hemley, J. J., 1967, Wall rock alteration, in Barnes, H. L., ed., Geochemistry of hydrothermal ore deposits: New York, Holt, Rinehart and Winston, p. 166-235.

Mitchell, P. A., Silberman, M. L., and O'Neil, J. R., 1981, Genesis of gold vein mineralization in an Upper Cretaceous turbidite sequence, Hope-Sunrise district, southern Alaska: U.S. Geological Survey Open-File Report 81-103, 20 p.

Moore, W. J., and Lanphere, M. A., 1971, The age of porphyry-type copper mineralization in the Bingham mining district, Utah--a refined estimate: Economic Geology, v. 66, no. 2, p. 331-334.

Morton, J. L., Silberman, M. L., Bonham, H. F., Jr., Garside, L. J., and Noble, D. C., 1977, K-Ar ages of volcanic rocks, plutonic rocks and ore deposits in Nevada and eastern California--determinations run under the USGS-NBMG cooperative program: Isochron/West, no. 20, p. 19-29.

Naeser, C. W., and Faul, Henry, 1969, Fission track annealing in apatite and sphene: Journal of Geophysical Research, v. 74, no. 2, p. 705-710.

Noble, D. C., and Silberman, M. L., 1984, Volcanic and hydrothermal evolution and K-Ar chronology of the Julcani district, Peru: Economic Geology [in press].

Noble, D. C., Vogel, T. A., Weiss, S. I., Erwin, J. W., McKee, E. H., and Younker, L. W., 1984, Stratigraphic relations and source areas of ash-flow sheets of the Black Mountain and Stonewall Mountain volcanic centers, Nevada: Journal of Geophysical Research [in press].

Norton, Dennis, and Cathles, L. M., 1979, Thermal aspects of ore deposition, in Barnes, H. L., ed., Geochemistry of hydrothermal ore deposits, (2d ed.): New York, John Wiley and Sons, p. 611-683.

O'Neil, J. R., Silberman, M. L., Fabbi, B. P., and Chesterman, C. W., 1973, Stable isotope and chemical relations during mineralization in the Bodie mining district, Mono County, California: Economic Geology, v. 68, no. 6, p. 765-784.

Petersen, Ulrich, Noble, D. C., Arenas, M. J., and Goodell, P. C., 1977, Geology of the Julcani mining district, Peru: Economic Geology, v. 72, no. 6, p. 931-949.

Ransome, F. L., 1909, The geology and ore deposits of Goldfield, Nevada: U.S. Geological Survey Professional Paper 66, 258 p.

Rose, A. W., and Burt, D. M., 1979, Hydrothermal alteration, in Barnes, H. L., ed., Geochemistry of hydrothermal ore deposits (2d ed.): New York, John Wiley and Sons, p. 173-235.

Rowen, L. C., Kingston, M. J., and Heald-Wetlaufer, Pamela, 1984, The Humboldt and Walker Lane structural zones: Post-Oligocene belts of mineralization in Nevada: Economic Geology [in press].

Silberman, M. L., 1982a, Geochronology of hydrothermal mineralization [abs.]: Geological Society of America Abstracts with Programs, v. 14, no. 7, p. 617.

_____1982b, Hot-spring type, large tonnage, low-grade gold deposits, in Erickson, R. L., compiler, Characteristics of mineral deposit occurences: U.S. Geological Survey Open-File Report 82-795, p. 131-143.

Silberman, M. L., and Ashley, R. P., 1970, Age of ore deposition at Goldfield, Nevada from K-Ar dating of alunite: Economic Geology, v. 65, no. 3, p. 352-354.

Silberman, M. L., Berger, B. R., and Koski, R. A., 1974, K-Ar age relations of granodiorite emplacement and tungsten and gold mineralization near the Getchell mine, Humboldt County, Nevada: Economic Geology, v. 69, no. 5, p. 646-656.

Silberman, M. L., Bonham, H. F., Jr., Garside, L. J., and Ashley, R. P., 1979a, Timing of hydrothermal alteration-mineralization and igneous activity in the Tonopah mining district and vicinity, Nye and Esmeralda Counties, Nevada, in Ridge, J. D., ed., Papers on mineral deposits of western North America: Nevada Bureau of Mines and Geology Report 33, p. 119-126.

Silberman, M. L., and Chesterman, C. W., 1972, K-Ar age of volcanism and mineralization, Bodie mining district and Bodie Hills volcanic field, Mono County, California: Isochron/West, no. 3, p. 13-22.

Silberman, M. L., Chesterman, C. W., Kleinhampl, F. J., and Gray, C. H., Jr., 1972, K-Ar ages of volcanic rocks and gold-bearing quartz-adularia veins in the Bodie mining district, Mono County, California: Economic Geology, v. 67, no. 5 p. 597-604.

Silberman, M. L., MacKevett, E. M., Jr., Connor, C. L., and Matthews, Alan, 1980, Metallogenic and tectonic significance of oxygen isotope data and whole-rock potassium-argon ages of the Nikolai Greenstone, McCarthy quadrangle, Alaska: U.S. Geological Survey Open-File Report 80-2019, 31 p.

Silberman, M. L., Morton, J. L., Cox, D. C., and Richter, D. H., 1977, K-Ar ages of disseminated copper and molybdenum mineralization in the Nebesna and Klein Creek batholiths, eastern Alaska Range, Alaska [abs.]: Geological Society

of Canada Abstracts with Programs, v. 2, p. 48.

Silberman, M. L., Noble, D. C., and Bonham, H. F., Jr., 1975, Ages and tectonic implications of the transition of calc-alkaline andesitic to basaltic volcanism, in the western Great Basin and the Sierra Nevada [abs.]: Geological Society of America Abstracts with Programs, v. 7, no. 3, p. 375.

Silberman, M. L., Stewart, J. H., and McKee, E. H., 1976, Igneous activity, tectonics, and hydrothermal precious-metal mineralization in the Great Basin during Cenozoic time: Society of Mining Engineers of AIME Transactions, v. 260, no. 3, p. 253-263.

Silberman, M. L., White, D. E., Keith, T. E. C., and Dockter, R. D., 1979b, Duration of hydrothermal activity at Steamboat Springs, Nevada, from ages of spatially associated volcanic rocks: U.S. Geological Survey Professional Paper 458-D, p. D1-D14.

Snyder, W. S., Dickinson, W. R., and Silberman, M. L., 1976, Tectonic implications of space time patterns of Cenozoic magmatism in the western United States: Earth and Planetary Science Letters, v. 32, p. 91-106.

Stewart, J. H., and Carlson, J. E., 1976, Cenozoic rocks of Nevada: Nevada Bureau of Mines and Geology, Map 52, scale 1:1,000,000, 4 sheets.

Strachan, D. G., Pettit, Paul, and Reid, R. F., 1982, The geology of the Borealis gold deposit, Mineral County, Nevada [abs.]: Geological Society of America Abstracts with Programs, v. 14, no. 7, p. 627.

Wallace, A. B., 1980, Geology of the Sulphur district, southwestern Humboldt County, Nevada: Society of Economic Geologists Field Conference, 1980, Road Log and Articles, p. 80-91.

Warnaars, F. W., Smith, W. H., Bray, R. W., Lanier, George, and Shafiquallah, Muhammed, 1978, Geochronology of igneous intrusions and porphyry copper mineralization at Bingham, Utah: Economic Geology, v. 73, no. 7, p. 1242-1249.

Whalen, J. B., Britten, R. M., and McDougall, Ian, 1982, Geochronology and geochemistry of the Frieda River prospect area, Papua New Guinea: Economic Geology, v. 77, no. 3, p. 592-616.

White, D. E., 1955, Thermal springs and epithermal ore deposits: Economic Geology, 50th anniversary volume, pt. 1, p. 99-154.

_____1974, Diverse origins of hydrothermal ore fluids: Economic Geology, v. 69, no. 6, p. 954-973.

____1981, Active geothermal systems and hydrothermal ore deposits: Economic Geology, 75th anniversary volume, p. 392-423.

Wilson, F. H., 1980, Late Mesozoic and Cenozoic tectonics and the age of porphyry copper prospects; Chignik and Sutwick Island quadrangles, Alaska Peninsula: U.S. Geological Survey Open-File Report 80-543, 94 p.

Characteristics of Bulk-Minable Gold-Silver Deposits in Cordilleran and Island-Arc Settings

By Harold F. Bonham, Jr.

CONTENTS

INTRODUCTION

Bulk-minable gold-silver deposits occur in various geologic environments in Cordilleran and island-arc settings, and some of these deposits have been mined on an intermittent basis, depending on prevailing gold-silver prices, for many years. Several deposits of this type were in production in the Western United States during the 1920's and 1930's, for example, Zortman, Mont., Yellow Pine, Idaho, and the Comstock Lode, Northumberland, and Gold Acres, Nev.

The relatively high price levels that have prevailed for gold and silver since 1979 have stimulated a worldwide search for bulk-minable precious-metal deposits. Favorable price levels and the development of improved metallurgical techniques for the treatment of low-grade ores, in particular heap leaching, have made possible the economic recovery of gold and silver from ores containing as little as 0.06 troy oz Au per ton (2 g Au/t) or 2.2 troy oz Ag per ton (75 g Ag/t).

A second factor that has stimulated the search for bulk-minable precious-metal deposits, particularly gold, was the discovery of the Carlin, Nev., gold deposit in 1961-62. The Carlin ore is of the so-called microscopic type, in which visible gold is rare or absent. Consequently, outcropping ore zones do not form a placer train. The real significance of the Carlin deposit is that as a large, relatively high grade (12 million tons containing 0.52 troy oz Au per ton [11 million t containing 18 g Au/t]), bulk-minable ore body, it received widespread publicity and focused the attention of the mining industry on this class of deposit. The relatively ordinary appearance of the oxidized sedimentary host rocks for this type of deposit had, for the most part, prevented their discovery in earlier years. Note, however, that several deposits of this type at Mercur, Utah, and at Getchell, Northumberland, and Gold Acres, Nev., were discovered and had produced significant amounts of gold well before the Carlin discovery.

The diversity of geologic environments in which low-grade precious-metal deposits occur in Cordilleran and island-arc settings is discussed by Sillitoe (1984), who proposes the following general mineralization types for low-grade gold deposits: (1) Porphyry copper deposits; (2) epithermal deposits hosted by intrusive rocks; (3) contact-metasomatic skarn deposits; (4) contact-metasomatic distal deposits, generated beyond the influence of skarn formation; (5) Carlin-type carbonate-hosted deposits; (6) hydrothermal-breccia-hosted deposits; (7) enargite-luzonite-bearing massive sulfide deposits of replacement origin; (8) epithermal deposits dispersed in felsic or intermediate volcanic rocks; (9) vein-type epithermal deposits; and (10) Kuroko-type massive sulfide deposits. Several of these classes are equally applicable to low-grade silver deposits.

Other classification schemes for low-grade gold-silver deposits are possible, including those based on geochemical associations, alteration types, specific host-rock associations, structural controls, and genetic models. Sillitoe's (1984) classification includes elements of all these categories. Owing to the inherent geologic complexity of many of these deposits—for example, a single deposit, such as the Blue Star mine, Nev., can contain disseminated gold ore in limy, carbonaceous

sediment as well as in porphyritic granodiorite—I propose the following simple, first-order classification scheme which is amenable to numerous subclasses under each major heading: (1) Deposits spatially related to intrusive granitic rocks, phaneritic, or porphyritic rocks, or true porphyries, including stocks, dikes, and sills; and (2) deposits spatially related to volcanic centers, including calderas, dome fields, and composite volcanoes. I recognize some overlap between these two categories. Sillitoe's (1984) types 1 through 5 fit into my category 1, his types 6 and 7 can belong in either category 1 or 2, and his types 8 through 10 belong in my category 2. The 1982 U.S. Geological Survey workshop was concerned principally with the Carlin or carbonate-hosted and breccia types and category 2. A very brief consideration of category 1 is included here for the purposes of comparison.

DEPOSITS RELATED TO GRANITIC INTRUSIVE ROCKS

Porphyry copper deposits

Sillitoe (1979, 1984) has discussed gold-rich porphyry copper deposits on a worldwide basis. He concluded (Sillitoe, 1979) that the gold in gold-rich porphyry deposits is present in potassium silicate alteration, which commonly carries a high magnetite content. A high Au content is not related to geotectonic setting, composition of the host intrusive body, age of mineralization, erosional level, or size of the ore body.

Sillitoe (1979) suggested that copper-poor porphyry gold deposits should be considered as an exploration target. Although no documented examples of precious-metal-bearing porphyry deposits are known, the Zortman-Landusky deposits in Montana may be of this type. Gold-silver mineralization at Zortman-Landusky (Koschman and Bergdahl, 1968; Graybeal, 1981) occurs partly in fractured syenite porphyry. Auriferous pyrite and sylvanite occur in a gangue of quartz and fluorite.

Epithermal deposits hosted by intrusive rocks

Sillitoe (1984) describes several examples of gold-silver mineralization of the epithermal type associated with intrusive rocks, including Porgera, Papua New Guinea; Salave, Spain; and the Yellow Pine deposit in the Stibnite district, Idaho. The Austin district, Nev. (McKee, 1974), would also fit into this category. At Austin, gold-silver mineralization occurs in narrow quartz veins that fill joints and fractures in quartz monzonite of the Austin pluton. Ore minerals include native silver, acanthite, proustite, pyragyrite, stephanite, polybasite, and electrum. The gangue consist of quartz, calcite, adularia, rhodochrosite, and ankerite. Associated sulfides include pyrite, molybdenite, galena, and sphalerite. The pluton is 157±6 m.y. old, according to K-Ar dating of biotite. Adularia from vein material is 94 m.y. old by K-Ar dating. The Austin district, which holds more than 110 million tons (100 million t) of ore containing 0.29 to 0.43 troy oz Ag per ton (10-15 g Ag/t) and minor gold, constitutes a potentially significant resource.

Contact-metasomatic skarn deposits

The contact-metasomatic skarn deposits listed by Sillitoe (1984) include Copper Canyon in the Battle Mountain district, Nev.; Ertsberg, Irian Jaya, Indonesia; La Luz, Nicaragua; and OK Tedi, Papua New Guinea. Deposits of this type typically consist primarily of gold-copper mineralization and may occur adjacent to an unmineralized or weekly mineralized stock, such as those at Battle Mountain and Ertsburg. They are genetically related to intrusive stocks of dioritic, monzonitic, or granodioritic composition. The gold in these deposits occurs in calc-silicate skarns associated with pyrite, pyrrhotite, chalcopyrite, and, commonly, magnetite.

Contact-metasomatic distal deposits

Contact-metasomatic distal deposits include those believed to be related to granitic intrusive rocks but which lie beyond the zone of well-developed skarn formation. The Copper Canyon deposit near Battle Mountain, Nev., is an excellent example of this type. Disseminated gold deposits occur beyond a copper-gold-bearing skarn in a 30-m-thick horizon within basal conglomerate of the Pennsylvanian Battle Formation. These gold deposits and the copper-gold-bearing skarn are zoned around a granodiorite porphyry stock that is altered and contains minor, noneconomic sulfide mineralization (Blake and Kretschner, 1980).

The conglomerate, which is the host for the gold ore bodies and the skarn deposit, has a calcareous matrix. In the vicinity of the gold mineralization, the conglomerate has been thermally metamorphosed to tremolite. The tremolite in the gold deposits is replaced by pyrrhotite, pyrite, and lesser amounts of sphalerite, galena, and chalcopyrite. Native gold, generally less than 0.05 mm in diameter, is associated with the pyrite and pyrrhotite. Silver mineralization in the deposits is related to the galena. Hydrothermal alteration associated with gold deposition has altered the tremolite to epidote, chlorite, and clay minerals (Blake and Kretschner, 1980). The Duval Corp. announced in November 1981 the discovery of additional reserves at Copper Canyon of 16 million tons (14.5 million t) averaging 0.135 troy oz Au per ton (4.67 g Au/t) and 0.514 troy oz Ag per ton (17.73 g Ag/t).

Another important deposit which fits into this category is the Equity (Sam Goosly) silver mine in British Columbia. Although the mineralization at the Equity deposit was originally interpreted as a volcanogenic sulfide deposit remobilized by later intrusive activity (Ney and others, 1972), more recent work (Wetherell, 1979) shows that the deposit is related to a quartz monzonite porphyry intrusion.

The copper-silver-antimony mineralization at the Equity deposit occurs in fine-grained tuff and volcaniclastic rocks. The chief sulfide minerals are pyrite, pyrrhotite, arsenopyrite, sphalerite, chalcopyrite, galena, and tetrahedrite. Tetrahedrite is

the main silver-bearing phase. The two main ore bodies are the Southern Trail zone and the Main zone. The ore in the Southern Trail zone is largely restricted to hydrothermal breccia, whereas that in the Main zone occurs as disseminated massive sulfide lenses and in hydrothermal breccia. Alteration minerals include andalusite, tourmaline, dumortierite, scorzalite, and late quartz-sericite. K-Ar ages of the quartz monzonite porphyry stock and alteration minerals in the ore zone are identical, within analytical error, at approximately 57 to 58 m.y. (Wetherell, 1979). The quartz monzonite porphyry stock contains subeconomic copper-molybdenum stockwork mineralization. Wetherell (1979) considered the ores to be distal to the copper-molybdenum mineralization in the porphyry stock. Announced reserves at the Equity mine are 7,509,000 tons (6,812,000 t) in the Southern Tail zone containing 0.48 weight percent Cu, 0.123 weight percent Sb, 3.82 troy oz Ag per ton (130.9 g Ag/t), and 0.040 troy oz Au per ton (1.381 g Au/t); and 23,323,000 tons (21,158,000 t) in the Main zone containing 0.353 weight percent Cu, 0.073 weight percent Sb, 2.87 troy oz Ag per ton (98.4 g Ag/t), and 0.024 troy oz Au per ton (0.825 g Au/t).

Sillitoe (1984) discusses the gold mineralization at Andacollo, Chile, which he considers to be distal to porphyry copper mineralization. Sillitoe (1984) also places the Windfall disseminated gold deposit in the Eureka district, Nev., into this category; however, the Windfall deposit seems to be genetically related to rhyodacite porphyry dikes present in the mine area rather than to the 100-m.y.-old quartz diorite stock referred to by Sillitoe (1984). The dikes are of mid-Tertiary age. The Windfall deposit probably should be classified as of the Carlin type.

The Golfo de Oro disseminated gold-silver deposit in northern Sonora, Mexico, also falls into the contact-metasomatic distal class. The Golfo de Oro deposit occurs in carbonaceous, calcareous shale and siltstone of the Barranca Formation of Mesozoic age. The gold-silver deposit occurs within a zone of hydrothermal alteration peripheral to the San Antonio del Cobre breccia pipe, which contains copper, molybdenum, and uranium mineralization and is genetically related to dacite porphyry dikes of Laramide age. The Golfo de Oro deposit occurs within a 2.5-km^2 area of hydrothermal alteration within which shale and siltstone locally are intensely silicified and brecciated and contain as much as 50 percent disseminated sulfides, principally pyrite and pyrrhotite, as well as minor tetrahedrite, galena, and sphalerite. The developed ore bodies occur in the oxidized zone and contain 0.12 to 0.15 troy oz Au per ton (4-5 g Au/t) and 0.29 troy oz Ag per ton (10 g Au/t). Developed reserves exceed 5.5 million tons (5 million t).

Carlin-type carbonate-hosted deposits

Carlin-type deposits are hydrothermal disseminated-replacement gold deposits, characterized by a high Au/Ag ratio and a geochemical association of gold, arsenic, antimony, mercury, and, in many deposits, thallium. Tungsten, molybdenum, tin, fluorine, and barium are commonly present in anomalous amounts. The host rock typically is carbonaceous, silty carbonate, or carbonaceous calcareous siltstone. Spatially associated with nearly all Carlin-type deposits are intrusive rocks ranging from granodiorite to rhyodacite in composition, and from stocks to dikes, sills, and plugs in form. The intrusive rocks are commonly altered and mineralized and in some deposits contain minable ore bodies. Silicified rocks, including abundant massive jasperoid, are present in most deposits. The jasperoid commonly shows evidence of multiple periods of hydrothermal brecciation and may occur either capping the main ore horizon, within it, or below it. In some places, the jasperoid is of ore grade. In addition to the ubiquitous silicification, alteration minerals typically present include illite, montmorillonite, kaolinite, chlorite, and sericite.

Primary controls on ore deposition in Carlin-type deposits are high-angle faults that transect a favorable host-rock type, typically a thin-bedded silty to sandy carbonaceous siltstone or carbonate rock. Hydrothermal breccia is invariably present in the ore zone and ranges from crackle breccia to pebble dikes and small breccia pipes.

The gold in Carlin-type deposits is typically submicroscopic and has particle sizes in the submicron to micron range (Radtke, 1981). The gold occurs as coatings on pyrite, dispersed on grains of amorphous-carbon grains as gold-organic complexes, in discrete grains in realgar, and in solid solution in realgar and native arsenic (Radtke, 1981).

Sulfide minerals present in Carlin-type deposits include pyrite (approx 2 percent) and, typically, widely varying amounts of cinnabar, realgar, orpiment, and stibnite. Small amounts of base-metal sulfides, including sphalerite, galena, chalcopyrite, and molybdenite, are commonly present. Several rare thallium-bearing minerals have been identified in a few deposits. The amount of arsenic present in Carlin-type deposits varies considerably; some deposits, such as Getchell, Nev., and Mercur, Utah, contain abundant arsenic sulfides, whereas others, such as Northumberland and Alligator Ridge, Nev., contain only small amounts of arsenic.

At several Carlin-type deposits, unoxidized primary ore is overlain by a zone of hypogene oxidation formed by a late stage of boiling of the hydrothermal solutions. Supergene oxidation may be superimposed on the zone of hypogene oxidation and can make separation of the hypogene and supergene alteration stages difficult in several of these deposits (Wells and others, 1969; Radtke, 1981).

The ages of Carlin-type deposits are a subject of controversy. Radtke and Dickson (1974) and Radtke (1981) prefer a late Tertiary age for virtually all deposits of this type, on the basis of presumed very shallow depositional environment, presumed control by basin-and-range faults of late Tertiary age, and an inferred relation to late Tertiary volcanism as a heat source for the hydrotheral fluids which produced the mineralization. K-Ar ages of hydrothermal sericite from Carlin-type deposits, however, indicate an age range from at least Cretaceous to late Tertiary. The Getchell, Nev., deposit has a K-Ar age of approximately 90 m.y. (Silberman and others, 1974), and the Pinson and Preble, Nev., deposits are also interpreted to be of Late Cretaceous age (Berger, 1980). The Gold Acres, Nev.,

deposit is spatially and, possibly, genetically related to a pluton dated at 94 m.y. (Silberman and McKee, 1971). The Cortez, Nev., deposit may be related to intrusive dikes that have a K-Ar age of 35 m.y. (Wells and others, 1971). The Gold Strike, Nev., deposit has been dated at 78.4 m.y. (Morton and others, 1977). Sericite from the Northumberland, Nev., deposit has a K-Ar age of 84 m.y. (H. F. Bonham, Jr., and M. L. Silberman, unpub. data, 1983). K-Ar ages of 131 m.y. have been obtained on sericite in mineralized dikes at the Carlin deposit (Radtke, 1981). Tertiary volcanic rocks near the Carlin mine have a K-Ar age of 14 m.y. (Radtke, 1981). The McLaughlin deposit in California, which has similarities to Carlin-type deposits, occurs partly in volcanic rocks which are approximately 2 m.y. old.

In summary, the available geologic and radiometric evidence for the ages of Carlin-type deposits indicates an age range of Cretaceous to late Tertiary or Quaternary. The close spatial relation of these deposits to intrusive rocks also implies a genetic relation. The argument that the deposits are geologically young because they were deposited at shallow depths and thus would not have persisted for any significant length of geologic time is defective on at least two counts. First, the Pueblo Viejo gold-silver deposit in the Dominican Republic was formed in a near-surface environment but is at least 80 m.y. old (Russell and others, 1981). Second, geologic evidence strongly indicates that many Carlin-type deposits have formed at depths of more than 1,000 m (Berger, 1980).

Several reports on the formation of Carlin-type deposits have strongly emphasized a hot-spring model (Radtke, 1981). The Carlin-type deposits are related to fossil geothermal systems, and although many of these systems may have vented to the surface as hot springs, none of the Carlin-type deposits have been shown to have formed in an actual hot-spring environment. In fact, of the Carlin-type deposits studied in some detail, the Carlin deposit itself is the only one for which a shallow (approx 200 m) depth of formation has been proposed (Radtke, 1981). The Gold Acres deposit, which is considered to have formed approximately 1,500 m below the surface, is believed to be genetically related to a granitic pluton present 120 m below the gold ore body. Hornfels and skarn containing scheelite and molybdenite occur in the open pit, and the gold ore is believed to have been deposited in the waning stage of the hydrothermal system that produced the skarns (Wrucke and Armbrustmacher, 1975). A similar geologic setting has been inferred for the disseminated gold mineralization at the Getchell mine (Silberman and others, 1974; Berger, 1980). Comparable geologic environments can be inferred for the Northumberland, Blue Star, Gold Strike, Bootstrap, Pinson, and Preble deposits in Nevada.

I believe, therefore, on the basis of most of the available evidence, that Carlin-type deposits formed at depths of 1,000 m or more below the paleosurface and can be related to a hot-spring model only in the context that hydrothermal ore deposits form in geothermal systems which generally, but not always, vent to the surface as hot springs and fumaroles.

The following attributes are exploration parameters for Carlin-type deposits.

1. The deposits typically occur in silty to sandy thin-bedded carbonaceous siltstone or carbonate rock and have a stratabound configuration.
2. Intrusive igneous rocks of intermediate composition are present as plugs, dikes, sills, or stocks in the deposit or nearby in the district, and have a spatial and, possibly, a genetic relation to the mineralizaton.
3. No specific age of mineralization is required. Known deposits range in age from Mesozoic to at least late Tertiary, and there seems to be no good geologic reason why deposits older than Mesozoic should not occur.
4. Gold typically predominates over silver in abundance and generally is submicroscopic. The gold is associated with mercury, arsenic, antimony, and, to a lesser extent, thallium, barium, fluorine, tungsten, molybdenum, and tin.
5. High-angle faults typically serve as conduits for ore fluids.
6. Hydrothermal breccias are invariably present in and adjacent to the ore zone.
7. Massive silicification in the form of jasperoid is commonly present. The jasperoid typically overlies the ore zone but in some places, as at Alligator Ridge, Nev., also underlies the ore zone.

Hydrothermal breccia-hosted deposits

The class of hydrothermal-breccia-hosted deposits, as proposed by Sillitoe (1984), includes those deposits in which the gold-silver mineralization is confined to hydrothermal breccias. He discusses two major classes of breccia deposits: collapse-breccia pipes and hydrothermal-intrusion breccias. The collapse-breccia pipes are typically associated with porphyry copper systems and commonly contain major copper and (or) molybdenum and minor gold. The hydrothermal-intrusion breccias are chiefly valuable for their precious-metal content and contain only minor base metals. Examples cited by Sillitoe (1984) include Kidston, Queensland, Australia; the Ortiz deposit in New Mexico; the Cresson pipe, Cripple Creek, Colo.; and the Balatoc pipe in the Baguio district, Philippines. The Golden Sunlight deposit in Montana and the Gilt Edge deposit, S.D., also occur in hydrothermal breccias.

The geology of the Ortiz deposit is described by Wright (1984) and summarized by Sillitoe (1984). The gold deposit occurs in a breccia pipe situated on the margin of a volcanic vent of Oligocene age; the volcanic vent is 2,400 m in diameter. Intrusive dikes, sills, and plugs of latite porphyry and trachyandesite occur in and adjacent to the vent. The breccia pipe cuts Cretaceous quartzite and argillite, and contains abundant fragments of quartzite and argillite fragments as well as of latite porphyry and trachyandesite. The breccia pipe contains gold, pyrite, scheelite, magnetite, galena, sphalerite, and chalcopyrite in the silicified matrix of the breccia. Alteration phases include silicification, seritization, and albitization. Anomalous gold and stockwork copper mineralization occur in several other hydrothermal breccias along the periphery of the volcanic vent. Announced reserves are 8.8 million tons (8 million t)

containing and 0.034 troy oz Au per ton (1.71 g Au/t) and 0.09 troy oz Ag per ton (3.1 g Ag/t).

The Golden Sunlight deposit in the Whitehall district, Jefferson County, Mont., occurs in and adjacent to a breccia pipe that transects late Precambrian rocks of the Belt Supergroup; the pipe is 180 to 240 m in diameter. The breccia fragments are angular and consist of quartzite and silicified argillite cemented by dark-gray chalcedonic quartz. Pyrite is the only visible sulfide mineral, but arsenic, copper, lead, and zinc are anomalous. The gold occurs in pyrite. Intrusive dikes, plugs, and sills of hydrothermally altered and mineralized latite porphyry that occur in the district are probably genetically related to the mineralization. Stockwork veinlets containing quartz, pyrite, chalcopyrite, and molybdenite occur in quartzite and argillite adjacent to the breccia pipe. The deposit contains developed open-pit reserves of 37.5 million tons (34 million t) grading and 0.05 troy oz Au per ton (1.74 g Au/t) and 0.05 troy oz Ag per ton (1.7 g Ag/t). A comparable tonnage of mineralization of approximately the same grade that occurs beneath open-pit limits could be mined by underground methods.

The Gilt Edge deposit in the Black Hills, S.D., occurs in a hydrothermal breccia associated with rhyolite porphyry dikes that intrude a latite porphyry stock. The rhyolite porphyry dikes contain disseminated molybdenite and pyrite. Fragments of the molybdenite-bearing porphyry occur in the hydrothermal breccia. The matrix of the breccia is silicified and contains moderate to abundant disseminated pyrite and sparse molybdenite. Several million tons of mineralized rock amenable to open-pit mining that averages more than 0.06 troy oz Au per ton (2 g Au/t) occurs at the Gilt Edge deposit.

DEPOSITS RELATED TO VOLCANIC CENTERS

Caldera-connected deposits

Several bulk-minable precious-metal deposits occur within collapse calderas of the Valles type. Disseminated silver mineralization at Creede, Colo., occurs in intracaldera tuff and in moat-fill sediment. Disseminated silver mineralization at the Hardshell deposit, Ariz., occurs in caldera fill consisting of volcaniclastic rocks and tuff (Graybeal, 1981). The disseminated silver deposits at DeLamar, Idaho, are associated with rhyolite domes that may have been emplaced along the ring fracture of a small caldera (M. Beebe, oral commun., 1981).

The important gold-silver deposit at Round Mountain, Nev., occurs in intracaldera tuff on the margin of a major Oligocene caldera (Berger and others, 1981). Potentially bulk minable gold mineralization at Goldfield, Nev., is present in hydrothermal breccia which occurs on the margin of a small caldera (Ashley, 1974).

Bulk-minable precious-metal deposits in caldera environments do not form a simple genetic grouping. In some deposits, the mineralization is apparently related to the caldera cycle, as at Round Mountain (Berger and others, 1981), whereas in other places the mineralization clearly postdates the caldera cycle, as at Goldfield (Ashley, 1974). Mineralization in a caldera which is genetically related to that caldera cycle is also related to intrusive rocks emplaced during the resurgent phase of caldera volcanism. In deposits unrelated to the caldera cycle, the mineralization is relatable to later intrusive and volcanic activity in and (or) adjacent to a preexisting caldera structure. The important parameters for mineralization in a caldera are favorable structural environments: ring-fracture zone; radial and longitudinal high-angle faults associated with caldera formation and resurgence; favorable zones of porosity and permeability, such as caldera moat-fill or volcaniclastic rocks; and nonwelded or poorly welded parts of pyroclastic flows.

Disseminated silver mineralization at Creede, Colo., occurs in both caldera moat-fill sediment and poorly welded tuff (Graybeal, 1981). The disseminated gold-silver mineralization at Round Mountain, Nev., occurs as a blanketlike ore body in the poorly welded zone of intracaldera ash-flow tuff and along intersecting joints and fractures in the more densely welded part of the tuff (Berger and others, 1981).

Hot spring-associated deposits

Hot-spring precious-metals deposits, in the context of this chapter, are those deposits that have been deposited at or within 100 m of the paleosurface. This classification does not include deposits inferred to have been deposited in the lower parts of fossil hot-spring systems. Although most geothermal systems that have formed "epithermal" deposits of gold-silver-mercury-arsenic-antimony probably must have vented at the paleosurface as hot springs, this inference is based on analogy with modern hot-spring systems which are currently depositing gold, silver, and so on, such as Steamboat Springs, Nev., and Broadlands and Waiotapu, New Zealand (Weissberg and others, 1979; White, 1980).

Positive evidence for a hot-spring environment of deposition is the actual occurrence of hot-spring sinter associated with the mineral deposition in the case of subaerial environments. Evidence for a subaqueous hot-spring depositional environment includes lenses or layers of originally opaline silica interlayered with lacustrine or marine sediment, mineralization clearly involved with soft-sediment deformation, the occurrence of stratiform mineralization concordant with the surrounding sediment, and a sharp upward termination of alteration and mineralization in the sediment overlying the mineralized zone. Other criteria may be used to define a subaqueous origin for Kuroko-type massive sulfide deposits, but these deposits are not considered here. Deposits for which a subaqueous hot-spring origin may be inferred are Waterloo, Calif. (Graybeal, 1981), and Pueblo Viejo, Dominican Republic (Kesler and others, 1981).

Bulk-minable precious-metal deposits for which a subaerial hot-spring depositional environment can be demonstrated include the McLaughlin deposit, Calif. (Albers, 1981), Sulphur, Nev. (Wallace, 1980), Hasbrouck, Nev. (Bonham and Garside, 1979), Buckskin, Nev. (P. G. Vikre, oral commun., 1981), and Gold Hill, Buckhorn, and Humboldt House, Nev. A deposit in which at least part of the mineralization formed in a

subaerial hot-spring environment is at DeLamar, Idaho. The Borealis deposit, Nev., probably formed within 100 m of the paleosurface, although sinter is absent. Deposits for which a subaerial hot-spring environment can be inferred for at least part of the precious-metal mineralization are the Great Barrier Island deposits, North Island, New Zealand (Ramsay and Kobe, 1974), and the Haile deposit, S.C. (Worthington and others, 1980).

The McLaughlin deposit in the old Knoxville mercury district, Napa County, Calif., is localized in Quaternary volcanic rocks and in Franciscan rocks of Mesozoic age (Averitt, 1945) at the site of the old Manhattan mercury mine. Hot-spring sinter at the Manhattan mine was mined as mercury ore (Averitt, 1945). Stibnite is associated with pyrite, marcasite, cinnabar, and gold at the deposit. Announced reserves are 20 million tons (18 million t) grading 0.14 troy oz Au per ton (5.0 g Au/t). Gold mineralization occurs in sinter, explosion breccia, and hydrothermaly brecciated sedimentary and volcanic rocks. Alteration types include silicification and argillization.

The Borealis deposit in Mineral County, Nev., was placed in operation in October 1981. This disseminated gold-silver deposit occurs in late Tertiary volcaniclastic sedimentary rocks, andesite flows, and brecciated rhyolite. The bulk of the gold mineralization occurs within a quartz-sulfide breccia, surrounded by an argillically altered zone and overlain by an acid-leached horizon. Ore minerals are electrum, pyrite, sphalerite, and minor bravoite and cobaltite. gold, silver, mercury, antimony, and arsenic are anomalous in near-surface rocks and show a systemetic decrease in abundance with depth; however, zinc increases in abundance with depth. Announced reserves are approximately 2.2 million tons (2 million t) grading and 0.098 troy oz Au per ton (3.4 g Au/t) and 0.49 troy oz Ag per ton (16.8 Ag/t) (Huang and Strachan, 1981).

Sulphur, Nev., was described by Wallace (1980). An acid-leached zone containing opaline silica, sulfur, alunite, and cinnabar is underlain by a silicified conglomerate containing disseminated gold-silver mineralization. Pyrite and stibnite occur in the silicified conglomerate, which is anomalous in arsenic and mercury. Late-stage alunite veins, as much as 2 m thick, which contain erratically high values in silver cut the silicified conglomerate. The Sulphur district is currently being explored for bulk-minable gold-silver deposits. Alunite from the Sulphur district has been dated at approximately 1 m.y.

COMPOSITE-VOLCANO- AND DOME-FIELD-RELATED DEPOSITS

A significant number of bulk-minable precious-metal deposits in Cordilleran and island-arc settings are related to composite volcanoes of intermediate composition and to silicic volcanic centers, including dome fields. Several deposits in Japan are related to Tertiary and Quaternary andesitic composite volcanoes. Most of these deposits are small—1.1 to 4.4 million tons (1-4 million t)—and grade 0.05 to 0.3 troy oz Au per ton (2-10 g Au/t). They commonly occur as silicified and brecciated pods in an advanced-argillic-alteration assemblage consisting of quartz, alunite, kaolinite, and, in some deposits, pyrophyllite, diaspore, zunyite, and topaz. Ore minerals include electrum, pyrite, enargite, stibnite, and, locally, galena, sphalerite, and arsenic sulfides. Anomalous amounts of tin are present in several deposits. Host rocks are andesitic flows, breccias, and volcaniclastic rocks.

The Comstock Lode, which is famous for its high-grade gold-silver ore bodies, also contains bulk-minable gold-silver deposits. The lode itself is essentially a quartz stockwork in andesite flows and breccia, emplaced along a major fault zone. High-grade parts of the Comstock Lode were mined underground in the period from 1860 to the early 1900's. Wide low-grade parts of the Comstock Lode have been mined by block-caving and open-pit methods on an intermittent basis since the early 1920's. The last major operation on the lode was an open-pit mine operated by Houston International during the period 1979-81 (McIntosh, 1980). The higher grade ore contained abundant base metals as well as electrum and silver sulfosalts. The low-grade ore contains pyrite, minor sphalerite, electrum, and argentite. Much of the ore that was mined by open-pit methods was oxidized and contained free gold, as well as silver halides. The andesite that forms the wall rock of the Comstock Lode is propylitized. Typical alteration minerals include chlorite, epidote, calcite, albite, montmorillonite, illite, and pyrite. In and within a few meters of the quartz stockwork that forms the lode, the andesite is altered to an assemblage of quartz, sericite, and adularia. Local zones of an advanced argillic assemblage of pyrophyllite, alunite, and kaolinite occur in the hanging wall of the lode.

REFERENCES CITED

Albers, J. P., 1981, A lithologic-tectonic framework for the metallogenic provinces of California: Economic Geology, v. 76, no. 4, p. 765-790.

Ashley, R. P., 1974, Goldfield mining district, in Guidebook to the geology of four Tertiary volcanic centers in central Nevada: Nevada Bureau of Mines and Geology Report 19, p. 49-66.

Averitt, Paul, 1945, Quicksilver deposits of the Knoxville district, Napa, Yolo and Lake Counties, California: California Journal of Mines and Geology, v. 41, no. 2, p. 65-89.

Berger, B. R., 1980, Geological and geochemical relationships at the Getchell mine and vicinity, Humboldt County, Nevada: at Society of Eonomic Geologists Epithermal Deposits Field Conference, 1980, field-trip guidebook, p. 111-134.

Berger, B. R., Tingley, J. V., Filipek, L. H., and Neighbor, J., 1981, Origin of pathfinder trace-element patterns associated with gold-silver mineralization in late Oligocene volcanic rocks, Round Mountain, Nye County, Nevada [abs.]: Association of Exploration Geochemists Precious Metals Symposium, Vancouver, British Columbia, Canada, 1981, Abstracts, p. 207.

Blake, D. W., and Kretschmer, E. L., 1980, Gold deposits at Copper Canyon, Lander County, Nevada: Society of Economic Geologists Epithermal

Deposits Field Conference, 1980, field-trip guidebook, p. 136-147.

Bonham, H. F., Jr., and Garside, L. J., 1979, Geology of the Tonopah, Lone Mountain, Klondike, and Northern Mud Lake quadrangles, Nevada: Nevada Bureau of Mines and Geology Bulletin 92, 142 p.

Graybeal, F. T., 1981, Characteristics of disseminated silver deposits in the western United States, in Relations of tectonics to ore deposits in the southern Cordillera: Arizona Geological Society Digest, v. 14, p. 271-281.

Huang, C.-I., and Strachan, D. G., 1981, Geochemistry and geology of a disseminated gold deposit at Borealis, Mineral County, Nevada [abs.]: Geological Society of America Abstracts with Programs, v. 13, no. 2, p. 62.

Kesler, S. E., Russell, N., Seward, M., Rivera, J., McCurdy, K., Cumming, G. L., and Sutter, J. F., 1981, Geology and geochemistry of sulfide mineralization underlying the Pueblo Vieja gold-silver oxide deposit, Dominican Republic: Economic Geology, v. 76, no. 5, p. 1096-1117.

Koschmann, A. H., and Bergendahl, M. H., 1968, Principal gold-producing districts of the United States: U.S. Geological Survey Professional Paper 610, 283 p.

McIntosh, L. L., 1980, Geology of the Consolidated-Imperial open pit Au-Ag mine, Comstock Lode district, Storey County, Nevada: Society of Economic Geologists Epithermal Deposits Field Conference, 1980, field-trip guidebook, p. 64-69.

McKee, E. H., 1974, Road log and trip guide, Austin-Northumberland Caldera-Carver Station, in Guidebook to the geology of four Tertiary volcanic centers in central Nevada: Nevada Bureau of Mines and Geology Report 19, p. 2-5.

Morton, J. L. Silberman, M. L., Bonham, H. F., Jr., Garside, L. J., and Noble, D. C., 1977, K-Ar ages of volcanic rocks, plutonic rocks and ore deposits in Nevada and eastern California--determinations run under the USGS-NBMG cooperative program: Isochron/West, no. 20, p. 19-29.

Ney, C. S., Anderson, J. M., and Panteleyev, Andre, 1972, Discovery, geologic setting and style of mineralization, Sam Goosly deposit, B. C.: Canadian Institute of Mining Bulletin, v. 65, no. 723, p. 53-64.

Radtke, A. S., 1981, Geology of the Carlin gold deposit, Nevada: U.S. Geological Survey Open-File Report 81-97, 154 p.

Radtke, A. S., and Dickson, F. W., 1974, Genesis and vertical position of fine-grained disseminated replacement-type gold deposits in Nevada and Utah, USA, in Problems of ore deposition: International Association on the Genesis of Ore Deposits Symposium, 4th, Varna, Bulgaria, 1974, v. 1, p. 71-78.

Ramsay, W. R. H., and Kobe, H. W., 1974, Great Barrier Island silver-gold deposits, Hauraki Province, New Zealand: Mineralium Deposita, v. 9, no. 2, p. 143-153.

Russell, N., Seaward, M., Rivera, J. A., McCurdy, K., Kesler, S. E., and Cloke, P. L., 1981, Geology and geochemistry of the Pueblo Viejo gold-silver oxide deposit, Dominican Republic: Institution of Mining and Metallurgy Transactions, sec. B, v. 90, p. B153-B162.

Silberman, M. L., and McKee, E. H., 1971, K-Ar ages of granitic plutons in north-central Nevada: Isochron/West, no. 1, p. 15-32.

Silberman, M. L., Berger, B. R., and Koski, R. A., 1974, K-Ar age relations of granodiorite emplacement and tungsten and gold mineralization near the Getchell mine, Humboldt County, Nevada: Economic Geology, v. 69, no. 5, p. 646-656.

Sillitoe, R. H., 1979, Some thoughts on gold-rich porphyry copper deposits: Mineralium Deposita, v. 14, no. 2, p. 161-174.

----- 1984, Low-grade gold potential of volcano-plutonic arcs, in Society of Mining Engineers of AIME Precious Metals Symposium, Sparks, Nev., 1980, Proceedings: Nevada Bureau of Mines and Geology Report 36 [in press].

Wallace, A. B., 1980, Geology of the Sulphur district, southwestern Humboldt County, Nevada: Society of Economic Geologists Epithermal Deposits Field Conference, 1980, field-trip guidebook, p. 80-91.

Weissberg, B. G., Browne, P. R. L., and Seward, T. M., 1979, Ore metals in active geothermal systems in Barnes, H. L., ed., Geochemistry of hydrothermal ore deposits (2d ed.): New York, John Wiley and Sons, p. 738-780.

Wells, J. D., Elliott, J. E., and Obradovich, J. D., 1971, Age of the igneous rocks associated with ore deposits, Cortez-Buckhorn area, Nevada, in Geological Survey research, 1971: U.S. Geological Survey Professional Paper 750-C, p. C127-C135.

Wells, J. D., Stoiser, L. R., and Elliott, J. E., 1969, Geology and geochemistry of the Cortez gold deposit, Nevada: Economic Geology, v. 64, no. 5, p. 526-537.

Wetherell, D. G., 1979, Geology and ore genesis of the Sam Goosly copper-silver-antimony deposit, British Columbia: Vancouver, British Columbia, Canada, University of British Columbia, M.S. thesis.

White, D. E., 1980, Steamboat Springs geothermal area: Society of Economic Geologists Epithermal Deposits Field Conference, 1980, field-trip guidebook, p. 44-51.

Worthington, J. E., Kiff, I. T., Jones, E. M., and Chapman, P. E., 1980, Applications of the hot springs or fumarolic model in prospecting for lode gold deposits: Mining Engineering, v. 32, no. 1, p. 73-79.

Wright, A., 1984, Geology and exploration of the Ortiz gold deposit, New Mexico, in Society of Mining Engineers of AIME Precious Metals Symposium, Sparks, Nev., 1980, Proceedings: Nevada Bureau of Mines and Geology Report 36 [in press].

Wrucke, C. T., and Armbrustmacher, T. J., 1975, Geochemical and geologic relations of gold and other elements at the Gold Acres open-pit mine, Lander County, Nevada: U.S. Geological Survey Professional Paper 860, 27 p.

Summary of the Steamboat Springs Geothermal Area, Nevada, with Attached Road-Log Commentary

By Donald E. White

CONTENTS

INTRODUCTION

The Steamboat Springs geothermal area is approximately 16 km south of downtown Reno, Nev., and mostly just west of Interstate Highway 395 (fig. 50). Thermal waters and gases have discharged from an area of approximately 5 km^2; postglacial (post-Lake Lahonton) hot-spring discharge has been restricted to the Main Terrace just west of the highway and to the Low Terrace to the southeast adjacent to Steamboat Creek. This hot-spring system has the longest and most complex geologic history of any active geothermal area yet studied in detail in the world (fig. 51; White and others, 1964; Silberman and others, 1979).

The area has attracted interest in its geothermal potential for many years. Hot-spring water was used in the local spas for bathing and heating during the early 1900's, and efforts were made to pipe the water to Reno for heating purposes in 1916 (White, 1968, p. C6, C7, C15-C16). The first geothermal well at Steamboat Springs was drilled about 1920 in efforts to obtain a dependable supply of hot water for the local resort (White, 1968, p. C45-C55), and the first well specifically searching for steam to generate electricity was drilled in 1950 (Rodeo well, fig. 50). During the late 1950's and early 1960's, 8 to 10 additional geothermal exploration wells were drilled in the immediate area, ranging in depth from 218 to 558 m; the maximum measured temperature was 186°C (White, 1968), but these early geothermal efforts were unsuccessful in identifying a reservoir of adequate temperature and permeability. Chemical geothermometers, however, predicted reservoir temperatures ranging from about 180° to 230°C (Brook and others, 1979; Nehring, 1979). A 930-m-deep geothermal test well was then drilled in 1979 by the Phillips Petroleum Co. 2.5 km southwest of the Main Terrace near the crest of the Steamboat Hills. The maximum temperature in this well is near the geochemical maximum, as now confirmed by the Phillips Petroleum Co.

GEOLOGY OF THE STEAMBOAT SPRINGS DEPOSITS

The Steamboat Springs area has been of long-standing interest to economic geologists for its bearing on hydrothermal ore deposits, and it is now viewed as the present-day equivalent of geothermal systems of Tertiary age that formed epithermal gold-silver deposits throughout the Great Basin of the Western United States and elsewhere (White and others, 1964; White, 1967, 1968, 1981). At Steamboat Springs, hot-spring sinter deposits, chemical sediment in spring vents, and veins intersected in drill holes all contain significant concentrations, in order of importance, of gold, silver, mercury, arsenic, antimony, thallium, and boron (table 7). The oldest hot-spring sinter was deposited about 3 m.y. B.P., before extrusion of basaltic andesite from a vent near the crest of the Steamboat Hills, 2.5 km southwest of the Main Terrace (fig. 50). This andesite, dated at 2.53±0.11 m.y. (Silberman and others, 1979), is a key unit in understanding the history of the hot-spring system. The basaltic andesite under Sinter Hill in the western part of the geothermal area (drill hole GS-6) was locally replaced almost completely by adularia (Schoen and White, 1967) that yielded a K-Ar age of 1.1±0.1 m.y.; this alteration probably occurred during deposition of the overlying chalcedonic-sinter deposits. Thermal activity that formed the younger sinter deposits has probably been continuous but varying in magnitude for a least the past 0.1 m.y., possibly longer. Other intervals of activity probably have occurred (fig. 51) but are not clearly decipherable from the preserved evidence.

The geothermal area lies approximately on a line that connects four rhyolite domes, the largest of which is 5 km southwest of the springs and is 1.14±0.04 m.y. old. Three domes from 1.5 to 5 km northeast of the springs yielded ages of 1.2 and 3.0 m.y. Vertical uplift under Sinter Hill is likely to have been caused by a shallow intrusion correlative with these younger domes (White and others, 1964).

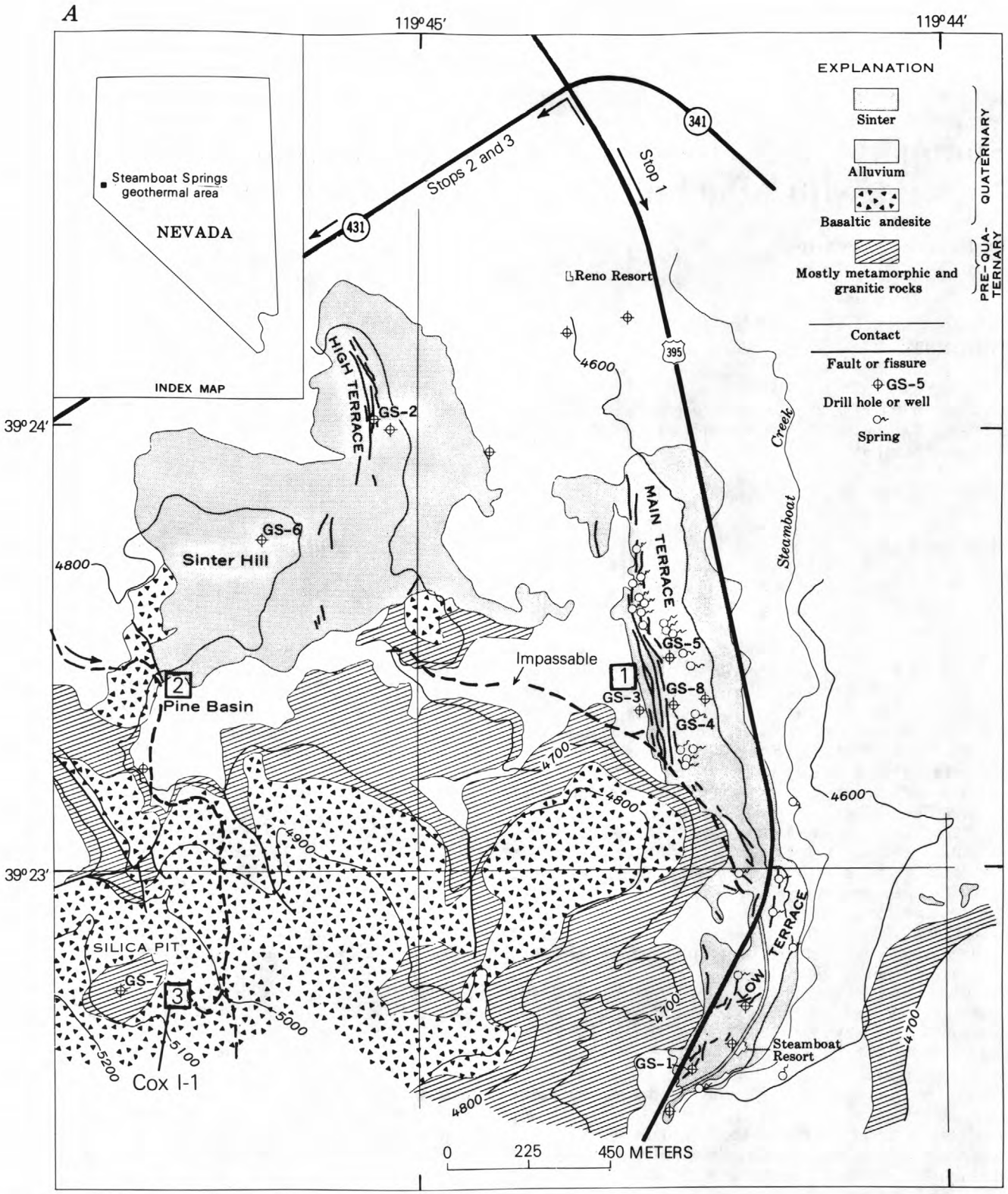

Figure 50. Steamboat Springs geothermal area, Washoe County, Nev. A, Geologic map, modified from White and others (1964, pl. 1) and Schoen and White (1967, fig. 1). B, Recommended local access roads.

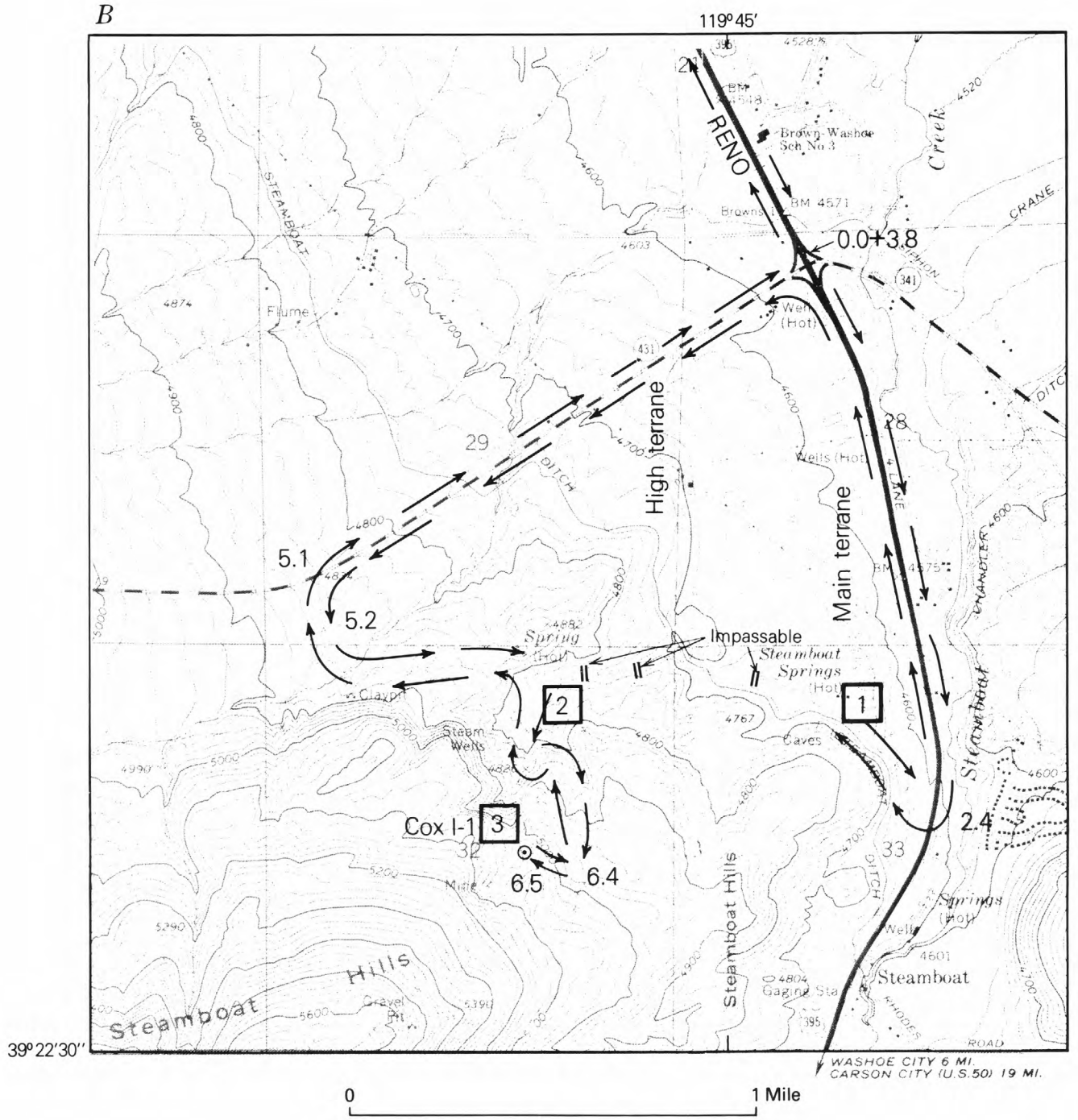

Figure 50. Continued.

White (1968) estimated that a magma volume equivalent to 100 km^3 must have cooled and crystallized just to supply the convective heat losses assumed at present rates for 100,000 years. About 3 m.y. of continuous activity at present rates would require 3,000 km^3 of magma, but this volume seems improbable, judging from mass- and heat-flow constraints. However, intermittent activity during at least 10 percent of the total interval (0.3 m.y.) is considered a reasonable estimate, especially in view of the complex history of volcanic activity.

The long timespan from the earliest hydrothermal activity to the present and the puny volume of rhyolite domes extruded during this time interval may be best explained by a huge magma chamber underlying the area, but at great depth. In view of the complex histories of most large silicic volcanic systems, two or more cycles of evolution of the magma system seem likely. No cycle culminated in the ash-flow-tuff eruptions and caldera collapse that many other such systems have undergone, possibly owing to the great depth of the Steamboat Springs system (R. L. Smith,

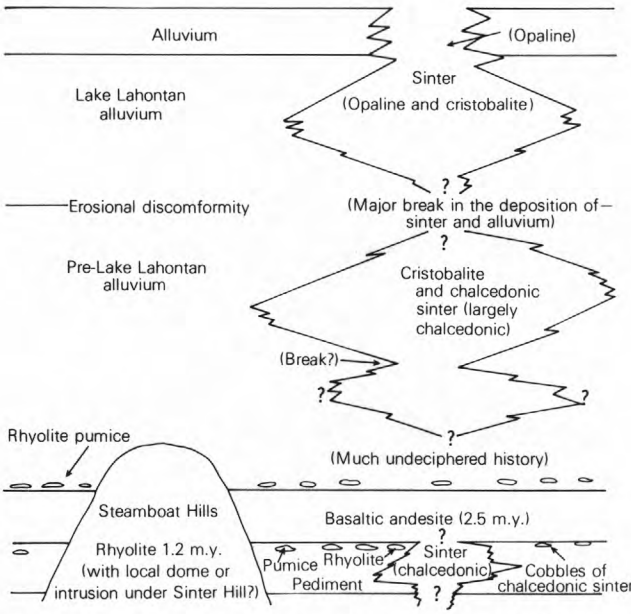

Figure 51. Composite stratigraphic relations at Steamboat Springs (from Silberman and others, 1979, fig. 3).

oral commun., 1975).

Sinter at Steamboat Springs generally contains detectable amounts of gold and silver, and dark siliceous mud deposited in the present springs contains as much as 15 ppm Au, 150 ppm Ag, 0.01 weight percent Hg, and 3.9 weight percent Sb as stibnite and metastibnite (table 7; Brannock and others, 1948; White, 1967). Mercury is notable in some chalcedonic sinter and has been mined and recovered in small amounts from acid-leached opaline residues resulting from solfataric alteration of granodiorite and basaltic andesite in the Silica Pit (fig. 50; White and others, 1964; Schoen and others, 1974). Elemental mercury (Hg^0) was identified in vapor from several drill holes and hot-spring vents, cinnabar is common in small amounts in association with native sulfur where vapor escapes through porous acid-decomposed sinter of the Main Terrace, and clusters of small crystals of cinnabar have been deposited on test specimens of sulfide minerals, especially galena, immersed for several months in nonproducing geothermal wells. Stibnite has been deposited as needlelike crystals on the walls of several hot-spring pools, such as spring 8 (fig. 50; table 7). Coatings of orange-red metastibnite (amorphous Sb_2S_3) also formed on the discharge apron of spring 8 at some unknown time after systematic spring measurements were terminated in 1952, and also formed in the initial discharge blasts of at least three erupting geothermal wells. Sample W-941c (table 7) has the highest contents of gold, silver, and other metals of any surface-formed deposit yet analyzed.

All the cinnabar identified in the Steamboat Springs geothermal area occurs within 15 m of the present topographic surface, and no mercury was found analytically in drill core at depths below 26 m (table 7). Some cinnabar occurs in acid-leached rocks above the water table in environments indicating deposition from a vapor phase, as in the Silica Pit (fig. 52). These relations may provide the keys for understanding the "opalite type" of mercury deposits that are rather common in western Nevada (Bailey and Phoenix, 1944).

Stibnite was recognized in veinlets and cavities in drill core to a maximum depth of 45 m below the surface. In six drill holes in the active Low and Main Terraces, the deepest observed stibnite occurred at temperatures that ranged from 100° to 146°C, although traces of Sb occurred at greater depths (table 7). In spite of the much higher As concentrations in the waters relative to Sb (White, 1967, table 13.3), no arsenic sulfides were recognized in surface deposits and drill core.

Spectrographic analyses of 11 samples of core from drill hole GS-5 (table 7) indicate mainly chemically precipitated SiO_2 (sinters to 84 ft 25.6 m and chalcedony-quartz-calcite veins at greater depths). These samples were analyzed spectrographically, using standard and newly developed short-wavelength-radiation (SWR) techniques to attain lower levels of detection for critical elements not sufficiently detectable by routine emission-spectrographic methods. Visible pyrargyrite (Ag_3SbS_3) had been identified previously in a sample at 273 ft (83.2 m) and subsequently in core samples at 238 and 353 ft (72.5 and 107.6 m), respectively (not analyzed), but silver minerals were not recognized in other core from this hole.

These data demonstrate that gold, arsenic, antimony, mercury, thallium, and boron all tend strongly to concentrate in the near-surface deposits of this active system, with contents commonly 10 to 100 times higher than in deeper deposits. Germanium also shows some upward concentration, but silver generally favors the middle and deeper parts of the explored system. Sample W-310d (table 7) is representative of metal-enriched deposits of thermal water that has flowed slowly to the surface; contents of the "epithermal" elements (Au, As, Sb, Hg, Tl, B) are relatively high in comparison with the base-metal elements (Cu, Zn, Pb). Silver favors the second group but also occurs with the first group. Sample 941c formed in the discharge blast of water erupted from a depth of 220 m in Nevada Thermal well No. 4 (west of Pine Basin, fig. 50), where the maximum temperature was approximately 185°C at the bottom of the well (221 m). Any base-metal elements in water erupted from this depth rapidly bypassed the natural environments of intermediate depths; thus, both groups of metals were still available for rapid precipitation in these unusual surface deposits. A metal-bearing dark siliceous mud (sample W-50, table 7) contained high concentrations of the epithermal elements and modest concentrations of the base-metal group. This mud was flushed out of the system as black suspended matter, conspicuous only during periods of near-maximum discharge (Brannock and others, 1948, p. 223); precipitation of gelatinous silica and metals had already occurred, largely below the surface at unknown depths. However, gold, arsenic, antimony, mercury, and thallium may have continued to precipitate as lower temperatures and depths were attained.

Table 7. Spectrographic analyses of chemical precipitates from the Steamboat Springs geothermal area, Nevada

[Six-step semiquantitative short-wavelength spectrographic analyses by Chris Heropoulos. All values in parts per million; n.d., not determined. Below limit of detection: Bi, Se, and Te]

Sample	Depth in drill hole GS-5 (ft [m])	Description	Temperature (°C)	Au	Ag	As	Sb	Hg	Tl	B	Cu	Zn	Pb
W-50	---	Siliceous mud, spring 24---------	95.5	15	150	700	1.5	100	700	500	20	50	7
W-310d	---	Sinter and stibnite, spring 8----	95	1.5	1	50	1.0	30	70	1,000	1	.2	--
W-941c	---	Metastibnite and opal, erupting Nevada thermal well No. 4.	96	60	400	600	>.2	<80	2,000	>2,000	>2,000	>2,000	400
---	11 (3.4)	Opaline sinter-------------------	42	.3	2	150	700	2	10	1,000	15	15	n.d.
---	19 (5.8)	do------------------------------	52	n.d.	.3	30	500	500	5	500	3	5	n.d.
---	42 (12.8)	do------------------------------	80	.2	.5	300	3,000	500	70	200	10	10	n.d.
---	84 (25.6)	Chalcedonic sinter---------------	122	n.d.	<.2	70	100	3	1.5	20	1.5	7	n.d.
---	113 (34.5)	Vein chalcedony------------------	137	1.5	30	30	50	n.d.	1.5	15	5	15	n.d.
---	174 (53.1)	Vein chalcedony-calcite----------	153	.7	20	50	50	n.d.	1.5	15	10	10	n.d.
---	231 (70.1)	do------------------------------	163	.3	70	70	30	n.d.	n.d.	15	3	30	n.d.
---	273 (83.2)	do------------------------------	168	n.d.	100	50	30	n.d.	n.d.	20	10	7	n.d.
---	346 (105.4)	Vein chalcedony-quartz-----------	171	n.d.	15	5	20	n.d.	n.d.	10	1	7	n.d.
---	363 (110.6)	Vein chalcedony-calcite----------	172	n.d.	100	30	30	n.d.	<1	20	5	30	n.d.
---	446 (135.8)	Vein chalcedony-quartz-calcite---	171	n.d.	.7	1.5	20	n.d.	n.d.	15	2	10	n.d.

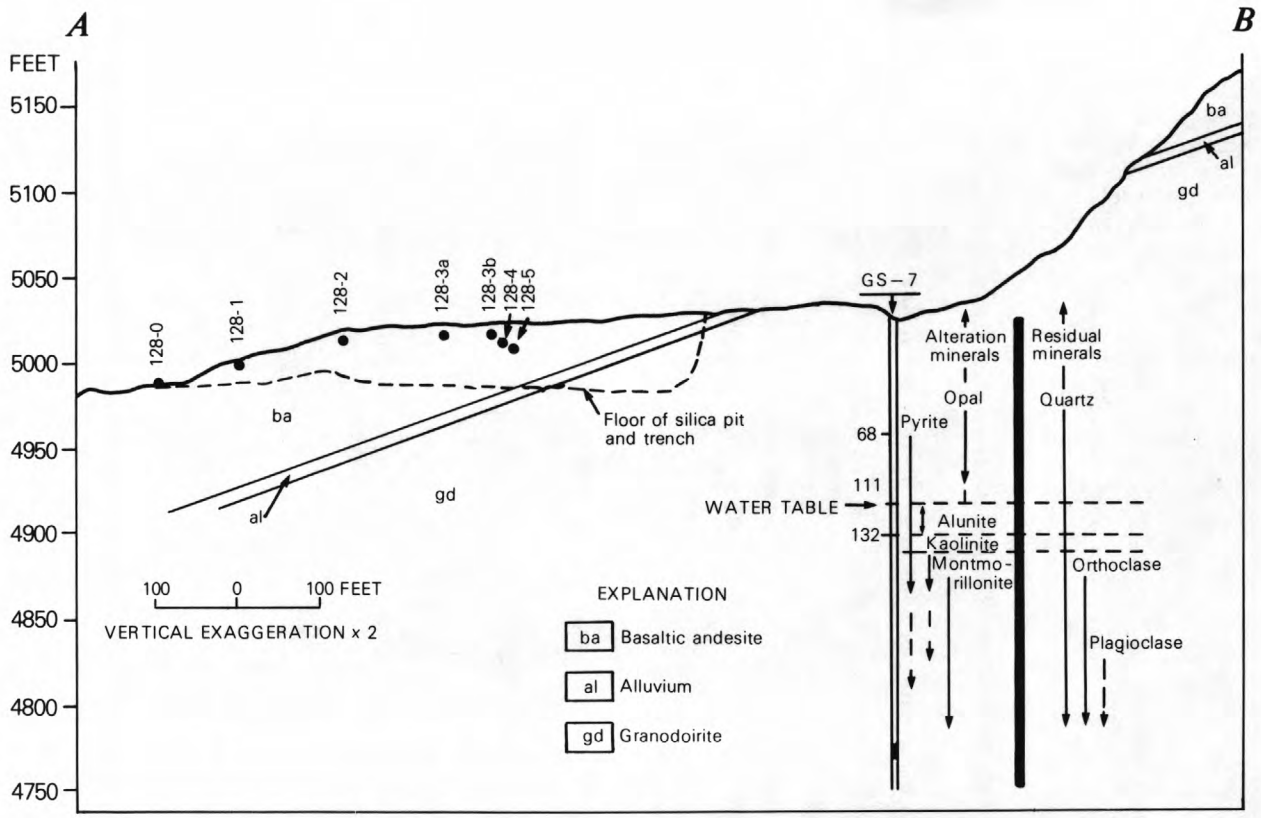

Figure 52. Geologic cross section of the Silica Pit, showing locations of samples and mineralogy of core from drill hole GS-7 (from Schoen and others, 1974, fig. 3).

Stable isotopes in Steamboat Springs thermal waters indicate a great dominance of meteoric water in the system, although as much as 10 percent of magmatic water could have been present but not identifiable isotopically (Craig, 1963; White and others, 1963). The isotopic relations show an increase in $\delta^{18}O$ of 2 to 3 permil in the hot water relative to the cold meteoric recharge, and little or no change in hydrogen isotopes. This oxygen shift, a phenomenon common in high-temperature geothermal waters, results from interaction at high temperatures between meteoric water (low in ^{18}O) and rock silicates (high in ^{18}O) during hydrothermal alteration.

ROAD LOG FOR THE STEAMBOAT SPRINGS GEOTHERMAL AREA, NEVADA

Interval Miles	(km)	Description
0.0	(0.0)	Intersection of Interstate Highway 395 with Nevada Highways 431 and 341 (north end of fig. 50A, approx 10 mi [16 km] S. of Reno). Drive south on the highway along the east-side base of the Main Terrace, Steamboat Springs.
1.4	(2.2)	Turn right (west) from Interstate Highway 395 onto rough road to the Main Terrace (turn is obscure; watch for break in the fence).
1.7	(2.7)	Take right fork to crest of the Main Terrace.
1.9	(3.0)	Stop 1 (on figs. 50A and 50B). Park vehicle. Cross zone of open and closed fissures about 300 ft (90 m) to southeast to corroded valve and 1.2-m-high vertical pipe of drill hole GS-4, a core hole drilled by the U.S. Geological Survey in 1949. Water level in fissures is approximately 10 ft (3 m) deep; all flowing springs are at lower altitudes to east and north, either seeping or discharging as much as several liters per minute. Notice the porous vugginess of most of the hot-spring sinter, formed from direct precipitation of SiO_2 as X-ray-amorphous common opal. The different varieties of sinter and their significance were described by White and others (1964, p. B30-B33), and details of the terraces and fissure systems were shown by White (1968, pls. 1, 3).

General: Three pumiceous rhyolite domes to northeast are 1.1 and 3.0 m.y. old. Beyond and to the east, volcanic rocks of the Virginia Range, largely andesite and rhyodacite, 10 to 15 m.y. old, exhibit alteration and bleaching related to the Comstock Lode district

(Virginia City, 7 mi [11 km] southeast).

To the north, Truckee Meadows and Reno. To the northwest, the low light-colored ridge is the High Terrace, still thermally active but with a water level 40 ft (12 m) below the surface and discharging subsurficially; probably no surface discharge in about the past 30,000 years. Farther to the west is Sinter Hill, with a few stunted pine trees, underlain by chalcedonic sinter ranging from about 1.1 to 3 m.y. old. (Stop 2 will be in Pine Basin, due west.) To the southwest is basaltic andesite lava, 2.5 m.y. old, that flowed out over a pediment cut on Mesozoic granodiorite and metamorphic rocks. The eroded cinder cone forming the apparent crest (from this view) of the Steamboat Hills lacks a crater form and is 1.6 mi (2.5 km) from the Main Terrace. The most productive geothermal well (Phillips Steamboat No. 1, S. edge of fig. 50A) drilled in the area is just this side (to the northeast) of the high point on the eroded cinder cone. The white dumps below the relict cone are acid-bleached andesite and granodiorite from the Silica Pit (figs. 50, 52, and stop 3).

Walk 300 ft (90 m) northeastward to a small sinter cone—spring 8, at the east lip of the terrace and just north of the powerline. Over many years, this spring discharged approximately a liter per minute of water high in Sb (0.4 ppm) and As (3.5 ppm); it was one of only three springs of the 27 monitored that discharged continuously during 7 years of systematic observation (1945-52; White, 1968, pl. 4). Stibnite needles have formed at times on the walls and bottom of the pool. The red-orange layer of sinter around the vent is colored by metastibnite (amorphous Sb_2S_3) deposited at some unrecorded time after the detailed studies ceased.

Walk upslope about 250 ft (75 m) northwestward to drill hole GS-5, 574 ft (175 m) deep, with a maximum temperature of 172°C, which has been studied in the most detail. Abundant quartz-calcite veins were as much as 7 ft (approx 2 m) thick and dipped 45°-80° E. Some pyrargyrite is visible, generally containing more than 20 ppm Ag (table 7).

Walk on northwestward to the highest springs that commonly discharge from open fissures about 10 ft (3 m) lower than the crest of the Main Terrace farther south). Springs 23 and 24, at times of very high turbulent discharge, deposited black siliceous mud in suspension, containing as much as 15 ppm Au, 150 ppm Ag, 3 weight percent Sb, and abundant Hg, As, Tl, and B (see table 1).

Near spring 24 and to the south, note that individual fissures "open" and "close." The open parts were formerly interpreted as "pullaparts," but, in places, nonmatching walls and abrupt closures demonstrate that the open parts resulted from dissolution and disintegration of sinter along fractures (White and others, 1964, p. B53-B54; 1968, pl. 3). Active disintegration is now occurring in the "closed" parts of fissures; dig down a few inches into the loose sinter rubble where hot vapor is escaping. Also, note the gradual change horizontally into coherent horizontally bedded sinter. Condensing steam containing Hg^0 and oxidizing H_2S produces native S, pink dispersed HgS, and strongly acidic condensates ($pH \leq 1$). The acidic condensate initially contains no SiO_2 but becomes rapidly saturated with soluble opaline SiO_2 (approx 300 ppm at 95°C).

Return south to vehicles, past the old Rodeo well, which was the first geothermal well (drilled in 1950) specifically exploring for steam to generate electricity. Drive southward to Interstate Highway 395 and original 0.0 point (now 3.8 mi; see fig. 50A).

3.8 (6.1) Drive 1.3 mi (2.1 km) westward on Nevada Highway 431.

5.1 (8.2) Turn left (south) onto gravel road for 1 mi (1.6 km), left bend (to the east). Kaolinite clay pit is to right (south; alteration of basaltic andesite). Note "forest" of stunted ponderosa pines, which are growing about 1,500 ft lower in altitude than their lowest limit in the Carson Range to the west. Their growth here is due to acidity produced by H_2SO_4 from oxidation of both H_2S. Normal sagebrush and other vegetation cannot grow in acidic soil that pines can tolerate, and so the pines have no competition for the limited moisture. (When driving, note ahead to the east in the Virginia

5.2 (8.4)

Range the presence of similar altered ground, due entirely to oxidizing of pyrite without H_2S, sustaining similar growth of anomalous ponderosa pines in soil with pH as low as about 3.5.)

5.9 (9.5) Stop 2 (return to geologic map, fig. 50) at road junction in Pine Basin. Leave cars and walk 300 ft (90 m) northward up the slope of Sinter Hill to an area of chalcedonic-sinter rubble. This was formerly an excellent outcrop of chalcedonic sinter (White and others, 1964, figs. 13, 14), interpreted as older than the 2.5-m.y.-old basaltic andesite. Chalcedonic sinter generally requires many thousands of years as well as temperatures of preferably near 125°C for conversion from opaline sinter. Note that 125°C requires burial to a depth of approximately 50 ft (15 m) to provide sufficient hydrostatic water pressure for water to coexist with steam at this temperature. Detailed relations in chalcedony-filled cavities of this sinter provide significant insights into the local geologic history. Gravity-stratified microbanding in former cavities now dips 30° SE., in comparison with the relict bedding, which dips 42° SE. These data indicate an initial dip of 12° SE. when the sinter was chalcedonized. At some later time, the chalcedonic sinter was tilted 30° southeastward, possibly owing to the rise of rhyolitic magma under Sinter Hill about 1.2 m.y. B.P. (see fig. 51; White and others, 1964, p. B34-35). Note the black surfaces of many exposed sinter fragments, then break open the darkest ones. The red-and-pink color is from cinnabar dispersed in chalcedony; the black color develops on exposure to sunlight, for reasons still not well understood.

Return to cars and drive on southward 0.1 mi (0.2 km) ("Steam wells," fig. 50A) to site of three former geothermal wells. The only visible one, Nevada thermal well No. 3, is 1,203 ft (385 m) deep and generally erupts intermittently as a manmade geyser. One of the older wells, no longer evident, was known as the mercury well because a metallic film of Hg^0 condensed on metallic objects held in the escaping steam and gases. Continue generally southward past the bend in the road and upslope 0.4 mi (0.6 km) to intersection, take turn and drive 0.1 mi (0.2 km) to bleached dump of the Silica Pit.

6.4 (10.3)

6.5 (10.5) Stop 3. The old Silica Pit has now been converted to a discharge sump for erupted water from Phillips geothermal well Cox I-1. The basaltic andesite is underlain by pediment gravel, entirely bleached and difficult to recognize except for relict outlines and slight color differences of clasts. The gravel, in turn, is underlain by white leached granodiorite consisting of original quartz plus opaline residues that retain the original volume of feldspars, biotite, and hornblende.

9.1 (14.6) Return route to Nevada Highway 431 and Interstate Highway 395. You will pass over the subdued north end of the High Terrace (fig. 50), which also has a fissure system, older and less well preserved than that of the Main Terrace. At a few places along the crest of the High Terrace, opaline sinter disconformably overlies chalcedonic sinter, some of which contains dispersed cinnabar. Drill hole GS-2 (now destroyed) penetrated 75 ft (23 m) of chalcedonic sinter lying on sediment and volcanic rocks. These rocks, in turn, are unconformable on granodiorite at 351-ft (107 m) depth. Chalcedony-quartz-calcite veins much like those in drill hole GS-5 are conspicuous from 90- to 333-ft (27-101 m) depth; several of these veins contain visible ruby silver (pyrargyrite).

REFERENCES CITED

Bailey, E. H., and Phoenix, D. A., 1944, Quicksilver deposits in Nevada: University of Nevada Bulletin, v. 38, no. 5 (Geology and Mining Series 41), 206 p.

Brannock, W. W., Fix, P. F., Gianella, V. P., and White, D. E., 1948, Preliminary geochemical results at Steamboat Springs, Nevada: American Geophysical Union Transactions, v. 29, no. 2, p. 211-226.

Brook, C. A., Mariner, R. H., Mabey, D. R., Swanson, J. R., Guffanti, Marianne, and Muffler, L. J. P., 1979, Hydrothermal convection systems with reservoir temperatures ≥ 90°C, in Muffler, L. J. P., ed., Assessment of geothermal resources of the United States--1978: U.S. Geological Survey Circular 790, p. 18-85.

Craig, Harmon, 1963, The isotopic geochemistry of water and carbon in geothermal areas, in Tongiorgi, Ezio, ed., Nuclear geology on geothermal areas: Pisa, Casiglio Nazionale delle

Ricerche, Laboratorio di Geología Nucleare, p. 17-54.

Nehring, N. L., 1980, Geochemistry of Steamboat Springs, Nevada: San Jose, Calif., San Jose State University, M.S. thesis, 61 p.

Schoen, Robert, and White, D. E., 1967, Hydrothermal alteration of basaltic andesite and other rocks in drill hole GS-6, Steamboat Springs, Nevada; in U.S. Geological Survey research, 1967: U.S. Geological Survey Professional Paper 575-B, p. B110-B119.

Schoen, Robert, White, D. E., and Hemley, J. J., 1974, Argillization by descending acid at Steamboat Springs, Nevada: Clays and Clay Minerals, v. 22, no. 1, p. 1-22.

Silberman, M. L., White, D. E., Keith, T. E. C., and Dockter, R. D., 1979, Duration of hydrothermal activity at Steamboat Springs, Nevada, from ages of spatially associated volcanic rocks: U.S. Geological Survey Professional Paper 458-D, D1-D14.

White, D. E., 1967, Mercury and base-metal deposits with associated thermal and mineral waters, in Barnes, H. L., ed., Geochemistry of hydrothermal ore deposits: New York, Holt, Rinehart and Winston, p. 575-631.

----- 1968, Hydrology, activity, and heat flow of the Steamboat Springs thermal system, Washoe County, Nevada: U.S. Geological Survey Professional Paper 458-C, C1-C109.

----- 1981, Active geothermal systems and related ore deposits: Economic Geology, 75th anniversary volume, p. 392-423.

White, D. E., Craig, Harmon, and Begemann, F., 1963, Summary of the geology and isotope geochemistry of Steamboat Springs, Nevada, in Tongiorgi, Exio, ed., Nuclear geology on geothermal areas: Pisa, Casiglio Nazionale delle Ricerche, Laboratorio di Geología Nucleare, p. 9-16.

White, D. E., Thompson, G. A., and Sandberg, C. H., 1964, Rocks, structure, and geologic history of Steamboat Springs thermal area, Washoe County, Nevada: U.S. Geological Survey Professional Paper 458-B, p. B1-B63.

Geologic Discussion of the Borealis Gold Deposit, Mineral County, Nevada

By Donald G. Strachan

CONTENTS

INTRODUCTION

Borealis is a volcanic-hosted disseminated gold deposit in west-central Nevada, 160 km southeast of Reno (fig. 53). The mine is owned and operated by Tenneco Minerals Inc. The descriptions and concepts presented herein pertain only to the original Borealis ore body and stem from my experience as project geologist during mine development, early production, and district-exploration stages from May 1980 to March 1983.

The stratigraphic, structural, and mineralogic characteristics of the Borealis deposit resemble those in several classic western Nevada and eastern California precious-metal districts, including the Comstock, Aurora, Bodie, Masonic, Tonopah, and Goldfield. All of these districts contain disseminated, vein, and (or) stockwork deposits of Miocene-Pliocene age in volcanic or associated sedimentary rocks. The Borealis deposit contains evidence of fossil geothermal activity, somewhat comparable to the McLaughlin deposit in California, the Hasbrouck Peak and Round Mountain deposits and Steamboat Springs in Nevada, and the DeLamar deposit in Idaho.

The purpose of this chapter is to discuss the regional setting of Borealis, describe the general characteristics of the Borealis ore types, and suggest a genetic model for the deposit.

Acknowledgement.—The information contained in this chapter is published with the permission of Tenneco Minerals Inc.

REGIONAL GEOLOGY

The Borealis deposit occurs near the west margin of the Basin and Range province on the east edge of Fletcher Valley, one of the structural basins in the region (Gilbert and Reynolds, 1973). Mesozoic basement rocks include granitic, metavolcanic, and metasedimentary rocks, overlain unconformably by thick sections of Cenozoic sedimentary and volcanic rocks. The Wassuk Range, forming the east side of Fletcher Valley, is composed of several granitic plutons that range in age from Late Jurassic into Cretaceous. The west flanks of this range are covered by Tertiary andesite and related rocks of intermediate composition, and include laharic breccias and minor lava flows (Stewart and others, 1982). These deposits, in turn, are overlain by Quaternary basalt flows, locally including cinder cones and the Aurora Crater, about 13 km southeast of Borealis. Fletcher Valley is filled with Quaternary alluvial-fan and pediment deposits. The Miocene and Pliocene volcanic and sedimentary rocks exposed along the margins of the basin are locally silicified and form bold outcrops. The uppermost parts of the Borealis breccias and sinters occur in one of these siliceous outcrops along the southeastern quadrant of the basin.

North-south- and northwest-trending steep normal faults, which may have displacements of 1,800 to 3,000 m, have created sharply defined ranges and valleys, such as the Wassuk Range and Fletcher Valley (Gilbert and Reynolds, 1973). This region also lies within the broad northwest-trending Walker Lane shear zone (Shawe, 1965), which is cut by northeast-trending faults (Gilbert and Reynolds, 1973).

Most ore deposits in the western part of the Basin and Range province are associated with complex uplift and doming, the result of the introduction of intrusive bodies (Silberman and others, 1976). Andesite is the predominant host rock for precious-metal deposition in this area; most of the gold produced in Nevada came

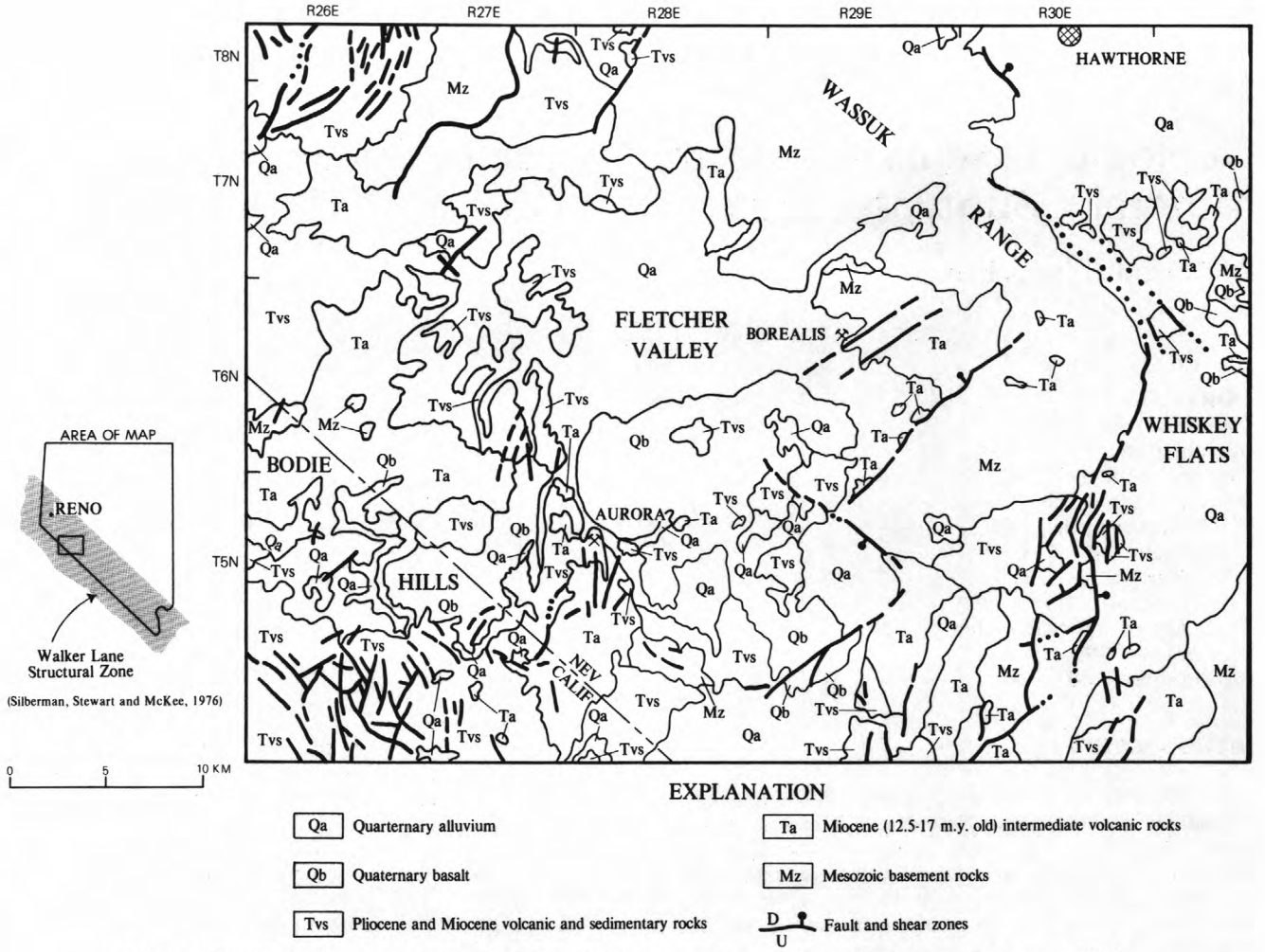

Figure 53. Geologic map of the Fletcher Valley area, Nev. (after Carlson and others, 1978).

from Cenozoic deposits along the Walker Lane zone (Silberman and others, 1976).

The western part of the Basin and Range province in Nevada contains numerous associated warm or hot springs (Stearns and others, 1937, p. 91-93). Many of the modern hot springs are situated along known normal faults, and there also is evidence of fossil hot-spring activity along these structures. The Borealis area has had a long history of magmatic volcanic activity from the Paleozoic through the Quaternary (Stewart and others, 1982; Silberman and others, 1976), which provides an extended source of heat for hydrothermal activity in the region. The deep faults promoted circulation of meteoric water to deep levels, where rock temperatures were elevated because of magmas.

MINE GEOLOGY

Stratigraphy

Stratigraphic units at Borealis include sedimentary- and volcanic-rock types, both of which host gold mineralization. The timespan represented by these units extends from prehydrothermal through posthydrothermal activity. Thus, some units in the stratigraphic section were deposited contemporaneously with hydrothermal activity and, as such, were altered either during or immediately after deposition. In addition, some units were actually formed by the hydrothermal system itself.

The oldest rocks at Borealis are Miocene hornblende andesite flows and laharic breccias. Tuffaceous sedimentary rocks are interbedded with the andesitic units; the sedimentary layers range from 1.5 to 15 m in thickness. The complete Miocene volcanic section is at least 450 m thick, possibly as thick as 900 m. This section of Miocene volcanic rocks and interbedded tuffaceous sedimentary rocks is equivalent to unit Ta_2 of Stewart and others (1982), which occurs throughout the Walker Lake $1^{o}x2^{o}$ sheet (fig. 53).

The Miocene andesitic section is unconformably overlain by a sequence of Pliocene rocks that host the Borealis deposit. The Pliocene rocks are divided into three units: (1) spring-vent deposits, (2) quartz breccia, and (3) talus deposits. Units 1 and 2 were formed by geothermal activity, whereas unit 3 was simply deposited over and around the active Pliocene geothermal system that was also responsible for gold deposition at Borealis.

The spring-vent deposits constitute a bleached unit that is varyingly silicified and argillized. It probably identifies an area near fossil geothermal vents of the Borealis hydrothermal system and is the earliest

geothermal deposit formed by the system. This unit is defined by strong bleaching, argillization, and silicification within Miocene andesite and Pliocene tuffaceous sedimentary rocks. The unit crops out at the present topographic surface and extends to depth, crosscutting the earlier andesitic section. Mineral assemblages that define the spring-vent deposits include opal-cristobalite and kaolinite-alunite. Oxides and sulfides occur in sparse amounts in both assemblages.

The quartz breccia unit was deposited unconformably over the spring-vent unit. The external geometry of the quartz breccia unit is broadly lenticular and shares a sharp contact with the underlying spring-vent deposits and the older andesitic section (fig. 54). Two end members are recognized in the quartz breccia unit, on the basis of matrix mineralogy: (1) quartz-sulfide, and (2) montmorillonite-hematite-opal.

The matrix of the quartz-sulfide end member is dark grey and contains cristobalite, chalcedonic quartz, and as much as 10 percent disseminated, extremely fine grained sulfides, dominantly pyrite and minor amounts of chalcopyrite, bravoite, and cobaltite. The breccia clasts are of red to pale-pink microcrystalline quartz with disseminated hematite.

The quartz-sulfide breccia grades laterally away from the center of the deposit to montmorillonite-hematite-opal breccia. The difference between these two breccia types is that the matrix of the second type is composed of montmorillonite, hematite, and opal instead of quartz and sulfides. Clasts of the montmorillonite-hematite-opal breccia can be of quartz-hematite-pyrite, opaline material, or andesite.

The talus deposits grade into the quartz breccia unit. The talus also contains clasts of andesite, opal, and quartz-hematite-pyrite in a loose silty-sandy matrix.

Quaternary colluvium overlies lateral stratigraphic equivalents of the mineralized Pliocene deposits at Borealis. The colluvium contains clasts of andesite and granodiorite from the highlands in the Wassuk Range, and altered Miocene and Pliocene clasts from the Borealis deposit and surrounding areas of hydrothermal alteration.

Structure

The Borealis deposit apparently occurs at the intersection of three nearly vertical but poorly exposed fault systems: (1) A northeast-trending shear zone, known locally as the Borealis trend, identified by outcrop and drilling data; (2) an east-west-trending set of shears, found by drilling and trenching; and (3) a north-south-trending normal fault, down on the west side, inferred from geophysical (electromagnetic and magnetic) and drilling data. The Borealis trend is a 5-km-long series of silicified and brecciated outcrops, trending approximately N. 50° E. The ore body itself, and the quartz breccia outcrops immediately east of the postulated north-southerly trending fault, constitute evidence for the Borealis trend in the mine area. The east-westerly trending shears, as identified in drill holes and a single trench, contain near-vertical quartz-hematite (after pyrite) breccias carrying anomalous gold.

Alteration

Alteration at the Borealis deposit includes a wide range of silicification and argillization. Silicification ranges from opal to quartz, and argillization from incipient alteration defined by montmorillonite to intense alteration defined by kaolinite-alunite.

The upper parts of the Miocene andesitic section were silicified and argillized by early extreme acid leaching. Remnant porphyritic textures are visible in strongly silicified, acid-leached rocks.

Acid leaching of the andesitic section and overlying tuffaceous sedimentary rocks produced an opal-cristobalite assemblage, locally referred to as sponge rock because of its open texture. This alteration is a near-surface phenomenon and grades with depth into an argillic-alteration assemblage defined by

Figure 54. Local unconformity (dashed line) separating earlier barren spring-vent deposits (light colored) from the later quartz breccia in the Borealis pit. View eastward. Photograph taken in 1982.

kaolinite and alunite. The contacts between the sponge rock and kaolinite-alunite alteration vary extremely and range from vertical to horizontal and from sharp to gradational.

Silicification has affected all the rock types; however, it is best characterized within the quartz breccia and spring-vent deposits. The quartz breccia unit is cemented by opal or chalcedonic quartz. Likewise, opal and chalcedony characterize the spring-vent deposits where both the tuffaceous sedimentary rocks and underlying andesite are intensely silicified.

The talus deposit is the least altered of the premineral and synmineral units. The matrix of the sedimentary breccia is locally altered to montmorillonite and hematite, with or without opal lining the insides of small vugs. This alteration is marginal and gradational into central masses of quartz-sulfide breccia.

Mineralization

Two types of ore occur at Borealis: (1) spring vent and (2) quartz breccia. Both ore types are characterized by diverse textures and alteration assemblages.

The spring-vent ores consist of sub-micron- and micron-size gold in combination with jarosite, alunite, barite, hematite, and sulfides of undetermined mineralogy. The yellow and brown oxides and gray sulfides are unconsolidated fine-grained bedded precipitates. Minor amounts of silt- to pebble-size detrital quartz and rock fragments are mixed with chemical precipitates in the spring-vent ores.

Most individual spring-vent-ore bodies are lenticular and range from 3 to 15 m in width, from 3 to 30 m in length, and from 0.15 to 3 m in thickness. Figures 55 and 56 show reconstructions of the spring-vent-ore bodies, developed from blasthole assays. Although these reconstructions ignore the true individual thicknesses of interleaved and superimposed spring-vent lenses, the end result documents the vertical stacking and alignment of the spring-vent-ore bodies over several bench levels in the pit.

The quartz breccia ores, like the spring-vent ores, consist of micron-size gold associated with oxides and minor sulfides in a siliceous to argillaceous matrix. Reflected-light microscopy of heavy-mineral separates from quartz-sulfide ores reveal that the largest gold particles are 25 μm; however, much of the gold is suspected to be smaller than 2 μm. Sulfides associated with the gold include pyrite, chalcopyrite, bravoite, and cobaltite.

Many of the highest grades of quartz-sulfide breccia contain a hydrothermal overprint of vuggy sugary quartz, crystalline barite, leucoxene, and fine hematite. Lower grades of oxidized quartz-sulfide breccia contain neither the vuggy quartz nor the oxides but, instead, are partially to pervasively oxidized, with little textural change.

The ore body within the quartz breccia unit is an east-northeast-elongate lens. Ore grades within this lens are consistent, with only a few barren internal zones. Lateral contacts of the ore body are gradational to fairly sharp, whereas the higher grades of the quartz-sulfide breccia pass into lower grades of montmorillonite-hematite-opal breccia. The upper ore-body boundaries are at the base of a thin (1.5-4.5 m thick) leached zone, unless covered by unmineralized sedimentary breccia.

Age of mineralization

The age of the Borealis deposit is bracketed by K-Ar ages on alunite and andesite. F. J. Kleinhampl and M. L. Silberman (written commun., 1980) obtained an age of 4.0±0.5 m.y. on alunite from the acid-leached zone, and R. F. Reid (written commun., 1982) obtained an age of 7.0±0.5 m.y. on hornblende in andesite from the Miocene section. This hornblende age is a maximum for the hydrothermal system because the andesitic section is altered, whereas the alunite age presumably represents the age of acidic alteration during boiling of hydrothermal solutions in the near-surface environment.

DISCUSSION

The genesis of the Borealis deposit has been considered in terms of the Steamboat Springs geothermal system (Schoen and others, 1974; White, 1981). The basis for this comparison is the similarity between the alteration types at Borealis and Steamboat Springs. Spring-vent-ore bodies are aligned in a northeastward direction, to the north-southerly alignment of spring vents at Steamboat Springs. This alignment at Borealis reflects control by underlying fluid conduits, defined by northeast-striking structures.

The spring vent deposits probably were precipitated just below the air-water interface in a subaerial hot-spring environment. Bedded oxides commonly overlie the sulfides in the spring-vent ores, but interbedding of the oxides and sulfides in some places suggests hypogene oxide formation, which would infer that the Eh of the precipitating fluid was partly responsible for oxide formation. A periodic variation in the proportionate mixing of hydrothermal and paleosurface waters, or an occasional waning of hydrothermal-fluid flow, may have been responsible for the indicated Eh change. Hypogene oxide precipitation has a bolder, clearer counterpart in the ores of the quartz breccia unit.

The quartz breccia unit was formed by explosive, repetitive hydrothermal activity. The resulting breccia was deposited contemporaneously with the talus deposits. Both units were subsequently altered by continued discharge of the geothermal system. The texture and mineralogy of the clasts indicate strong quartz recrystallization and oxidation during each hydrothermal cycle before the introduction of matrix sulfides under reducing conditions. Clast boundaries in these two units are sharp. The oxidized quartz-hematite clasts, the later quartz-sulfide matrix, and the still-later oxide overprint indicate wide and, possibly, cyclic fluctuations in the Eh (and pH?) of the hydrothermal fluids which mineralized the quartz breccia unit. These redox fluctuations may reflect variations in the chemistry and (or) volume of rising

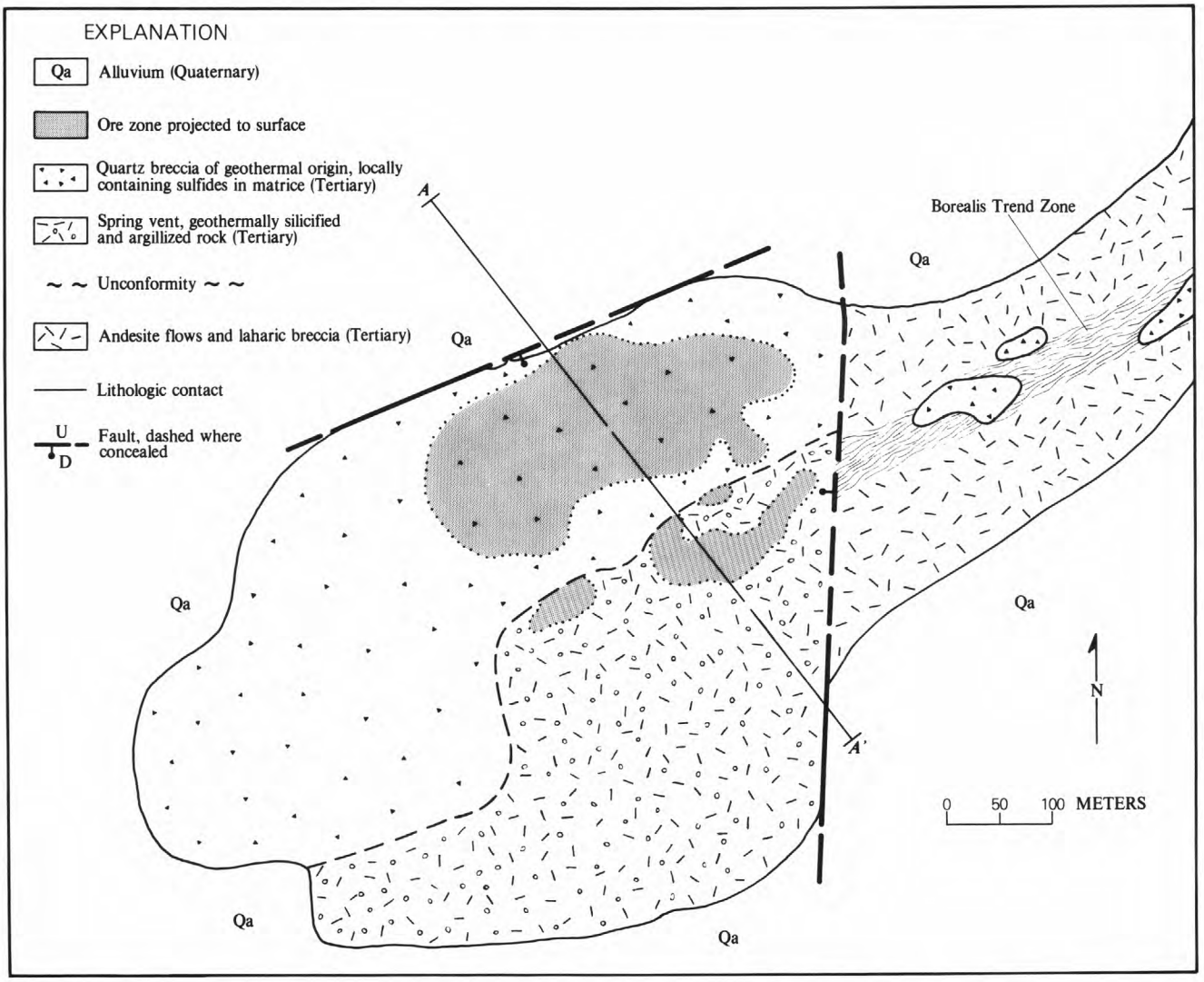

Figure 55. Generalized sketch of geologic relations at the Borealis minesite.

hydrothermal fluids during deposition of the quartz breccia unit.

The acid-leached sponge rock and the less intensely leached kaolinite-alunite alteration assemblages in the spring-vent unit could have formed in a subaerial to vadose environment. The genetic environment of sponge rock and similar acid-leached alteration types at Steamboat Springs, Nev., was described by Schoen and others (1974). Hydrothermal fluids at Steamboat Springs are venting beneath a subaerial surface. Vapors with a pH as high as 2, derived from boiling fluids, condense on vent walls and nearby rock or soil surfaces. These acidic condensates percolate into the substrate and downward to the water table, where they leach away most major components except silica, zirconium, and titanium. In extreme acid leaching above the water table, even silica is mobilized for short distances and redeposited as opal. A similar mechanism is envisioned to have occurred at Borealis and formed the sponge rock.

Precious metals and sulfides precipitate from spring waters at Steamboat Springs. Similarly, the spring-vent ores at Borealis precipitated from geothermal water near the top of the paleowater table. A rising water table, possibly aided by the gradually sinking northeast margin of the Fletcher basin, created the vertical stacking of spring-vent-ore bodies at Borealis. Some of the lower spring-vent-ore bodies may have formed in leached zones within the upper few meters of andesite. Later, the higher spring-vent-ores developed in overlying hot-spring-associated breccias and tuffaceous sedimentary rocks.

During the last stages of spring-vent activity, a series of normal dislocations may have existed along the north-southerly trending fault on the present east margin of the deposit, and along the northeasterly Borealis trend. These dislocations created a local depression on the northwest side of the present acid-leached spring-vent edifice (figs. 55, 56). Taluslike sedimentary breccia immediately began to accumulate, and hydrothermal fluids (previously venting in the subaerial and vadose spring-vent environment) were diverted to conduits beneath the accumulating talus. Spring-vent activity or, at least, the associated

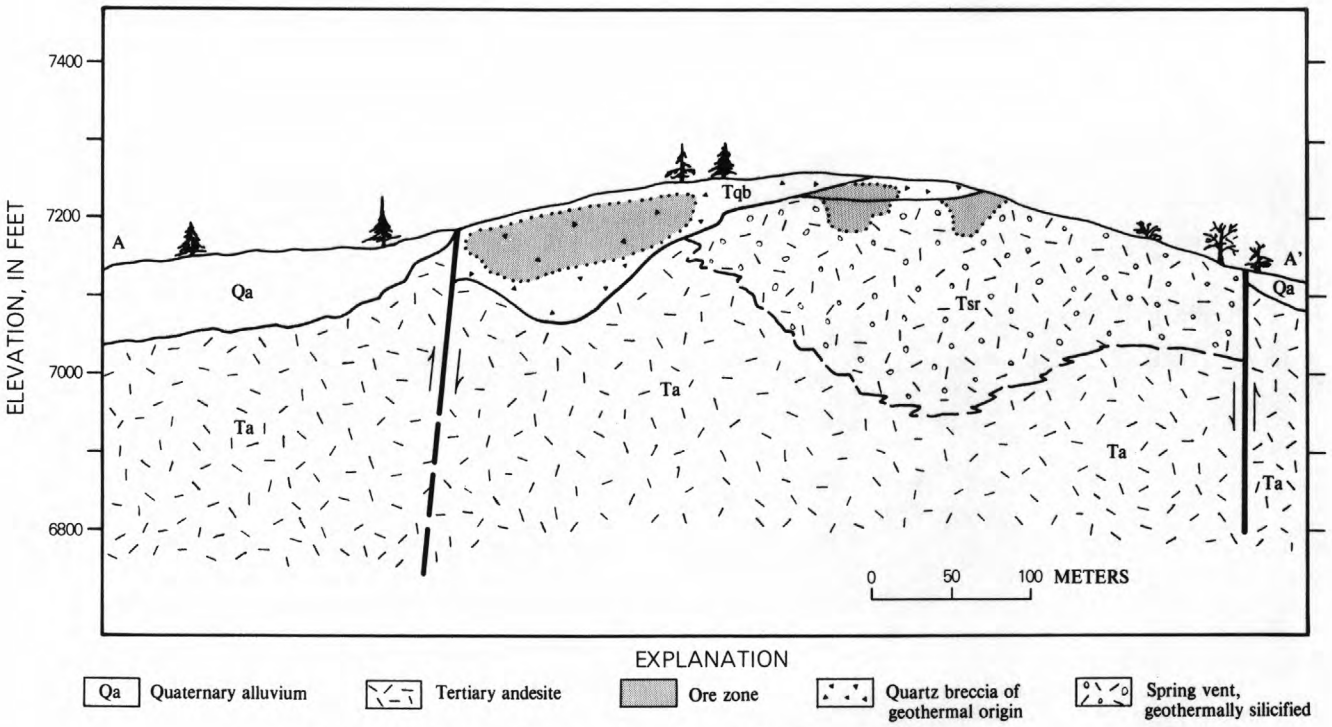

Figure 56. Schematic cross section of the Borealis minesite.

subaerial acid leaching terminated approximately contemporaneously.

Fluids venting upward into the sedimentary and hydrothermal breccias silicified and mineralized both the finer grained matrix and constituent clasts. However, acid leaching of the spring-vent type did not affect the quartz breccia unit, probably because the vents and overlying sedimentary breccia were below the local water table.

A cyclic explosive/passive aspect to hydrothermal venting is apparent in the development of the quartz breccia ore body. The explosiveness of the mineralizing fluids is attested to by: (1) the craterlike walls at the base of the quartz breccia ores; (2) vertical collapsed pipes, at least 3 m in diameter, cutting argillically altered andesite below the pre-quartz breccia unconformity; and (3) explosive fluid-streaming textures in some of the highest grades of quartz-sulfide breccia ores. Passive, waning stage(?), more highly oxidizing hydrothermal fluids produced the quartz-barite-hematite assemblages in the highest grade quartz-sulfide breccia ore.

Borealis seems to be part of the fossil surficial vent area of a structurally controlled epithermal system cutting Tertiary volcanic rocks. The cyclicity of paleosurface ores at Borealis may be a manifestation of the same mechanisms that cause cyclicity in vein mineralogy, as observed in other, more deeply eroded epithermal deposits.

REFERENCES CITED

Carlson, J. E., Stewart, J. H., Johannesen, D. C., and Kleinhampl, F. J., 1978, Geologic map of the Walker Lake 1° by 2° quadrangle, Nevada-California: U.S. Geological Survey Open-File Report 78-523, scale 1:250,000.

Gilbert, C. M., and Reynolds, M. W., 1973, Character and chronology of basin development, western margin of the Basin and Range province: Geological Society of America Bulletin, v. 84, no. 8, p. 2489-2509.

Schoen, Robert, White, D. E., and Hemley, J. J., 1974, Argillization by descending acid at Steamboat Springs, Nevada: Clays and Clay Minerals, v. 22, no. 1, p. 1-22.

Shawe, D. R., 1965, Strike-slip control of Basin-Range structure indicated by historical faults in western Nevada: Geological Society of America Bulletin, v. 76, no. 12, p. 1361-1378.

Silberman, M. L., Stewart, J. H., and McKee, E. H., 1976, Igneous activity tectonics, and hydrothermal precious-metal mineralization in the Great Basin during Cenozoic time: Society of Mining Engineers of AIME Transactions, v. 260, no. 3, p. 253-263.

Stearns, N. D., Stearns, H. T., and Waring, G. A., 1937, Thermal springs in the United States: U.S. Geological Survey Water Supply Paper 679-B, 206 p.

Stewart, J. H., Carlson, J. E., and Johannesen, D. C., 1982, Geologic map of the Walker Lake 1° by 2° quadrangle, California and Nevada: U.S. Geological Survey Map MF-1382-A, scale 1:250,000.

White, D. E., 1981, Active geothermal systems and hydrothermal ore deposits: Economic Geology, 75th anniversary volume, p. 392-423.

The Geology of the Enfield Bell Mine and the Jerritt Canyon District, Elko County, Nevada

By Donald J. Birak and Robert B. Hawkins

CONTENTS

INTRODUCTION

The discovery of disseminated gold deposits in the Jerritt Canyon district and the development of the Enfield Bell mine have contributed greatly to a resurgence in exploration for disseminated gold deposits in Nevada and the Western United States. The Jerritt Canyon project and the Enfield Bell mine is a 70:30 joint venture between the Freeport Gold Co. and FMC Gold Inc., which are wholly owned subsidiaries of their parent companies, Freeport-McMoRan Inc. and FMC Inc., respectively.

The Jerritt Canyon district lies within the Independence Mountains in north-central Elko County, Nev., approximately 80 km north of Elko (fig. 57). The Enfield Bell mine is located in the center of the Independence Range in the Jerritt Canyon window of the Roberts Mountains thrust. Ore is mined from carbonaceous and oxidized parts of the Roberts Mountains and Hanson Creek Formations, and is treated in a standard cyanidation mill, located approximately 12.8 km east of the mine.

Acknowlegments.—We gratefully acknowledge the management of the Freeport Gold Co. and the Freeport Exploration Co. for permission to publish this report. We thank Freeport geologists, especially those of the Jerritt Canyon District Office, for their critical reviews of the manuscript and stimulating discussions of the complex geology of the deposit; these reviews and discussions have contributed greatly to our current level of understanding of the history of the Jerritt Canyon district and the Enfield Bell mine.

HISTORY AND PRODUCTION

The discovery of gold mineralization in the Jerritt Canyon district was preceded by an antimony-exploration program initiated by FMC Inc. in 1971, on the basis of the antimony occurrences in the area reported by Lawrence (1963). Exploration emphasis shifted to gold when geologists recognized similarities between this area and the Carlin ore bodies. Mapping, sampling, and geochemical analyses led to the discovery of a gold anomaly along the north fork of Jerritt Creek. Drilling of this anomaly in 1973 revealed significant grades and thicknesses of gold mineralization in the lower part of the Roberts Mountains Formation. On the basis of this discovery, additional drilling was performed that delineated several small pods of low-grade gold mineralization; the mineralization was significant but not in sufficient amounts to constitute a minable discovery.

In 1976, the Freeport Exploration Co. assumed management of the project through a joint-venture agreement with FMC Inc. and began an expanded program of geologic mapping and geochemical sampling that led to a new understanding of the geology of the district. Several new geochemical anomalies and drilling targets were defined, including the Marlboro Canyon ore body, which is now part of the Enfield Bell mine. Although a classic "bull's-eye" geochemical target was the clue that led to the initial discovery in the north fork of Jerritt Creek, the bulk of current reserves were found beneath a cover of colluvium and soil that was geochemically barren.

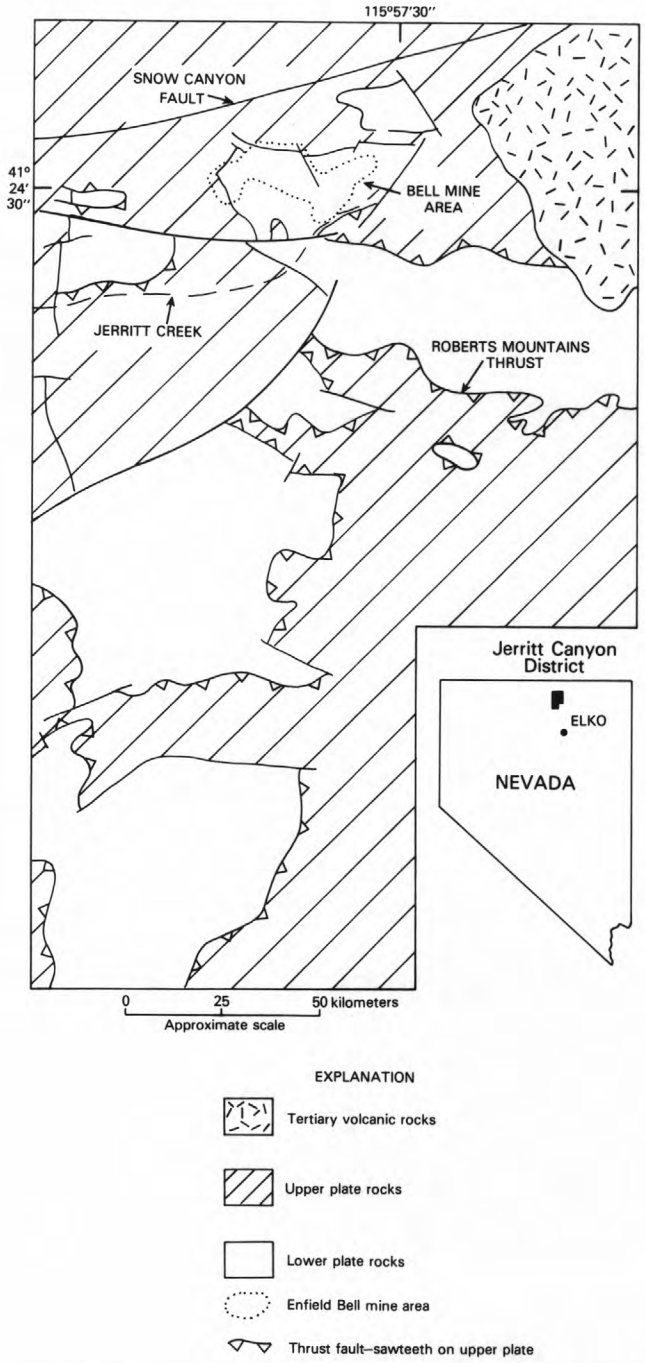

Figure 57. Location and general geology of the Jerritt Canyon district and the Enfield Bell mine area. Diagonal lines, exposures of upper-plate rocks; unpatterned, exposures of lower-plate rocks.

A decision to proceed with the construction of a mine and mill was made in 1979, and full-scale mill production began in July 1981. Current reserves are in four ore bodies, designated the Marlboro Canyon, North Generator Hill, West Generator Hill, and Alchem deposits. Mining has proceeded for the past 3 years within the Marlboro Canyon deposit and in part of the North Generator Hill deposit, referred to as Lower North Generator Hill. Milling proceeds at a design rate of 3,200 tons per day (2,900 t/d) of oxidized and carbonaceous ore.

REGIONAL GEOLOGY

The geology of the Jerritt Canyon district (Hawkins, 1973) is similar to that of the Lynn window (Radtke and others, 1980), insofar as much of the district is composed of Paleozoic sedimentary and volcanic rocks of the upper and lower plates of the Roberts Mountains thrust (fig. 57). The upper plate consist of an Ordovician eugeosynclinal sedimentary and volcanic assemblage composed of shale, argillite, chert, quartzite, intermediate to mafic flows, and lesser amounts of limestone and bedded barite. Basinal miogeosynclinal rocks compose the lower plate and consist of Ordovician and Silurian siltstone, limestone, chert, and quartzite. Deformation during the Late Devonian Antler orogeny moved the eugeosynclinal rocks (allochthon) eastward over the miogeosynclinal assemblage (autochthon), along the Roberts Mountains thrust (Merriam and Anderson, 1942). Good exposures of the thrust are uncommon in the Jerritt Canyon district. Where it is exposed, the thrust contact may be highly undulatory. Folding of the lower- and upper-plate rocks is recognized locally as a manifestation of this thrusting. A major southwest-plunging asymmetric anticline, referred to as the Map anticline, may have formed at that time.

Contemporaneous with the Robert Mountains thrust, several imbricate low-angle normal and reverse faults within the upper and lower plates were formed. These faults are important insofar as they caused locally significant truncations of stratigraphy that provided excellent pathways for hydrothermal fluids. Several of these structures have been recognized within the lower-plate rocks in the Enfield Bell mine area.

Tertiary igneous activity in the district produced several extrusive and intrusive rock types, none of which are found in the immediate mine area. A granodioritic to tonalitic pluton, measuring approximately 4,000 m^2 in outcrop area, was emplaced in the southwestern part of the district. Although no age determinations have yet been made on this pluton, it maybe as old as 120 m.y., equivalent in age to the Gold Strike stock north of the Carlin mine (Hausen and Kerr, 1968), or as young as 38 m.y., equivalent in age to the Mount Neva stock near the town of Tuscarora, Nev. (Coats and McKee, 1972). Possibly contemporaneous with granitic plutonism was the formation of several intermediate to mafic dikes and sills. These intrusive bodies are widely scattered across the district and are relatively small; their outcrops generally measure less than 10 m wide by 30 m long.

Deposition of andesitic and rhyolitic flows and ash flows occurred about 43 to 34 m.y. B.P. (Stewart, 1980). Deposition of the andesitic volcanic rocks is interpreted, from mapping evidence, to be the earlier of these two events. Subsequent faulting and erosion have limited exposures of the volcanic rocks to the extreme northeast corner of the district. Regional magnetic data suggest that these volcanic rocks continue beneath

valley-fill gravel to the east.

Basin-and-range-associated tectonism during the Miocene (Stewart, 1980) created a steep block-faulted terrain. Three conspicuous basin-and-range fault sets trend east-west, northwest, and northeast within the district. Hawkins (1982) postulated that the east-west-trending fault set may have been active during the Mesozoic, and was followed by the development of northeast- and northwest-trending faults during the basin-and-range event. The Snow Canyon fault, one of the major east-west-trending faults, occurs just north of the Jerritt Canyon window (fig. 57). Similar but smaller scale east-west-trending faults in the Enfield Bell mine are are the Marlboro Canyon, Bell, and Ridge faults (fig. 58), which may have also formed first during the Mesozoic.

Erosion of uplifted blocks along these faults has locally removed the upper-plate rocks and exposed the lower plate as windows in the Roberts Mountains thrust (fig. 58). In most areas, the contact between upper- and lower-plate rocks in the Jerritt Canyon district is thought to be a high-angle fault. Exposure of the Roberts Mountains thrust is limited. Continued erosion has resulted in a steep terrain and the locally thick alluvial and colluvial cover in the district.

REGIONAL STRATIGRAPHY

Most of the rocks in the Jerritt Canyon district are Paleozoic sedimentary and volcanic rocks that have been assigned to the upper and lower plates of the Roberts Mountains thrust (Hawkins, 1973).

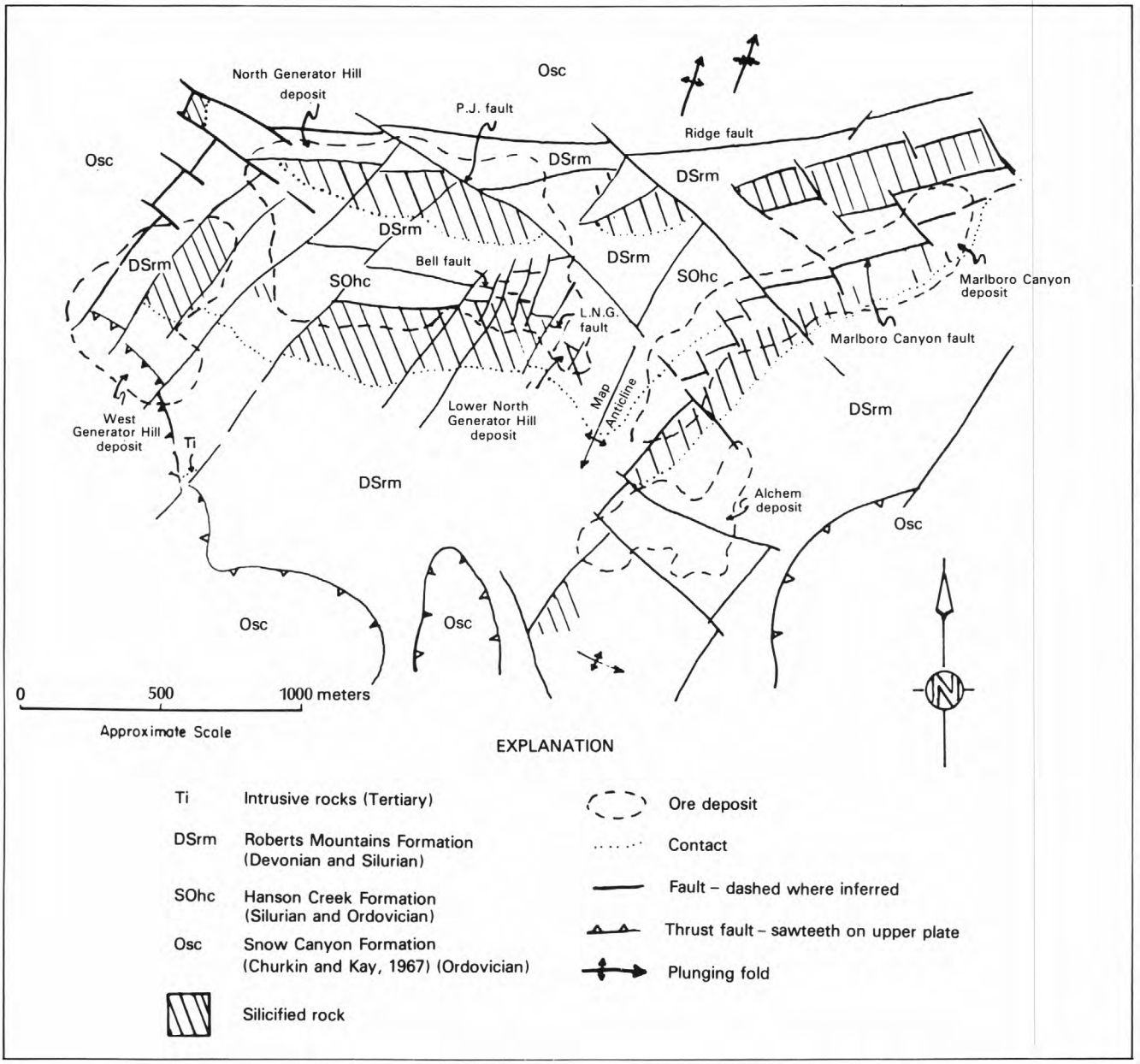

Figure 58. Preliminary geologic map of the Enfield Bell mine, Jerritt Canyon district, Elko County, Nevada.

Lower-plate rocks

Lower-plate stratigraphy within the Independence Mountains was described by Kerr (1962) and Hawkins (1973). Although a continuous, undisturbed stratigraphic section has not yet been recognized, sufficient exposures are present to enable the reconstruction of a complete section from the base of the Eureka Quartzite through the Roberts Mountains Formation (fig. 59).

The Eureka Quartzite of Middle Ordovician age is recognized throughout most of central Nevada as a prominent cliff-forming member of the autochthonous assemblage. Exposures of the formation in the district are limited to the southern parts of the Jerritt Canyon window, where it is composed of thick-bedded orthoquartzite. Fresh rock is generally light grey, with scattered grains of oxidized pyrite; weathered surfaces may be slightly yellow brown. Quartz grains are cemented by silica except near the contact with the laminated fissile, varyingly calcareous to dolomitic siltstone. The rock is composed of well-rounded well-sorted quartz silt grains, with carbonate as cement. Accessory minerals include illite-sericite, chlorite, anastamosing carbon filaments, disseminated pyrite, and a distinctive heavy-mineral suite. Black lenses composed of carbon, pyrite euhedra, and fibrous chalcedony, 0.5 cm thick and 2 to 5 cm long, oriented parallel to bedding, are common in the basal part of the formation. Fossils are rare and are limited to graptolite molds on parting surfaces.

A 10- to 15-m-thick bed of laminated to thin-bedded silty limestone occurs near the base of the formation. The more fissile siltstone beds commonly weather into small platy fragments and form gradual slopes, whereas the silty limestone unit is more resistant and can be traced in outcrop for hundreds of meters along strike.

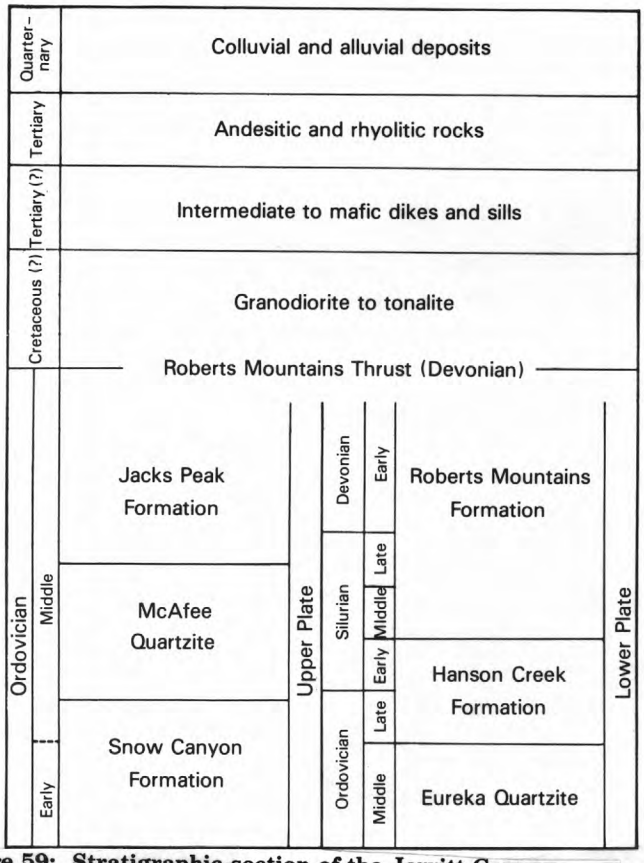

Figure 59: Stratigraphic-section of the Jerritt Canyon district. Stratigraphy for upper-plate rocks from Churkin and Kay (1967), for lower-plate rocks from Merriam and McKee (1976), Matte and others (1975), and Mullens and Poole (1972).

Upper-plate rocks

The upper-plate rocks (western facies) in the Independence Mountains have been correlated with eugeosynclinal rocks of the Ordovician Valmy Group (Churkin and Kay, 1967). Three formations of Ordovician age are recognized locally, in ascending order: The Snow Canyon Formation (Early and Middle Ordovician), the McAfee Quartzite (Middle Ordovician), and the Jacks Peak Formation (Middle Ordovician).

Whereas exposures of the McAfee Quartzite and the Jacks Peak Formation are limited to the northernmost part of the Jerritt Canyon district, the Snow Canyon Formation commonly flanks lower-plate rocks throughout the district. Only the Snow Canyon Formation is described here.

The rocks that compose the Snow Canyon Formation in the Jerritt Canyon district are predominantly siliceous sedimentary rocks, estimated at 350 m thick (Churkin and Kay, 1967). Except for the more resistant members, the Snow Canyon does not crop out well and forms smooth talus-covered slopes.

Shale, fissile siltstone, and argillite form the bulk of the Snow Canyon section. These rocks are carbonaceous and much less calcareous or dolomitic than those of the Roberts Mountains Formation. Weathered exposures show a characteristic orange-brown staining. Bedding generally is very wavy and contorted, and soft-sediment-compaction features are common. Graptolite molds are locally abundant.

Interspersed with the clastic rocks are multicolored wavy chert beds that exhibits a knobby texture on their bedding planes, referred to locally as overlying Hanson Creek Formation, where carbonate cement may also occur. Although bedding is indistinct, beds are generally massive and more than 3 m thick. Fossils are rare, but local exposures yield graptolite molds. Measured thicknesses of the Eureka Quartzite range from 150 to 190 m. Although the base of the formation has not been well studied, the upper contact is interpreted to be gradational with the Hanson Creek Formation.

The Hanson Creek Formation, considered to be of Late Ordovician and Early Silurian age by Matti and others (1975), is the major host rock at the Enfield Bell mine and is exposed in many parts of the Jerritt Canyon window. On the basis of surface and subsurface data, the Hanson Creek Formation is here subdivided into five lithologic units—unit 1 (youngest) through unit 5 (oldest) (fig. 60). Because the upper parts of the Hanson Creek Formation are much better known and occur more commonly in outcrop than the lower units, the units are numbered consecutively from the top down.

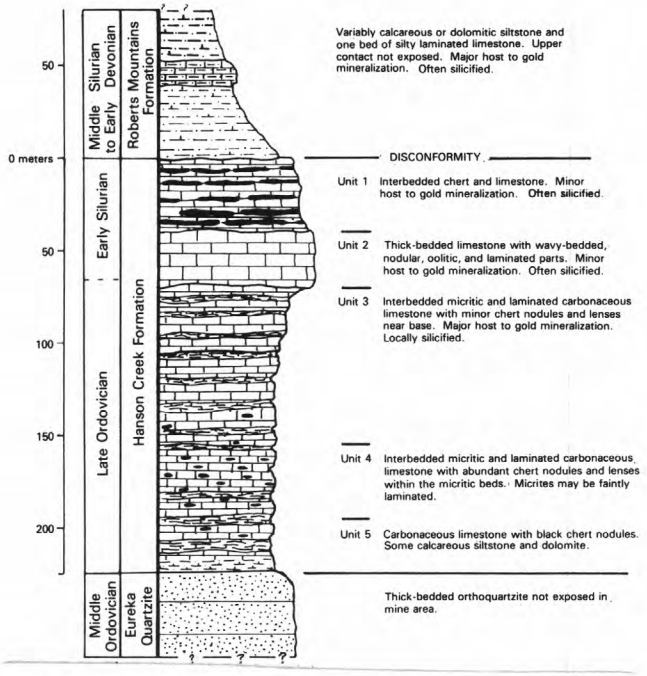

Figure 60. Generalized stratigraphic section of lower-plate rocks in the Bell mine area.

The lower three units of the Hanson Creek Formation, units 3 through 5, are carbonaceous banded limestones. The banding, best developed in unit 3, results from alternating beds of micritic limestone and laminated dolomitic limestone, in which the laminated beds are the most carbonaceous. Pyrite occurs in both types of beds, although it is more abundant in the laminated beds.

The basal unit, unit 5, as measured, consists of 5 to 30 m of dolomitic limestone and thin-bedded micritic limestone, with some laminated calcareous siltstone near the basal contact. Fossils recognized throughout are crinoidal, brachiopod, bryozoan, and radiolarian fragments. Near the top of unit 5, an intraclastic layer has been recognized in which the intraclasts contain fossil debris mixed with carbon stringers and pods and sparry calcite cement. Locally, lenses and pods of black, carbonaceous chert have been recognized.

The overlying unit 4 is a 30- to 40-m-thick sequence of carbonaceous banded limestone containing abundant black chert nodules and lenses, 5 to 25 cm long, oriented parallel to bedding. Micrite beds may be faintly laminated, whereas laminated dolomitic limestone beds are locally absent. Fossil fragments are similar to those found in the basal unit.

The middle unit of the Hanson Creek Formation, unit 3, is a sequence of alternating carbonaceous micritic limestone beds and laminated carbonaceous dolomitic limestone beds. This unit, which is the main host for gold mineralization in the Enfield Bell mine (fig. 60), has been measured at more than 90 m thick in exposures in the southern part of the district. Chert beds, generally less than 0.1 m long and 2 cm thick, occur sporadically in the lower part of the unit. Fossils recognized in this unit are similar to those in the lower two units, with the addition of trilobite fragments. Studies have shown that gold mineralization favors the more permeable laminated beds, which occur locally in tenfold greater abundance than in the micrite beds.

Overlying unit 3 is a varyingly textured 30-m-thick unit of limestone—unit 2. Four different rock types have been recognized in this unit: (1) Thick-bedded limestone, (2) wavy thin-bedded to nodular limestone, (3) oolitic limestone, and (4) wavy-laminated limestone. The rock is weak to noncarbonaceous, weakly pyritic, and locally is entirely composed of dolomite. Fossils are fairly evenly distributed and resemble those recognized in the lower three units; however, trilobite fragments have not been recognized in this unit.

The uppermost unit of the Hanson Creek Formation, unit 1, is composed of 3 to 40 m of interbedded black chert and carbonaceous limestone. Chert beds are more consistent than in units 3, 4, or 5 and may exceed 1 m in length and 5 cm in thickness. Pinching and swelling of the chert as a result of soft-sediment deformation is common. Sponge spicules, radiolarians, and the absence of diagenetic-replacement textures suggest a sedimentary, nondiagenetic origin for the chert. The limestone beds, which are thicker than the chert beds, compose as much as 75 percent of a measured thickness near the base of the unit. Both laminated and nonlaminated limestone beds have been recognized.

The contact between the Roberts Mountains and Hanson Creek Formations appears to be disconformable, a contention that was also supported by the work of Matti and others (1975). Whereas previously published reports (Mullens and Poole, 1972; Merriam and McKee, 1976) placed the uppermost unit of the Hanson Creek Formation as part of the overlying Roberts Mountains Formation, Freeport Gold Co. geologists cite the sharpness of the contact between this uppermost unit and siltstone of the Roberts Mountains Formation, as well as the similar textures and mineralogy within the five Hanson Creek Formation, as evidence that the uppermost unit, 1, more properly belongs within the Hanson Creek Formation.

The Roberts Mountains Formation of Middle Silurian to Early Devonian age (Matti and McKee, 1977) is exposed throughout the Jerritt Canyon district. The basal 30 m of this formation is host to gold mineralization in the Enfield Bell mine (fig. 60). The estimated thickness of the Roberts Mountains Formation is 300 m; however, the uppermost part has been truncated by the Roberts Mountains thrust, which forms the upper contact of the formation. The major rock type of the Roberts Mountains Formation is a cobblestone texture. Bedding is generally less than 10 cm thick. Bedded grey barite locally occurs with the chert.

Discontinuous layers of grey to brown quartzite, generally less than 3 m thick, occur within the finer grained clastic sequence. A thicker quartzite unit, with scattered shale horizons, apparently caps the Snow Canyon Formation. Both types of quartzite are composed of quartz sand grains and scattered pyrite cemented with silica or carbonate. Carbon and random quartz veinlets are recognized locally. Crossbedding,

though sparse, has been observed in the thinner quartzite and siltstone beds.

Mafic pillow lavas occur within the Snow Canyon Formation, sandwiched between argillaceous-rock sequences. Chert and limestone can be found sporatically within the lavas. The limestone beds occur between successive pillow structures. Alteration of these lavas has changed the primary minerals to chlorite, sericite, and carbonate. Phenocrysts of plagioclase and pyroxene commonly are totally altered to calcite.

Limestone is the least continuous rock type in the Snow Canyon Formation. Besides occurring within altered mafic lavas, limestone has been recognized interspersed with laminated chert, shale, and siltstone. A section of shaly carbonaceous limestone capped by a cliff-forming intraformational limestone breccia apparently occurs near the base of the formation on the west margin of the Enfield Bell mine area.

GEOLOGY OF THE ENFIELD BELL MINE

The Enfield Bell mine is located in the northern part of the Jerritt Canyon window, in an area approximately 3,300 m long east-west by 1,200 m wide north-south (fig. 58). The mine comprises four known ore deposits, in order of decreasing size: the Marlboro Canyon, North Generator Hill, West Generator Hill, and Alchem deposits. Current reserves are 13.7 million tons (12.5 million t) at an average grade of 0.199 troy oz Au per ton (7.03 g Au/t), occurring in both oxidized and carbonaceous sedimentary rocks. Mineralization is structurally and lithologically controlled within the upper banded limestone of the Hanson Creek Formation, unit 3, and the lower siltstone of the Roberts Mountains Formation (fig. 60). Lesser amounts of ore occur in silicified sections of both formations. Small slices of geochemically barren upper-plate rock have been recognized in the Marlboro Canyon pit. Gold currently is being mined from Marlboro Canyon and a part of North Generator Hill known as Lower North Generator Hill (fig. 58).

Structure

Faulting is common in the Enfield Bell mine area and is the most important structural feature related to mineralization; folding may have been contemporaneous with a premineral set of faults. The four sets of faults in the Enfield Bell mine area range in age from Devonian to Tertiary. The oldest faults are the Roberts Mountains thrust and sympathetic subparallel low-angle normal and reverse faults within the upper- and lower-plate assemblages. The presence of imbricate low-angle faults became evident when detailed mapping revealed reversals and truncations of stratigraphy along brecciated low-angle shears.

East-west-trending faults are the next-younger set of major faults in the mine area. These faults are cut by younger northwest- and northeast-trending faults. The ages of these three fault sets is somewhat equivocal; however, the east-west-trending system is postulated to have formed first during the Mesozoic, with an overprint of Tertiary motion. One such fault is the Snow Canyon fault (Hawkins, 1982), which occurs immediately north of the mine area (fig. 57). Smaller scale east-west-trending faults within the mine area are the Marlboro Canyon fault in the Marlboro Canyon ore body, the Bell and L.N.G. faults in the Lower North Generator Hill ore body, and the Ridge fault, which forms the north boundary of the Jerritt Canyon window (fig. 58).

Figures 61A and 61B show typical cross sections through the Lower North Generator Hill and Marlboro Canyon deposits that illustrate the characteristics of the Bell and Marlboro Canyon faults, which were the main conduits for mineralization in their respective ore bodies. In each deposit, rocks of the Roberts Mountains and Hanson Creek Formations form the footwall block (north) against rocks of the Hanson Creek Formation in the hanging wall (south). Estimated relative vertical displacement on these faults is 100 m. Both faults dip steeply south but change dip and strike directions over short vertical and horizontal distances. The Marlboro Canyon fault changes strike in the western part of the Marlboro Canyon ore body to more northeasterly, whereas the Bell fault changes strike to northeasterly in the east end of the Lower North Generator Hill ore body (fig. 58). Both faults became shallower in dip on progressively deeper mine levels.

The L.N.G. fault is also an east-west-trending fault that may have formed as a result of uplift along the Bell fault; it appears, for the most part, to be a bedding-plane fault. This fault, which dips gently south, is believed to have formed as a result of slippage along the boundary between silicified and unsilicified parts of the Hanson Creek Formation. The amount of displacement on the L.N.G. fault is small, and the strike of the fault changes to northwesterly on the east side of the Lower North Generator Hill ore body (fig. 58).

After formation of the Marlboro Canyon and Bell faults, the high-angle northwest- and northeast-trending faults were formed during Basin and Range tectonism. Mapping evidence of active mine faces suggests that the northeast-trending faults postdate the northwest-trending faults. However, the fact that the northwest-trending P. J. fault in the North Generator Hill deposit cuts both east-west- and northeast-trending faults indicates that some of the northwest-trending faults postdate the northeast-trending faults. Although the genetic relations of faulting in the mine area is still equivocal, all the faults are interpreted to predate gold mineralization. Ore coincides with faults and blossoms at fault intersections. Figure 62, a geologic map of a typical ore bench in the Lower North Generator Hill pit, shows the relation of these structures.

The Map anticline, a southwest-plunging asymmetric fold that occurs between the North Generator and Marlboro Canyon ore bodies (fig. 58), is believed to have formed as a result of thrusting. The western limb of this fold strikes west-northwest and dips south-southwest, whereas the eastern limb strikes north-northeast and dips east-southeast. Dips on each limb range from 25° to 65°; the eastern limb is the steepest. The fold limbs are delineated by dipping beds of jasperoid, which can be readily seen in aerial photographs.

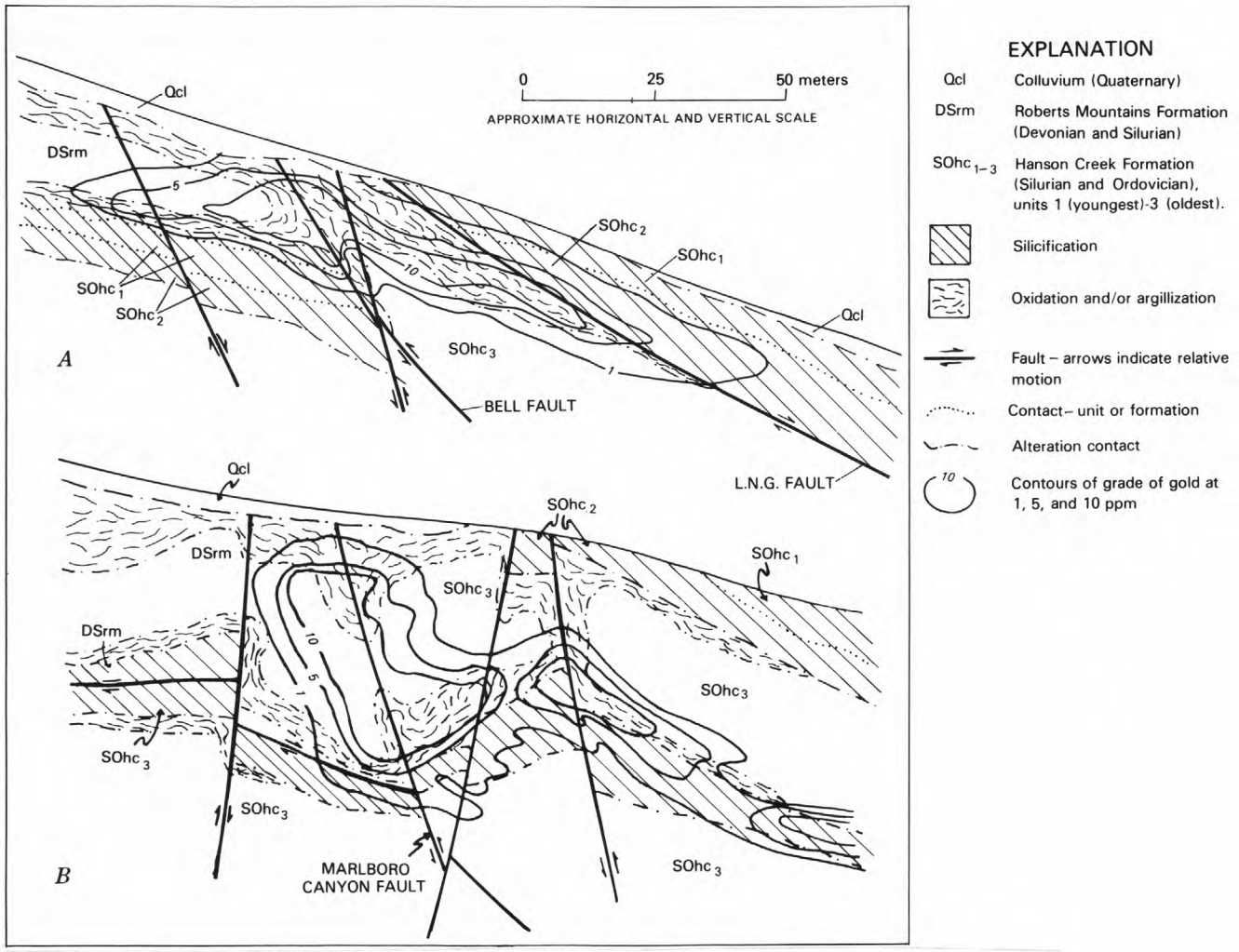

Figure 61. A, North-south cross section through the central part of the Lower North Generator Hill deposit. Contours of gold grade are 1, 5, and 10 ppm. B, North-south cross section, looking east, through the central part of the Marlboro Canyon ore body. Gold mineralization is strongly structurally controlled, with greater vertical than horizontal continuity. Contours of gold grade are 1, 5, and 10 ppm.

Ore-body morphology

The ore in the Enfield Bell mine occurs in two distinct modes. The largest ore zone, containing the most continuous and highest grades of gold, are elongate, steeply to moderately dipping tabular zones (Marlboro-type ore zones), which are typical sites for ore deposition in North Generator Hill and in most of Marlboro Canyon. The second type of ore zone (Alchem-type ore zone) is also tabular but is associated with low-angle faults, commonly containing stratiform jasperoid bodies. The bulk of the ore tonnage in the western Marlboro Canyon, Alchem, and West Generator Hill deposits are from Alchem-type ore zones.

Figure 61B shows a cross section of a typical Marlboro-type ore zone. A mushroomlike appearance is created by gold values increasing in large increments from the surface down, tapering off more gradually below the main ore intervals. Figure 63 shows a typical cross-sectional view of an Alchem-type ore zone. The ore occurs in both unsilicified and silicified parts of the Roberts Mountains Formation and in silicified sections of the underlying Hanson Creek Formation. The contact between the two formations is interpreted to be, at least in part, a low-angle fault. The best ore grades occur in rocks of the Roberts Mountains Formation, and the ore zone may be highly undulatory.

Gold in both types of ore zones is disseminated in the rock- quite typical of ore zones observed in other Nevada gold deposits, such as Carlin. Gold grains observed in thin section may exceed 5 μm in diameter but are generally smaller than 2 μm. Where large enough to be observed petrographically, gold grains are commonly spatially associated with goethite, pseudomorphic after pyrite.

Alteration

Three major hydrothermal events have altered the rocks of the Enfield Bell mine: (1) Silicification, (2) oxidation and argillization, and (3) carbonization. Silicification, the predominant event, resulted in alteration of the limestone to hard dense varicolored

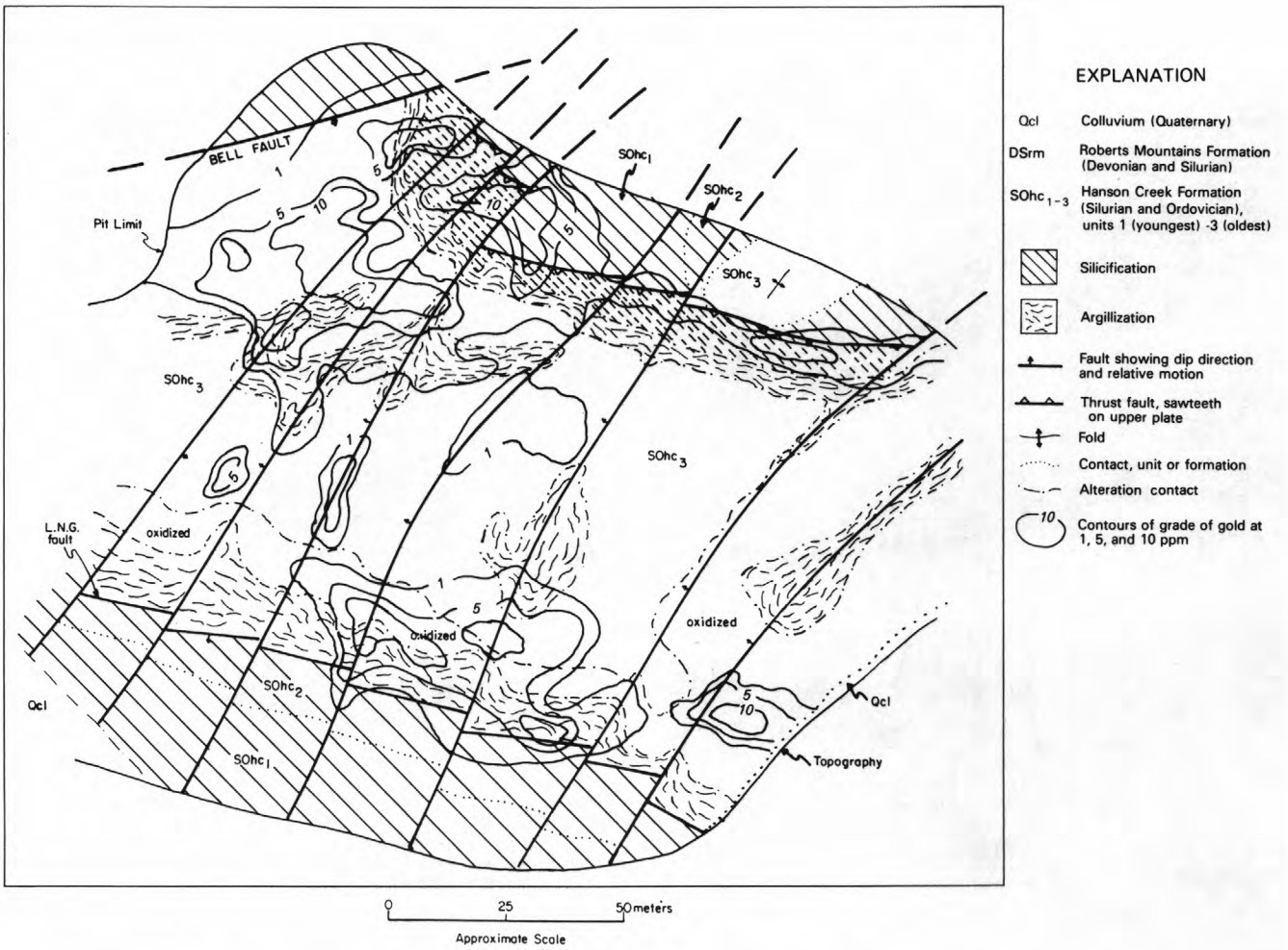

Figure 62. Geologic map of a typical mine level in the Lower Generator Hill ore body.

jasperoid. The jasperoid bodies in the mine area stand out in strong relief from the surrounding terrain and are approximately tabular in shape. Although about 35 to 40 percent of the rocks in the mine area are jasperoid, jasperoid constitutes less than 10 percent of the ore. The degree of silicification recognized in the mine area ranges from scattered quartz veining to complete replacement of the carbonate fraction. Silicification has affected rocks of both the Roberts Mountains and Hanson Creek Formations but is more intense in limestone of the Hanson Creek Formation. Mine mapping suggests that all but possibly the latest phase of silicification occurred before Tertiary block faulting. Jasperoid can be seen in razor-sharp contact against unsilicified rocks, horizontally juxtaposed along high-angle faults. The nearly stratiform appearance of the jasperoid bodies is interpreted to be the result of silicification along low-angle faults as well as replacement of chemically favorable rock types. The major stage of silicification that formed the jasperoid bodies is also believed to predate gold mineralization. Gold values occur in silicified and unsilicified rocks on either side of high-angle faults. Gold mineralization does not normally occur in ore-grade concentrations in jasperoid and generally is homogeneously distributed and of lower grade relative to the range of values found in the main ore zones. Locally, the jasperoid bodies may host gold mineralization higher than 30 ppm, but generally it ranges from less than 0.05 to 1.5 ppm.

Oxidation and argillization may be the most economically important alteration events to have taken place in the Enfield Bell mine area; the oxidized and argillized rocks contain the highest gold values and are relatively easy to treat with conventional cyanidation techniques of gold recovery. These two types of alteration coincide spatially and are believed to have similar, but not necessarily contemporaneous, genesis. Oxidation of the Roberts Mountains Formation produced a tan to light-orange-brown semifriable siltstone. Pyrite grains are well oxidized to limonite and goethite, and carbon is generally absent. The rock may also be noncalcareous, owing to associated but limited decalcification. Oxidation within the Hanson Creek Formation is similar to that recognized in the Roberts Mountains Formation, except for (1) local oxidation of black, carbonaceous chert lenses and beds to light-brown chert or black chert with brown rims, and (2) preferential oxidation of the more permeable laminated beds of unit 3 of the Hanson Creek Formation. Again, as in the Roberts Mountains

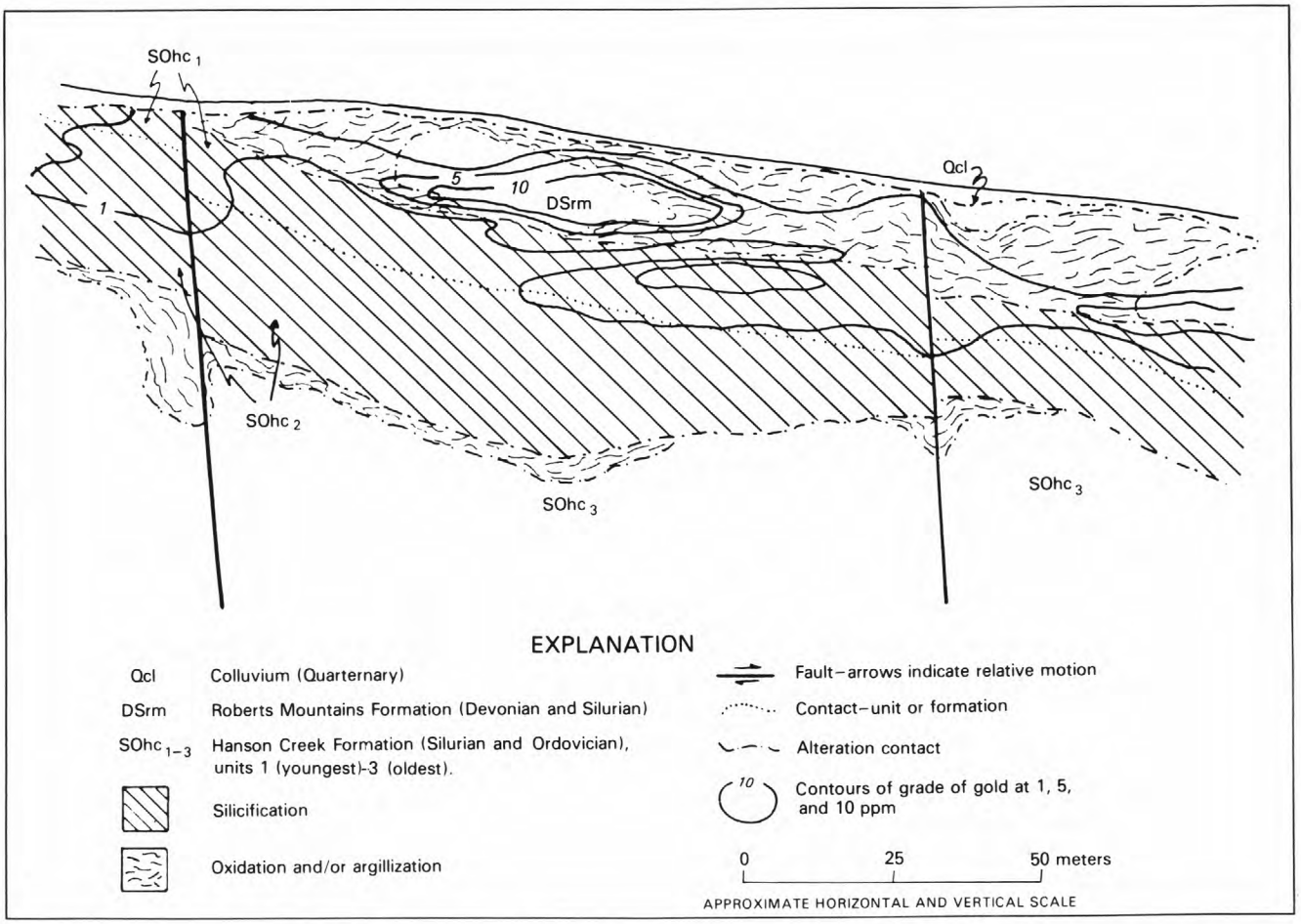

Figure 63. North-south cross section through the western part of the Marlboro Canyon ore body, showing the stratiformity of gold mineralization in an Alchem-type ore zone. Contours of gold grade are 1, 5, and 10 ppm.

Formation, oxidation of the Hanson Creek Formation may have been accompanied by decalcification.

Argillization of the Enfield Bell mine rocks took place along structurally controlled zones and is considered an advanced, more localized stage of the oxidation process. This alteration produced clay-rich zones within the Hanson Creek and Roberts Mountains Formations that are highly tabular, with greater vertical than horizontal continuity. Their shape is due to formation along high-angle structures, such as the Marlboro Canyon and Bell faults, where argillized Hanson Creek limestone occurs against argillized Roberts Mountains siltstone (fig. 61A, 61B). Argillization is also recognized in rocks directly above and below jasperoid bodies. One such occurrence is along the L.N.G. fault, where argillized and oxidized Hanson Creek limestone forms the footwall of the fault against unargillized jasperoid in the hanging wall (fig. 61A). Whereas primary rock textures are commonly preserved in the argillically altered rock, primary minerals are not. Dominant alteration minerals are kaolinite, sericite, illite, smectites, alunite, jarosite, quartz, and iron oxide; carbonate, pyrite, and carbon are rare. Gold values in the argillized and oxidized rocks range from less than 0.05 to more than 150 ppm; the highest gold value measured to date was within argillized Roberts Mountains siltstone, assaying 685 ppm.

Most of the observed effects of oxidation and argillization are believed to have formed nearly contemporaneously after silicification. Argillized rock grades into oxidized rock, whereas razor-sharp contacts between argillized and silicified or carbonaceous rock have been observed. Some oxidation may have occurred before argillization and silicification, as evidenced by oxidized, decalcified, unsilicified beds of limestone interbedded with silicified limestone. Replacement of carbonate by silica normally results in a highly impermeable rock that would resist the effects of oxidation and argillization.

Carbonization of the rocks in the Enfield Bell mine area is strongly controlled by structure. Carbonization produced black, sooty carbonaceous zones within much less carbonaceous or oxidized rock. High- and low-angle fault zones may have localized the carbon. Commonly the carbonized rock is sheared and may be host to realgar and orpiment. It is believed that primary sedimentary hydrocarbons migrated or were concentrated in the highly permeable fault zones, possibly through the action of large-scale pressure solution. Gold values within the remobilized carbon zones may be high along main ore trends, generally

ranging from less than 0.05 to 35 ppm. Locally, values of more than 150 ppm have been detected.

Accessory mineralogy

Several gangue minerals occur in the rocks of the Enfield Bell mine, some of which locally are excellent indicators of gold mineralization, whereas others are simply indicate hypogene activity on a districtwide scale. The most reliable mineralogic indicators of gold mineralization are realgar and orpiment. Realgar is by far the most abundant arsenic mineral, whereas orpiment occurs as an oxidation of realgar. Minor arsenopyrite has been detected through x-ray diffraction. Realgar and orpiment are found in carbonaceous rock in veins, intermixed with white sparry calcite, as veins in carbonaceous rocks, and as small scattered grains with remobilized carbon along fractures and shears. Although arsenic minerals have not been recognized in completely oxidized or argillized rock, significant arsenic values have been detected. Districtwide geochemical arsenic values range from traces to more than 1,000 ppm; higher concentrations are generally associated with higher gold grades.

Cinnabar is also a good indicator of gold mineralization, although it is far less abundant than the arsenic minerals. Dull blood-red grains of cinnabar have been found disseminated in high-grade ore zones. Districtwide geochemical analyses have yielded mercury values from traces to more than 50,000 ppb. The highest mercury values are invariably associated with high arsenic values in remobilized carbon zones, where cinnabar may be found finely disseminated with realgar and orpiment.

Barite and stibnite constitute the rest of the volumetrically important accessory minerals. Although they are not reliable indicators of gold mineralization, these two minerals are abundant in the mine area, where they are almost entirely restricted to jasperoid bodies. Barite occurs as euhedral encrustations on fractures or in vugs, as thin white veinlets, or as massive mosaic-textured pods and veins in jasperoid bodies and, less commonly, in oxidized siltstone. Euhedral dipyramidal barite crystals, as much as 10 cm long, have been found in clay-filled vuggy zones in jasperoid. Although barite may be locally abundant, the geochemical data for barium distribution are inconclusive.

Stibnite forms euhedral acicular crystals in radiating clusters or vein fillings of anhedral to subhedral grains. Veins of stibnite range from less than 1 to more than 15 cm in width. Stibnite and barite are commonly found intermixed, and mantling of stibnite with barite in some occurrences indicates a slightly earlier deposition for stibnite. Alteration of stibnite through hypogene and supergene processes formed three common antimony oxides as rims or complete replacements of stibnite crystals: Stibiconite ($H_2Sb_2O_5$), valentinite (Sb_2O_3), and kermesite (Sb_2S_2O). Both stibnite and antimony oxides have been observed as coatings and encrustations on euhedral quartz crystals. Geochemical antimony values from traces to as much as 500 ppm have been detected district wide. Some native sulfur crystals occur with stibnite, presumably as a more advanced oxidation product of the stibnite.

Other accessory minerals that have been recognized either megascopically, microscopically, or with x-ray diffraction are calcite, jarosite, alunite, variscite, dolomite, lepidocrocite, collophane, possibly scorodite ($FeAsO_4 \cdot 2H_2O$), and dusserite ($Ca_3(AsO_4)_2 \cdot 3Fe(OH)_3$). Except for calcite and jarosite, these minerals are only sparse, and it is equivocal whether they formed through hypogene processes. Calcite is most commonly found as white blocky veins in Hanson Creek limestone and in lesser amounts in Roberts Mountains siltstone or in jasperoid bodies. Botryoidal encrustations of calcite (travertine?) occur in vugs in oxidized limestone or jasperoid bodies and can contain as much as 1.5 ppm Au. Jarosite, which is a fairly common constituent of argillized rock, also occurs as small cinnamon-brown crystals on fracture surfaces in silicified and unsilicified rock.

Base-metal sulfides have not been observed in the Enfield Bell mine area, although they have been reported in other disseminated gold deposits (Harris and Radtke, 1976). Anomalous geochemical values of copper, lead, and zinc have been obtained from surface samples in the Enfield Bell mine area.

Silver values in the Enfield Bell mine are typical of those in other disseminated systems and range from less than 0.05 to 1.5 ppm. Typically the Au/Ag ratio exceeds 20:1. Data on other common trace elements, such as Mn, Tl, or W, are inconclusive.

SUMMARY AND CONCLUSIONS

Gold mineralization in the Jerritt Canyon district and the Enfield Bell mine is hosted within carbonaceous and oxidized parts of autochthonous lower-plate rocks of the Roberts Mountains thrust. Thrusting and associated imbricate low-angle faults provided excellent pathways for the movement of hydrothermal fluids, especially where intersected by high-angle faults. These conduits allowed the gold-bearing fluids to migrate upward into structurally and chemically favorable horizons. Alteration events, such as silicification, oxidation, argillization, and carbonization, occurred during the hypogene history of the deposit, though not necessarily contemporaneously with gold mineralization. A preliminary genetic sequence for the Enfield Bell mine ore bodies is as follows: (1) Deposition of Paleozoic miogeosynclinal and eugeosynclinal rocks in separate basins; (2) thrusting and folding of eugeosynclinal rocks over the miogeocline during Antler tectonism; (3) high-angle faulting during the Mesozoic; (4) small-scale oxidation of parts of the lower-plate rocks; (5) silicification of the lower-plate rocks to form jasperoid bodies; (6) high-angle block faulting during the Tertiary, possibly contemporaneously with intrusive activity; (7) formation of zones of remobilized carbon; (8) deposition of gold; (9) oxidation and argillization of carbonaceous rocks; and (9) deposition of stibnite, barite, realgar, and orpiment.

Although many questions on the hydrothermal history of the Jerritt Canyon district remain to be answered, continued production and exposure of the ore body are still adding to the knowledge gained thus far.

REFERENCES CITED

Churkin, Michael, Jr., and Kay, Marshall, 1967, Graptolite-bearing Ordovician siliceous and volcanic rocks, northern Independence Range, Nevada: Geological Society of America Bulletin, v. 78, no. 5, p. 651-684.

Coats, R. R., and McKee, E. H., 1972, Ages of plutons and types of mineralization, northwestern Elko County, Nevada, in Geological Survey research, 1972: U.S. Geological Survey Professional Paper 800-C, p. C165-C168.

Harris, Michael, and Radtke, A. S., 1976, Statistical study of selected trace elements with reference to geology and genesis of the Carlin gold deposits, Nevada: U.S. Geological Survey Professional Paper 960, 21 p.

Hausen, D. W., and Kerr, P. F., 1968, Fine gold occurrences at Carlin, Nevada, in Ridge, J. D., ed., Ore deposits of the United States, 1933-1967 (Graton-Sales volume): New York, American Institute of Mining, Metallurgical, and Petroleum Engineers, v. 1, p. 908-940.

Hawkins, R. B., 1973, The geology and mineralization of the Jerritt Creek area, northern Independence Mountains, Nevada: Pocatello, Idaho State University, M.S. thesis, 104 p.

----- 1982, Discovery of the Bell gold mine--Jerritt Canyon district, Elko County, Nevada: Mining Congress Journal, v. 68, no.2, p. 28-32.

Kerr, J. W., 1962, Paleozoic sequences and thrust slices of the Seetoya Mountains, Independence Range, Elko County, Nevada: Geological Society of America Bulletin 73, no. 4, p. 439-460.

Langenheim, R. L., Jr., and Larsen, E. R., 1973, Correlation of Great Basin stratigraphic units: Nevada Bureau of Mines and Geology Bulletin 72, 36 p.

Lawrence, E. F., 1963, Antimony deposits of Nevada: Nevada Bureau of Mines Bulletin, v. 61, 248 p.

Matti, J. C., and McKee, E. H., 1977, Silurian and lower Devonian Paleogeography of the outer continental shelf of the Cordilleran miogeocline, central Nevada, in Stewart, J. H., Stevens, C. H., and Fritsche, A. E., eds., Paleozoic paleogeography in western United States: Pacific Coast Paleogeography Symposium 1: Los Angeles, Society of Economic Paleontologists and Mineralogists, Pacific Section, p. 181-215.

Matti, J. C., Murphy, M. A., and Finney, S. C., 1975, Silurian and lower Devonian basin and basin-slope limestones, Copenhagen Canyon, Nevada: Geological Society of America Special Paper 159, 48 p.

Merriam, C. W., and Anderson, C. A., 1942, Reconnaissance survey of the Roberts Mountains, Nevada: Geological Society of America Bulletin, v. 53, no. 12, pt. 1, p. 1675-1727.

Merriam, C. W., and McKee, E. H., 1976, The Roberts Mountains Formation, a regional stratigraphic study with emphasis in rugose coral distribution, with a section on Conodonts, by J. W. Huddle: U.S. Geological Survey Professional Paper 973, 51 p.

Mullens, T. E., and Poole, F. G., 1972, Quartz-sand-bearing zone and early Silurian age of upper part of the Hanson Creek Formation in Eureka County Nevada, in Geological Survey research, 1972: U.S. Geological Survey Professional Paper 800-B, p. B21-B24.

Radtke, A. S., Rye, R. O., and Dickson, F. W., 1980, Geology and stable isotope studies of the Carlin gold deposit, Nevada: Economic Geology, v. 75, no. 5, p. 641-672.

Stewart, J. H., 1980, Regional tilt patterns of late Cenozoic basin-range fault blocks, western United States: Geological Society of America Bulletin, pt. 1, v. 91, no. 8, p. 1460-1464.

Discussion of the Disseminated-Gold-Ore-Occurrence Model

By Edwin W. Tooker

CONTENTS

INTRODUCTION

The ultimate objective of the 1982 workshop was, if possible, to develop an ore-occurrence model for the disseminated-gold-deposit type. Such a model should assure a common vocabulary and body of factual data that define the common classifiable deposit characteristics and lead to the systematic identification of favorable geologic environments of deposition. Several ore-occurrence models for other types of deposits at various qualitative and quantitative levels have been created to organize data systematically for meeting special-purpose needs (Erickson, 1982; Cox, 1983a, b), but the seeming diversity between sediment- and volcanic-hosted disseminated gold occurrences appeared, at the outset, to pose difficulties in arriving at a simple model. Options for framing a model were considered first, and the elements composing one followed.

Recently, two types of occurrence models have been developed, each of which provides an example of model technology. A genetic-geologic uranium model, for example, encompasses the widely ranging igneous, sedimentary, and metamorphic environments in which uranium forms (Finch and others, 1980). The environment and processes of formation of deposits thought to have a common origin are considered in a time-process sequence. The matrix is intended to consider every event, condition, and process that influenced mineralization, and thus aid in evaluation of the resources. As an example of the second type of model, the computer program "Prospector" (Duda, 1980) was designed for the identification or recognition of specific types of deposits (for example, porphyry copper, massive sulfide) and links field and laboratory observable or inferred evidence with an inference network of plausible rules based on probabilistic reasoning. Such a model provides a systematic methodology for creating a useful resource model and may assist in evaluating geologic terranes and the discovery of unrecognized resources.

The consensus of the workshop was that a definitive or quantitative model, such as those described above, may be premature for disseminated gold deposits; however, documentation of the geologic attributes as well as of existing gaps in data is an important first step in establishing the status of knowledge.

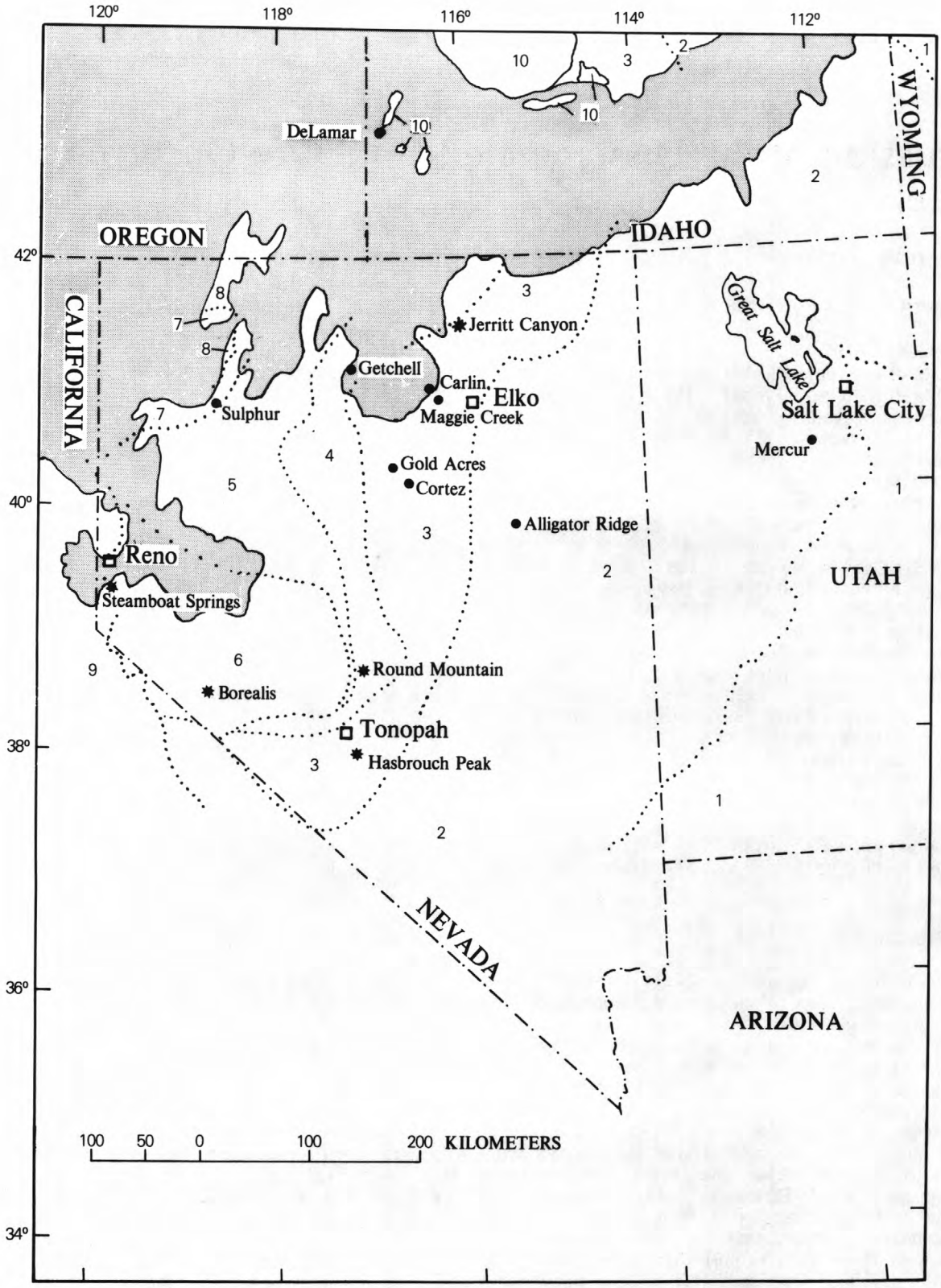

Figure 64. Nevada and adjacent parts of neighboring States, showing geologic host terranes and locations of deposits visited or observed (stars), or listed in checklist (dots). Shading, postaccretionary volcanic cover; dotted line, terrane boundary. Terranes shown (after Silberling and others, 1984) include: (1) cratons, (2) miogeoclinal cratonal shelf, (3) Roberts Mountains, (4) Golconda, (5) Mesozoic overlap, (6) Walker Lane, (7) Jackson, (8) Black Rocks, (9) Sierra Nevada batholith, and (10) Idaho batholith.

CHECKLISTS OF THE REGIONAL, DISTRICT, AND DEPOSIT ATTRIBUTES OF DISSEMINATED GOLD OCCURRENCES

The workshop participants collaborated in organizing the current level of understanding about disseminated gold deposits in the following series of checklists of regional, district, and deposit attributes, based on examples of current models. These checklists represent a diverse group of disseminated deposits that include examples of the sediment-, volcanic-, and hot-spring-hosted types shown in figure 64. The size of a deposit is reported in short tons and troy ounces, and ore grades in troy ounces of gold per short ton; S.I. equivalents are given in parentheses.

ATTRIBUTES OF DISSEMINATED GOLD DEPOSITS

Table 8, which summarizes the deposit checklists, provides evidence of an emerging systematic, though at present qualitative, characterization of the commonly shared regional, district, and deposit features of some typical disseminated gold occurrences. However, all the returns are not yet in; not all the variations in the types of deposits are known, and new such deposits in different geologic terranes continue to be discovered.

Regional features

Most of the disseminated gold deposits considered in this volume are concentrated in central and western Nevada, in a complex geologic region already well known for its lode, vein-and-replacement, dispersed (subvolcanic porphyry), skarn, bonanza, and placer gold deposits. This region is made up of several geologic terranes whose distinct stratigraphic and structural compositions and, in some cases, diverse geographic points of origin are believed to be evidence for their accretion to the North American craton, beginning in the middle Paleozoic and continuing through the Mesozoic. Oceanic island arcs, scraps of oceanic basins with ophiolitic basement, and fragments of continental margins, some with Precambrian basement (Jones and others, 1982; Jones, 1983), are thought to have been attached successively to the craton, which is composed of continental crustal material. The Roberts Mountains and Golconda terranes (fig. 64) are composed of an oceanic-basin sequence of sedimentary layers that are believed to have been thrust over the miogeoclinal platform shelf of the North American craton; other adjoining oceanic and continental terranes, some of which were apparently derived from other parts of the Pacific Basin, were rafted into place and also welded to the expanding continental margin. On the basis of isotopic data on intrusive rocks, Kistler and Peterman (1978) concluded that continental Precambrian crust underlies a large part of the thrusted, oceanically derived crustal terranes as far west as central Nevada.

This broad zone of accreted terranes in Nevada is also the locus of extensive volcanism and intrusion of magmatic materials, hydrothermal alteration, and, locally, the occurrence of late thermal activity in hot springs (Silberman and others, 1976). A direct genetic or only casual relation between disseminated gold deposits and discrete igneous formations remains unclear. Some, but not all, of the sediment-hosted deposits in the checklists are demonstratably associated with igneous rocks; a more obvious genetic and age association may be verified or assumed in the case of the volcanic-hosted deposits (Silberman, this volume; White, this volume).

Locally, at least, the sedimentary and volcanogenic rocks in these terranes and in the underlying craton contain and are, therefore, potential sources of gold and associated metals that are concentrated in the disseminated deposits (Dickson and others, 1979; Rytuba and Glanzman, 1979; Rye, this volume). This observation leads to the conclusion that circulating hot-water systems, a large part of which is meteoric water (White, 1981), are important factors necessary for gold concentration and deposition, and that volcanism provided a source of the heat and at least some of the structures that facilitated transport. The host rocks in the productive terranes include carbonaceous limestone, siltstone, shale, quartz-rich clastic sedimentary rocks, and andesitic to rhyolitic volcanic and volcaniclastic rocks whose original and (or) altered compositions and resulting permeability provided favorable sites for the precipitation of disseminated gold. In Nevada, at least, these sedimentary rocks may be of either oceanic or miogeoclinal origin.

Elsewhere in the region, however, comparable rocks are not known to be sites for gold deposition. Similarly, gold is not associated with all the volcanically derived hydrothermal systems in the region. Table 8, nevertheless, shows a marked similarity of deposit attributes in the known sediment- and volcanic-hosted gold deposits. This similarity leads to the conclusion that disseminated deposits share some common process attributes. Volcanic caldera and other fault and breccia structures, as well as permeable volcaniclastic and sedimentary rocks near the surface, may make their primary contribution to ore deposition as channelways and depositional traps, utilized by rising hydrothermal solutions in the low (epithermal)-temperature range derived from late stages of volcanism and plutonism. This process may be fueled by more deeply buried intrusive sources of heat that have leached gold from crustal rocks, as well as trace amounts of gold that may occur in near-surface sediment. Silberman (this volume) describes evidence of more than one period of activity.

If we speculate that the broad similarity of disseminated deposits investigated precludes attributing a local origin for the main source of gold from one or more of the great variety of upper-crustal near-surface sedimentary and igneous host rocks in tectonostratigraphic terranes in the region, can a deeper buried source be justified? Exposed cratonal rocks in northern Arizona are known to contain gold-bearing quartz veins of Proterozoic age in metamorphosed basement rocks, followed by Late Cretaceous veins associated with intrusion of two-mica monzogranite and, finally, disseminated visible gold associated with a late-magmatic altered pipelike bodies of syenite (Theodore and others, 1982). A belt of Phanerozoic muscovite-bearing, generally small plutons that trends north-south through Nevada along the inferred edge of the Precambrian crust corresponds to areas of deformation

Alligator Ridge, Nevada

[Data from J. J. Rytuba. n.d., no data available]

A. Name/location	Alligator Ridge mine, secs. 14, 23, T. 22 N., R. 57 E., White Pine County, Nev.
B. Deposit type	Carbonate-hosted disseminated deposit.
C. Other examples	Carlin, Cortez, Jerritt Canyon, Nev.
D. Regional attributes	
1. Presence of gold	New district.
2. Terrane	Miogeosynclinal facies.
3. Basement	Not exposed.
4. Igneous association	No intrusive igneous rocks.
5. Structural regime	Normal faults, northeast-trending, related to Basin and Range extension.
6. Level of erosion	At surface and shallow depth.
E. District attributes	
1. Host rocks	Siltstone of the Pilot Shale.
2. Traps	Faulted, fractured, and brecciated siltstone above massive limestone.
3. Preparation	Jasperoid breccia development at contact of the Pilot Shale and the Devils Gate Limestone. Silicification, oxidation, carbon removal.
4. Size	Five ore bodies over a strike length of about 1-1/2 km; no past production.
5. Extensions	Adjacent ore bodies likely.
F. Deposit attributes	
1. Host rocks	Thin-bedded platy carbonaceous lower member of the Pilot Shale.
2. Size/shape	90 to 120 by 120 to 180 m; 5 million ton at 0.11 oz Au/t (4.5 million t at 3.8 g Au/t); no past production.
3. Physical characteristics	
a. Ore/gangue mineralogy	Ore: free gold (micron size), unoxidized ore, and unknown species in carbonaceous ore. Gange: pyrite, carbon, quartz, minor barite.
b. Structures	Disseminations in permeable reactive host rock.
c. Textures	Fine grained; open fractures and breccias coated with quartz.
d. Host-rock type/age	Siltstone (Mississippian); unknown.
e. Paragenesis	n.d.
4. Chemical characteristics	
a. Solution chemistry	
(1) Inclusions	n.d.
(2) Stability	n.d.
(3) Solubility	n.d.
(4) Isotopes	n.d.
(5) Cause of deposition	n.d.
b. Temperature	n.d.
c. Associated anomalies	As, Hg, Sb, Tl.
d. Alteration/zonation	Carbon removal, limonite staining.
e. Oxidized or carbonaceous materials.	Carbonaceous and oxidized ore.
f. Chemical evolution	n.d.
5. Source of elements	n.d.
6. Geophysical signatures	
a. Gravity	n.d.
b. Magnetic	n.d.
c. Induced polarization	n.d.
d. Seismic	n.d.
e. Radiometric	n.d.
7. Summary of apparent depositional environment.	Deposition in faulted-fractured siltstone above jasperoid breccia developed at contact with underlying massive limestone. Ore in both carbonaceous and oxidized strata.
8. Byproduct metals	Hg.
G. Summary, features for resource evaluation.	Low-grade As, Au, Hg, Sb anomalies adjacent to and above jasperoid breccia developed at contact with carbonaceous siltstone and massive limestone. No mineralization previously recognized in this area.

Borealis, Nevada

[Data from H. F. Bonham, Jr., Nevada Bureau of Mines and Geology. n.d., no data available]

A. Name/location	Borealis district, 19 km south of Hawthorne, Nev.
B. Deposit type	Volcanic-hosted disseminated gold.
C. Other examples	Iwato, Kasuga, and Akeshi, Japan; Pueblo Viejo, Dominican Republic; Baguio district, Lepanto, Phillipines; Masonic district, Nev.
D. Regional attributes	
1. Presence of gold	Known gold province, along with Bodie, Aurora, and Masonic districts, Nev. Veins and stockworks.
2. Terrane	Continental margin, mobile-belt volcanic rocks.
3. Basement	Mesozoic plutonic and metamorphic rocks; possible accreted late Paleozoic volcanic-arc terrane.
4. Igneous association	Andesitic composite volcano. Rhyolite flow-domes.
5. Structural regime	Subduction-related volcanoes in arc setting.
6. Level of erosion	Favorable.
E. District attributes	
1. Host rocks	Volcanic flows and volcaniclastic rock-types.
2. Traps	Favorable stratigraphy (see D1 above).
3. Preparation	Hydrothermal alteration widespread.
4. Size	Previous minor production of gold.
5. Extensions	Excellent.
F. Deposit attributes	
1. Host rocks	Subaerial andesitic volcanic rocks, flow-banded rhyolites and volcaniclastics rocks and flows.
2. Size/shape	Deposit is in quartz-sulfide breccia, irregular; 2 million tons at 0.08 oz Au/ton (1.8 million t at 2.5 g Au/t), which is 160,000 oz Au (4.5 million g Au).
3. Physical characteristics	
a. Ore/gangue mineralogy	Pyrite, sphalerite, minor bravoite and cobaltite. Geochemically anomalous Ag, As, Au, Hg, and Sb. Hg decreases with depth, whereas Zn increases.
b. Structures	Silicified hydrothermal breccias cutting volcaniclastic rocks and flows.
c. Textures	Silicified breccias with multiple periods of brecciation and silicification. Late period of boiling resulted in acid-leached zone (sponge rock of local usage).
d. Host-rock type/age	Miocene andesite and associated volcaniclastic rocks. Mineralization age, 5 m.y.(?).
e. Paragenesis	Several stages of silicification and brecciation, with associated precious and base-metal mineralization. During late stage, lowering of water table combined with boiling resulted in formation of acid-leached rock in upper part of ore zone.
4. Chemical characteristics	
a. Solution chemistry	
(1) Inclusions	n.d.
(2) Stability	n.d.
(3) Solubility	n.d.
(4) Isotopes	n.d.
(5) Cause of deposition	Probably, boiling and oxidation of bisulfide species.
b. Temperature	Silicate and sulfide mineralogy are temperature indicators. Available data not diagnostic at this time; probably 120°C.
c. Associated anomalies	Anomalous Ag, Au, and Hg.
d. Alteration/zonation	Wallrock alteration: Silicification, argillization, acid leaching with alunite, and alteration in deeper levels; adjacent to deposit is advanced argillic alteration with pyrophyllite, diaspore, and quartz-alunite ledges.
e. Oxidized or carbonaceous materials.	Late-stage hematite and barite indicate increase of f_{O_2} in hydrothermal system. No carbonaceous material.
f. Chemical evolution	Early quartz-sulfide deposition, late-stage oxidizing environment.
5. Source of elements	Not known. Two main possibilities are (1) magmatic and (2) leaching of andesitic pile by convecting meteoric waters.

6. Geophysical signatures	
a. Gravity	n.d.
b. Magnetic	n.d.
c. Induced polarization	n.d.
d. Seismic	n.d.
e. Radiometric	n.d.
7. Summary of apparent depositional environment.	High-level system associated with low-pH hydrothermal solutions (Huang and Strachan, 1981). Argillic and advanced argillic alteration. No evidence of former paleosurface or true sinter, and so not a hot-spring deposit. Ore is in quartz-sulfide breccias, in part oxidized by late-stage hypogene solutions. Has many similarities to other gold deposits associated with advanced argillic alteration--for example, Goldfield, El Indio, and Lepanto--but apparenty lacks typical enargite-luzonite-tennantite assemblages that are characteristic of this group of deposits, although these minerals may be present elsewhere within the district. The Borealis deposit also appears to contain only minor amounts of high-grade (more than 1 oz Au/t (34.3 g Au/t)) ore, whereas Goldfield-type deposits typically contain significant zones of very high-grade Au mineralization. The top of the Borealis deposit probably formed within 100 m of the paleosurface at temperatures of about 200°C. There apparently was a high temperature gradient with depth (pyrophyllite-diaspore assemblage), and the solutions were low pH. The gold was transported as a bisulfide complex and precipitated by boiling and bisulfide oxidation. Late-stage solutions were oxidizing and formed hematite and barite and partially oxidized previously deposited sulfides. The deposit occurs in flow-banded rhyolite domes and marginal breccias and in andesitic volcanic rocks and associated volcaniclastic rocks. High-angle faults were the primary solution channelways. Stockwork mineralization may occur at depth, and a significant increase in base metals at depth is to be expected. Silicified hydrothermal breccias elsewhere in the district may well contain significant Au mineralization in association with enargite-group minerals. The occurrence of a granodiorite porphyry intrusion at depth is indicated. The deposit setting is that of an eroded composite volcano.
8. Byproduct metals	Ag, possibly Cu, elsewhere in the district.
G. Summary, features for resource evaluation.	Faulted and extensively altered volcanic rocks, similar to those in known gold deposits in region geochemical anomalies.

Carlin, Nevada

[Data from C. E. Ekburg, Carlin Gold Mining Co., with additions from W. C. Bagby. n.d., no data available]

A. Name/location	Carlin gold mine, approximately 32 km north of Carlin, Nev.
B. Deposit type	Carbonate-hosted, hydrothermal, disseminated.
C. Other examples	Cortez, northern Nevada; Bell, northern Nevada.
D. Regional attributes	
1. Presence of gold	Carlin is located on a northwestward trend shared by several other loci of gold mineralization. Gold is generally submicroscopic, however, the oldest known occurrences contain coarse ($\leq$0.5 mm) gold. The gold mineralization at Carlin is accompanied by antimony, mercury, and arsenic.
2. Terrane	Sedimentary host rocks of miogeosynclinal origin.
3. Basement	Cambrian sedimentary rocks are exposed, but basement rocks do not crop out.
4. Igneous association	Premineral intrusive dikes of acidic composition. Dikes are indiscriminately mineralized.
5. Structural regime	Carlin is located along a northwest-trending lineament of probable crustal origin in the Antler orogenic belt and below the Roberts Mountains thrust.
6. Level of erosion	No apparent significant supergene enrichment.

E. District attributes

1. Host rocks	Porous, permeable sedimentary rocks.
2. Traps	Favorable stratigraphic horizon, with unaltered massive limestone unit lying stratigraphically above.
3. Preparation	Carbonate removal, addition of clay minerals and silica.
4. Size	Five mines, all gold.
5. Extensions	n.d.

F. Deposit attributes

1. Host rocks	Gold mineralization is in top 90 m of the Roberts Mountains Formation (stratiform).
2. Size/shape	Strike of 1675 m on a N. 45 E. trend dipping 30^{o}-40^{o} NW. As of 1977, 3 million oz Au (93 million g Au) produced from 9.4 million tons (8.5 million t) milled.
3. Physical characteristics	
a. Ore/gangue mineralogy.	Oxidized gold ore major minerals: clay, silica, quartz (detrital); minor minerals: oxides, some exotic sulfates. Carbon gold ore major minerals: clay, silica, quartz (detrital); minor minerals: carbon, pyrite, realgar, cinnabar, other minor sulfides.
b. Structures	Replacement and dissemination.
c. Textures	Acid leaching(?).
d. Host-rock type/age	Silurian and Devonian Roberts Mountains Formation. Mineralization is Tertiary.
e. Paragenesis	Radtke (1981) indicated early introduction of silica, pyrite, illite, and sericite, followed by Au associated with Hg, As, Sb, and Tl minerals. Early stage of silicification was preceded and (or) accompanied by removal of dolomite and calcite. Minor Pb, Zn, and Cu sulfides were introduced slightly later than the Au. Late acid-leaching oxidation included carbonate, sulfide, and organic-carbon removal, introduction of barite and quartz veins and anhydrite, and kaolinite alteration.
4. Chemical characteristics	
a. Solution chemistry	
(1) Inclusions	Type I: 0.0-17 weight percent NaCl equivalent, 152^{o}-338^{o}C; type II: less than 1 weight percent NaCl equivalent, 198^{o}->350^{o}C; type III: rarely containing liquid CO_2. Radtke (1981) indicated that the solutions evolved from low-temperature (175^{o}-200^{o}C) nonboiling solutions during main-stage activity to high-temperature (200^{o}-300^{o}C) boiling during the acid-leaching stage.
(2) Stability	Experimental work on the stabilities of pyrite, cinnabar, mercury, orpiment, realgar, and gold suggests that the solutions were low temperature (150^{o}-200^{o}C) and that total sulfide was low (0.001-0.0001 m) (Rytuba, this volume).
(3) Solubility	Rytuba (this volume) suggests that gold solubility was controlled by sulfide complexing under low temperature, low ionic strength, low total sulfide, and low f_{O_2} and f_{S_2}.
(4) Isotopes	δD=-153 to -139 permil; stage I, $\delta^{18}O$=-6 to +3 permil; stage II, $\delta^{18}O$=+3 to +6 permil; stage III, $\delta^{18}O$=+6 to +10 permil; stage IV, $\delta^{18}O$=-15 to -10 permil. Rye (this volume) noted that the fluid isotopes indicate meteoric-dominated water and that substantial exchange with carbonate or igneous rocks occurred in a low water-rock system.
(5) Cause of deposition	Radtke (1981) suggested that a combination of factors, including changes in ionic strength and pH due to boiling, and supersaturation due to temperature decrease, caused deposition of sulfide and sulfosalt minerals. Deposition of gold was presumably controlled by these same processes.
b. Temperature	200^{o}-400^{o}C (?)
c. Associated anomalies	As, Hg, Sb, Tl.
d. Alteration/zonation	Carbonate removal, clay introduction, silica introduction.
e. Oxidized or carbonaceous materials.	The Roberts Mountains Formation contains trace amounts of syngenetic carbon. In altered parts of the Roberts Mountains Formation, carbonaceous material has been remobilized, and additional carbon introduced. A small proportion of the gold was precipitated on carbon particles.

f. Chemical evolution -----	See 4a(1) above.
5. Source of elements --------	Leached from deep-seated intrusive(?) and (or) surrounding sedimentary rocks.
6. Geophysical signatures	
a. Gravity ----------	n.d.
b. Magnetic ----------	The Lynn window (locus of the Roberts Mountains Formation) is situated at a magnetic "high".
c. Induced polarization ---	n.d.
d. Seismic ----------	n.d.
e. Radiometric ----------	n.d.
7. Summary of apparent depositional environment.	Low-pressure low-temperature near-surface deposition.
8. Byproduct metals ----------	Hg.
G. Summary, features for resource evaluation.	Anomalously high geochemical values for As, Au, Hg, Sb, and Tl in a carbonate sedimentary sequence that contains silicification and argillization as the major alteration types.

Cortez, Nevada

[Data from J. J. Rytuba. n.d., no data available]

A. Name/location ----------	Cortez. T. 27 N., R. 47, 48 E., Lander County, Nev.
B. Deposit type ----------	Carbonate-hosted, disseminated.
C. Other examples ----------	Horse Canyon and Gold Acres, Nev.
D. Regional attributes	
1. Presence of gold ----------	Ag-Au district.
2. Terrane ----------	Tectonostratigraphic accreted oceanic crust over miogeoclinal shelf of craton.
3. Basement ----------	Concealed.
4. Igneous association -------	Several felsic dikes of biotite-quartz-sanidine porphyry of age and composition to those of the Caetano Tuff.
5. Structural regime ---------	North-northwest-striking normal faults.
6. Level of erosion ----------	Apparently near-surface, as evidenced by open breccia and vein.
E. District attributes	
1. Host rocks ----------	Finely laminated carbonaceous siltstone beds of the Roberts Mountains Formation.
2. Traps ----------	Ore bodies follow general strike and dip of dikes.
3. Preparation ----------	Silicification; brecciation and fracturing, formation of jasperiod.
4. Size ----------	0.8 by 6.4 km. Cortez main production: 4.5 million oz Ag, 24,000 oz Au (139.9 million g Ag, 146,000 g Au) and some minor Pb, Cu, and Zn from mantos in the Hamburg dolomite.
5. Extensions ----------	New discovery in district being put into production at Horse Canyon, which holds 3.4 million ton (3.08 million t) of ore containing .05 oz Au/t (1.9 g Au/t).
F. Deposit attributes	
1. Host rocks ----------	Deposit occurs in thin bedded siltstone of the Roberts Mountains Formation (Wells and others, 1969).
2. Size/shape ----------	3.4 million st of ore containing 0.29 oz Au/t (3.1 million mt at 9 g Au/t) in irregular to tabular ore bodies striking north-northwest and dipping 30°-40° SW.
3. Physical characteristics	
a. Ore/gangue mineralogy --	Native gold, pyrite, Au-, As-, Sb-, and Hg-bearing pyrite and gangue minerals of quartz, calcite, and very minor barite.
b. Structures ----------	Disseminated and fracture controlled. Some minor quartz-gold veins.
c. Textures ----------	Fine-grained, locally open breccias and fractures.
d. Host-rock type/age -----	Silurian and Devonian Roberts Mountains Formation and 34-m.y.-old felsic dikes.
e. Paragenesis ----------	n.d.

4. Chemical characteristics	
a. Solution chemistry	
(1) Inclusions	n.d.
(2) Stability	n.d.
(3) Solubility	n.d.
(4) Isotopes	n.d.
(5) Cause of deposition	n.d.
b. Temperature	175°-200°C from fluid inclusions (Rye, this volume).
c. Associated anomalies	As, Sb, Hg, W, Tl.
d. Alteration/zonation	Silicification, carbon oxidation, argillization of felsic dikes to montmorillonite.
e. Oxidized or carbonaceous materials.	Both carbonaceous and oxidized ore present.
f. Chemical evolution	n.d.
5. Source of elements	n.d.
6. Geophysical signatures	
a. Gravity	n.d.
b. Magnetic	n.d.
c. Induced polarization	n.d.
d. Seismic	n.d.
e. Radiometric	n.d.
7. Summary of apparent depositional environment.	Deposition in faulted and fractured silty limestone adjacent to felsic dikes. Ore solutions rose along contact of felsic dikes and laterally spread out into the carbonate rocks. Silicification was accompanied by gold and pyrite deposition, along with trace amounts of As, Sb, Hg, Tl, and W
8. Byproduct metals	Ag.
G. Summary, features for resource evaluation.	Low-grade geochemical anomalies of As, Au, Hg, Sb, and W in and adjacent to jasperoid replacement bodies in carbonate rocks.

DeLamar, Idaho

[Data from W. C. Bagby. n.d., no data available]

A. Name/location	DeLamar silver mine, Owyhee Mountains, southwestern Idaho.
B. Deposit type	Volcanic-hosted disseminated silver/gold.
C. Other examples	Waterloo(?), Calif.; Rochester(?), Nev.
D. Regional attributes	
1. Presence of gold	The region is known for placer gold discovered in 1863, and for silver and gold production from veins in the Silver City area until 1914.
2. Terrane	Cretaceous-Paleocene plutonic terrane overlain by Miocene volcanic rocks. Would be considered an inner continental margin.
3. Basement	Outliers of the Idaho batholith, with small roof pendants of metasedimentary rock.
4. Igneous association	Granodiorite of the Idaho batholith and alkali olivine basalt and rhyolite of the Owyhee volcanic field. The volcanic field is marginal to the Snake River rift.
5. Structural regime	The basement rocks are associated with Mesozoic subduction. The volcanic rocks are associated with later rifting possibly associated with Basin and Range development. The regional structure is dominated by N. 10°-20° W.-trending oblique-slip normal faults.
6. Level of erosion	Erosion is considerable but varies regionally. Epithermal veins in the region indicate that erosion has not yet stripped away those deposits.

E. District attributes

1. Host rocks	Rhyolitic flows, tuff, breccia, and volcaniclastic sediment; basalts.
2. Traps	Brittle rhyolite, zones of intense faulting in plutonic rocks.
3. Preparation	Faulting and widespread alteration(?).
4. Size	The district includes DeLamar and Silver City. Between 1888 and 1914, estimated production was 400,000 oz Au (12.4 million g Au) and 6 million oz Ag (187 million g Ag) from 800,000 tons (725,000 t) of ore (Panze, 1975).
5. Extensions	Excellent

F. Deposit attributes

1. Host rocks	Rhyolitic domes, lavas, and pyroclastic deposits
2. Size/shape	Published reserves (Rogers and others, 1980) are 10 million tons at 3.5 oz Ag ton and 0.025 oz Au/ton (9 million t at 120 g Au/t and 3.737 g Ag/t). The deposit is irregular, and its shape is controlled in part by structure as well as by the geomorphology of the rhyolitic domes.
3. Physical characteristics	
a. Ore/gangue mineralogy	Naumannite (Ag_2Se), argentite, native gold, marcasite, pyrite (colloform variety, malnikovite), and trace amounts of chalcopyrite and galena are primary ore minerals. Secondary mineralogy includes native silver, jarosite, argentojarosite, cerargerite, goethite, hematite, and lepidocrocite. Gangue mineralogy is predominantly silica as quartz and chalcedony.
b. Structures	Mineralization is essentially confined to stockwork veinlets. Silicified rhyolite porphyries also carry ore.
c. Textures	Argentite occurs as coarse grains, as large as 2 mm in diameter. Naumannite occurs as replacement rinds on argentite and as growths on top of quartz. Gold occurs as anhedral blobs in quartz and is associated with naumannite either in fractures, absorbed on the surface, locked in naumannite, or in solid solution.
d. Host-rock type/age	Rhyolite is dated by K-Ar methods at 15.6 to 15.7±0.3 m.y. Panze (1975) considered volcanism and mineralization contemporaneous.
e. Paragenesis	Early hydrothermal mineralization was quartz and sericite, followed by pyrite (colloform variety, malnikovite) on quartz. Marcasite followed pyrite and was less abundant; it occurs as a crust on malnikovite and as small laths in quartz. Exact paragenesis of the chalcopyrite is uncertain, although it is commonly locked in and is replaced by naumannite. Argentite was after marcasite and was followed by naumannite. Gold partly overlaps naumannite deposition in time.
4. Chemical characteristics	
a. Solution chemistry	
(1) Inclusions	n.d.
(2) Stability	n.d.
(3) Solubility	n.d.
(4) Isotopes	n.d.
(5) Cause of deposition	Probable causes include change of temperature with boiling and (or) mixing with ground water. Oxidation may also have been important.
b. Temperature	Mineral assemblage of malnikovite, argentite, and naumannite suggests a range of 133°-200°C. Early pyrite with quartz may have been in the range 200°-300°C.
c. Associated anomalies	Anomalously high Ag, Au, Hg, and Se. Hg delineates ore bodies best.
d. Alteration/zonation	Strong argillic alteration; sericite, kaolinite, Na-montmorillonite, illite, and pyrite. Pyrophyllite is reported as fracture coatings but is rare. Intense silicification.
e. Oxidized or carbonaceous materials.	No carbonaceous material.
f. Chemical evolution	Early fluids were rich in silica and iron, and later evolved to silver- and selenium-rich fluids. At times, pH was low enough to cause strong argillic alteration.

5. Source of elements --------	n.d.
6. Geophysical signatures	
a. Gravity ----------	n.d.
b. Magnetic ----------	n.d.
c. Induced polarization ---	n.d.
d. Seismic ----------	n.d.
e. Radiometric ----------	n.d.
7. Summary of apparent depositional environment.	Early intrusion/extrusion of rhyolitic lavas along major normal faults. Zones of intrusion served later as conduits for a high-level (quite possibly hot spring) hydrothermal system. Fluids rose along fractures in the volcanic rocks and deposited minerals in the conduits, as well as beneath clay zones that capped the system locally. The presence of chalcedonic sinters suggests that the hydrothermal system vented.
8. Byproduct metals ----------	Only gold and silver produced.
G. Summary, features for resource evaluation.	Faulted Tertiary rhyolite dome field. The rhyolite is altered, and chalcedonic sinters are present. Mercury anomalies of 0.2 to more than 1 ppm over ore bodies.

Getchell, Nevada

[Data from B. R. Berger. n.d., no data available]

A. Name/location ----------	Getchell Mine, Humboldt County, Nev.
B. Deposit type ----------	Carbonate-hosted disseminated gold deposit.
C. Other examples ----------	Carlin Mine, Nev.; Cortez Mine, Nev.; Mercur Mine, Utah; Ermont Mine, Mont.
D. Regional attributes	
1. Presence of gold ----------	Other precious-metal districts and types of deposits in the region: Dutch Flat, Hot Springs Range--placers, gold-quartz veins; Midas--Au quartz veins, breccia pipes; Adelaide--quartz fissure veins, placers; Iron Point (including Preble)--disseminated, quartz veins. Other deposits in the Potosi (Getchell) mining district: Ogee-Pinson--disseminated; Pinson--disseminated; Section 9--disseminated; Richmond--Ag-Au veins and skarn. Zoned district and regional anomalies: No specific zoning in space recognized; age relationships suggest early porphyry-type and skarn mineralization, with Mo+W+Cu, some Ag+Au+base metal quartz veins, then disseminated Au. Regional geochemical anomalies for As, Au, Hg, Mo, Sb, W. The Osgood Mountain stock is anomalous in Au.
2. Terrane ----------	Transitional-facies carbonate rocks, black shale, greenstone, chert, and quartzite. Considered to be the edge of the continent, with distal-facies carbonate turbidites into troughs or basins with restricted water flow (anoxic) giving way to chert and mafic volcanic rocks over time.
3. Basement ----------	Considered to be continental; not exposed.
4. Igneous association -------	Spatially associated with granodiorite and dacite porphyry dikes intruded along the Getchell fault zone.
5. Structural regime ---------	Major deposits occur along major throughgoing Getchell fault system. Normal fault bounds entire east flank of the Osgood Mountains. The fault is at least as old as the Osgood Mountains stock.
6. Level of erosion ----------	Flanks of range suitable for high-level deposits.

E. District attributes

1. Host rocks	Carbonate-rich parts of sandy to argillaceous limestone-dolomite; thin-bedded, carbonaceous, fractured or broken by high-angle faults (Joralemon, 1951).
2. Traps	Highest grades common along small-scale fold noses, and in repeatedly fractured and silicified zones in limestone (I believe these were main fluid-conduit zones).
3. Preparation	Host rocks prepared by faulting, hydrothermal brecciation, and decarbonization.
4. Size	District is large; the Getchell mine by itself consists of the North Pit, Center Pit, South Pit, and Section 4 Pit over a strike length of about 3-4 km; the Getchell mine produced 4 million ton (3.6 million t) averaging about 0.25 oz Au/ton (8.6 g Au/t) equivalent to 1 million oz Au (31.1 million g Au), with known reserves of >4 million tons (3.6 million t) averaging about 0.20 oz Au/ton (6.8 g Au/t), equivalent to 800,000 oz Au (24.5 million g Au). About 10 to 13 km south of Getchell, the Pinson mine is currently producing >3 million ton (2.7 million t)averaging 0.10-0.15 oz Au/ton (3.4-5.1 g Au/t), equivalent of 300,000-450,000 oz Au (9.3-14.0 million g Au). Gold is the only major product of the gold mines. Other mines are mainly WO_3 skarn, with $10-15 million recorded production, mainly from the Granite Creek, Pacific, Kirby, Riley, Alpine, Richmond, and Tip Top mines.
5. Extensions	Substantial additional reserves at Getchell and Pinson; excellent exploration targets near Getchell.

F. Deposit attributes

1. Host rocks	Replacement of carbonate-bearing parts of the Cambrian Preble and Ordovician Comus Formations where sedimentary rocks are within the Getchell fault zone. Mineralized zones are essentially long narrow sheets along the strike of formations. Mineralization does not trail out to any extent along bedding away from the fault zone.
2. Size/shape	The deposit occurs as sheetlike mineralized zones, elongate along strike and downdip, and narrow. The ore zones may be more than 300 m long and extend downdip at least 300 to 900 m. No bottom has been found to the ore. Thicknesses vary considerably, ranging from 4 to more than 15 m. Grade is erratically distributed, but highest grades near vertical shoots of intense silicification suggest fluid conduits. Highly silicified high-grade zones show multiple brecciation events, intermittently recemented with silica.
3. Physical characteristics	
a. Ore/gangue mineralogy	Ore: Native Au (mostly smaller than 1 μm), native Ag (minor), scheelite (not recovered), orpiment (very abundant), realgar (very abundant), stibnite (common), cinnabar (uncommon), getchellite (rare), galkhaite (very rare). Gangue: Quartz, pyrite, marcasite, arsenopyrite, fluorite, calcite, dolomite, chabazite, ilsemmanite, barite. Alteration: Silicification, illite (mixed layer sericite), kaolinite, calcite, dolomite, nontronite. Quartz and illite are generally very fine grained; some coarse illite after biotite; kaolinite very fine grained, found mostly in argillaceous sedimentary rocks and coarse-grained granodiorite; calcite common, generally coarse grained; nontronite present as fine green masses in silica breccia.

b. Structures ---------- Ore is mainly associated with pyrite and arsenopyrite, secondly with quartz, and only to a minor extent with orpiment and realgar. Gold is truly disseminated and along microfractures in silicified brecciated limestone, with overall configuration of sheets along faults. Isoclinal folds play an important role locally in control of ore shoots; highest grades follow the rake and plunge of fold noses. Hydrothermal breccias are common, generally subtle.

c. Textures ---------- Gold is very fine grained; visible gold is very rare. Evidence for boiling is fine-grained quartz, multiple breccias, and pods of kaolinite.

d. Host-rock type/age ----- Wallrock: Cambrian Preble Formation. Age of mineralization: K-Ar on sericite, 89 m.y.

e. Paragenesis ----------

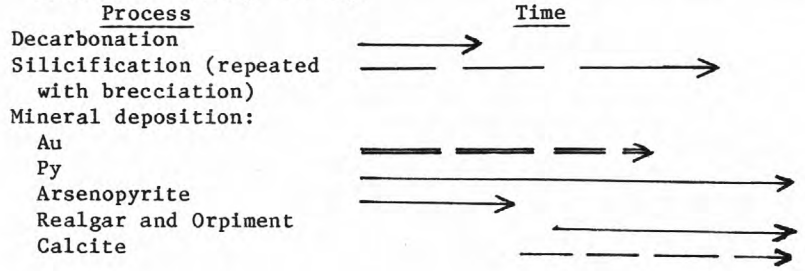

4. Chemical characteristics

a. Solution chemistry

(1) Inclusions --------- n.d.

(2) Stability ---------- n.d.

(3) Solubility --------- n.d.

(4) Isotopes ---------- Some data available for S, more in progress.

(5) Cause of deposition n.d.

b. Temperature ---------- n.d.

c. Associated anomalies --- As, Sb, Hg, Tl, F, some U_3O_8 in carbonaceous material, Mo, W.

d. Alteration/zonation ---- Bio → Chl + illite + py; Plag → Kaol + illite; CO_3 → SiO_2 replacement. No K-feldspar recognized.

e. Oxidized or carbonaceous materials. Carbonaceous material present in host rock, some remobilized during mineralization.

f. Chemical evolution ----- The evolution of this deposit is inferrable from the paragenesis. As the system develops, the carbonate is leached and silica is dumped--considerable silica in the upper parts of the system. The high-level silicification results in the jasperoid bodies, an important ingredient to the overall development of the "productive" aspects of the system.

5. Source of elements -------- n.d.

6. Geophysical signatures

a. Gravity ---------- n.d.

b. Magnetic ---------- Ground magnetics proved useful for mapping structure, aeromagnetics at 0.4-km line spacing outlined the stock and major faults.

c. Induced polarization --- n.d.

d. Seismic ---------- n.d.

e. Radiometric ---------- Aerorad survey was only useful in outlining the general Getchell fault trend but did not specifically delineate any alteration zones.

f. Other ---------- At Getchell, very low frequency electromagnetic (EM) methods were able to trace the main fault structures; tried SP to map out the trace of the Getchell fault (worked, but was slower and less useful than EM).

7. Summary of apparent depositional environment - The Getchell deposits formed along the high-angle Getchell Fault System with the highest gold grades occurring in favorable carbonate horizons in a Paleozoic organic-rich sedimentary sequence. The main hydrothermal conduits form pipe-like zones of intense silicification with repeated episodes of brecciation and accompanying mineralization and resilicification. The grades of gold mineralization decreases laterally away from these apparent centers of hydrothermal activity.

8. Byproduct metals ---------- As, Hg.

Gold Acres, Nevada

[Data from C. T. Wrucke. n.d., no data available]

A. Name/location	Gold Acres, Lander County, Nev. The deposit is on the east flank of the Shoshone Range, 42 km northeast of Battle Mountain. The nearest town is Crescent Valley, about 25 km to the northeast. In 1984 the Gold Acres mine consisted of two nearly connected open pits, one approximately north-northwest of the other. The northern open pit was operated mainly in the 1940's and 1950's but has been mined briefly at other times. The southern pit was opened in the 1970's.
B. Deposit type	The deposit is in siliceous and carbonate sedimentary rocks of accreted terrane.
C. Other examples	The Gold Acres deposit resembles the ore body at Carlin, 80 km to the northeast, in several ways, including the presence of gold in carbonate rocks of the Roberts Mountains Formation and siliceous rocks of Devonian age. However, the Gold Acres deposit differs from the deposit at Carlin and from other disseminated gold deposits in northern Nevada in many details, particularly in its situation in the upper plate of the Roberts Moutains thrust.
D. Regional attributes	
1. Presence of gold	Gold Acres is in a part of north-central Nevada known for numerous disseminated gold deposits that are hosted in Paleozoic sedimentary rocks and are broadly considered as deposits of the Carlin type. Gold Acres is in the central part of that province (Armbrustmacher and Wrucke, 1978).
2. Terrane	Rocks in north-central Nevada in the vicinity of Gold Acres are part of the North American craton. Deposit is in overlying accreted oceanic plate.
3. Basement	A basement of Proterozoic rocks is believed to underlie Gold Acres, but it is nowhere exposed in the Shoshone Range or in the adjacent mountain ranges. Evidence of a Proterozoic basement is based on regional studies by Kistler and Peterman (1978) of strontium isotopes. Paleozoic rocks are widely exposed in the Shoshone Range and consist of an eastern assemblage composed principally of carbonate strata and a western assemblage consisting mainly of siliceous sedimentary rocks and basalt (now greenstone). The eastern assemblage was deposited in the miogeocline that formed along the west margin of North America, whereas the western assemblage was deposited on the ocean floor west of the miogeocline. Exposed eastern-assemblage rocks at Gold Acres are Devonian in age, and they probably overlie Cambrian, Ordovician, and Silurian formations. Western-assemblage rocks in the area are of Cambrian to Devonian age.
4. Igneous association	A granitic pluton underlies the Gold Acres deposit but is nowhere exposed. Biotite from core drilled from the pluton was dated at 98.8±2.0 m.y. (Silberman and McKee, 1971). A few quartz porphyry dikes are exposed at the mine. Sericite from one of these dikes was dated at 94.3±1.9 m.y. (Silberman and McKee, 1971). Other dikes, largely argillized and exposed mainly on the west walls of both open pits, resemble 32-35 m.y.-old intrusive rhyolite exposed at the Cortez mine, 14 km to the southeast, and at Tenabo, 6 km to the northeast. This rhyolite is thought to be correlative with the Caetano Tuff. Preliminary analyses of samples from this dike at Gold Acres indicate the dikes have the same suite of trace elements in about the same range of concentration as the dikes at Cortez and therefore may be Oligocene in age (J. Rytuba and R. J. Madrid, oral commun., 1984).
5. Structural regime	The Roberts Mountains thrust is the dominant structural feature at Gold Acres. Western-assemblage siliceous rocks form the upper plate of the thrust, and eastern-assemblage carbonate rocks form the lower plate.

6. Level of erosion ----------	Depth of burial of the host rocks during Cretaceous mineralization has been estimated at about 610 to 2,400 m, possibly about 1,500 m (Wrucke and Armbrustmacher, 1975), on the basis of the assumed thickness of the upper plate of the Roberts Mountains thrust in the Gold Acres area during Late Cretaceous time and taking into account that erosion reduced the Roberts Mountains allochthon to a thickness of 1,000 m or less near Walti Hot Spring, about 40 km southeast of Gold Acres, by middle Cretaceous time. Independent evidence of the thickness of overburden during mineralization at Gold Acres has not been found. Depth of burial in Oligocene time has not been determined.
E. District attributes	
1. Host rocks ----------	Limestone of the Roberts Mountains Formation of Silurian and Devonian age and of the Wenban Limestone of Devonian age are favored host rocks in the Gold Acres mine, but some of the gold at the mine and all of the gold at Tenabo, a small mineralized area 7 km north-east of Gold Acres, is in chert and argillite of Devonian age.
2. Traps ----------	Intensely fractured rock and fault zones are sites of mineral occurrences at Gold Acres and in areas of gold mineralization in surrounding areas, including Tenabo. The strongest mineralization occurred in the lower part of the Roberts Mountains allochthon at Gold Acres, especially in thrust lenses of carbonate rocks.
3. Preparation ----------	Host rocks at Gold Acres have been metamorphosed by the buried granitic pluton. The metamorphism locally converted argillite, chert, and greenstone to hornfels, and carbonate rock to skarn. The metamorphosed rocks trend northwest and are exposed in an area about 4 km long by about 1 km wide. Sericitic alteration occurred in the Cretaceous igneous rocks. The metamorphic rocks locally have been so kaolinized that the identity of the original rock is almost completely masked.
4. Size ----------	Numerous gold deposits are present on the east side of the Shoshone Range, most with little or no production. The Gold Acres mine has had considerably greater production than all other mines in the area. Gold and silver ores are the only commodities produced for metals in the area.
5. Extensions ----------	Additional mineralized rock may occur at Gold Acres in areas of intensely fractured rocks in the Roberts Mountains allochthon near the buried pluton. The areas are likely to be south and southwest of the Gold Acres mine, but the mineralized ground may be deeply buried. An intriguing possibility at Gold Acres is that the Roberts Mountains Formation may lie beneath exposed Devonian rocks in the lower plate of the Roberts Mountains thrust, and could be mineralized.
F. Deposit attributes	
1. Host rocks ----------	The Gold Acres deposit is in carbonate and siliceous rocks low in the upper plate of the Roberts Mountains thrust at the southwest margin of a window in the thrust sheet.
2. Size/shape ----------	The ore body mined at Gold Acres was tabular and dipped at shallow angles southwest, parallel to the attitude of the Roberts Mountains thrust and of thrust slices above the sole of that thrust. The mine, as developed from 1942 to 1961, was an irregular pit about 450 m in longest dimension and 350 m in maximum width. In the early 1970's, the mine was expanded into a series of open pits extending on a northwestward trend an additional 750 m to the southeast. The Gold Acres mine was one of the largest producers of gold in Nevada during the 1950's. The mine produced gold and silver worth nearly $10 million in the period 1942-61 (Wrucke and Armbrustmacher, 1975), and estimated to have yielded approximately 280,000 oz Au (8.7 million g Au). Production since 1961 has not been reported but probably exceeded the total for the earlier period. Estimates of the gold resources remaining at Gold Acres have not been made.

3. Physical characteristics

a. Ore/gangue mineralogy -- Gold occurs in faults and in iron-oxide-coated fracture surfaces. The highest concentrates of gold were found in zones consisting of iron-oxide-rich clayey gouge. This gouge was found to consist mainly of kaolinite, 1 M muscovite, quartz, and hydrated amorphous iron oxides. Goethite, hematite, jarosite, gypsum, hexahydrite, dolomite, and calcite occur locally. No unoxidized gold ore was found. Zonation of minerals was not discovered, and no data are available on the trace-element chemistry of the minerals.

b. Structures ---------- The faults that contain ore are both low and high angle. Low-angle faults are interpreted as thrust faults within the upper plate of the Roberts Mountains thrust; high-angle faults occur within thrust blocks and more commonly as faults that cut across the thrust plate. Faults that cut thrust sheets may be of Cretaceous age, as some of these faults are occupied by porphyry dikes about 94 m.y. old. A few blocks in waste dumps in the open-pit have open fractures lined with calcite.

c. Textures ---------- The original gold ore has been completely oxidized, and original textures are not preserved. Data on boiling are not available.

d. Host-rock type/age ----- Host rocks for gold consist principally of silty limestone of the Roberts Mountains Formation (Silurian and Devonian), chert, argillite, and greenstone of the Slaven Chert (Devonian), and skarn formed from the Wenban Limestone (Devonian).

e. Paragenesis ---------- Gold and a geochemically associated suite of elements were deposited at Gold Acres after deposition of a base-metal suite of elements, which, in turn, were introduced after molybdenum deposited as molybdenite and tungsten deposited as scheelite. The molybdenite and scheelite, which occur in skarn beneath the gold deposit, are interpreted as having been deposited during a late stage of contact metamorphism. The base-metal suite, consisting of copper, lead, zinc, and other metals (Armbrustmacher and Wrucke, 1978), was deposited in hornfels, skarn, and metagreenstone. Introduction of the base-metal suite took place at a lower temperature than for the molybdenum and tungsten. The molybdenum, tungsten, and base-metal suite mineralization is considered to be Late Cretaceous and probably occurred shortly after sericitization of the quartz porphyry dikes dated, at about 93 m.y. (Silberman and McKee, 1971). Gold formed at relatively low temperatures, probably in the root zone of a thermal-spring system. The gold mineralization once thought to be related to Cretaceous intrusive bodies (Wrucke and Armbrustmacher, 1975), may be related to Oligocene(?) rhyolite dikes.

4. Chemical characteristics

a. Solution chemistry

(1) Inclusions --------- n.d.

(2) Stability ---------- n.d.

(3) Solubility --------- n.d.

(4) Isotopes ---------- n.d.

(5) Cause of deposition n.d.

b. Temperature ---------- Homogenization temperatures were determined from studies of fluid inclusions (J. T. Nash, written commun., 1972). These estimates, corrected for a possible lithostatic overburden of about 1,500 m and assuming 10 percent salinity for the molybdenite and base-metal mineralization and for hydrostatic pressures for the gold mineralization, are $380^{\circ}\pm50^{\circ}C$ for the molybdenite mineralization, 150°–$225^{\circ}C$ and, possibly, 265° for the base-metal mineralization, and 160°–$195^{\circ}C$ for the gold mineralization.

c. Associated anomalies --- The trace-element suite associated with gold mineralization consists of gold, Ag, As, Au, B, and Hg. Distinctive suites of trace elements are associated with the other mineralizing events at Gold Acres (Wrucke and Armbrustmacher, 1975). No gas sniffing was conducted at Gold Acres, and no CO_2/CO ratios were obtained.

d. Alteration/zonation ----	See E3 and F3a above. Some limestone of the Roberts Mountains Formation in the mine has been weakly silicified.
e. Oxidized or carbonaceous materials.	The gold ore zone is strongly oxidized at Gold Acres (see F3a above). Carbonaceous material occurs in the limestone of the Roberts Mountains Formation. Some thrust blocks of carbon-rich silty limestone in the mine have had part of the original calcite and dolomite removed and are now coal black. Solution chemistry has not been studied.
f. Chemical evolution -----	n.d.
5. Source of elements --------	The trace-element suite associated with the gold mineralization at Gold Acres is similar to that associated with many low-temperature gold deposits around the world. This observation suggests that the gold may have a source derived from silicic igneous rocks of the kind commonly found at these gold deposits.
6. Geophysical signatures	
a. Gravity ----------	n.d.
b. Magnetic ----------	A magnetic high centered over the Gold Acres area (Philbin and others, 1963; Wrucke and others, 1968) is thought to reflect the granitic pluton that underlies the area.
c. Induced polarization ---	n.d.
d. Seismic ----------	n.d.
e. Radiometric ----------	n.d.
7. Summary of apparent depositional environment.	See F3e.
8. Byproduct metals ----------	Silver was produced from the gold ore at Gold Acres during the period 1942-61. Annual production averaged 9.8 percent Ag and ranged from 5.9 to 13.8 percent Ag.
G. Summary, features for resource evaluation.	The so-called gold suite of trace elements--that is, As, Au, Hg, Sb, W, and, locally, other elements--is the principal geochemical guide to the type of deposit at Gold Acres. This type of deposit can occur in the upper or lower plate of the Roberts Mountains thrust in Nevada and should be looked for in the brecciated and intricately slices lower part of the allochthon.

Hasbrouck Peak, Nevada

[Data from R. P. Ashley. n.d., no data available]

A. Name/location ----------	Hasbrouck deposit, Hasbrouck Mountain, 8 km SSW. of Tonopah, SE1/4 sec. 28 and NE1/4 sec. 33, T. 2 N., R. 42 E., Esmeralda County, Nev.
B. Deposit type ----------	Volcanic-hosted disseminated gold, with hot-spring features in upper parts.
C. Other examples ----------	Round Mountain, Bodie (in part), Hayden Hill(?), McLaughlin(?).
D. Regional attributes	
1. Presence of gold ----------	A northwest-trending belt in western Nevada and eastern California containing many epithermal precious-metal deposits, most associated with volcanic rocks.
2. Terrane ----------	Roberts Mountain allochthon (Paleozoic), foreland(?) of the Golconda thrust belt (Mesozoic), active subduction followed by backarc extension and (or) continental rifting (Tertiary).
3. Basement ----------	Pb and Rb-Sr isotopic data indicate near edge of Precambrian craton (to east). Near east edge of Sierran plutonic belt (plutons in vicinity are Jurassic in age).
4. Igneous association -------	Most rocks are basinal sediment with abundant silicic volcanic component. Silicic plugs nearby, possible small dikes in vicinity of deposit. Sediment includes interbedded hot-spring sinters.

5. Structural regime	Walker Lane structural zone of right-lateral displacement, also coeval basin-and-range extension faulting. Possibly on margin of buried caldera.
6. Level of erosion	Oe zone near and at present surface; much of the ore body is preserved in a topographic high. Sinter preserved near the top of the deposit suggests that present erosional level was close to the paleosurface at time of mineralization.
E. District attributes	
1. Host rocks	Volcanic sediment, including tuffaceous shale and sandstone, coarse tuff and lapilli tuff, and volcanic conglomerate of the Siebert Formation of Bonham and Garside (1979). Age range, 13 to 17 m.y.
2. Traps	Intense alteration (silicification) is localized along relatively coarse permeable beds and along small high-angle faults. Hydrothermal brecciation of the silicified rocks provided space for later-stage gold-bearing quartz, which forms breccia fillings and fracture fillings.
3. Preparation	Hydrothermal alteration (silicification) and hydrothermal brecciation
4. Size	Similar mineralization occurs locally in sedimentary rocks of the Siebert Formation over an area of at least 10 km^2. Past production from this type of mineralization is minor. Spatially closely associated with Ag-Au mineralization of the Tonopah district (mineralization slightly older) and the Divide district (mineralization nearly coeval).
5. Extensions	Only modest additional tonnages are likely to be found around the known ore bodies. There is a fair to good possibility that more ore bodies may exist at greater depths. A much larger area than that presently known may be prospective for new ore bodies.
F. Deposit attributes	
1. Host rocks	Silicified tuffaceous shale and sandstone, coarse tuff, lapilli tuff, and volcanic conglomerate.
2. Size/shape	Horizontal projection of ore body covers area of about 1 km^2. 5 million ton (4.5 million t) at an average grade of 0.1 oz Au/ton (3.4 g Au/t), with a cutoff grade of .04 to .05 oz Au/ton (1.4 to 1.7 g Au/t), which represents about 500,000 oz Au (15.3 million g Au). At this cutoff grade, the ore body has root zones that extend downward from the main ore mass, which is shaped like a thick disc.
3. Physical characteristics	
a. Ore/gangue mineralogy	Ore: Gold with simple sulfide assemblage, mostly pyrite and minor chalcopyrite and argentite. Gangue: Quartz and adularia in veinlets and silicified rock. Silicified rock is replacement quartz with mosaic texture.
b. Structures	Irregular areas representing silica fillings of hydrothermally brecciated parts of silicified masses, as well as representing microfracture-controlled disseminations in silicified masses.
c. Textures	Quartz veinlets filling silicified-rock breccias and fracture fillings are banded, some bands are relatively rich in sulfides and, probably, gold.
d. Host-rock type/age	Volcaniclastic rocks, mainly silicic, including tuffaceous shale and sandstone, coarse tuff and lapilli tuff and volcanic conglomerate, with interbedded sinter. Lapilli tuff is predominant in the mineralized part of the section. Ages of host rocks, mineralization, and nearby silicic plugs are all approximately coeval at 16 m.y.
e. Paragenesis	Quartz-sulfide-gold is always later than quartz-adularia flooding (silicification). Details of paragenesis unknown.

4. Chemical characteristics	
a. Solution chemistry	
(1) Inclusions ---------	n.d.
(2) Stability ----------	Gold deposited with quartz and adularia. Moderate f_{O_2}(?). Relatively low to possibly moderate f_{S_2} and δS. Low SO_4 relative to H_2S.
(3) Solubility ---------	Available data do not provide useful constraints on conditions of ore deposition.
(4) Isotopes ----------	n.d.
(5) Causes of deposition	Boiling a likely possibility, because ore minerals and gangue fill hydrothermal breccias.
b. Temperature ----------	Silicate and sulfide assemblages not definitive for temperature determination. Presence of surface sinter and hydrothermal brecciation suggests relatively low hydrostatic pressure, and temperatures at boiling curve, thus equal to or less than 200°C at 150 m, or a maximum of 230°-240°C in deeper parts of the deposit with some overpressure.
c. Associated anomalies ---	As, Hg, Sb, and low-level W anomalies.
d. Alteration/zonation ----	Ore-grade material confined to silicified zone (quartz+K feldspar±sericite), which is surrounded by successive argillic (quartz+mixed-layer montmorillonite/illite+kaolinite) and propylitic zones. Hot-spring sinters near top of system are still chalcedonic and opaline. K-metasomatism involving addition of K above initial values has probably occurred at least locally. Nearby silver-rich veins are in argillic rocks, but their relations to the main gold mineralization are unclear.
e. Oxidized or carbonaceous materials.	Carbonaceous material not involved in localizing ore minerals or silicification. Any organic material originally present in the altered host-rock sediment is now gone.
f. Chemical evolution -----	Throughout the entire sequence of alteration and ore deposition, fluids were silica-saturated. Metal, sulfide, and total sulfur concentrations presumably increased over time. Gold, pyrite, and other sulfide minerals precipitated with declining temperature and (or) boiling. Repeated boiling may have been important in the concentration process, whereas declining temperature may have been important for ore deposition, but direct evidence from fluid-inclusion and ore-paragenesis studies is unavailable. Some lamellar quartz totally replacing early calcite is present. Because pressures were generally low and the calcite was completely removed, this feature is probably due to retrograde solubility of calcite with decreasing temperature.
5. Source of elements --------	Speculative; no isotopic or trace-element data are available that provide constraints.
6. Geophysical signatures	
a. Gravity ----------	n.d.
b. Magnetic ----------	n.d.
c. IP ----------	n.d.
d. Seismic ----------	n.d.
e. Radiometric ----------	Limited parts of silicified zones may be detectable in radiometric surveys, owing to K content, but present data are inconclusive.
7. Summary of apparent depositional environment.	A continental basin receiving abundant volcanic debris from nearby dominantly rhyolitic eruptions. Conditions ranged from subaerial through fluvial to lacustrine. Repeated intrusions were associated with the rhyolitic volcanism; one or more such intrusions provided the heat that drove the hydrothermal system.
8. Byproduct metals ----------	Ag.
G. Summary, features for resource evaluation.	(1) A volcanic environment, including volcaniclastic rocks and domes but not excluding flows, with permeable units and enough structural disruption to provide conduits (not necessarily major faults). (2) Silicification is essential, and brecciation and veining of silicified rocks--the more complex, the better--are probably essential for ore-grade material. (3) Sinter may not be essential but is favorable because it suggests that a substantial part of the system is likely preserved beneath it. (4) In a regional assessment, argillic alteration may help home in on targets. (5) The best trace-element indicator is gold itself. As, Hg, and Sb may also be useful, especially As.

Jerritt Canyon, Nevada

[Data from R. C. Banghart, D. J. Birak, and W. E. Daly, Freeport Minerals Co. n.d., no data available]

A. Name/location	Jerritt Canyon district (Bell mines), sec. 33, 34, 35, T. 41 N., R. 53 E., Elko County, Nev.
B. Deposit type	Carbonate-hosted disseminated gold.
C. Other examples	Carlin, Cortez, Pinson, Aligator Ridge, and Windfall, Nev.
D. Regional attributes	
1. Presence of gold	A known antimony district, commonly in association with gold.
2. Terrane	Accreted Roberts Mountains tectonostratigraphic oceanic sediment overlies miogeosynclinal (eastern)-facies lower-plate ore host rock seen in windows of thrust plates.
3. Basement	Not exposed.
4. Igneous association	Absence of major intrusive igneous rocks; small felsic stock, scattered dioritic dikes and sills and rhyodacite flow, local travertine hot-spring deposit.
5. Structural regime	Basin-and-range and extensional faults, Roberts Mountain thrust fault.
6. Level of erosion	Deposits now near surface; some may have been eroded.
E. District attributes	
1. Host rocks	Sedimentary limestone, siltstone, and chert of the Hanson Creek (Ordovician and Silurian) and Roberts Mountains Formations (Silurian and Devonian), underlain by the Eureka Quartzite (Ordovician).
2. Traps	Fault intersections, silica capping, thrust fault.
3. Preparation	Hydrothermal alteration (silicification, argillization, oxidation) weathering.
4. Size	260 km^2; two current pits, four minable ore bodies; gold, silver, antimony, and barite present; past production insignificant.
5. Extensions	Good possibilities.
F. Deposit attributes	
1. Host rocks	Banded fine-grained gray black carbonaceous middle limestone unit in the Hanson Creek Formation, and laminated medium-gray calcareous locally carbonaceous siltstone of the Roberts Mountains Formation, overlain by the upper plate of the Roberts Mountains thrust, containing chert, argillite, shale, greenstone and quartzite (Hawkins, 1982).
2. Size/shape	30 by 2,400 m; extremely irregular along faults and bedding; 13.7 million ton containing 0.205 oz Au/ton (12.5 million t at grade of 7.0 g Au/t), which approximates 2.8 million oz Au (87.3 million g Au); no past production.
3. Physical characteristics	
a. Ore/gangue mineralogy	Ore: free gold (max 1-4 m) and unknown mineralogic species in carbonaceous and oxidized types of ore; gangue: includes stibnite, pyrite, carbon, realgar, orpiment, barite, quartz, cinnabar, aragonite, variscite.
b. Structures	Microveins at fault intersection with favorable strata below thrust fault, and disseminations in permeable reactive host rocks.
c. Textures	Fine grained, open vuggy silicification, permeable host.
d. Host-rock type/age	Chert-carbonate-silt sedimentary rocks of Ordovician to Devonian ages.
e. Paragenesis	n.d.
4. Chemical characteristics	
a. Solution chemistry	
(1) Inclusions	n.d.
(2) Stability	n.d.
(3) Solubility	n.d.
(4) Isotopes	n.d.
(5) Cause of deposition	n.d.
b. Temperature	Generally low in ranges of simple sulfides and silicates (clays and jasperoid?) open vuggy silicification suggests shallow, low-temperature environment.

c. Associated anomalies ---	As, Hg, Sb.
d. Alteration/zonation ----	Carbon redistribution, clay mineral formation, limonite staining, calcite in ore zone.
e. Oxidized or carbonaceous materials.	Iron oxides, sulfates, and organic carbon.
f. Chemical evolution -----	n.d.
5. Source of elements --------	n.d.
6. Geophysical signatures	
a. Gravity ----------	n.d.
b. Magnetic ----------	n.d.
c. Induced polarization ---	n.d.
d. Seismic ----------	n.d.
e. Radiometric ----------	n.d.
7. Summary of apparent depositional environment.	Primary rock types formed in deep-water miogeosynclinal environment, giving rise to laminated carbonaceous rock types. Silicified (jasperoid) altered host rock near faults; low-temperature, near-surface mineral assemblage.
8. Byproduct metals ----------	Ag, Hg.
G. Summary, features for resource evaluation.	Located in a gold-bearing region, favorable host rocks, alteration zonation, and geochemical anomalies.

Maggie Creek/Gold Quarry, Nevada

[Data from W. C. Bagby. n.d., no data available]

A. Name/location ----------	Maggie Creek/Gold Quarry, 16 km northwest of Carlin, Nev.
B. Deposit type ----------	Sediment-hosted disseminated gold.
C. Other examples ----------	Carlin, Cortez, and Jerritt Canyon, Nev.
D. Regional attributes	
1. Presence of gold ----------	The deposits occur on the southwest edge of the Carlin window, which is part of the northwest alinement of similar windows, commonly referred to as the Lynn-Pinyon or Carlin belt. Gold is regionally highly anomalous in this belt, and eight known disseminated gold deposits occur within it.
2. Terrane ----------	Both allochthonous and autochthonous rocks of the Antler orogeny occur within the region.
3. Basement ----------	Cambrian sedimentary rocks are the oldest exposed.
4. Igneous association -------	Mesozoic and Tertiary plutons occur along the Lynn-Pinyon belt.
5. Structural regime ---------	The Lynn-Pinyon belt may represents an underlying major crustal flaw zone.
6. Level of erosion ----------	Erosion has cut through the Roberts Mountains allochthon and exposed autochthonous rocks within the Lynn-Pinyon belt. The absence of any significant supergene enrichment in the gold deposits within this belt suggests relatively recent exposure.
E. District attributes	
1. Host rocks ----------	Host rocks are silty finely laminated carbonaceous dolomitic limestone and carbonaceous shale and siltstone (Cress, 1972).
2. Traps ----------	Permeable horizons in Paleozoic sediment, and fracture zones associated with faults.
3. Preparation ----------	Carbonate removal, brecciation (either fault or hydrothermal), silicification, and argillization.
4. Size ----------	The district includes Maggie Creek/Gold Quarry, Carlin, Blue Star, Bootstrap, and Dee, all gold mines.
5. Extensions ----------	Potentially very good; n.d.
F. Deposit attributes	
1. Host rocks ----------	Host rocks are thin-bedded chert, shale, and siltstone sequence and an argillaceous dolomitic limestone and siltstone sequence, with minor interbedded sandstone.

2. Size/shape	Maggie Creek: 4.8 million tons (4.4 million t) containing 0.092 oz Au/ton (3.15 g Au/t); resource of 442,000 oz Au (13.9 million g Au). Gold Quarry: 175 million tons (159 million t) containing 0.046 oz Au/Ton (1.58 g Au/t); resource of 8 million oz Au (254 million g Au)
3. Physical Characteristics	
a. Ore/gangue mineralogy	Minerals present in the ore zones include pyrite, iron oxides, illite, kaolinite, alunite, quartz, and dolomite (Hausen and others, 1982).
b. Structures	The ore zones are localized in host sedimentary rock where they intersect near-vertical fault zones.
c. Textures	n.d.
d. Host-rock type/age	Host rocks are lower Paleozoic western- and transitional-facies rocks. Mineralization age unknown; possibly Tertiary or Cretaceous.
e. Paragenesis	n.d.
4. Chemical characteristics	
a. Solution chemistry	
(1) Inclusions	n.d.
(2) Stability	n.d.
(3) Solubility	n.d.
(4) Isotopes	n.d.
(5) Cause of deposition	n.d.
b. Temperature	n.d.
c. Associated anomalies	Maggie Creek: As, Zn, Ba; Gold Quarry: As, Sb, Pb, Zn, Ba.
d. Alteration/zonation	Carbonate (calcite) removal, dolomitization, argillization (illite, kaolinite, alunite), silicification.
e. Oxidized or carbonaceous materials.	Carbonaceous material is present in limestone and shale. Although most ore is oxidized, carbon-rich ore is also present.
f. Chemical evolution	n.d.
5. Source of elements	Leached(?) from Paleozoic section with input(?) from buried intrusive rocks.
6. Geophysical signatures	
a. Gravity	n.d.
b. Magnetic	n.d.
c. Induced polarization	n.d.
d. Seismic	n.d.
e. Radiometric	n.d.
7. Summary of apparent depositional environment.	The depositional environment is considered to be similar to that of Carlin: Relatively low pressure (1-2 km) and low temperature (200°-300°C).
8. Byproduct metals	n.d.
G. Summary, features for resource evaluation.	Anomalously high geochemical values for Au, As, Sb, Hg in silty dolomitic limestone and shale lithologies.

McLaughlin, California

[Data from J. P. Albers. n.d., no data available]

A. Name/location	McLaughlin deposit, Napa and Yolo Counties, Calif.
B. Deposit type	Hot-spring deposit.
C. Other examples	Baguio(?), Philippines; Kushikino(?), Japan; Wilbur Springs, Calif.
D. Regional attributes	
1. Presence of gold	McLaughlin is the only known economic deposit of its type in the Coast Ranges. Regionally, the area is known for its mercury deposits. Wilbur Springs, New Almaden, and Stayton mercury deposits all reportedly carry minor gold.
2. Terrane	The deposit occurs in the uplifted accreted terrain of the California Coast Ranges, which consists of Mesozoic ophiolitic rocks (the Coast Range ophiolite), overlying sediment of the Great Valley sequence, and underthrust and accreted sediment and ophiolites of the Franciscan Complex.

3. Basement	Neither pre-Cambrian nor Paleozoic rocks are known within the terrane. The oldest rocks in the region are accreted Jurassic-Cretaceous oceanic rocks that presumably form the oceanic-crust basement.
4. Igneous association	The deposit is located near an outlier of the Clear Lake volcanic field. These volcanic rocks and the earlier Sonoma Volcanics are of regional extent. Oceanic basalt of the Coast Range ophiolite occurs in the McLaughlin region. However, the deposit is probably more closely related in time to the late Cenozoic Clear Lake Volcanics than to the Jurassic-Cretaceous oceanic igneous suites.
5. Structural regime	The deposit appears to lie on the Knoxville fault of Averitt (1945), a regional structure, which extends for several kilometers southeast of the deposit and appears to be offset by younger crossfaults northwest of the deposit (Averitt, 1945). If the deposit is associated in time with Clear Lake volcanism, then the structural environment during deposition was one of extension associated with San Andreas transform faulting (Hearn and others, 1981).
6. Level of erosion	The Coast Ranges are continuing to be uplifted, and erosion is probably fast, regionally owing to the relatively wet climate of northern California. However, sinter is reportedly present at McLaughlin. If this is so, then the deposit is hardly eroded at all and must be quite young.
E. District attributes	
1. Host rocks	Sedimentary rocks of the Great Valley sequence, ophiolitic rocks of the Coast Range ophiolite, and tuff and lavas of Clear Lake volcanism occur within the district. These rocks could all potentially serve as host rocks to gold within the district.
2. Traps	Structural traps may be important if regional structures, such as the Knoxville fault, do control mineralization. Sandstone of sedimentary rocks of the Great Valley sequence could also serve as sedimentary traps to disseminated gold, owing to their permeability. Averitt (1945) mentioned silicified tuff at the Manhattan mercury mine (now McLaughlin). This observation suggests that pyroclastic deposits associated with Clear Lake volcanism could also serve as traps for ore.
3. Preparation	Silica carbonate alteration of serpentinite is common within the district (Averitt, 1945). Such alteration may prepare ophiolitic rocks for gold mineralization. Otherwise, rock preparation within the district is unknown.
4. Size	The McLaughlin gold deposit is within the Knoxville mercury district, which has no previous gold production. The district includes the Reed, Harrison, Soda Springs, Red Elephant, Knoxville, and Manhatten/Royal (now McLaughlin gold) mercury mines. Mercury production between 1862 and 1943 totaled 156,000 flasks (Averitt, 1945).
5. Extensions	n.d.
F. Deposit attributes	
1. Host rocks	The deposit is at the faulted contact of the Coast Range ophiolite (upper part) and the Great Valley sequence. Both are overlain by Clear Lake volcanic rocks. Although data are unavailable, all of these rocks could host the ore.
2. Size/shape	The deposit reportedly contains 3.2 million oz Au (99.5 million g) (Engineering and Mining Journal, 1983). The shape of the deposit is unknown.
3. Physical characteristics	
a. Ore/gangue mineralogy	On the basis of the reports by Becker (1888, p. 271-290) and Averitt (1945), the mineralogy must include native gold, cinnabar, pyrite, stibnite, and silica.
b. Structures	n.d.
c. Textures	n.d.
d. Host-rock type/age	If all rocks near the deposit are mineralized, they include: (1) Jurassic-Cretaceous ophiolitic rocks and sandstone, and (2) late Cenozoic lavas and pyroclastic debris.
e. Paragenesis	n.d.

4. Chemical characteristics	
a. Solution chemistry	
(1) Inclusions ---------	n.d.
(2) Stability ----------	n.d.
(3) Solubility ---------	n.d.
(4) Isotopes ----------	n.d.
(5) Cause of deposition	The presence of sinter at McLaughlin suggests a water-dominated hot-spring system. If gold is associated with sulfides (pyrite, stibnite, cinnabar) as surmised, then the gold may have been carried in solution as a sulfide complex. Under these conditions, fluid temperature is likely to have been controlled by the boiling-with-depth curve. As the rising hydrothermal solutions cooled and boiled, and (or) mixed with near-surface waters, gold-sulfide complexes destabilized, and gold was precipitated with sulfides and silica. Precipitation of gold could also have been in response to oxidation of the fluids (Seward, 1973).
b. Temperature ----------	Most likely controlled by the boiling-with-depth curve.
c. Associated anomalies ---	On the basis of the known mineralogy of the deposit, there probably are at least high Hg and Sb geochemical anomalies associated with the deposit.
d. Alteration/zonation ----	Averitt (1945) mentioned kaolinized and silicified volcanic rock at McLaughlin. Zonation is unknown.
e. Oxidized or carbonaceous materials.	n.d.
f. Chemical evolution -----	n.d.
5. Source of elements --------	The deposit is located near and possibly within mafic ophiolitic rocks. Many of the worlds largest and richest gold deposits have this same association. Thus, it is possible that the ophiolite served as a source of gold (Keays and Scott, 1976).
6. Geophysical signatures	
a. Gravity ----------	n.d.
b. Magnetic ----------	n.d.
c. Induced polarization ---	n.d.
d. Seismic ----------	n.d.
e. Radiometric ----------	n.d.
7. Summary of apparent depositional environment.	The depositional environment for the deposit was a water-dominated hot-spring system. The Knoxville fault (Averitt, 1945) probably acted as a conduit for the fluids. Metals (Hg, Au, Sb) were carried to the surface and deposited near and, possibly, on the surface in response to rapid changes in chemical and physical parameters due to boiling, oxidation, and dilution of the fluids.
8. Byproduct metals ----------	Hg, Sb(?).
G. Summary, features for resource evaluation.	Guides for recognizing this type of deposit include: (1) High, anomalous Hg, Sb, and Au; (2) silicification and argillation; and (3) the presence of siliceous sinter. Because this type of deposit is formed near the surface and thus is easily eroded, young volcanic terranes (heat engine) are most likely to retain surface manifestations of hot-spring gold deposits.

Mercur, Utah

[Data from L. D. Kornze, Getty Mining Co., and E. W. Tooker. n.d., no data available]

A. Name/location	Mercur mining (Camp Floyd) district, secs. 5-8, T. 6 S., R. 3 W., Tooele County, Utah.
B. Deposit type	Carbonate-hosted disseminated gold.
C. Other examples	Carlin and Alligator Ridge, Nev.
D. Regional attributes	
1. Presence of gold	A known gold, silver, and mercury district, organized in 1870 (Butler and others, 1920).
2. Terrane	Miogeoclinal-shelf sedimentary (Paleozoic and Mesozoic) sequence on the edge of the craton, subsequently thrust eastward during the Sevier orogeny.
3. Basement	Precambrian (Proterozoic).
4. Igneous association	Sheets, dikes, and plugs of granodioritic porphyry (36.7 m.y.) and rhyolite porphyry (31.6 m.y.).
5. Structural regime	District close to axis of Ophir anticline in the Bingham sequence on upper plate of the Midas thrust fault (Sevier thrust belt) (Tooker and Roberts, 1970). Faults in district are related to folding, intrusion of porphyries, and basin-and-range faults.
6. Level of erosion	Deposits now near surface; some erosion presumed.
E. District attributes	
1. Host rocks	Major gold deposition in the Mercur mine series of Getty Mining Company comprising several upper carbonaceous limestone layers of lower member of the Great Blue Limestone (Mississippian) (Gilluly, 1932).
2. Traps	Stratabound permeable reactive carbonate layers.
3. Preparation	Silicification-argillization, decalcification, oxidation, weathering.
4. Size	0.8 by 3-km main zone along strike of strata outcrop; smaller area is 5 km south.
5. Extensions	Now being developed in Mercur and explored in adjoining Sunshine and West Dip areas.
F. Deposit attributes	
1. Host rocks	Interbedded shaly, silty, sandy, carbonaceous, and fossiliferous (bioclastic) thin-bedded limestone and brecciated jasperoid in upper part of the lower member of the Great Blue Limestone. Locally bleached, silicified, and leached. Overlain by Long Trail Shale Member of Great Blue Limestone. Cut by sills/dikes of rhyolite porphyry and breccia pipes close to mineralized zones. Brecciated jasperoid in upper part of the lower member of the Great Blue Limestone. Locally bleached, silicified, and leached. Age relations to mineralization are uncertain.
2. Size/shape	Currently being evaluated along linear cross faulted zone. Irregular linear main ore zone of old surface and underground workings, about 60 by 4,600 m. Ore occurs in discontinuous stratiform bodies, as long as 120 m along strike and 300 m downdip. Pre-1960 production, about 1 million oz Au (31.1 million g Au). Reserves announced for new open-pit ore zones about 14.9 million tons (13.5 million t) at 0.09 oz Au/ton (3.1 g Au/t), which is about 1.3 million oz Au (41.7 million g Au).
3. Physical characteristics	
a. Ore/gangue mineralogy	Free gold (smaller than 1 μm), disseminated; species of unoxidized gold undetermined. Gold associated with realgar, orpiment, stibnite, and cinnabar. Gangue: Quartz, carbon, pyrite, marcasite, barite, hematite, calcite, sulfates, and jasperoid (Guenther, 1973; Lenzi, 1971).
b. Structures	Gold occurs in strata, on the east limb of the Ophir anticline, cut by numerous steep normal faults--also sites for rhyolite porphyry sills and dikes. At least two breccia pipes are located in the Mercur district, possibly vents for a phreatic explosion and local collapse of strata.

c. Textures	Fine-grained, porous, not well studied to date.
d. Host-rock type/age	Host is strongly fractured carbonaceous limestone of Mississippian age; associated rhyolite porphyry, 31.6 m.y. old (K-Ar). No gold mineralization observed in rhyolite, very weakly argillized.
e. Paragenesis	Calcite replaced by quartz, sericite and illite in limestone. Pyrite and marcasite are earlier than orpiment and realgar, which are later vug coatings; calcite and barite are late. Gold- and mercury-ore relations uncertain. Realgar also is latter and associated with late calcite veins. Pyrite and marcasite formed during mineralization are in small fine grained pitted grains.
4. Chemical characteristics	
a. Solution chemistry	
(1) Inclusions	n.d.
(2) Stability	n.d.
(3) Solubility	n.d.
(4) Isotopes	n.d.
(5) Cause of deposition	n.d.
b. Temperature	Mineralogy suggests low temperature epithermal range (85°-200°C).
c. Associated anomalies	Ag, As, Hg, Sb, Tl.
d. Alteration/zonation	Jasperoid irregular replacement of limestone, decalcification and solution of limestone to increase porosity, silicification, kaolinite and sericite formation, carbon redistribution, oxidation, and weathering (Klatt and Tafuri, 1976). Jasperoid extends beyond mineralized area.
e. Oxidized or carbonaceous materials.	Both oxidized and carbonaceous materials occur: in sulfide zone, gold occurs as minute inclusions in pyrite and marcasite, in carbon complexes, and as free gold associated with quartz and calcite; in oxidized zone, all gold is in native state. No supergene enrichment in Au.
f. Chemical evolution	Removal of Ca, replacement by Si, Al, K, Au, As, Ba, Fe, Hg, S, Ti, Tl, and organic C introduced in mineralized zone. Mo and B present in enrichment levels; Sb is in some mineralized zones. Gold-bisulfide complex suspected, deposition caused by mixing with meteoric water.
5. Source of elements	Unknown, but in region of intense metallization.
6. Geophysical signatures	
a. Gravity	n.d.
b. Magnetic	n.d.
c. Induced polarization	n.d.
d. Seismic	n.d.
e. Radiometric	n.d.
7. Summary of apparent depositional environment.	Host rocks formed miogeoclinal shelf of craton during the Paleozoic and early Mesozoic, thrust eastward and folded by the Cretaceous Sevier orogeny, then fractured. Igneous intrusive bodies introduced low temperature (approx. 200°C) hydrothermal solutions introduced during late stages of magmatic cycle into host strata, evidence of boiling and venting, sedimentary rocks in ore horizon altered, silica, sulfides, and gold deposited.
8. Byproduct metals	Ag, Hg.
G. Summary, features for resource evaluation.	Located in a known gold-producing region, favorable stratigraphic section, geochemical anomalies present.

Round Mountain, Nevada

[Data from D. R. Shawe. n.d., no data available]

A. Name/location	Round Mountain, Nye County, Nev.
B. Deposit type	Volcanic-hosted stockwork-disseminated gold deposits.
C. Other examples	No closely similar gold deposits known elsewhere.
D. Regional attributes	
1. Presence of gold	Within a known gold province that contains a great variety of gold-deposit types: Vein deposits (including bonanza type) in Tertiary volcanic rocks and Paleozoic and Mesozoic sedimentary and volcanic rocks, and replacement and disseminated (stockwork) deposits in Paleozoic and Mesozoic sedimentary and volcanic rocks and Tertiary volcanic rocks. Round Mountain is one of several early Miocene (19-25 m.y. old) gold deposits in a northwest-trending belt centered along the northeast margin of the Walker Lane in southwestern Nevada, associated with rhyolitic-andesitic flows and tuffs of similar geologic age. No relation to regional geochemical anomalies is evident. Minerals and metals in the deposit are nondiagnostic because all are widely and irregularly distributed in the region.
2. Terrane	Accreted terrane of some complexity; mixed oceanic-shelf derivation, emplaced near continent margin. Probably several successive episodes of accretion, beginning with the Antler orogeny (Roberts Mountains allochthon) of Devonian-Mississippian age, and possibly including two or more Mesozoic events.
3. Basement	Lower Paleozoic marine sedimentary rocks, consisting of quartzite, silty argillite, argillite, limy argillite, limestone, dolomite, and chert, locally metamorphosed to schist and calc-silicate carbonate rocks, and Cretaceous granite. Not known whether or not "crystalline" Precambrian rocks underlie the Paleozoic and Mesozoic rocks. Ore deposits of a great variety are widely known in basement rocks throughout the basin-and-range structural province.
4. Igneous association	Silicic volcanic rocks within which the Round Mountain gold deposits formed are favored hosts elsewhere in the region. Closeness in the ages of the gold ore and host volcanic rocks (26-25 m.y.) suggests that the ore deposits are related to magmatic activity. However, no 25-m.y.-old intrusive rocks are known in the near vicinity. Nearby 35-m.y.-old rhyolitic and andesitic dikes and granodiorite stock predated formation of the gold ores.
5. Structural regime	Round Mountain lies close to a major crustal tectonic zone, the northwest-trending Walker Lane, of probable great geologic vintage (Mesozoic or older?). Some northwest-trending faults at Round Mountain had a major influence on the localization of ore. The district also is marginal to a large Cretaceous granitic pluton that may have served as a structural control on localization of the gold mineralization.
6. Level of erosion	Erosion has not progressed sufficiently to remove the relatively shallow and low-temperature environment of the Round Mountain volcanic-hosted stockwork-disseminated deposits. However, the deposits may not have formed just below the surface, as indicated by a temperature of formation (250°-260°C, Nash, 1972) suggesting a depth of 0.5 to 1 km (see data from Broadlands thermal area, New Zealand, Grindley, 1970).
E. District attributes	
1. Host rocks	Silicic (quartz latitic to rhyolitic) ash-flow tuff.
2. Traps	Lower unwelded porous unit of the ash-flow tuff, and similar porous tuff in an underlying volcanic megabreccia, served as a permeable zone that controlled deposition of the main disseminated lower ore body.

3. Preparation ----------	Silicification of volcanic rock in the welded upper part of the ash-flow tuff, controlled by major mineralized northwest-trending fractures in the core of the district, accounts for the erosion-resistant Round Mountain hill. Early-stage silicification probably increased the brittleness of the silicic ash-flow tuff and permitted extensive fracturing that controlled stockwork mineralization in the upper ore body.
4. Size ----------	District is about 2 by 3 km. Early production (1906-59) came from several underground lode mines and surface and underground placer workings. Total production of gold during the early period was about 537,000 oz Au (16.7 million g Au) (Koschmann and Bergendahl, 1968, p. 194). According to Ferguson (1921, p. 395-397), fineness of the gold mined from lodes was 574-696, and that of placer gold only slightly higher. Thus, probably about 250,000 oz Ag (7.8 million g Ag) was produced in the early period. Current production started in about 1977 from the stockwork ore body in silicified welded ash-flow tuff. Through 1983, in addition, more than 300,000 oz Au (9.4 million g Au) (Simpson and Getz, 1981; Paul Sonerholm, written commun, 1984), and more than 150,000 oz Ag (4.7 million g Ag), has been produced.
5. Extensions ----------	Mining company (Smoky Valley Mining Division of the Copper Range Co., a subsidiary of Louisiana Land and Exploration) is continuing to drill in the district and, in addition to a large new (lower) ore body, has found other new zones of gold-silver-mineralized rock. Large additional potential resources may exist.

F. Deposit attributes

1. Host rocks ----------	The upper body at Round Mountain (now being mined) lies in welded rhyolitic ash-flow tuff, dated as 26.1 m.y. old. Early-mined lode ore bodies were distributed throughout the total present thickness of the welded tuff, about 250 m vertically from the base of the welded tuff to the top of Round Mountain hill. Presently mined stockwork has a similar distribution. The lower ore body at Round Mountain (explored by drilling but not yet developed for mining) is in underlying porous tuff, and it extends locally into underlying Paleozoic rocks.
2. Size/shape ----------	Early-mined ore bodies were thin quartz veins, commonly brecciated, along steep east-west- to northwest-striking faults, and on north- and south-dipping low-angle faults. The flat veins were richer in gold than were the steep veins, and richest ore shoots occurred along intersections of the flat faults with the steep faults (Ferguson, 1921). The veins generally were no more than a few centimeters wide but locally were both thicker and thinner. Numerous vertical nearly parallel northwest-striking fissures filled with thin quartz seams formed a "sheeted" zone at the southwest edge of Round Mountain hill that was mined in a large glory hole. More than half (approximately 330,000 oz Au (10.2 million g Au)) of the gold production during the early period (1906-59) came from the lode deposits at Round Mountain. During the first 10 years of production, grade averaged about 2 oz Au/ton (68.6 g Au/t) and generally diminished thereafter. The presently mined ore body is an oval zone, about 0.4 by 0.8 km, centered on northwest-striking faults of the sheeted zone. Numerous mineralized fractures of different orientations, together with the northwest-striking fractures of the sheeted zone, constitute a stockwork. Reserves in this ore body were initially reported as 11 million tons (10 million t) at .06 oz Au/ton (20 g Au/t) or 660,000 oz Au (20 million g Au). The newly discovered, but not yet mined, lower ore body is also an oval zone, about 1.0 by 1.3 km and as much as 250 m thick, containing an announced 193 million ton (175 million t) averaging .043 oz Au/ton (1.5 g Au/t) or 8.3 million oz Au (262 million g Au). This ore body is more silver rich than the upper ore body and contains about 15.7 million oz Ag (488 million g Ag).

3. Physical characteristics

a. Ore/gangue mineralogy -- Veins of the early-mined deposits consisted of a gangue of quartz and accessory adularia, alunite, and, rarely, fluorite; primary metallic minerals were gold (electrum), pyrite, and, rarely, realgar (Ferguson, 1921, p. 391). Chalcedonic silica is a late-stage mineral. Limonite, manganese oxide, and clay minerals are locally abundant, and jarosite is present in places. Limonite is the product of oxidation of pyrite. Ferguson (1921, p. 393) reported widespread supergene mineralization in which fissures, filled with iron and manganese oxides, or clay, and free gold, transected primary quartz veins. B. R. Berger and P. I. Eimon (unpub. data, 1981) attributed the formation of clays and manganese oxide to a second stage of hydrothermal mineralization. The presently mined (upper) ore body encompasses some of the mined-out veins of the earlier period of mining. It is a stockwork that, in effect, is simply an extension of the veins, as thin seams and fracture fillings in the wallrocks between the veins, that, though of low grade, is minable owing to the present high price of gold. Its mineralogy is essentially that of the veins; it is distinguishable, however, by the occurrence outside a zone of strong alunite development, and fluorite is a common component that occurs in pockets in strongly altered rhyolite. The newly discovered (lower) ore body contains disseminated gold-bearing pyrite and minor base-metal sulfides. The mineralogic residence of the silver is not fully known. Geochemical data reported by Berger and others (1981) indicate that a broad zone of arsenic and antimony enrichment lies near the top of the zone of gold and silver mineralization that constitutes the upper and lower ore bodies. The Au/Ag ratio in the upper ore body is about 2:1, whereas that in the lower ore body is about 1:2.

b. Structures ---------- Faults, both high and low angle, commonly bounded by wallrock breccia and locally filled with gouge and displaying anastomosing slickensided shears, localized the quartz veins that were mined during the early period. The high-angle faults are characterized by nearly horizontal slickensides and mullions, attesting to dominantly strike-slip displacement. Other fractures subparallel to the high-angle faults, and myriad fractures of different orientations, localized the stockwork mineralization of the upper ore body. The lower ore body, though centered on conspicuous zone of northwest-striking fractures, is characterized by disseminated mineralization in porous tuff, a feature suggesting that permeability of the porous tuff beneath a cap of densely welded and, in places, silicified ash-flow tuff was a major factor in ore localization.

c. Textures ---------- No specific ore textures are known that are diagnostic evidence of boiling. Many veins show that a period of silicification was followed by rupture (shearing and brecciation) and, in turn, by renewed silicification. A possible corollary is that silicification sealed the system to allow a buildup of pressure, which, after deformation (breaking), was released in an episode of boiling. Alternatively, hydrothermal-pressure buildup, after sealing by silicification, was sufficient to cause rupture (hydrobrecciation) and boiling. Neither mechanism, however, is required by the evidence.

d. Host-rock type/age ----- The rhyolitic welded ash-flow-tuff host rock has been approximately dated at 26.1±0.8 m.y. (Silberman and others, 1975, p. 1). The age of gold mineralization has been established at approximately 25.2±0.8 m.y. (K-Ar age on adularia; Silberman and others, 1975, p. 2). Alunite in thin veins in the core zone of alteration has been dated at about 10 m.y. old (B. R. Berger, oral commun., 1981). Whether these veins are hypogene or supergene is not known.

e. Paragenesis ---------- In view of the uncertainly as to whether some of the late mineralizing events at Round Mountain were hypogene or supergene, the evolution of the mineral system cannot be described with any confidence.

4. Chemical characteristics

a. Solution chemistry

(1) Inclusions --- Fluid-inclusion studies by Nash (1972, p. C17) indicated that some of the quartz veins (early stage) were deposited from solutions of very low salinity (0.2-1.4 weight percent NaCl equivalent).

(2) Stability --- The presence of chalcedonic silica in late-stage (post-primary ore?) veins suggests that the temperature of deposition at that time was no higher than about 200°-230°C, possibly much lower. Little, if any, additional evidence of depositional conditions based on mineral stabilities is available.

(3) Solubility --- Solubility data for silica do not add significant understanding of the environment of gold deposition at Round Mountain.

(4) Isotopes --- No stable-light-isotope data are available from Round Mountain.

(5) Cause of deposition --- Boiling is a possible mechanism to account for the deposition of gold and associated minerals, but no direct evidence exists for it. Nash (1972, p. C17) stated that "Boiling does not seem to be characteristic of***" a group of Nevada gold-quartz-adularia vein deposits, including Round Mountain. There is insufficient direct evidence to determine the cause of deposition of the gold deposits.

b. Temperature --- The temperature of deposition of some of the quartz veins at Round Mountain, based on fluid-inclusion studies, was about 250° to 260°C (Nash, 1972, p. C17). Berger (this volume) reported temperatures in the range 210-268°C.

c. Associated anomalies --- Associated elements that provide geochemical anomalies which are guides to the location of the Round Mountain gold deposits are Ag, As, Cu, K, Mo, Zn (Shawe, 1977), and F, Hg, Sb, Tl, and W (B. R. Berger and P. I. Eimon, unpub. data 1981).

d. Alteration/zonation --- The work of Tingley (Berger and Tingley, 1980) showed that the northeastern part of the Round Mountain district, encompassing the area of Stebbins Hill to the north and the top and northeast flank of Round Mountain hill farther south, where high-angle west-northwest-trending veins as well as low-angle veins were mined, shows pervasive alteration of tuff in which biotite of the tuff has been altered to chlorite, sericite, and clay. The core of this zone is extensively silicified, and local zones of alunite in veins are present. Peripheral to the altered core is a zone of propylitization of tuff in which biotite of the tuff was altered to chlorite and sericite. Within this peripheral zone southwest of Round Mountain hill are the presently mined upper ore body (stockwork) and newly discovered lower ore body, both centered on the northwest-trending sheeted zone. A patch of breccia at the southeast end of the top of Round Mountain hill and within the altered core, was interpreted by Berger and Tingley (1980) to be a breccia pipe and part of the structural system that localized alteration in the core of the mineralized system. Drill-hole data (Paul Sonerholm, oral commun., 1982), however, do not confirm downward projection of the breccia zone.

e. Oxidized or carbonaceous materials. --- There is no evidence that oxidized or carbonaceous material in the host rock influenced ore deposition.

f. Chemical evolution --- Incomplete understanding of and inadequate data on the Round Mountain gold deposits prevent reconstruction of the chemical evolution of the mineral system.

5. Source of elements --- n.d.

6. Geophysical signatures

a. Gravity --- n.d.

b. Magnetic --- Aeromagnetic mapping (U.S. Geological Survey, 1979) indicates west-facing arc of magnetic highs that encloses the Round Mountain district; the ore is similar to areas of magnetic highs that mark the margins of nearby Mount Jefferson and Manhattan calderas. The magnetic highs near Round Mountain may indicate a volcanic--at least igneous--center concealed beneath alluvium and the silicic volcanic rocks exposed at the surface, to which the gold deposits are related.

c. Induced polarization --- n.d.

d. Seismic --- n.d.

e. Radiometric --- Gold ore from the presently mined ore body at Round Mountain contains minor uranium, and so the deposit could have a radiometric signature.

7. Summary of apparent depositional environment.	Ore deposition followed emplacement of rhyolitic welded ash-flow tuff, possibly by as much as about 1 m.y. and probably at a depth of about 500 m. The temperature of formation of the early veins was about 250° to 260°C, and deposition was from fluids of low salinity (0.2-1.4 weight percent NaCl equivalent), though not necessarily under boiling conditions. Deposition of veins and the stockwork ore body occurred in brittle rhyolitic welded ash-flow tuff and was controlled by tectonically formed faults and fractures. Deposition of the large disseminated ore body underlying the veins and stockwork occurred in laterally permeable porous ash tuff, although tectonically formed faults probably provided the channels for ingress of hydrothermal fluids from a deeper level. The altered core zone (of silicification and alunitization) northeast of the stockwork and disseminated ore bodies, and coincident with part of the area of vein mineralization, is not clearly related to the stockwork and disseminated ore bodies. If the main ingress of hydrothermal fluids into the district was upward through "flues" (breccia pipes) in the altered core zone, as suggested by Berger and Tingley (1980) and by B. R. Berger and P. I. Eimon (unpub. data, 1981), it is not evident how the bulk (approx. 95 percent) of the gold mineralization occurred outside the altered core and at a lower level than the zone of silicification and alunitization. Moreover, the localization of the stockwork and disseminated ore bodies along a tectonic fault zone outside the altered core zone suggests that the major solution flow that formed those ore bodies was upward from deeper levels along the tectonic fault zone. Further work, including stable-light-isotope studies, will be needed to clarify the nature of the separate mineralizing stages that have been recognized in the vein deposits. These stages will have to be correlated with the formation of the stockwork and disseminated ore bodies, and the ambiguous age (10 m.y.) of the alunite veins in the altered core zone explained. Judged from the nearby presence of several mineral systems of different ages and separated in age by many millions of years (D. R. Shawe and others, unpub. data, 1983), the possibility of multiple ages of gold mineralization at Round Mountain should be considered.
8. Byproduct metals ----------	Silver is the only byproduct metal, but a major one, recovered.
G. Summary, features for resource evaluation.	The geologic setting that appears to be favorable for the occurrence of gold deposits of the type present at Round Mountain is a stack of silicic volcanic rocks underlain by an igneous center (zone of igneous intrusion). Evidence of widespread mineralization recurring throughout geologic time marks the region as a metal-rich province. A relatively near-surface environment seems essential for the formation of epithermal gold-silver deposits, but it is not at all clear that boiling and the near-surface (acid leaching) zone of a hot-spring system are essential to the model. Geochemical characteristics of the Round Mountain gold-silver district include the presence of anomalous Ag, As, Cu, F, Hg, K, Mo, Sb, Tl, W, and Zn. Although the relation of various alteration minerals to the major ore bodies at Round Mountain is unclear, the presence in and around the ores of hydrothermal quartz, adularia, alunite, sericite, chlorite, fluorite, clay, manganese oxide, pyrite, and other (base metal) sulfides appears to be important to recognition of an appropriate alteration and mineralization environment.

Round Mountain mine, Nevada

[Data from J. V. Tingley, Nevada Bureau of Mines and Geology, and B. R. Berger. n.d., no data available]

A. Name/location	Round Mountain gold mine. West flank of the Toquima Range, mining area located in portions of secs. 19, 20, 30, and 31, T. 10 N., R. 44 E., Mount Diablo Baseline Meridian, Nye County, Nev.
B. Deposit type	Volcanic-hosted; veins, sheeted zones, breccia, blanket dissemination.
C. Other examples	Similar to occurrences at Hasbrouck Mountain, Divide district, Esmeralda County, Nev., and generally to the DeLamar mine, Owyhee County, Idaho. Except for variations in host-rock type and slightly different positions within the hydrothermal systems, the occurrence also is similar to the deposits at Creede, Colo.
D. Regional attributes	
1. Presence of gold	Located within a known gold province--central Nevada. It is a known type; there may be some districtwide zoning, especially if the nearby Jefferson-district mineralization can be correlated with Round Mountain. The other metal occurrences within the Round Mountain district (W, Hg, Ag at Silver Point) are related to much earlier periods of mineralization and so cannot be used to establish mineral zoning within the district. Other precious metal districts in the region are as follows:
	District — Type of deposit
	Round Mountain — Placer.
	Jefferson City — Ag-Au quartz veins; breccias.
	Gold Hill — Au-Ag quartz veins; breccias.
	Shale Pit-Silver Pit — Disseminated Au; Ag/base-metal veins.
	Manhattan — Ag-Au quartz veins; disseminated Au.
	Northumberland — Disseminated Au.
2. Terrane	The Round Mountain deposits formed in the ring-fracture zone of a late Oligocene caldera; the disseminated and veinlet ores formed in nonwelded intracaldera fill, and the lodes in densely welded intracaldera fill. The basement is continental crust, immediately beneath the ash flows are Paleozoic argillite, limestone, and quartzite, and Cretaceous granite.
3. Basement	Continental crust.
4. Igneous association	Igneous host rock (welded biotite quartz rhyolite ash-flow tuff); tufficite dikes are present. A plug of intrusive material is probably present beneath Round Mountain (rhyolite domes are exposed at Jefferson City and Gold Hill).
5. Structural regime	Caldera. The inferred plug may have intruded at a point on the ring structure of a caldera. Important deeper structures appear to be north-southerly and northeasterly-trending features not exposed on the surface. Ores are mostly concentrated on northwest-trending high-angle fractures, also somewhat on northeast-trending fractures.
6. Level of erosion	Shallow; deposit formed near the surface and has been eroded only a few tens of meters.
E. District attributes	
1. Host rocks	(a) Silicified nonwelded tuff (upper part of flow) was fractured and thus was favorable for the formation of narrow high-grade gold veins. (b) Welded tuff (middle portion of flow sheet) was fractured, but wider zones developed, filled with quartz veins to form sheeted zones. These wider areas are being mined in the present open-pit operation. (c) Soft nonwelded tuff (lower part of flow) was porous and permitted a blanketlike disseminated occurrence to form. This deposit forms the bulk of the new reserves at Round Mountain.

2. Traps	(a) The upper nonwelded, middle welded, lower nonwelded "stratigraphy" of the host ash-flow tuff served as a stratigraphic as well as a structural trap. (b) Classic structural traps appear to have controlled formation of ore shoots within the major veins mined during the life of the old underground-mining operation. High-grade shoots occurred at multiple vein intersections, vein breccia intersections, and so on.
3. Preparation	Not apparent and not considered important. Alteration was not a prerequisite for ore formation.
4. Size	The original Round Mountain gold district is relatively small, it extends only about 2 1/2 km east-west by about 1 1/2 km north-south. Numerous adjoining mining operations were consolidated at an early date at Round Mountain into one operating company, which mined what is essentially a single ore occurrence. Gold and silver are (and have been) the only metals recovered at Round Mountain. Production of lode mines and related gold placers during 1907-68 was about $12,000,000. Reserves announced by the present operators, the Smoky Valley Mining Co., total more than 200 million tons (181.4 million t) averaging nearly 0.05 oz Au/ton (1.7 g Au/t) which is 8-10 million oz Au (248.8 million g Au) and more than 15 million oz Ag (466.5 million g Ag). Older mining produced 800,000-900,000 oz Au (24.9-28 million g Au), mainly from placers. Many early mines were eventually consolidated into the Sunnyside and Fairview as only important producers. The only significant product is Au-Ag bullion. Elsewhere in area is minor tungsten production from quartz-huebnerite veins, silver from quartz veins (Silver Pit), and gold from Paleozoic sedimentary rocks (Shale Pit).
5. Extensions	Possibilities are good for the discovery of extensions; Smoky Valley continues to develop ore as they continue to drill. Other, similar ore bodies could exist in the Round Mountain area, possibly related to Mount Jefferson caldera or to the inferred other caldera at Round Mountain.

F. Deposit attributes

1. Host rocks	Volcanic (welded tuff). Some ore is localized in hydrothermal breccia; disseminated ores are stratabound (in nonwelded-tuff horizons), breccia ores are pods or veinlike. Ores occur (a) in quartz-feldspar veins and veinlets, (b) in silica-cemented breccia, (c) in association with disseminated pyrite, and (d) replacing pumice fragments.
2. Size/shape	Deposits are generally elongate and vertical along the primary controlling structures, ranging from narrow veins in the tightest rock to flat wide blanket forms in the porous tuff. Three general forms can be described: (a) Narrow, quartz-adularia veins in silicified nonwelded tuff (the "silica cap"). These veins were very narrow, 0.6 to 2.5 cm thick, but several closely spaced veins and the silicified rock nearby were commonly mined in stopes as much as 1 1/2 m wide several meters feet along strike, and from the surface down to about 120 m. No records exist on this (early) period of mining, but tonnage was small and the ore quite probably good. (b) Wide zones in the welded part of the tuff. The rock was not so silicified and fractured in a less brittle fashion. Wide sheeted zones occurred along vertical structures, a system of parallel flat structures, related to centers of hydrothermal brecciation. Tonnage of this material mined underground until about 1930 totaled about 500,000 ton (453,500 t) grading from $4 to $50 per ton (in the approximate range of 0.11-1.4 oz Au/ton (3.4-43.5 g Au/t)). The present open-pit operation is mining one of the widest of the vertical sheeted zones. Announced tonnages of this part of the deposit were 12 million ton (10.9 million t) at 0.055 oz Au/ton (1.7 g Au/t). (c) Blanketlike zone, formed at the intersection of the wide sheeted zone with the lower, nonwelded tuff. The top of this zone is reported to be about 120 m below the level of the present pit; values

(mineralization) have been reported to 360 m in some holes. The zone is several hundred meters wide and is elongate along the controlling N.40°-50° W.-trending sheeted zone. Exploration of this zone has resulted in defining more than 195 million ton (177 million t) of ore averaging just under 0.05 oz Au/ton (1.6 Au/t). Exploration is still in progress.

3. Physical characteristics - Mineralogy--not well studied. Native Au, electrum, pyrite, and realgar. Mineralization is zoned:

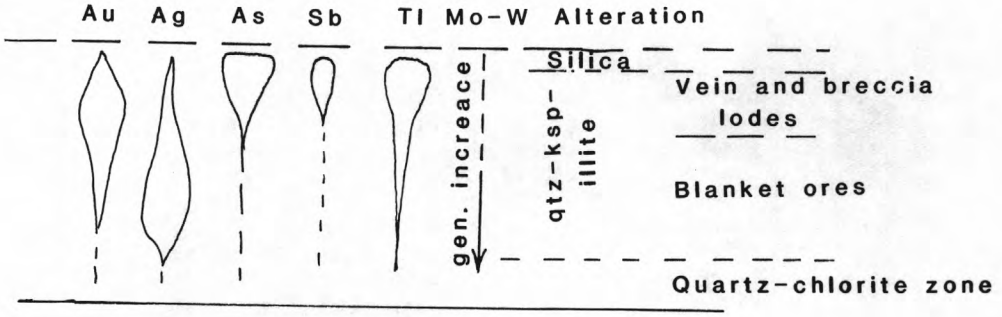

Types of ore:

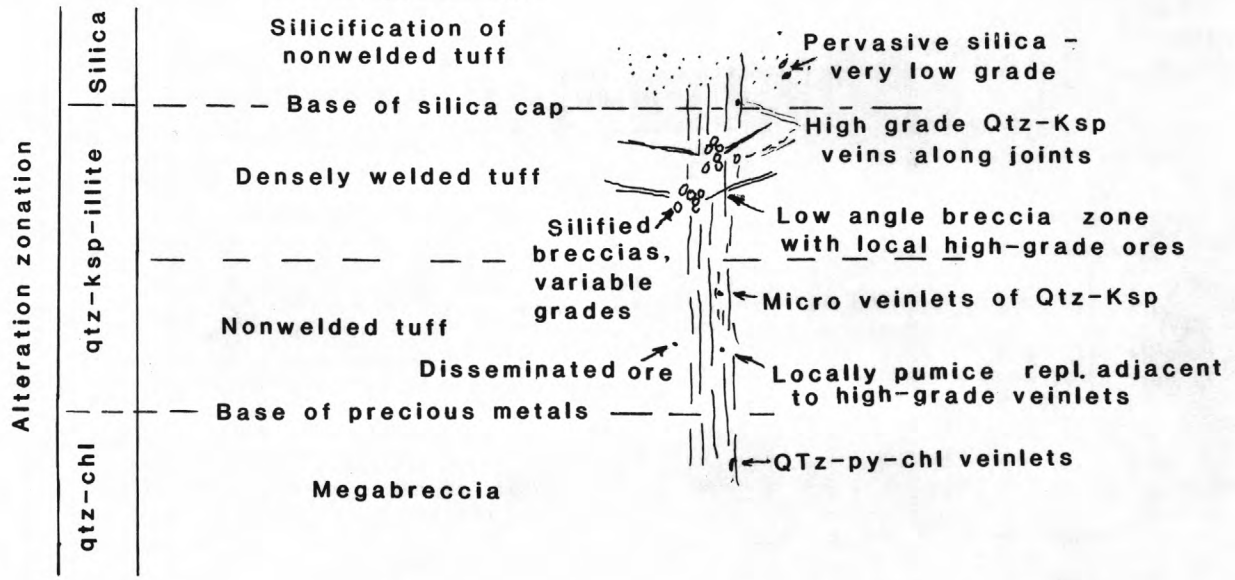

a. Ore/gangue mineralogy -- Quartz and various iron oxides are the only common gangue minerals. Manganese oxides are common on some structures, and fluorite occurs in the breccias and in the main sheeted zones. Pyrite is a gangue mineral in the disseminated ores.

b. Structures ---------- Deposits in the upper part of the tuff occur as veins, vein-filled sheeted zones, and breccia. The deposit in the lower, nonwelded part of the ash flow is an open-space, dissemination, a blanketlike occurrence controlled by the intersection of a wide sheeted zone with the porous part of the tuff.

c. Textures ---------- Open-space filling, banded quartz and adularia, and tiny clear quartz crystals lining open cavities are commonly seen; some lamellar quartz after calcite also occurs.

d. Host-rock type/age ----- Rhyolite welded tuff, dated at 26.1±.8 m.y. (biotite) and 25.7±0.7 (sanidine). Mineralization has been dated at 25.2±.8 m.y. (adularia), 25.4±0.8 (sericite), 25.1±0.8 (altered dike).

e. Paragenesis ---------- n.d.

4. Chemical characteristics	
a. Solution chemistry	
(1) Inclusions ---------	Abundant in quartz; very dilute solutions with essentially no depression of feezing point.
(2) Stability ----------	n.d.
(3) Solubility ---------	n.d.
(4) Isotopes -----------	n.d.
(5) Cause of deposition	Evidence from fluid inclusions suggests boiling important mechanism
b. Temperature ----------	From fluid inclusions: variation 170°C to 270°C; average, approximately 230°C.
c. Associated anomalies ---	Arsenic, thallium, molybdenum, tungsten, antimony, mercury
d. Alteration/zonation ----	Essentially all the ash-flow tuff at Round Mountain displays propylitic alteration. The major veins display alteration envelopes which grade outward from each vein-filled fracture, ranging from a thin clay selvage next to the vein which immediately grades out to propylitically altered rock, to large areas of argillic alteration associated with the hydrothermal-breccia centers. Areas of alunitic alteration coincide with the small centers of hydrothermal brecciation and are mappable by the presence of alunite veinlets, with some disseminated jarosite. Silicification is physically within a larger zone of argillic alteration.
e. Oxidized or carbonaceous materials.	No carbonaceous materials within ore deposit.
f. Chemical evolution -----	n.d.
5. Source of elements --------	n.d.
6. Geophysical signatures	
a. Gravity ----------	Gravity has been used to map the major structures at Round Mountain by the use of indirect methods. Therefore, ore zones have been defined with some (reported) success.
b. Magnetic ----------	n.d.
c. Induced polarization ---	n.d.
d. Seismic ----------	The internal stratigraphy of the tuff unit (welded-nonwelded boundary) is apparently mappable by the use of seismic techniques.
e. Radiometric ----------	n.d.
7. Summary of apparent depositional environment.	The Round Mountain deposit formed, probably very near the surface, in favorable horizons within an ash-flow tuff. Early silicification (formation of a "silica cap") caused portions of a hydrothermal system to "overpressure." The resultant fracturing, resealing, refracturing, and so on, caused the formation of podlike hydrothermal breccias and related quartz veins.
8. Byproduct metals ----------	Gold is the principal metal, and silver the only byproduct.
G. Summary, features for resource evaluation.	The caldera setting is important. Localization of later, but related, plugs and (or) vent systems along the ring fractures have provided important mineralization controls. Host rocks could be any porous or brecciated rock. An impervious or less porous capping rock is important. Areas of widespread propylitic alteration occur with localized centers of argillic, advanced argillic; alunitic and locally pervasive silicification seems to be characteristic. At Round Mountain, the mineralogy appears to be simple: Free gold, silver, iron and manganese oxides containing gold and silver, and pyrite.

Sulphur, Nevada

[Data from A. B. Wallace, Cordex Exploration Co. n.d., no data available]

A. Name/location	Sulphur district, southwesternmost Humboldt County, 153 km northeast of Reno, 97 km west of Winnemucca, T. 35 N., R. 28 and 29 E., Nev.
B. Deposit type	Disseminated gold hosted in volcanic and volcaniclastic rocks and alluvium showing abundant hot-spring features.
C. Other examples	Steamboat Springs and Borealis, Nev.
D. Regional attributes	
1. Presence of gold	In northwestern Nevada, numerous "epithermal" gold deposits are associated with volcanic rocks.
2. Terrane	Poorly known; "basement" of Mesozoic volcanic and clastic sedimentary rocks with uncertain relation to Mesozoic tectonism, overlain by Tertiary bimodal basalt/rhyolite volcanic rocks associated with continental rifting(?).
3. Basement	See 2 above.
4. Igneous association	Abundant rhyolitic tuff and lavas overlain by rhyolitic ash. Rhyolitic dikes associated closely in time with ore formation.
5. Structural regime	Basin-and-range faulting. Possibly near a rhyolitic volcanic center.
6. Level of erosion	Ore formed near surface, which is preserved and marked by siliceous spring sinter. Near-surface blanket of acid-leached rock overlies gold/silver mineralization and is well preserved.
E. District attributes	
1. Host rocks	Tertiary alluvial gravel and volcaniclastic sediment. Veins in underlying rhyolite lavas and ash flows.
2. Traps	Intense silicification is controlled in a coarse conglomerate overlying a thick section of rhyolitic air-fall or lacustrine tuff. Late basin-and-range faulting controls dikes and late veins of alunite and quartz (with silver), and earlier basin-and-range faulting may have controlled gold and silicification.
3. Preparation	Silicification.
4. Size	Low-grade mineralization present in an area of 6 km^2. Economic concentrations are much smaller but of undetermined size (approx 1-2 million ton (.9-1.8 million t).
5. Extensions	n.d.
F. Deposit attributes	
1. Host rocks	Conglomerate and lacustrine/air-fall tuff.
2. Size/shape	Unknown low-grade mineralization in large (3-6 km^2) blanket of silicification in conglomerate bed. Economic concentrations may be small (1 millions ton) pipelike bodies near feeders. Overlain by zone leached by acid condensate containing sulfur and mercury.
3. Physical characteristics	
a. Ore/gangue mineralogy	Not totally known. Gold apparently is associated with pyrite in highly silicified conglomerate. Some stibnite. Gangue is replacement quartz, with minor vugs and microveinlets of quartz. Silver mineralogy is unknown.
b. Structures	Minor microveining. Late (postgold) coarse alunite veins cut silicification.
c. Textures	Replacement quartz has a mosaic texture, with disseminated pyrite. Late quartz in microveinlets and euhedral crystals coating vugs. Late (postgold) mineralization consists of veins of alunite and distinctly separate veins of banded quartz with calcite replacement textures.
d. Host rock type/age	Conglomerate is probably Pliocene alluvium. Sinter may be synore deposition, that is, approximately 1.7 m.y. old or Pleistocene.
e. Paragenesis	n.d.

4. Chemical characteristics	
a. Solution chemistry	
(1) Inclusions ---------	n.d.
(2) Stability ----------	Gold deposited with quartz and pyrite. Moderate f_{O_2}(?). Low to moderate f_{S_2} and δS. Low SO_4^{2-} relative to H_2S(?).
(3) Solubility ---------	Not constraining enough to matter.
(4) Isotopes -----------	n.d.
(5) Cause of deposition	Boiling important. Evidence for boiling includes a well preserved zone of acid leaching formed by the oxidation of condensate overlying a boiling water table below which gold/silver were deposited.
b. Temperature ----------	Unknown, but siliceous sinter suggests approximately 200°C at 150 m and 270° C at depth in deposit.
c. Associated anomalies ---	Not fully known; definitely As, Hg, Sb, and Tl.
d. Alteration/zonation ----	Ore-grade material associated with intense silicification, which grades progressively outward into less intense silicification and argillization. Acid-leached zone of opal/alunite overlies deposit. Silicification grades downward into montmorillonite argillic alteration except, possibly, along keel-shaped feeder zones.
e. Oxidized or carbonaceous materials.	No carbonaceous material is known. Oxidation is very shallow; in intense silicification pyrite is present at surface.
f. Chemical evolution -----	Unknown in detail; silica-saturated fluids migrated laterally in porous conglomerate and boiled near the water table. Eventually, silicification sealing of the system allowed overpressures. Late fracturing released pressures and allowed vapor-dominated emplacement of coarse alunite.
5. Source of elements --------	n.d.
6. Geophysical signatures	
a. Gravity ----------	n.d.
b. Magnetic ----------	n.d.
c. Induced polarization ---	n.d.
d. Seismic ----------	n.d.
e. Radiometric ----------	n.d.
7. Summary of apparent depositional environment.	Boiling, shallow geothermal/hydrothermal system developed along range-front normal faults with development of hot springs and sinter.
8. Byproduct metals ----------	n.d.
G. Summary, features for resource evaluation.	(1) Nearly exact replica of the Steamboat Springs geothermal area; (2) silicification, (3) sinter representing the surface at the time of mineralization; (4) volcanic environment; and (5) As, Sb, and Hg associated, but not directly to the grade of gold.

Table 8. Summary of critical attributes

[n.d., not

Attribute	Carbonate hosted					
	Carlin, Nev.	Cortez, Nev.	Gold Acres, Nev.	Jerritt Canyon, Nev.	Alligator Ridge, Nev.	Getchell, Nev.
Terrane	Accreted oceanic crust overlying cratonal miogeoclinal sediment.	Accreted oceanic crust overlying cratonal miogeoclinal sediment.	Accreted oceanic crust overlying cratonal miogeocline.	Accreted oceanic crust overlying cratonal miogeoclinal sediment.	Miogeoclinal cratonal margin.	Transitional-facies carbonate and siliceous accreted oceanic crust.
Basement	Unexposed Precambrian craton(?).	Unexposed Precambrian craton(?).	Unexposed Proterozoic craton(?).	Unexposed Precambrian craton(?).	Unexposed Precambrian and miogeoclinal Paleozoic sediment(?).	Unexposed Precambrian craton(?).
Igneous-rock association.	Premineral acidic dikes	Several felsic porphyritic dikes (biotite-quartz-sanidine).	Unexposed granitic pluton, 98.8 m.y. old. Quartz porphyry dikes exposed in mine, 94.3 m.y. old; rhyolite dikes, 32 to 35 m.y.(?) old.	Undetermined; nearby dioritic plug, andesite flow; travertine hot-spring deposit in vicinity.	None exposed	Granodiorite and dacite porphyry dikes in area along fault zone.
Structure	Basin-and-range Antler orogenic belt in windows below the Roberts Mountains thrust.	Basin-and-range north-northwest-striking normal faults.	Siliceous rocks of the Roberts Mountains thrust overlying carbonate lower-plate rocks.	Basin-and-range normal extensional faults, Roberts Mountains thrust fault.	Basin-and-range normal extensional faults.	Basin-and-range normal extensional faults.
Level of erosion	No apparent supergene enrichment; shallow.	Deposits near surface (open breccias).	Depth of erosion, about 1,500 m.	Deposits near surface; some probably eroded.	Deposits at surface or at shallow depth.	Deposits near surface
Host lithology	Carbonaceous siltstone; porous permeable sedimentary rocks of the Roberts Mountains Formation (Silurian and Devonian).	Carbonaceous siltstone of the Roberts Mountains Formation (Silurian and Devonian).	Limestone of the Roberts Mountains Formation (Silurian and Devonian) and the Wenban Limestone (Devonian).	Ordovician-Silurian siltstone, and chert sediment.	Carbonaceous siltstone in the Mississippian Pilot Shale.	Sandy to argillaceous carbonate sedimentary rocks of Cambrian and Ordovician age.
Traps	Favorable stratigraphic horizon; faulted.	Ore bodies follow dikes	Intense fracturing of lowermost part of the Roberts Mountains thrust.	Fault intersection under silica cap and regional thrust fault.	Faulted fractured brecciated siltstone above bedded limestone.	Small-scale folds, fractured silicified zones in limestone.
Preparation	Carbonate removal, argillization.	Silicification, brecciation, fracturing, and formation of jasperoid.	Rocks metamorphosed by pluton; local argillization, chert hornfels, skarn, sericitic alteration.	Hydrothermal silicification and argillization, oxidation, and weathering.	Jasperoid breccia formation, oxidation, carbon removal.	Faulting, hydrothermal brecciation, decarbonization.
Size	Five gold mines	0.8 by 6 km; 24,000 troy oz (746,400 g) Au, 4.5 million troy oz (139 million g) Ag.	Small	Four known deposits in 260-km^2 area; no significant past production.	Five ore bodies over 1-1/2-km strike; no past production.	Four pits along strike of 3 to 4 km; past production.
Associated metals	Au, Hg, As, Sb, Tl, minor Pb, Cu, Zn.	Au, Ag, Pb, Cu, Zn	Au, Hg, As, B	Au, Sb, Ba, Ag, Hg	Au, Hg, Sb, As	WO_3 from area, but not associated with Au.
Potential extensions	Excellent	Excellent (in Horse Canyon, 3.40 million tons (3.08 million t) of ore grading 0.055 troy oz Au per ton (1.9 g Au/t).	Highly probable	Good	Very likely	Known (at Pinson, 10-13 km south).
Ore host rock	Porous, permeable rocks of upper 300 ft of the Roberts Mountains Formation.	Finely laminated thin-bedded carbonaceous siltstone in limestone sequence.	Carbonate and siliceous rocks low in upper plate of the Roberts Mountains thrust.	Banded carbonaceous limestone and calcareous siltstone (Cambrian-Ordovician).	Thin platy fractured carbonaceous siltstone lower member of the Pilot Shale.	Replacement of carbonate parts of formation along strike of fault zone.
Shape, size, grade	Stratiform; strike along 1,645 m, N. 45° E.; dip, 30°-40° NW. Production: 3 million troy oz (93 million g) Au from 7.7 million tons (8.5 million t) of ore grading 0.39 troy oz Au per ton (13.4 g Au/t).	Irregular, tabular; 3.4 million tons (3.1 million t) of ore grading 0.29 troy oz Au per ton (9 g Au/t), or 986,000 troy oz (30.7 million g) Au.	Shallow-dipping tabular body; 300- by 450-m pit (originally), expanded by 250 m to southwest; approximately 280,000 troy oz (8.7 million g) Au; grade unavailable.	Irregular along fault, 30 by 2,400 m. Reserves: 13.7 million tons (12.4 million t) of ore grading 0.205 troy oz Au per ton (6.4 g Au/t), or 2.8 million troy oz (79.4 million g) Au.	Pit, average 107 by 150 m; 5 million tons (4.5 million t) of ore grading 0.11 troy oz Au per ton (3.4 g Au/t), or 550,000 troy oz (15.3 million g) Au.	Sheetlike zones on walls of faults, more than 300 m long, 300 to 900 m downdip, 5 to 15 m thick. Production: 1 million oz (31 million g) Au at a grade of 0.25 troy oz Au per ton (8.6 Au/t). Resources: 800,000 troy oz (21.9 million g) Au at a grade of 0.20 troy oz Au per ton (6.8 g Au/t).
Ore/gangue minerals	Oxidized ore: clay, silica, detrital quartz, and sulfates; carbonaceous ore: clay, silica, quartz, carbon, realgar, cinnabar, and sulfides.	Native gold with Au-As-Sb-Hg-bearing pyrite, quartz, calcite, and minor barite.	Oxidized ore in faults and fractures, associated with quartz, kaolinite, iron oxides, dolomite, and calcite.	Free gold (1-4 m) with stibnite, pyrite, carbon, realgar, orpiment, and cinnabar; barite, quartz, and aragonite gangue.	Free gold (micrometer size) in oxidized ore; form of gold in carbonaceous ore undetermined. Pyrite, carbon, quartz, and barite gangue.	Free gold (less than 1 m) with pyrite, arsenopyrite, native silver, scheelite, orpiment, realgar, stibnite, cinnabar, getchellite, quartz, pyrite, marcasite, fluorite, calcite, dolomite, barite, and chebazite.
Structure	Replacement and dissemination in beds and along faults.	Dissemination fracture controlled; minor quartz veins.	Low-angle faults and crosscutting high-angle faults.	Microveins at fault intersections with host strata; dissemination in permeable reactive host.	Dissemination in permeable reactive host.	Dissemination along microfractures in silicified brecciated limestone; associated with pyrite and quartz; sheetlike along faults, concentrated along nose of microanticlines.
Texture of ore	Acid leached	Fine-grained, locally open breccias and fractures.	Oxidized, no original texture preserved; boiling(?).	Fine-grained open vuggy silicification.	Fine grained; fractures and breccia coated with quartz.	Fine-grained quartz, multiple breccia, pods of kaolinite and alunite.
Age of ore	Tertiary	Undetermined; less-than-34-m.y.-old felsic dikes and Silurian host rocks.	Gold mineralization now believed to be related to Oligocene(?) rhyolite dikes.	n.d.	n.d.	89 m.y. (K-Ar)
Ore-formation temperature (°C).	175-200	175-200 (fluid inclusions).	160-380 (fluid inclusions).	n.d.	n.d.	n.d.
Associated geochemical anomalies.	As, Sb, Ag, Tl	As, Sb, Hg, W, Tl	Ag, Hg, As, B	Hg, As, Sb	Hg, As, Sb, Tl	As, Sb, Hg, Tl, F, U_3O_8, Mo, W.
Alteration/zonation	Carbon removal, clay introduction, silica introduction.	Silicification, carbon oxidation, argillization of felsic dikes to montmorillonite.	Weak silicification of limestone, sericitization of Cretaceous dikes, kaolinitization of Tertiary dikes.	Carbonization, argillization, oxidation.	Carbon removal, limonite staining.	Silicification, carbonization, oxidation.
Byproduct metals	Hg	Ag		Hg, As	Hg	Hg, As

of disseminated gold deposits

determined]

Carbonate hosted	Volcanic hot spring hosted			Volcanic hosted		
Mercur, Utah	Hasbrouck Peak, Nev.	McLaughlin, Calif.	Sulphur, Nev.	Borealis, Nev.	Round Mountain, Nev.	DeLamar, Idaho
Miogeoclinal-shelf sedimentary sequence on margin of craton.	Accreted oceanic volcanogenic crust.	Accreted ophiolitic volcanic oceanic crust.	Mesozoic volcaniclastic accreted(?) sediment.	Continental margin, accreted oceanic crust.	Paleozoic-Mesozoic accreted oceanic volcaniclastic crust.	Plutonic rocks overlain by Miocene volcanic rocks on inner continental margin.
Unexposed Precambrian craton.	Near outer edge of craton; Precambrian and miogeoclinal Paleozoic sediment(?).	Jurassic-Cretaceous oceanic crust.	Uncertain; near edge of craton and accreted oceanic crust.	Uncertain; Mesozoic plutonic and metamorphic rocks, oceanic andesitic volcanic rocks.	Undetermined; Precambrian craton(?).	Idaho batholith outliers (granodiorite).
Sills, dikes, and plugs of rhyolite porphyry and granodiorite porphyry.	Silicic volcanogenic sedimentary rocks and silicic plugs and dikes nearby; interbedded hot-spring sinter.	Nearby volcanic field, oceanic basalt; the Clear Lake and Sonoma Volcanics (Jurassic-Cretaceous).	Abundant rhyolitic tuff and lavas; dikes.	Andesitic volcanic rocks----	Silicic volcanic tuff underlying plug (?).	Alkali olivine basalt and rhyolite of the Owyhee volcanic field, margin of the Snake River rift.
Flanks of anticline of thrust-sheet allochthon close to Uinta-Cortez axis.	Basin-and-range normal extensional faults; margin of caldera(?), Walker Lane zone.	Extensional faults, San Andreas transform fault.	Basin-and-range normal extensional faults; possibly near volcanic center.	Volcanic-arc setting in basin-and-range Walker Lane zone.	Walker Lane zone; marginal to Cretaceous granitic pluton caldera(?).	Basin-and-range faulting.
Deposits near surface---------	Deposits near or at present surface.	Deposits at or near present surface.	Ore formed and at near surface.	Ore at or near present surface.	Ore at near-surface to moderate depth.	At or near surface.
Mississippian carbonaceous limestone.	Volcanogenic sedimentary rocks, 13 to 17 m.y. old (Miocene).	Sediment, ophiolites, tuff, and lavas, Jurassic-Cretaceous to Pliocene-Pleistocene.	Tertiary alluvial gravel and volcaniclastic sedimentary rocks.	Andesitic volcanic flows and volcaniclastic sedimentary rocks, Tertiary.	Silicic ash-flow tuff------	Rhyolitic flows, tuff, breccias, and volcaniclastic sedimentary rocks; basalt.
Stratabound permeable reactive layers in limestone and at crossfaults.	Altered along permeable beds and small faults; hydrothermal breccia.	Permeable sandstone and pyroclastic deposit.	Silicified conglomerate, late basin-and-range-fault-controlled dikes.	Favorable stratigraphy, veins, stockworks.	Upper beds, nonwelded tuff breccia; lower body in porous tuff, permeable zone, and volcanic megabreccia.	Brittle rhyolite faulted zones.
Jasperoid formation, silicification, argillization, oxidation, carbon introduction.	Hydrothermal silicification and brecciation.	Silica carbonate alteration of serpentine(?); mostly unknown.	Silicification----------	Hydrothermal alteration, silicification.	Silicification along northwest-trending fracture system.	Faulting and silicification.
Area along strike of limestone; past production, 1 million troy oz (31 million g) Au.	Area, 10 km^2; minor past production.	Six mines; no previous gold production; Old Knoxville mercury district.	Area unknown, probably about 8 to 15 km^2; irregular distribution.	Undetermined; previous minor gold production.	Area, 2 to 3 km^2; past production, 500,000 troy oz (15.6 million g) Au.	DeLamar/Silver City area; past placer and lode production, 400,000 troy oz (12.4 million g) Au and 6.0 million troy oz (190 million g) Ag.
Au, Ag, Hg, Sb, As, Tl--------	Au, Ag----------	Au, Hg, Sb----------	Sb, Hg, As, Tl----------	Au, Hg, As, Ag, Sb----------	Au, Ag----------	Au, Ag.
Known (at Sunshine and West Dip).	Modest laterally; may be none at depth.	Unknown, but probably good.	Undetermined----------	Possible to excellent in area.	Highly probable----------	Excellent.
Shaly silty carbonaceous fossiliferous limestone layers in the Great Blue Limestone (Mississippian).	Silicified tuffaceous shale and sandstone, tufa, lapilli tuff, and volcanic conglomerate of the Siebert Formation (Miocene).	Coast Range ophiolite and Great Valley sequence sedimentary rocks along contact overlain by the Clear Lake Volcanics.	Tertiary alluvial gravel and volcaniclastic sedimentary rocks; veins in underlying lavas and ash flows.	Miocene subaerial andesitic volcaniclastic rocks, sediment, and flows.	Upper body, welded rhyolite tuff (25 m.y.) and hydrothermal-breccia stockwork; lower body, disseminated in porous tuff.	Rhyolite domes, lavas, and pyroclastic deposits; K-Ar age, 15.6 to 15.7 m.y.
Linear zone along strike of formation, 60 by 4,600 m. Production: 1 million troy oz (31 million g) Au at a grade of 0.1 troy oz Au per ton (3.4 g Au/t). Resources: 1.4 million troy oz (41 million g) Au at a grade of 0.09 troy oz Au per ton (3.1 g Au/t).	Discoid; 1-km^2 area with root zone. Resource: More than 500,000 troy oz (15.6 million g) Au at a grade of 0.1 troy oz Au per ton (3.4 g Au/t).	Shape unknown. Resource: 3.2 million troy oz (100 million g) Au at a grade of about 0.15 troy oz Au per ton (5.1 g Au/t).	Shape unknown; 3- to 6-km^2 blanket of silicified conglomerate. Pipelike bodies near feeders and overlain by acid-leached zone. Resource: Possibly 1 million tons (0.9 million t) of ore, grade undetermined.	Irregular shape in quartz sulfide breccia. Resource: 2 million tons (1.8 million t) of ore grading 0.08 troy oz Au per ton (2.7 g Au/t), or 160,000 troy oz (5 million g) Au.	Thin brecciated quartz veins along steep faults; flatter veins are richer. Production: More than 150,000 troy oz (4.7 million g) Au at a grade of 2 troy oz Au per ton (66 g Au/t). Resource: 10.2 million troy oz (317 million g) Au at an average grade of 0.05 troy oz Au per ton (1.7 g Au/t). Reserves: 8.4 million troy oz (260 million g) Au and 15.7 million troy oz (488 million g) Ag.	Irregular; structure controlled by domes. Production: 400,000 troy oz (12.4 million g) Au and 6 million troy oz (187 million g) Ag. Resource: 250,000 troy oz (7.8 million g) Au at a grade of 0.025 troy oz Au per ton (0.86 g Au/t) and 35 million troy oz (1.09 million g) Ag at a grade of 3.5 troy oz Ag per ton (120 g Ag/t).
Free gold (less than 1 m) with arsenopyrite, pyrite, base-metal sulfides, realgar, orpiment, stibnite, cinnabar, quartz, illite, kaolinite, carbon, barite hematite, and calcite.	Free gold with pyrite, chalcopyrite, argentite, quartz, and adularia.	Free gold, cinnabar, pyrite, stibnite, and silica.	Not well known. Gold with pyrite in silicified host with stibnite, silver, and quartz.	Gold with pyrite, sphalerite, bravoite, cobaltite, silica, barite, and hematite. No carbonaceous material.	Free gold, pyrite, realgar, chalcedonic silica, quartz, adularia, alunite, fluorite, limonite, manganese oxide, and clay minerals.	Native gold and silver, argentite, marcasite, pyrite, chalcopyrite, galena, iron oxides, quartz, and chalcedony gangue.
Folded sediment, faults, breccia pipes.	Veinlets, hydrobreccia, microfractures.	n.d----------	Minor microveins, dissemination in silicified host; postore alunite veins cut silicification.	Silicified hydrobreccias cutting volcanic rock.	Veins in sheeted zones; stockwork breccias in upper part. Open-space dissemination in lower part, ash-flow tuff.	Stockwork veinlets and silicified rhyolite.
Fine-grained permeable carbonate.	Quartz veinlets, silicified breccia, fracture fillings banded.	n.d----------	Replacement quartz mosaic with pyrite, late mineralized veins of alunite, and banded quartz-calcite.	Silicified multiple breccia and acid-leached zones from late boiling.	Open-space filling, banded quartz-adularia silicification, boiling(?), multiple fracturing.	Au as anhedral blobs in quartz associated with naumannite (Ag_2Se) in fractures, adsorbed onto surface, or in solid solution.
Undetermined; older than 31.6 m.y. (K-Ar)(?).	n.d.	n.d.	1.7 m.y. (Pleistocene)	5 m.y.(?)	Younger than 25.2±0.8 m.y. (K-Ar).	Contemporaneous with volcanic rocks.
n.d., but in estimated epithermal range.	Max 200-240	n.d.	n.d.	Approx 120	200-230	130-200
Hg, As, Sb, Ag, Cu, Tl, Ti, Mo, B.	As, Sb, Hg, W----------	Hg, Sb, As, Te----------		Hg, Ag----------	Ag, Cu, Zn, Mo, Hg, As, Sb, Tl, F, W.	Se, Hg, Ag, Au.
Jasperoid, silicification-argillization.	Silicification, argillization, hot-spring system.	Silicification, argillization.	Inner silicification, outer argillization; no carbonaceous material.	Silicification, argillization, propylitization, alunite acid leaching.	Silicified core outward to argillic and propylitic; no oxidized or carbonaceous material.	Strong argillization, sericite, kaolinite, montmorillonite, illite, porphyllite, rare intense silicification.
Hg, Ag----------	Ag----------	Hg, Sb(?)----------		Hg, Ag----------	Ag----------	

and metamorphism during Mesozoic and early Cretaceous time (earlier than 120 to later than 50 m.y. B.P.) (Miller and Bradfish, 1980). This timespan approximately corresponds to the ages of disseminated deposits in Nevada and to the inference that they may represent reconcentration of gold from deep basement terranes, comparable with those in Arizona or Canada, which has been remobilized by granitic intrusions and volcanic activity. More data are required to prove this thesis.

Gold bearing porphyry (dispersed)-type deposits, however, seem to be directly associated with deeper, high-temperature intrusions and associated zoned magmatic hydrothermal processes than those of interest here. There is sufficient reason, in my opinion, to consider that a dispersed porphyry system differs from (or is a deeper manifestation of) a disseminated system, which occurs at or near the surface.

Disseminated gold occurrences are now being found in accreted and cratonal terranes elsewhere in the Cordilleran region and beyond (in California, Arizona, New Mexico, Washington, Montana, and Utah). In addition to common occurrences in an existing gold province associated with igneous systems, they generally are related to present-day or fossil hot-spring or vented (brecciated) systems. The concentration of disseminated gold deposits in Nevada and, possibly, Idaho-Montana seems to be related to broad regional northeast-trending subparallel linear suture zones or structural flaws in the crust, as proposed by Tooker (1979), that traverse the craton inboard from its outer edge. Such broad basement structural zones may also provide channels for the introduction of heat from yet deeper seated sources and thus facilitate the remobilization of metals during geologic time, and may account for the anomalous age correlations between igneous and gold-depositing activity.

One final critical regional factor is that the rate of erosion in the Nevada area has been sufficient only to uncover, but not to remove, these presumed near-surface deposits.

District characteristics

Comparison of the data listed in table 8 provides some generalizations about the geologic attributes characterizing the sediment- and volcanic-hosted disseminated gold districts and deposits. In the following summations, distinctive features are listed in separate columns, whereas common features are listed across both columns:

	Sediment hosted	Volcanic hosted
Host lithology	Paleozoic carbonaceous limestone, calcareous siltstone, and chert.	Volcanogenic sediment, ash-flow tuff, lavas, and ophiolite.
Gold traps	Permeable strata, reactive beds, faults and breccias, breccia pipes, impermeable capping, small-scale fold structures, and thrust faults.	
Sources of heat	Generally indirect evidence: Intrusive plugs, dikes, and sills; hot-spring activity; volcanic caldera center.	
Preparation	Hydrothermal silicification, argillization, and brecciation-boiling.	
	Increased permeability due to solution, jasperoid formation, and decarbonization.	Serpentinization.
Size	A few square kilometers to tens of square kilometers, some including mines or former mines; generally no former gold production indicated.	
Persistent geochemical associations.	Au, Ag, Hg, Sb, As, and Tl.	
Potential extensions.	Generally favorable or possible.	

The main differences observed in district attributes are directly related to differences in host-rock lithology and structures, and in their responses to hydrothermal alteration.

Deposit traits

Similar comparison of the deposit traits listed in table 8 brings out more differences between the sediment- and volcanic-hosted deposits, as follows:

	Sediment hosted	Volcanic hosted
Ore host rock	Thin-bedded banded calcareous limestone, calcareous siltstone, and shale; fractured, altered.	Silicified tuff, volcanogenic conglomerate, volcanic flows, and associated sedimentary rocks; fractured, altered.
Shape	Generally discontinuous sheetlike zones along faults and along permeable sedimentary layers.	Irregular bodies controlled by shear and breccia zones, faults, and permeable volcaniclastic sedimentary rocks, commonly stockwork root zones.
Size	0.5 to more than 3 million troy oz (16-93 million g) Au.	0.2 to more than 3 million troy oz (6.2-93 million g) Au.
Grade	0.1-0.25 troy oz Au/ton (3.4-8.6 g Au/t).	0.05-0.1 troy oz Au/ton (1.7-3.4 g Au/t).
Ore minerals	Free gold (less than 1 μm), generally invisible; native silver (locally), cinnabar, stibnite, realgar, orpiment, and, locally, base-metal sulfides.	Free gold (less than 1 μm), locally visible; argentite and native silver, arsenopyrite, cinnabar, realgar, orpiment, and stibnite.
Ore gangue	Barite, carbon, quartz, pyrite, fluorite, calcite and hematite.	Quartz, barite, adularia, pyrite, and hematite.
Ore structures	Stratabound dissemination in permeable strata, with microfaults, breccias, minor folds, shears, crossfaults and breccia pipes.	Veinlets, hydrobreccia, dissemination in porous host, sheeted zones, stockworks, and breccia pipes.
Ore texture	Fine-grained, locally silicified banded coatings and replacements on fractures and open vugs; generally evidence of boiling and multiple brecciation; gold generally invisible.	
Age of ore	Mostly undetermined, ranging from 1.7 to 90 m.y.	
Temperature of ore formation.	Mostly undertermined, but mineralogic and textural associations suggest a range of 200° to 250°C.	
Alteration zonation.	Silicification, jasperoid formation, argillization, carbonization, later oxidation.	Silicification, argillization, and propylitization; absence of carbon; alunite acid leaching.
Associated geochemical anomalies.	Au, Ag, Hg, As, Sb, locally Tl, F, and W.	Au, Ag, Hg, Sb, Cr, Mo, locally Tl, F, and W.

A reasonable conclusion from these comparisons is that the present data base provides a generalized occurrence model for disseminated gold deposits.

Overlaps of the features described above contrast with seemingly distinctive characteristics of some individual deposits in the checklists. This comparison of data may be as close to describing a model for disseminated gold deposits as is possible at this time. Thus, this volume is a summary of the current status of knowledge.

REFERENCES CITED

Armbrustmacher, T. J., and Wrucke, C. T., 1978, The disseminated gold deposit at Gold Acres, Lander County, Nevada, in Lovering, T. G., and McCarthy, J. H., Jr., eds., Conceptual models in exploration geochemistry: The Basin and Range Province of the western United States and northern Mexico: Journal of Geochemical Exploration, v. 9, no. 2-3 (special issue), p. 195-203.

Averitt, Paul, 1945, Quicksilver deposits of the Knoxville district, Napa, Yolo, and Lake Counties, California: California Journal of Mines and Geology, v. 41, no. 2, p. 65-89.

Becker, G. F., 1888, Geology of the quicksilver deposits of the Pacific slope, with an atlas: U.S. Geological Survey Monograph 13, 486 p.

Berger, B. R., and Tingley, J. V., 1980, Geology and geochemistry of the Round Mountain gold deposit, Nye County, Nevada [abs.]: American Institute of Mining Engineers Precious Metals Symposium, Reno, Nev., 1980, Abstracts, p. 18c.

Berger, B. R., Tingley, J. V., Filipek, L. H., and Neighbor, J., 1981, Origin of pathfinder trace-element patterns associated with gold-silver mineralization in late Oligocene volcanic rocks, Round Mountain, Nye County, Nevada [abs.]: Association of Exploration Geochemists Precious Metals Symposium, Vancouver, British Columbia, Canada, 1981, Abstracts, p. 207.

Bonham, H. F., Jr., and Garside, L. J., 1979, Geology of the Tonopah, Lone Mountain, Klondike, and Northern Mud Lake quadrangles, Nevada: Nevada Bureau of Mines and Geology Bulletin 92, 142 p.

Butler, B. S., Loughlin, C. F., Heikes, V. C., and others, 1920, The deposits of Utah: U.S. Geological Survey Professional Paper 111, 672 p.

Cox, D. P., ed., 1983a, U.S. Geological Survey-Ingeominas mineral resource assessment of Columbia: Ore deposit models: U.S. Geological Survey Open-File Report 83-423, 62 p.

----- 1983b, U.S. Geological Survey-Ingeominas mineral resource assessment of Columbia: Additional ore deposit models: U.S. Geological Survey Open-File Report 83-901, 31 p.

Cress, L. D., 1972, Geology of the Carlin window area, Eureka County, Nevada: San Jose, California State University, M.S. thesis, 103 p.

Dickson, F. W., Rye, R. O., and Radtke, A. S., 1979, The Carlin gold deposits as a product of rock-water interactions, in Ridge, J. D., ed., Papers on mineral deposits of western North America: Nevada Bureau of Mines and Geology Report 33, p. 101-108.

Duda, R. V., 1980, The Prospector system for mineral exploration: Menlo Park, Calif., SRI International, 120 p.

Engineering and Mining Journal, 1983, California, in This month in mining: v. 184, no. 1, p. 111.

Erickson, R. L., compiler, 1982, Characteristics of mineral deposit occurrences: U.S. Geological Survey Open-File Report 82-795, 248 p.

Ferguson, H. G., 1921, The Round Mountain district, Nevada: U.S. Geological Survey Bulletin 725-I, p. 383-406.

Finch, W. I., Cragen, H. C., Lupe, Robert, and McCammon, R. B., 1980, Genetic-geologic models--a systematic approach to evaluate geologic favorability for undiscovered uranium resources, pt. 1 of Research on uranium resource models--a progress report: U.S. Geological Survey Open-File Report 80-2018, 53 p.

Gilluly, James, 1932, Geology and ore deposits of the Stockton and Fairfield quadrangles, Utah: U.S. Geological Survey Professional Paper 173, 171 p.

Grindley, G. W., 1970, Subsurface structures and relation to steam production in the Broadlands geothermal field, New Zealand: Geothermics, Special Issue 2, v. 2, pt. 1, p. 248-261.

Guenther, E. M., 1973, The geology of the Mercur gold camp, Utah: Salt Lake City, University of Utah, M.S. thesis, 79 p.

Hausen, D. M., Ekburg, C., and Kula, F., 1982, Geochemical and XRD-computer logging method for lithologic ore type classification of Carlin-type gold ores, in Hagen, R. D., ed., Process Mineralogy II: Metallurgical Society of AIME, Process Mineralogy Committee Symposium, Dallas, Tex., 1982, Proceedings.

Hawkins, R. B., 1982, Discovery of the Bell gold mine—Jerritt Canyon district, Elko County, Nevada: Mining Congress Journal, v. 68, no. 2, p. 28-32.

Hearn, B. C., Donnelly-Nolan, J. M., and Goff, F. E., 1981, The Clear Lake Volcanics: Tectonic setting and magma sources, in McLaughlin, R. J., and Donnelly-Nolan, J. M., eds., Research in the Geysers-Clear Lake geothermal area, northern California: U.S. Geological Survey Professional Paper 1141, p. 25-46.

Huang, C.-I., and Strachan, D. G., 1981, Geochemistry and geology of a disseminated gold occurrence at Borealis, Mineral County, Nevada [abs.]: Geological Society of America Abstracts with Programs, v. 13, no. 2, p. 62.

Jones, D. L., 1983, Tectonostratigraphic terranes of western North America--an overview [abs.]: Geological Society of America Abstracts with Programs, v. 15, no. 5, p. 384.

Jones, D. L., Cox, Allan, Coney, Peter, and Beck, Myrl, 1982, The growth of western North America: Scientific American, v. 247, no. 5, p. 70-84.

Joralemon, Peter, 1951, The occurrence of gold at the Getchell mine, Nevada: Economic Geology, v. 46, no. 3, p. 267-310.

Keays, R. R., and Scott, R. B., 1976, Precious metals in ocean-ridge basalts: Economic Geology, v. 71, no. 4, p. 705-720.

Kistler, R. W., and Peterman, Z. E., 1978, Reconstruction of crustal blocks of California on the basis of initial strontium isotopic compositions of Mesozoic granitic rocks: U.S. Geological Survey Professional Paper 1071, 17 p.

Klatt, H. R., and Tafuri, W. J., 1976, Gold mineralization in the Mercur mining district, Utah: paper presented at Northwest Mining Association Meeting, Spokane, Wash., 1976.

Koschmann, A. H., and Bergandahl, M. H., 1968, Principal gold-producing districts of the United States: U.S. Geological Survey Professional Paper 610, 283 p.

Lenzi, G. W., 1971, Geochemical reconnaissance at Mercur, Utah: Utah Geological and Mineral Survey Special Studies 43, 16 p.

Miller, C. F., and Bradfish, L. J., 1980, An inner Cordilleran belt of muscovite-bearing plutons: Geology, v. 8, no. 9, p. 412-416.

Nash, J. T., 1972, Fluid-inclusion studies of some gold deposits in Nevada, in Geological Survey research, 1972: U.S. Geological Survey Professional Paper 800-C, p. C15-C19.

Panze, A. J., 1975, Geology and ore deposits of the Silver City-DeLamar-Flint region, Owyhee County, Idaho: Idaho Bureau of Mines and Geology Pamphlet 161, 79 p.

Philbin, P. W., Meuschke, J. L., and McCaslin, W. E., 1963, Aeromagnetic map of the Roberts Mountains area, central Nevada: U.S. Geological Survey open-file map, scale 1:25,000.

Radtke, A. S., 1981, Geology of the Carlin gold deposit, Nevada: U.S. Geological Survey Open-File Report 81-97, 154 p.

Rodgers, W. H., Moss, K. L., and Thomason, R. E., 1980, The DeLamar silver mine--an update: DeLamar silver mine report, 5 p.

Rytuba, J. J. and Glanzman, R. K., 1979, Relation of mercury, uranium, and lithium deposits to the McDermitt caldera complex, Nevada-Oregon, in Ridge, J. D., ed., Papers on mineral deposits of western North America: Nevada Bureau of Mines and Geology Report 33, p. 109-117.

Seward, T. M., 1973, Thio complexes of gold and the transport of gold in hydrothermal ore solutions: Geochimica et Cosmochimica Acta, v. 37, no. 3, p. 379-399.

Shawe, D. R., 1977, Geochemical and generalized geologic maps showing distribution of iron, copper, lead, zinc, silver, molybdenum, antimony, arsenic, tungsten, barium, boron, and potassium in the Round Mountain quadrangle, Nye County, Nevada: U.S. Geological Survey Miscellaneous Field Studies Maps MF-835-A through MF-835-L, scale 1:24,000.

----- 1981, U.S. Geological Survey workshop on nonfuel mineral-resource appraisal of wilderness and CUSMAP areas: U.S. Geological Survey Circular 845, 18 p.

Silberman, M. L., Shawe, D. R., Koski, R. A., and Goddard, B. B., 1975, K-Ar ages of mineralization in Round Mountain and Manhattan, Nye County, Nevada: Isochron/West, no. 13, p. 1-2.

Silberman, M. L., Stewart, J. H., and McKee, E. H., 1976, Igneous activity, tectonics, and hydrothermal precious-metal mineralization in the Great Basin during Cenozoic time: Society of Mining Engineers of AIME Transactions, v. 260, no. 3, p. 253-263.

Simpson, D. L., and Getz, A. J., 1981, Leaching of silver and gold ores at Smoky Valley Mining Division, Copper Range Company: Nevada Institute of Technology International Gold/Silver Conference, Reno, Nev., 1981, Proceedings, p. 11.

Theodore, T. G., Blain, W. N., and Nash, J. T., 1982, Preliminary report on the geology and gold mineralization of the Gold Basin-Lost Basin mining district, Mohave County, Arizona, with sections on K-Ar chronology of mineralization and igneous activity, by E. H. McKee, and Implications of the composition of lode and placer gold, by J. C. Antweiller and W. L. Campbell: U.S. Geological Survey Open-File Report 82-1052, 322 p.

Tooker, E. W., and Roberts, R. J., 1970, Upper Paleozoic rocks in the Oquirrh Mountains and Bingham mining district, Utah, with a section on Biostratigraphy and correlation, by Mackenzie Gordon, Jr., and H. M. Duncan: U.S. Geological Survey Professional Paper 629-A, p. A1-A76.

Tooker, E. W., 1979, Metal provinces and plate tectonics in the conterminous United States, in Ridge, J. D., ed., Papers on mineral deposits of western North America: Nevada Bureau of Mines and Geology Report 33, p. 33-38.

U.S. Geological Survey, 1979, Aeromagnetic map of the Manhattan area, Nevada: U.S. Geological Survey Open-File Report OF-1454, scale 1:62,500.

Wells, J. D., Stoiser, L. R., and Elliott, J. E., 1969, Geology and geochemistry of the Cortez gold deposit, Nevada: Economic Geology, v. 64, no. 5, p. 526-537.

White, D. E., 1981, Active geothermal systems and hydrothermal ore deposits: Economic Geology, 75th anniversary volume, p. 392-423.

Wrucke, C. T., and Armbrustmacher, T. J., 1975, Geochemical and geologic relations of gold and other elements at the Gold Acres open-pit mine, Lander County, Nevada: U.S. Geological Survey Professional Paper 860, 27 p.

Wrucke, C. T., Armbrustmacher, T. J., and Hessin, T. D., 1968, Distribution of gold, silver, and other metals near Gold Acres and Tenabo, Lander County, Nevada: U.S. Geological Survey Circular 589, 19 p.

WORKSHOP AGENDA

Registration and dinner, May 16, 1982, Holiday Inn, Reno, Nev.

Conference session, May 17, Reno

Presentations and discussions of the geologic characteristics and depositional processes for volcanic- and carbonate-hosted disseminated gold deposits.

D. E. White, Hot spring metal-bearing systems in the Great Basin with a focus on metal zoning.

R. O. Fournier, Gold in hot spring water with respect to hydrothermal transport and deposition of gold.

M. L. Silberman, Ages of gold deposition and associated volcanic and tectonic activity.

R. O. Rye, Isotopes and temperature of disseminated deposits, implications regarding the hydrothermal system at Carlin and Cortez, Nevada.

H. F. Bonham, Jr., Overview and contrasts between types of carbonate- and volcanic-hosted deposits.

J. J. Rytuba, Geochemical transport in the gold-depositing environment.

B. R. Berger, Regional geochemical characteristics and zoning patterns with examples from Getchell, Cortez, and Round Mountain, Nevada.

C. G. Cunningham, Proposed model for gold deposition in the volcanic caldera environment.

Field-trip sessions, May 18, 19, and 20

Steamboat Springs, Nevada, an active metal-bearing hot springs area, D. E. White, leader.

Borealis, Nevada, a gold deposit in a mixed volcanic and fossil hot spring area, D. G. Strachan, leader.

Hasbrouck Peak, Nevada, a complex volcanic basin area and fossil hot spring deposit, A. B. Wallace, leader.

Round Mountain, Nevada, a volcanic-hosted deposit, comments by J. V. Tingley, B. R. Berger, and D. P. Shawe.

Jerritt Canyon, Nevada, a carbonate-hosted type deposit, R. C. Banghart, leader.

Model workshop session, Elko, Nev., May 21

Discussion of proper elements for an ore-occurrence model for the various disseminated gold deposits. Outline for checklist prepared. Participants prepared checklists for several typical deposits.

WORKSHOP PARTICIPANTS

Ashley, R. P.[1]	Chief, Branch of Western Mineral Resources, U.S. Geological Survey, Menlo Park, Calif. (also Survey gold commodity
Bagby, W. C.	Homestake Mining Co., Napa, Calif.; now with Branch of Western Mineral Resources, U.S. Geological Survey, Menlo Park, Calif.
Banghart, R. C.	Freeport Minerals, Jerritt Canyon, Nev.
Berger, B. R.	Branch of Exploration Research, U.S. Geological Survey, Denver, Colo.
Bonham, H. F., Jr.	Nevada Bureau of Mines and Geology, Reno, Nev.
Cunningham, C. G.	Branch of Central Mineral Resources, U.S. Geological Survey, Denver, Colo.
Fournier, R. O.	Branch of Igneous and Geothermal Processes, U.S. Geological Survey, Menlo Park, Calif.
Newell, R. A.	Newmont Exploration Company, Tucson, Ariz.
Rye, R. O.	Branch of Isotope Geology, U.S. Geological Survey, Denver, Colo.
Rytuba, J. J.[1]	Branch of Western Mineral Resouces, U.S. Geological Survey, Menlo Park, Calif.
Shawe, D. P.	Branch of Central Mineral Resources, U.S. Geological Survey, Denver, Colo.
Silberman, M. L.	Anaconda Minerals Co., Reno, Nev.; now with Branch of Exploration Geochemistry, U.S. Geological Survey, Denver, Colo.
Smith, C. L.	Branch of Exploration Geochemistry, U.S. Geological Survey, Denver, Colo.
Strachan, D. G.	Consulting geologist, Hawthorne, Nev.; formerly with Houston International Minerals Company, Hawthorne, Nev.
Taylor, R. B.[1]	Staff, Office of Mineral Resources, U.S. Geological Survey, Denver, Colo.
Tingley, J. V.	Nevada Bureau of Mines and Geology, Reno, Nev.
Tooker, E. W.[1]	Branch of Western Mineral Resources, U.S. Geological Survey, Menlo Park, Calif.
Wallace, A. B.	Cordex Exploration, Reno, Nev.
White, D. E.	Branch of Igneous and Geothermal Processes, U.S. Geological Survey, Menlo Park, Calif.

[1]Workshop organizing committee.

SUGGESTED READING ON DISSEMINATED GOLD DEPOSITS

Ashley, R. P., and Silberman, M. L., 1976, Direct dating of mineralization at Goldfield, Nevada, by potassium-argon and fission-track methods: Economic Geology, v. 71, no. 5, p. 904-924.

Berger, B. R., and Eimon, P. I., 1982, Conceptual models of epithermal silver-gold deposits: American Institute of Mining, Metallurgical, and Petroleum Engineers Preprint 82-13, 32 p.

Browne, P. R. L., 1971, Mineralization in the Broadlands geothermal field, Taupo volcanic zone, New Zealand, in International Mineralogical Association-International Association of the Genesis of Ore Deposits Joint Symposium, Tokyo-Kyoto, 1971, Proceedings: Society of Mining Geologists of Japan Mining Geology Special Issue 2, p. 64-75.

Browne, P. R. L., and Ellis, A. J., 1970, The Ohaki-Broadlands hydrothermal area, New Zealand: Mineralogy and related geochemistry: American Journal of Science, v. 269, no. 1, p. 97-131.

Dickson, F. W., Rye, R. O., and Radtke, A. S., 1979, The Carlin gold deposit as a product of rock-water interaction, in Ridge, J. D., ed., Papers on mineral deposits of western North America: Nevada Bureau of Mines and Geology Report 33, p. 101-108.

Ewers, G. R., and Keays, R. R., 1977, Volatile and precious metal zoning in the Broadlands geothermal field, New Zealand: Economic Geology, v. 72, no. 7, p. 1337-1354.

Henley, R. W., and Ellis, A. J., 1983, Geothermal systems ancient and modern: A geochemical review: Earth Science Reviews, v. 19, p. 1-50.

Nash, J. T., 1972, Fluid-inclusion studies of some gold deposits in Nevada, in Geological Survey research, 1972: U.S. Geological Survey Professional Paper 800-C, p. C15-C19.

Radtke, A. S., 1981, Geology of the Carlin gold district, Nevada: U.S. Geological Survey Open-File Report 81-97, 154 p.

Radtke, A. S., and Dickson, F. W., 1974, Genesis and vertical position of fine-grained disseminated replacement-type gold deposits in Nevada and Utah, USA: International Association on the Genesis of Ore Deposits Symposium, 4th, Varna, Bulgaria, 1974, Proceedings, v. 1, p. 71-78.

Radtke, A. S., Rye, R. O., and Dickson, F. W., 1980, Geology and stable isotope studies of the Carlin gold deposit, Nevada: Economic Geology, v. 75, no. 5, p. 641-672.

Roberts, R. J., Radtke, A. S., and Coats, R. R., 1971, Gold-bearing deposits in north-central Nevada and southwestern Idah, with a section on Periods of plutonism in north-central Nevada, by M. L. Silberman and E. H. McKee: Economic Geology, v. 66, no. 1, p. 14-33.

Seward, T. M., 1973, Thio complexes of gold and the transport of gold in hydrothermal ore solutions: Geochimica et Cosmochimica Acta, v. 37, no. 3, p. 379-399.

Silberman, M. L., Stewart, J. H., and McKee, E. H., 1976, Igneous activity, tectonics, and hydrothermal precious-metal mineralization in the Great Basin during Cenozoic time: Society of Mining Engineers of AIME Transactions, v. 260, no. 3, p. 253-263.

Weissburg, B. G., 1969, Gold-silver ore-grade precipitates from New Zealand thermal waters: Economic Geology, v. 64, no. 1, p. 95-108.

White, D. E., 1981, Active geothermal system and hydrothermal ore deposits: Economic Geology, 75th anniversary volume, p. 392-423.

GPO 587-044/10017